RADIOLOGY AND ONCOLOGY

vol.53 no.4
december 2019

NOVO

CABOMETYX®
(kabozantinib) tablete
60 mg | 40 mg | 20 mg

- **PFS**[2]
- **OS**[2]
- **ORR**[2]

CABOMETYX® pomembno izboljša PFS, OS in ORR v drugi liniji zdravljenja napredovalega karcinoma ledvičnih celic[1]

RAZŠIRITEV INDIKACIJE:

Sedaj tudi za zdravljenje napredovalega karcinoma ledvičnih celic (KLC) pri predhodno nezdravljnenih odraslih bolnikih s srednje ugodnim ali slabim prognostičnim obetom.[2]

ORR: objektivna stopnja odziva; OS: celokupno preživetje; PFS: preživetje brez napredovanja bolezni

Referenci:
1. Choueiri TK, Escudier B, Powles T, *et al.* Cabozantinib versus everolimus in advanced renal cell carcinoma (METEOR): final results from a randomised, open-label, phase 3 trial. The Lancet Oncology. 2016;17(7):917-27.
2. Povzetek glavnih značilnosti zdravila Cabometyx.

Skrajšan povzetek glavnih značilnosti zdravila

CABOMETYX 20 mg filmsko obložene tablete
CABOMETYX 40 mg filmsko obložene tablete
CABOMETYX 60 mg filmsko obložene tablete
(kabozantinib)

▼ Za to zdravilo se izvaja dodatno spremljanje varnosti. Tako bodo hitreje na voljo nove informacije o njegovi varnosti. Zdravstvene delavce naprošamo, da poročajo o katerem koli domnevnem neželenem učinku zdravila.

TERAPEVTSKE INDIKACIJE Zdravljenje napredovalega karcinoma ledvičnih celic (KLC) pri predhodno nezdravljenih odraslih bolnikih s srednje ugodnim ali slabim prognostičnim obetom ter pri odraslih bolnikih po predhodnem zdravljenju, usmerjenem v vaskularni endotelijski rastni faktor (VEGF). V monoterapiji zdravljenje hepatocelularnega karcinoma (HCK) pri odraslih bolnikih, ki so se predhodno že zdravili s sorafenibom. **ODMERJANJE IN NAČIN UPORABE** Pri bolnikih s KLC in HKC je poročeni odmerek 60 mg enkrat na dan. Zdravljenje je treba nadaljevati tako dolgo, dokler bolnik več nima kliničnih koristi od terapije ali do pojava nesprejemljive toksičnosti. Pri sumu na neželene reakcije na zdravilo bo morda treba zdravljenje začasno prekiniti in/ali zmanjšati odmerek. Če je treba odmerek zmanjšati, se priporoča zmanjšanje na 40 mg na dan in nato na 20 mg na dan. Prekinitev odmerka se priporoča pri obravnavi toksičnosti 3. ali višje stopnje po CTCAE (*common terminology criteria for adverse events*) ali nevzdržni toksičnosti 2. stopnje. Zmanjšanje odmerka se priporoča za dogodke, ki bi lahko čez čas postali resni ali nevzdržni. V primeru pojava neželenih učinkov 1. in 2. stopnje, ki jih bolnik prenaša in jih je možno enostavno obravnavati, prilagoditev odmerjanja običajno ni potrebna. Treba je uvesti podporno oskrbo. V primeru pojava neželenih učinkov 2. stopnje, ki jih bolnik ne prenaša in jih ni mogoče obravnavati z zmanjšanjem odmerka ali podporno oskrbo, je treba zdravljenje prekiniti, dokler neželeni učinki ne izzvenijo do ≤ 1. stopnje, uvesti podporno oskrbo in razmisliti o ponovni uvedbi zdravljenja z zmanjšanim odmerkom. V primeru pojava neželenih učinkov 3. stopnje je treba zdravljenje prekiniti, dokler neželeni učinki ne izzvenijo do ≤ 1. stopnje, uvesti podporno oskrbo in ponovno uvesti zdravljenje z zmanjšanim odmerkom. V primeru pojava neželenih učinkov 4. stopnje je treba zdravljenje prekiniti, uvesti ustrezno zdravniško oskrbo, in če neželeni učinki izzvenijo do ≤ 1. stopnje, ponovno uvesti zdravljenje z zmanjšanim odmerkom. Če neželeni učinki ne izzvenijo, je treba trajno prenehati z uporabo zdravila. Pri bolnikih z blago ali zmerno ledvično okvaro je treba kabozantinib uporabljati previdno. Uporaba se ne priporoča pri bolnikih s hudo ledvično okvaro. Pri bolnikih z blago okvaro jeter odmerka ni treba prilagajati. Pri bolnikih z zmerno okvaro jeter (Child Pugh B) priporočil za odmerjanje ni možno podati. Pri teh bolnikih je priporočljivo skrbno spremljanje celokupne varnosti. Pri bolnikih s hudo okvaro jeter (Child Pugh C) uporaba kabozantiniba ni priporočljiva. Način uporabe: Tablete je treba pogoltniti cele in jih ni dovoljeno drobiti. Bolnikom je treba naročiti, naj vsaj 2 uri pred uporabo zdravila in 1 uro po tem ničesar ne jedo. **KONTRAINDIKACIJE** Preobčutljivost na učinkovino ali katero koli pomožno snov. **POSEBNA OPOZORILA IN PREVIDNOSTNI UKREPI** Večina dogodkov se pojavi zgodaj v teku zdravljenja, zato mora zdravnik bolnika v prvih 8 tednih zdravljenja skrbno spremljati, da oceni, ali je treba odmerek prilagoditi. Dogodki, ki se običajno pojavijo zgodaj, vključujejo hipokalciemijo, hipokaliemijo, trombocitopenijo, hipertenzijo, sindrom palmarno-plantarne eritrodisestezije (PPES), proteinurijo in gastrointestinalne dogodke (bolečine v trebuhu, vnetje sluznice, zaprtje, driska, bruhanje). Pred uvedbo zdravljenja s kabozantinibom je priporočljivo izvesti preiskave delovanja jeter (ALT, AST in bilirubin), vrednosti skrbno spremljati med zdravljenjem in po potrebi prilagoditi odmerek. Bolnike je treba spremljati glede znakov in simptomov jetrne encefalopatije. Bolnike, ki imajo vnetno bolezen črevesja (npr. Crohnovo bolezen, ulcerozni kolitis, peritonitis, divertikulitis ali apendicitis), ki imajo tumorsko infiltracijo prebavil ali so imeli pred posegom na prebavilih zaplete (zlasti v povezavi z zapoznelim ali nepopolnim celjenjem), je treba pred uvedbo zdravljenja skrbno oceniti, nato pa natančno spremljati za pojav simptomov perforacij in fistul, vključno z abscesi in sepso. Trajna ali ponavljajoča se driska med zdravljenjem je lahko dejavnik tveganja za nastanek analne fistule. Uporabo kabozantiniba je treba pri bolnikih, pri katerih se pojavi gastrointestinalna perforacija ali fistula, ki je ni možno ustrezno obravnavati, prekiniti. Driska, navzea/bruhanje, zmanjšanje apetita in vnetje ustne sluznice/bolečina v ustni votlini so nekateri od najpogosteje poročanih neželenih učinkov na prebavila. Nemudoma je treba uvesti ustrezne medicinske ukrepe, vključno s podpornim zdravljenjem z antiemetiki, antidiaroiki ali antacidi, da se prepreči dehidracija, neravnovesje elektrolitov in izguba telesne mase. Če pomembni neželeni učinki na prebavila vztrajajo ali se ponavljajo, je treba presoditi o prekinitvi odmerjanja, zmanjšanju odmerka ali trajni ukinitvi zdravljenja s kabozantinibom. Kabozantinib je treba uporabljati previdno pri bolnikih, pri katerih obstaja tveganje za pojav venske trombembolije, vključno s pljučno embolijo, in arterijske trombembolije ali imajo te dogodke v anamnezi. Z uporabo je treba prenehati pri bolnikih, pri katerih se razvije akutni miokardni infarkt ali drugi klinično pomembni znaki zapletov trombembolije. Kabozantiniba se ne sme dajati bolnikom, ki hudo krvavijo, ali pri katerih obstaja tveganje za hudo krvavitev. Med zdravljenjem s kabozantinibom je treba spremljati vrednosti trombocitov in odmerek prilagoditi glede na resnost trombocitopenije. Zdravljenje s kabozantinibom je treba ustaviti vsaj 28 dni pred načrtovanim kirurškim posegom, vključno z zobozdravstvenim, če je mogoče. Kabozantinib je treba ukiniti pri bolnikih z zapleti s celjenjem rane, zaradi katerih je potrebna zdravniška pomoč. Pred uvedbo kabozantiniba je treba dobro obvladati krvni tlak. Med zdravljenjem je treba vse bolnike spremljati za pojav hipertenzije in jih po potrebi zdraviti s standardnimi antihipertenzivi. V primeru trdovratne hipertenzije, kljub uporabi antihipertenzivov, je treba odmerek kabozantiniba zmanjšati. Z uporabo je treba prenehati, če je hipertenzija resna ali trdovratna kljub zdravljenju z antihipertenzivi in zmanjšanemu odmerku kabozantiniba. V primeru hipertenzijske krize je treba zdravljenje prekiniti. Pri resni PPES je treba razmisliti o prekinitvi zdravljenja. Nadaljevanje zdravljenja naj se začne z nižjim odmerkom, ko se PPES umiri do 1. stopnje. V času zdravljenja je treba redno spremljati beljakovine v urinu. Pri bolnikih, pri katerih se razvije nefrotični sindrom, je treba z uporabo kabozantiniba prenehati. Pri uporabi kabozantiniba so opazili sindrom reverzibilne posteriorne levkoencefalopatije (RPLS), znan tudi kot sindrom posteriorne reverzibilne encefalopatije (PRES). Na ta sindrom je treba pomisliti pri vseh bolnikih s številnimi prisotnimi simptomi, vključno z epileptičnimi napadi, glavobolom, motnjami vida, zmedenostjo ali spremenjenim mentalnim delovanjem. Pri bolnikih z RPLS je treba zdravljenje prekiniti. Kabozantinib je treba uporabljati previdno pri bolnikih s podaljšanjem intervala QT v anamnezi, pri bolnikih, ki jemljejo antiaritmike, in pri bolnikih z relevantno obstoječo boleznijo srca, bradikardijo ali elektrolitskimi motnjami. Uporaba kabozantiniba je bila povezana z večjo pojavnostjo elektrolitskih nepravilnosti (vključno s hipokaliemijo, hiperkaliemijo, hipomagneziemijo, hipokalciemijo in hiponatriemijo), zato je priporočljivo spremljati biokemijske parametre in po potrebi uvesti ustrezno nadomestno zdravljenje v skladu s standardno klinično prakso. Bolniki z redko dedno intoleranco za galaktozo, laponsko obliko zmanjšane aktivnosti laktaze ali malabsorpcijo glukoze/galaktoze ne smejo jemati tega zdravila. Plodnost, nosečnost in dojenje: Ženskam v rodni dobi je treba svetovati, da v času zdravljenja s kabozantinibom ne smejo zanositi. Zanositev morajo preprečiti tudi ženske partnerice moških bolnikov, ki uporabljajo kabozantinib. Med zdravljenjem in še vsaj 4 mesece po končanju terapije morajo tako bolniki in bolnice kot tudi njihovi partnerji uporabljati zanesljiv način kontracepcije. Kabozantiniba se ne sme uporabljati med nosečnostjo, razen če zdravljenje ni nujno potrebno zaradi kliničnega stanja ženske. Matere med zdravljenjem s kabozantinibom in še 4 mesece po končanju terapije ne smejo dojiti. Zdravljenje s kabozantinibom lahko predstavlja tveganje za plodnost pri moških in ženskah. **INTERAKCIJE** Kabozantinib je substrat za CYP3A4. Pri sočasni uporabi močnih zaviralcev CYP3A4 (npr. ritonavirja, itrakonazola, eritromicina, klaritromicina, soka grenivke) je potrebna previdnost. Kronični sočasni uporabi močnih induktorjev CYP3A4 (npr. fenitoina, karbamazepina, rifampicina, fenobarbitala ali pripravkov zeliščnega izvora iz šentjanževke) se je treba izogibati. Razmisliti je treba o sočasni uporabi alternativnih zdravil, ki CYP3A4 ne inducirajo in ne zavirajo ali pa inducirajo in zavirajo le neznatno. Pri sočasni uporabi zaviralcev MRP2 (npr. ciklosporin, efavirenz, emtricitabin) je potrebna previdnost, saj lahko povzročijo povečanje koncentracij kabozantiniba v plazmi. Učinka kabozantiniba na farmakokinetiko kontraceptivnih steroidov niso preučili, vendar pa se priporoča dodatna kontracepcijska metoda (pregradna metoda). Zaradi visoke stopnje vezave kabozantiniba na plazemske beljakovine je možna interakcija z varfarinom v obliki izpodrivanja s plazemskih beljakovin, zato je treba spremljati vrednosti INR. Kabozantinib morda lahko poveča koncentracije sočasno uporabljenih substratov P-gp v plazmi. Osebe je treba opozoriti na uporabo substratov P-gp (npr. feksofenadina, aliskirena, ambrisentana, dabigatran eteksilata, digoksina, kolhicina, maraviroka, posakonazola, ranolazina, saksagliptina, sitagliptina, talinolola, tolvaptana) sočasno s kabozantinibom. **NEŽELENI UČINKI** Za popolno informacijo o neželenih učinkih, prosimo, preberite celoten povzetek glavnih značilnosti zdravila Cabometyx. Najpogostejši resni neželeni učinki zdravila v populaciji bolnikov s KLC so bili driska, hipertenzija, dehidracija, hiponatriemija, navzea, zmanjšanje apetita, embolija, utrujenost, hipomagneziemija in PPES. Najpogostejši neželeni učinki katere koli stopnje (ki so se pojavili pri vsaj 25 % bolnikov) v populaciji bolnikov s KLC so bili driska, hipertenzija, utrujenost, zvišanje vrednosti AST, zvišanje vrednosti ALT, navzea, zmanjšanje apetita, PPES, paragevzija, zmanjšanje števila trombocitov, stomatitis, anemija, bruhanje, zmanjšanje telesne mase, dispepsija in konstipacija. Najpogostejši resni neželeni učinki zdravila v populaciji bolnikov s HCK so bili jetrna encefalopatija, PPES, astenija in driska. Najpogostejši neželeni učinki katere koli stopnje (ki so se pojavili pri vsaj 25 % bolnikov) v populaciji bolnikov s HCK so bili driska, PPES, utrujenost, zmanjšanje apetita, hipertenzija in navzea. *Zelo pogosti (≥ 1/10):* anemija, hipotiroidizem, zmanjšan apetit, hipomagneziemija, hipokaliemija, paragevzija, glavobol, omotica, hipertenzija, krvavitev, disfonija, dispneja, kašelj, driska, navzea, bruhanje, stomatitis, konstipacija, bolečine v trebuhu, dispepsija, bolečina v zgornjem predelu trebuha, PPES, izpuščaj, bolečine v okončinah, utrujenost, vnetje sluznice, astenija, periferni edem, zmanjšanje telesne mase, zvišanje vrednosti ALT v serumu, zvišanje vrednosti AST. *Pogosti (≥ 1/100, < 1/10):* absces, trombocitopenija, nevtropenija, dehidracija, hipoalbuminemija, hipofosfatemija, hiponatriemija, hipokalciemija, hiperkaliemija, hiperbilirubinemija, hiperglikemija, hipoglikemija, periferna senzorična nevropatija, tinitus, venska tromboza, arterijska tromboza, pljučna embolija, gastrointestinalna perforacija, fistula, gastroezofagealna refluksna bolezen, hemoroidi, bolečina v ustni votlini, suha usta, jetrna encefalopatija, pruritus, alopecija, suha koža, akneiformni dermatitis, sprememba barve las oz. dlak, mišični krči, artralgija, proteinurija, zvišanje vrednosti ALP v krvi, GGT, kreatinina v krvi, amilaze, lipaze, holesterola v krvi, zmanjšanje števila belih krvnih celic. *Občasni (≥ 1/1.000, < 1/100):* limfopenija, konvulzije, pankreatitis, glosodinija, holestatični hepatitis, osteonekroza čeljusti, zvišanje vrednosti trigliceridov v krvi, zapleti z ranami. *Neznana pogostnost (ni mogoče oceniti iz razpoložljivih podatkov):* možganska kap, miokardni infarkt. **Vrsta ovojnine in vsebina:** Plastenka vsebuje 30 filmsko obloženih tablet. **Režim izdaje:** Rp/Spec **Imetnik dovoljenja za promet z zdravilom:** Ipsen Pharma, 65 quai Georges Gorse, 92100 Boulogne-Billancourt, Francija **Pred predpisovanjem, prosimo, preberite celoten povzetek glavnih značilnosti zdravila!**
CAB-121118

IPSEN
Innovation for patient care

PharmaSwiss
Choose More Life

SAMO ZA STROKOVNO JAVNOST
CAB0219-01, februar 2019

Odgovoren za trženje v Sloveniji:
PharmaSwiss d.o.o., Brodišče 32, 1236 Trzin
telefon: +386 1 236 47 00, faks: +386 1 283 38 10

RADIOLOGY AND ONCOLOGY

December 2019
Vol. 53 No. 4
Pages 373-496
ISSN 1318-2099
UDC 616-006
CODEN: RONCEM

Publisher
Association of Radiology and Oncology

Affiliated with
Slovenian Medical Association – Slovenian Association of Radiology, Nuclear Medicine Society,
Slovenian Society for Radiotherapy and Oncology, and Slovenian Cancer Society
Croatian Medical Association – Croatian Society of Radiology
Societas Radiologorum Hungarorum
Friuli-Venezia Giulia regional groups of S.I.R.M.
Italian Society of Medical Radiology

Aims and scope
Radiology and Oncology is a journal devoted to publication of original contributions in diagnostic and interventional radiology, computerized tomography, ultrasound, magnetic resonance, nuclear medicine, radiotherapy, clinical and experimental oncology, radiobiology, radiophysics and radiation protection.

Editor-in-Chief
Gregor Serša, Institute of Oncology Ljubljana, Department of Experimental Oncology, Ljubljana, Slovenia (Subject Area: Experimental Oncology)

Executive Editor
Viljem Kovač, , Institute of Oncology Ljubljana, Department of Radiation Oncology, Ljubljana, Slovenia (Subject Areas: Clinical Oncology, Radiotherapy)

Deputy Editors
Andrej Cör, University of Primorska, Faculty of Health Science, Izola, Slovenia (Subject Areas: Clinical Oncology, Experimental Oncology)
Maja Čemažar, Institute of Oncology Ljubljana, Department of Experimental Oncology, Ljubljana, Slovenia (Subject Area: Experimental Oncology)
Igor Kocijančič, University Medical Center Ljubljana, Institute of Radiology, Ljubljana, Slovenia (Subject Areas: Radiology, Nuclear Medicine)
Karmen Stanič, Institute of Oncology Ljubljana, Department of Radiation Oncology, Ljubljana, Slovenia (Subject Areas: Radiotherapy; Clinical Oncology)a
Primož Strojan, Institute of Oncology Ljubljana, Department of Radiation Oncology, Ljubljana, Slovenia (Subject Areas: Radiotherapy, Clinical Oncology)

Editorial Board

Subject Areas:
Radiology and Nuclear Medicine

Sotirios Bisdas, National Hospital for Neurology and Neurosurgery, Department of Neuroradiology, London, UK
Karl H. Bohuslavizki, Nuklearmedizin Spitalerhof, Hamburg, Germany
Boris Brkljačić, University Hospital "Dubrava", Department of Diagnostic and Interventional Radiology, Zagreb, Croatia
Maria Gődény, National Institute of Oncology, Budapest, Hungary
Gordana Ivanac, University Hospital Dubrava, Department of Diagnostic and Interventional Radiology, Zagreb, Croatia
Damir Miletić, Clinical Hospital Centre Rijeka, Department of Radiology, Rijeka, Croatia
Katarina Šurlan Popovič, University Medical Center Ljubljana, Clinical Institute of Radiology, Ljubljana, Slovenia
Jernej Vidmar, University Medical Center Ljubljana, Clinical Institute of Radiology, Ljubljana, Slovenia

Subject Areas:
Clinical Oncology and Radiotherapy

Luca Campana, Veneto Institute of Oncology (IOV-IRCCS), Padova, Italy
Christian Dittrich, Kaiser Franz Josef - Spital, Vienna, Austria
Dirk Rades, University of Lubeck, Department of Radiation Oncology, Lubeck, Germany
Luka Milas, UT M. D. Anderson Cancer Center, Houston, USA
Csaba Polgar, National Institute of Oncology, Budapest, Hungary
Mirjana Rajer, University Clinic of Pulmonary and Allergic Diseases Golnik, Golnik, Slovenia
Luis Souhami, McGill University, Montreal, Canada
Borut Štabuc, University Medical Center Ljubljana, Division of Internal Medicine, Department of Gastroenterology, Ljubljana, Slovenia
Andrea Veronesi, Centro di Riferimento Oncologico- Aviano, Division of Medical Oncology, Aviano, Italy
Branko Zakotnik, Institute of Oncology Ljubljana, Department of Medical Oncology, Ljubljana, Slovenia
Serena Bonin, University of Trieste, Department of Medical Sciences, Cattinara Hospital, Surgical Pathology Blg, Molecular Biology Lab, Trieste, Italy

Subject Area:
Experimental Oncology

Metka Filipič, National Institute of Biology, Department of Genetic Toxicology and Cancer Biology, Ljubljana, Slovenia
Janko Kos, University of Ljubljana, Faculty of Pharmacy, Ljubljana, Slovenia
Tamara Lah Turnšek, National Institute of Biology, Ljubljana, Slovenia
Damijan Miklavčič, University of Ljubljana, Faculty of Electrical Engineering, Ljubljana, Slovenia
Geoffrey J. Pilkington, University of Portsmouth, Institute of Biomedical and Biomolecular Sciences, School of Pharmacy and Biomedical Sciences, Portsmouth, UK
Justin Teissié, CNRS, IPBS, Toulouse, France
Gillian M. Tozer, University of Sheffield, Academic Unit of Surgical Oncology, Royal Hallamshire Hospital, Sheffield, UK

Subject Area: Radiophysics

Robert Jeraj, University of Wisconsin, Carbone Cancer Center, Madison, Wisconsin, USA
Häkan Nyström, Skandionkliniken, Uppsala, Sweden
Ervin B. Podgoršak, McGill University, Medical Physics Unit, Montreal, Canada
Matthew Podgorsak, Roswell Park Cancer Institute, Departments of Biophysics and Radiation Medicine, Buffalo, NY ,USA

Advisory Committee
Tullio Giraldi, University of Trieste, Faculty of Medicine and Psyhology, Department of Life Sciences, Trieste, Italy
Vassil Hadjidekov, Medical University, Department of Diagnostic Imaging, Sofia, Bulgaria
Marko Hočevar, Institute of Oncology Ljubljana, Department of Surgical Oncology, Ljubljana, Slovenia
Miklós Kásler, National Institute of Oncology, Budapest, Hungary
Maja Osmak, Ruder Bošković Institute, Department of Molecular Biology, Zagreb, Croatia
Tomaž Benulič, Institute of Oncology Ljubljana, Department of Radiation Oncology, Ljubljana, Slovenia

Editorial office

Radiology and Oncology
Zaloška cesta 2
P. O. Box 2217
SI-1000 Ljubljana
Slovenia
Phone: +386 1 5879 369
Phone/Fax: +386 1 5879 434
E-mail: gsersa@onko-i.si

Copyright © Radiology and Oncology. All rights reserved.

Reader for English
Vida Kološa

Secretary
Mira Klemenčič
Zvezdana Vukmirović

Design
Monika Fink-Serša, Samo Rovan, Ivana Ljubanović

Layout
Matjaž Lužar

Printed by
Tiskarna Ozimek, Slovenia

Published quarterly in 400 copies

Beneficiary name: DRUŠTVO RADIOLOGIJE IN ONKOLOGIJE
Zaloška cesta 2
1000 Ljubljana
Slovenia

Beneficiary bank account number: SI56 02010-0090006751
IBAN: SI56 0201 0009 0006 751
Our bank name: Nova Ljubljanska banka, d.d.,
Ljubljana, Trg republike 2,
1520 Ljubljana; Slovenia

SWIFT: LJBASI2X

Subscription fee for institutions EUR 100, individuals EUR 50

The publication of this journal is subsidized by the Slovenian Research Agency.

Indexed and abstracted by:

- *Baidu Scholar*
- *Case*
- *Chemical Abstracts Service (CAS) - CAplus*
- *Chemical Abstracts Service (CAS) - SciFinder*
- *CNKI Scholar (China National Knowledge Infrastructure)*
- *CNPIEC - cnpLINKer*
- *Dimensions*
- *DOAJ (Directory of Open Access Journals)*
- *EBSCO (relevant databases)*
- *EBSCO Discovery Service*
- *Embase*
- *Genamics JournalSeek*
- *Google Scholar*
- *Japan Science and Technology Agency (JST)*
- *J-Gate*
- *Journal Citation Reports/Science Edition*
- *JournalGuide*
- *JournalTOCs*
- *KESLI-NDSL (Korean National Discovery for Science Leaders)*
- *Medline*
- *Meta*
- *Microsoft Academic*
- *Naviga (Softweco)*
- *Primo Central (ExLibris)*
- *ProQuest (relevant databases)*
- *Publons*
- *PubMed*
- *PubMed Central*
- *PubsHub*
- *QOAM (Quality Open Access Market)*
- *ReadCube*
- *Reaxys*
- *SCImago (SJR)*
- *SCOPUS*
- *Sherpa/RoMEO*
- *Summon (Serials Solutions/ProQuest)*
- *TDNet*
- *Ulrich's Periodicals Directory/ulrichsweb*
- *WanFang Data*
- *Web of Science - Current Contents/Clinical Medicine*
- *Web of Science - Science Citation Index Expanded*
- *WorldCat (OCLC)*

This journal is printed on acid- free paper

On the web: ISSN 1581-3207
https://content.sciendo.com/raon
http://www.radioloncol.com

contents

clinical oncology

radiophysics

slovenian abstracts

review

The multidisciplinary team for gastroenteropancreatic neuroendocrine tumours: the radiologist's challenge

Vincenza Granata[1], Roberta Fusco[1], Sergio Venanzio Setola[1], Elisabetta de Lutio di Castelguidone[1], Luigi Camera[2], Salvatore Tafuto[3], Antonio Avallone[3], Andrea Belli[4], Paola Incollingo[5], Raffaele Palaia[4], Francesco Izzo[4], Antonella Petrillo[1]

[1] Division of Radiology, "Istituto Nazionale Tumori IRCCS Fondazione Pascale – IRCCS di Napoli", Naples, Italy
[2] Division of Radiology, "Università degli Studi di Napoli Federico II", Naples, Italy
[3] Division of Gastrointestinal Oncology, "Istituto Nazionale Tumori IRCCS Fondazione Pascale – IRCCS di Napoli", Naples, Italy
[4] Division of Hepatobiliary Surgical Oncology, "Istituto Nazionale Tumori IRCCS Fondazione Pascale – IRCCS di Napoli", Naples, Italy
[5] Operative Unit of Genaral surgery and Kidney Transplantation, Advanced Biomedical Science Department University Federico II of Naples, Italy

Radiol Oncol 2019; 53(4): 373-387.

Received 30 March 2019
Accepted 15 July 2019

Correspondence to: Dr. Roberta Fusco, Department of Radiology, Istituto Nazionale Tumori Fondazione G. Pascale. Phone: +390 81 590 714; Fax: +390 815 903 825; E-mail: r.fusco@istitutotumori.na.it

Disclosure: No potential conflicts of interest were disclosed.

Background. Gastroenteropancreatic neuroendocrine tumours (GEP-NETs) are a heterogeneous group of tumours. An effective diagnosis requires a multimodal approach that combines evaluation of clinical symptoms, hormonelevels, radiological and nuclear imaging, and histological confirmation. Imaging plays a critical role in NETs diagnosis, prognosis and management, so the radiologists are important members of the multidisciplinary team. During diagnostic work-up two critical issues are present: firstly the need to identify tumor presence and secondly to define the primary site and assess regional and distant metastases.

Conclusions. The most appropriate imaging technique depends on the type of neuroendocrine tumour and the availability of specialized imaging techniques and expertise. There is no general consensus on the most efficient imaging pathway, reflecting the challenge in reliably detection of these tumours.

Key words: neuroendocrine tumours; ultrasound; contrast-enhanced ultrasound; computed tomography; magnetic resonance imaging

Introduction

Gastroenteropancreatic neuroendocrine tumours (GEP-NETs) are a heterogeneous group of tumours, arising from neuroendocrine cells present in the gastrointestinal tract and into the islets of Langerhans of the pancreas.[1] Thanks to their capability to synthesize and secrete peptides and hormones, these tumours can cause clinical syndromes, although more often may be asymptomatic and discovered as an incidental finding.[2] Functioning tumours usually reveal themselves relatively early, so it might be difficult for the radiologist to localize the lesions since they are often too small to be detected. Non-functioning tumours generally present non-specific symptoms and frequently manifest as locally advanced or metastatic desease. The neuroendocrine tumour of the gastroenterict tract can cause vague abdominal symptoms and may be diagnosed as an irritable bowel syndrome (IBS).[3] Between 60% and 90% of GEP-NETs of pancreas (p-NETs) are non-functioning tumors, so they can be diagnosed at advanced stages because of their relatively indolent nature and slow

growth.[4] The diagnosis of functional (F)-p-NETs is clinical with laboratory test that should confirm the hypothesis. An effective diagnosis of NET requires a multimodal approach that combines evaluation of clinical symptoms, hormone levels, radiological and nuclear imaging, and histological confirmation.[3] Imaging plays a critical and indispensable role in NETs diagnosis, prognosis and management; therefore radiologists are important members of the multidisciplinary NET team.[5] Two critical issues are present in diagnostic work-up of NETs: firstly the need to identify tumor presence and secondly to define the primary site and assess regional and distant metastases.[6] In fact, primary site, stage, grade and functionality are prognostic factors that the radiologist should assess in order toguide prognosis and management.[6-7] Although imaging itself is not able to discriminate between a functioning and a non-functioning NET, the imaging identification of a large tumor burden in a patient without specific symptoms strongly suggests a non-functional tumor (Figure 1). Functional imaging can also suggest tumor grade.[7] The most appropriate imaging technique depends on the type of neuroendocrine tumour and the availability of specialized imaging techniques and expertise.[8]

Anatomical and functional imaging

Imaging modalities can be anatomic, which assess the physical characteristics of the tissue, or functional, which assess the biochemical characteristics.[7] The increase of knowledge about these tumours andNETs' characteristic of expressing somatostatin receptors (SSTRs) make them target of specific therapy (target therapy) and functional imaging. Currently, five main subtypes of SSTR have been identified (SSTR-1, SSTR-2A and SSTR-2B, SSTR-3, SSTR-4, and SSTR-5). SSTR-2 is the predominantly expressed one. The expression of SSTR is especially high in well-differentiated NETs compared to poorly differentiated ones.[9-10] In this scenario, molecular imaging techniques, with the ability to acquire informations on the SSR expression, have a pivotal role in diagnosis, staging, treatment selection and follow-up of NETs.[11] However, the technique should always be complemented with computed tomography (CT) or magnetic resonance imaging (MRI), inasmuch as these tecniques allow the exact identification of the tumor site, vascular and or biliary involvement and detection of metastatic disease, all parameters that impact on surgical planning and prediction of the response to treatment.[11-12]

The European Neuroendocrine Tumor Society (ENETS) has proposed a tumor–node–metastasis staging and grading system for various types of GEP-NETs.[4,5,13-19] Preoperative staging should include, whenever possible, somatostatin receptor scintigraphy (SSRS).[11] Although SSRS is highly efficient for whole-body imaging, detection of lesions is difficult in organs with intense physiologic uptake, with low receptors' density, or small size. 68Ga-DOTATATE PET/CT is more efficient than SSRS to evaluate small NET lesions, also considering that the affinity of 68Ga-DOTATATE to bind somatostatin receptor 2 is higher than 111In-octreotide's one.[20] However, the higher costs and the 68Ga generators limitated availability to specialized centers, due to the short half-life of 68Ga that requires in-house labelling of the tracer, still remain impediments to its routine use in clinical care.[21] MRI of the liver is complementary to 68Ga-DOTATATE PET/CT and is highly recommended

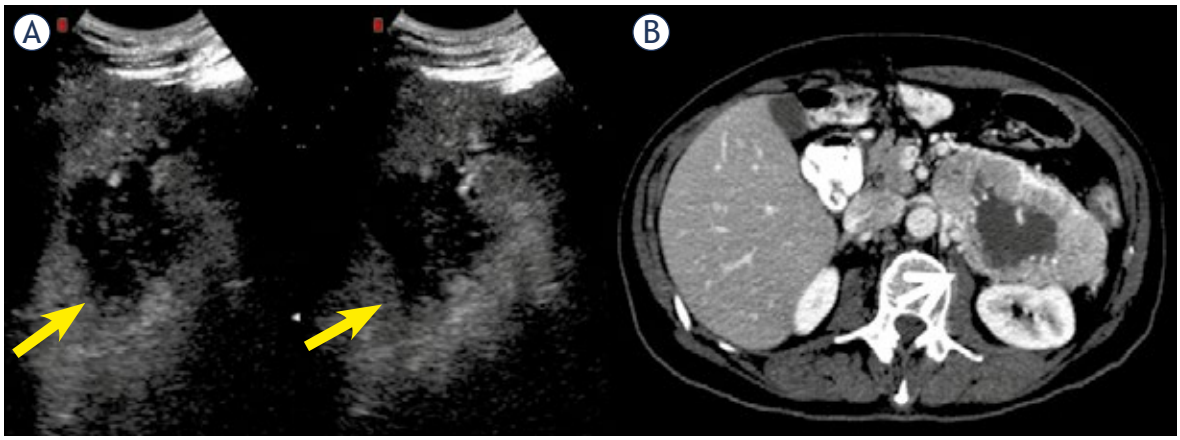

FIGURE 1. A 45 yrs old female: CEUS study of inhomogeneous pancreatic lesion **(A)**, with necrotic central area (arrow). CT **(B)**, during late arterial phase of contrast study shows the same vascular profile (arrow) seeing during CEUS study.

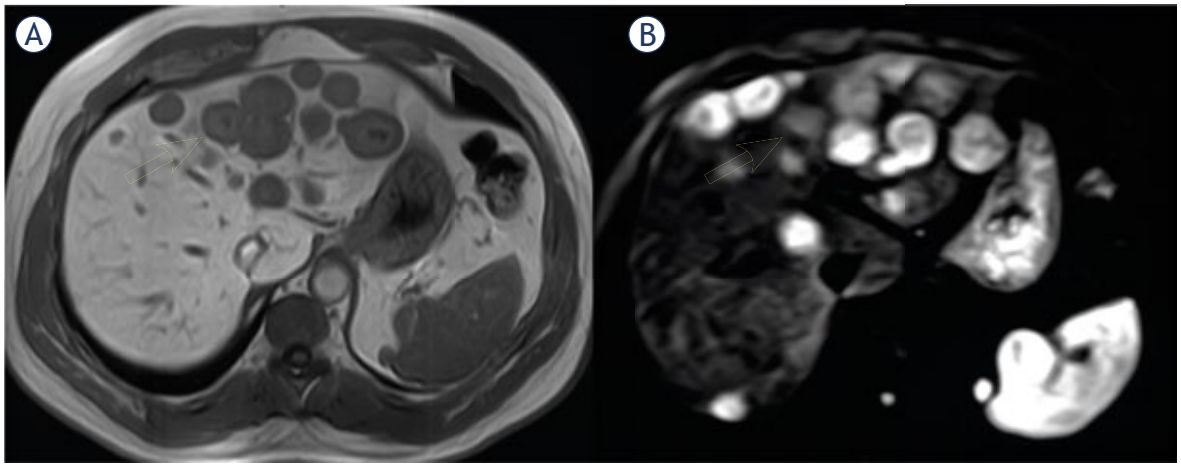

FIGURE 2. A 64 yrs old male with pancreatic NET. Liver metastases in IV, II and III segment, with a "target" appearance (arrow) during hepatobiliary phase of EOB-MR study **(A)** and restricted diffusion (arrow) on b800 s/mm^2**(B)**.

before any liver surgery and for monitoring liver metastases (Figure 2).[11]

The optimization of imaging techniques

The optimization of techniques is mandatory to assess GEP-NETs patients. CT is a widely available technique with high spatial and temporal resolution. Therefore, it represents the most common initial tool to assess suspected abdominal lesions. Contrast-enhanced CT protocols are mandatory for NET imaging. To achieve a good separation of the contrast phases, short scan times and high flow rates of the contrast agent (above 3 ml/s) should be used. Scans before contrast (calcifications), in the arterial phase (typical NET enhancement) and the portal phase should be carried out. Correct timing of the arterial phase is crucial for successful NET imaging. As GEP-NETs and their metastases are often hypervascular, they are easily detected in the early arterial phase of contrast study protocol (Figure 3).[21] For small-bowel tumors, CT enterography or enteroclysis can be performed.[23] The performance of CT is related to the study protocol, as well as the lesion size, location, and contrast with the surrounding tissue.[24,25] MR imaging offers higher intrinsic soft-tissue contrast[22]; moreover, recent advances in the hardware and software have also improved the spatial resolution and acquisition time for each sequence, resulting in shorter breath holds. Furthermore, MR imaging does not use ionizing radiation. Thanks to its capability to provide functional data by diffusion weighted imaging (DWI) and dynamic contrast-enhanced (DCE) imaging, MRI is a valuable tool in oncologic patient as perfusion dual energy CT.[26-30] However,

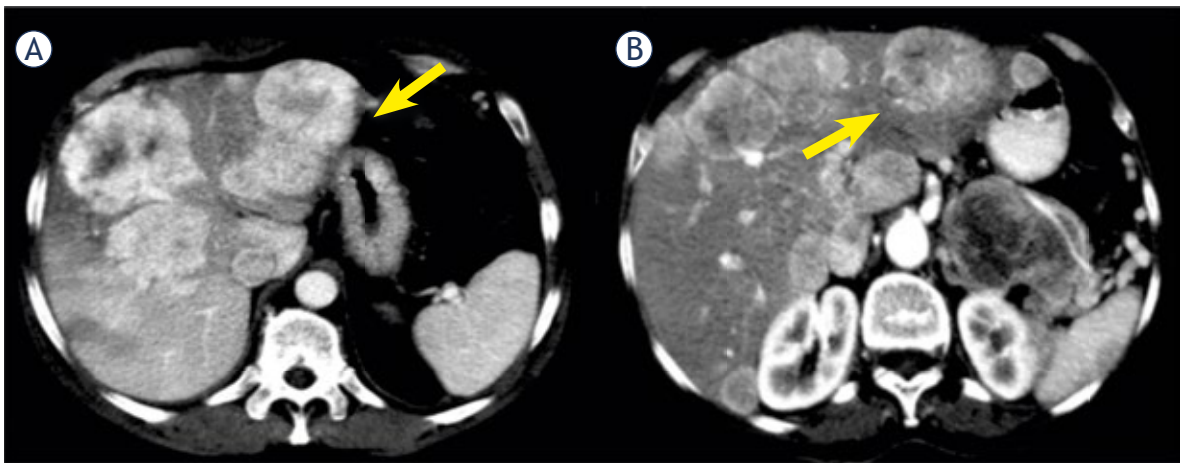

FIGURE 3. A 52 yrs old female with pancreatic NET. Liver metastases show hypervascular appearance (arrow) during arterial phase of contrast study on CT **(A, B)**.

MR imaging is less readily available, is more expensive, and often requires more time and patient cooperation.[22] MR abdominal acquisition protocols for NET imaging should include T1-weigthed and T2-weighted sequences and multiphase contrast enhancement studies, including unenhanced, arterial, venous and delayed phases Nowadays, the inclusion of DWI for the upper abdomen seems to be indispensable.[22] DWI is a relatively mature non-invasive imaging modality that could display functional information without contrast media.[22] DWI signal depends on the water mobility that reflects indirectly tissue biological characteristics. DWI has been applied to liver imaging as an excellent tool for detection and characterization of lesions, increasing clinical confidence and decreasing false positives.[22] Oncology is one of the main fields of application of DWI.[22] Water mobility is restricted in malignant tissue due to the increase of cellular density. Diffusion is quantified by ADC diffusion coeficient. The ADC map is the graphical representation of the ratio of DW signal intensities and its measurements may discriminate between benign and malignant lesions. The ADC measurements are related to the sequence acquisition protocol and suffer from a lack of reproducibility, especially in respiratory triggering techniques.[22] The main technical limits of MR imaging are costs, lack of availability and long examination time.[12]

Detection and localization of the primary tumour

Gastroduodenal neuroendocrine neoplasms

According to Delle Fave *et al.*, gastric neuroendocrine neoplasms (g-NENs) represent the most frequent digestive NENs and are increasingly recognized due to expanding indications of upper gastrointestinal endoscopy.[14] G-NENs may be divided into three types: type 1 and 2 are ECLomas, due to chronic hypergastrinemia, respectively associated with chronic atrophic gastritis (CAG) and Zollinger-Ellison's syndrome; type 3 g-NENs are rare and sporadic tumors not consequent to underlying gastric mucosal abnormality, the latter are mostly single large lesions with high metastatic potential and with high grade (often G3 NEC).[14] Duodenal neuroendocrine neoplasms (d-NENs) may be sporadic or associated with multiple endocrine neoplasia type 1 (MEN-1) and may present with a functional syndrome.[14] Gastroscopy and endoscopic US (EUS) are essential to localize the primary lesion and usually sufficient in small Type I and II g-NENs. Furthermore, the invasiveness of the gastric wall can be assessed with a EUS.[31] In gastric tumours larger than 1 cm and duodenal NETs, EUS is used to detect invasion and regional lymph node metastases.[32] For invasive gastric NETs, all Type III tumours and duodenal NETs staging is performed by CT and MRI.[14]

Ileal NETs

Ileal NETs are usually sporadic and multiple in 26%–30% of cases.[33] At the time of diagnosis hepatic metastases are already present in 20% of cases.[34-36] The lesion is indolent with non-specific symptoms (vague pain, bleeding, intermittent partial bowel obstruction). The classic carcinoid syndrome is present in 6%–30% of patients, and it is associated with hepatic metastases in more than 95% of cases.[37] CT or MR scan are often the preferred imaging tests, and small-bowel distention (enterography or enteroclysis) is desirable. The lesions are small, hypervascular, polypoid; high lesions can appear as asymmetric or concentric bowel wall thickening (Figure 4).[22] More often the radiologist easily detects secondary features, such as desmoplastic reaction in the mesentery and lymphadenopathy with or without calcification, these features are re-

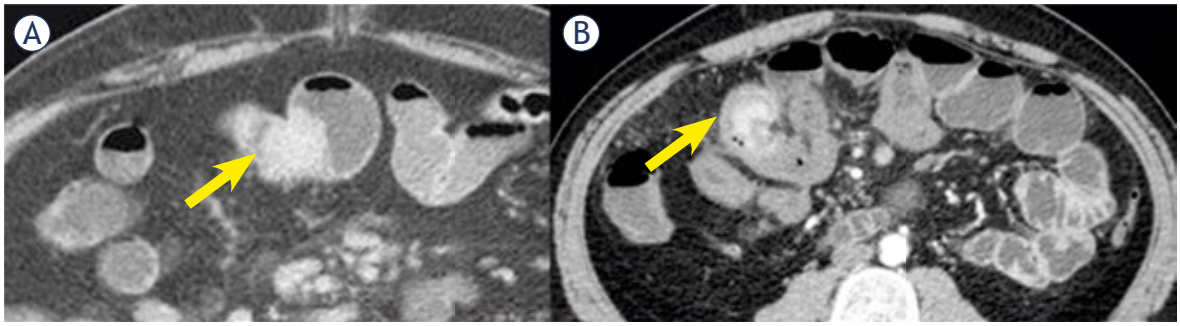

FIGURE 4. A 41 yrs old male. CT enteroclysis examination shows lesion, in **(A)**, as small, hypervascular, polypoid (arrow) and, in **(B)**, as an asymmetric bowel wall thickening (arrow).

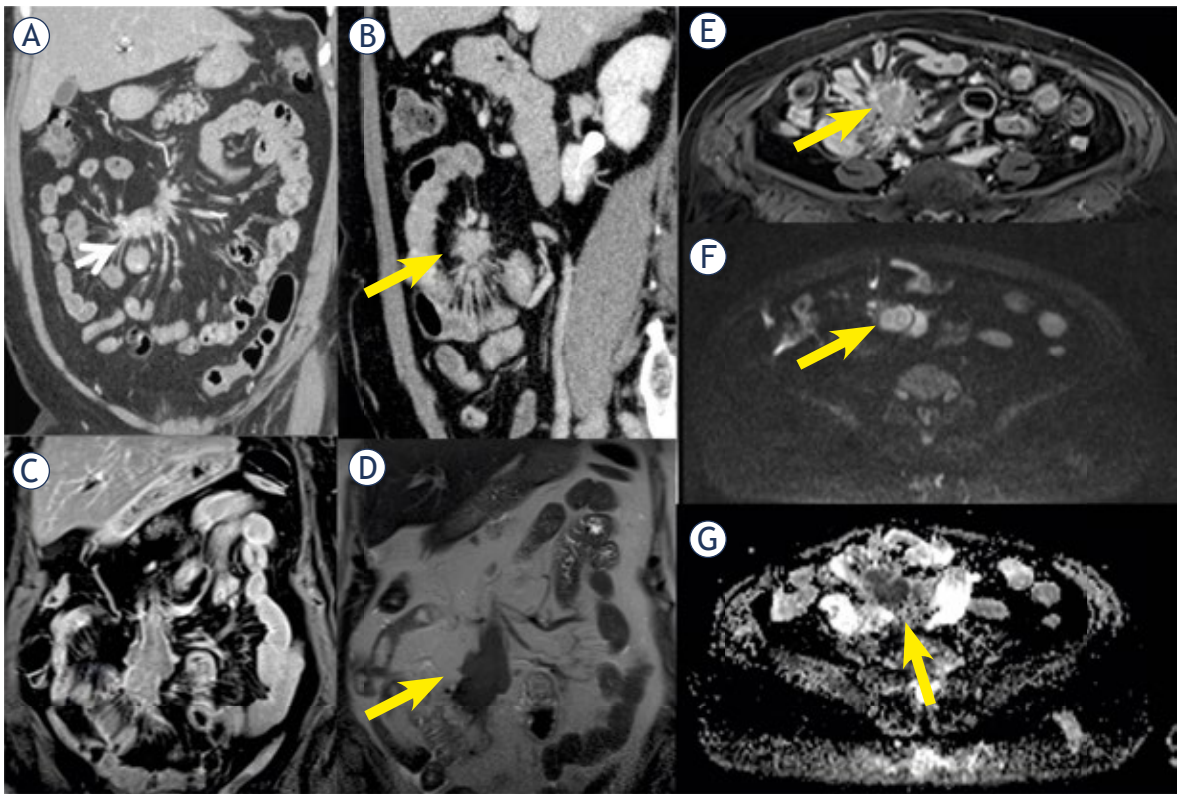

FIGURE 5. A 48 yrs old male with ileal net. CT during portal phase shows **(A**, coronal plane and **B** sagittal plane) desmoplastic reaction in the mesentery and lymphadenopathy (arrow); these features in T1-W post contrast study **(C** and **E** portal phase) show hypointense signal (arrow) and hypintense signal (arrow) in T2- W sequence **(D)** with restricted diffusion (arrow) in b800 s/mm^2 **(F)** and hypointense signal in ADC **(G)** map.

lated to the presence of the primary lesion in the neighboring small-bowel (Figure 5). Some times, the radiologists work in emergency setting with the patient affected by a bowel obstruction, intussusception or ischemia due to desmoplastic response compromising bowel lumen or mesenteric circulation.[12,22,24] Some researches have shown that CT enterography and MR enteroclysis improved sensitivity (100% and 86%–94%, respectively) and specificity (96.2% and 95%– 98%, respectively) for tumor diagnosis.[23,38-40] In addition, MR enterography (MRE) is one of the few imaging modalities that can provide an accurate evaluation of the small-bowel loops, as well as the whole abdominal cavity, without any radiation exposure and at reasonable healthcare costs. Owing to the undoubted advantages, it is realistic to look with a fresh eye at MRE, beyond the well-established role in the intestinal assessment of Crohn's disease (CD) patients. According to ENETS guidelines enteroclysis is beneficial to assess small bowel in patients with NET, in case of failure of CT scan in the localization ofthe primary tumour.[18] Nowadays, thanks to the increasing use of 68Ga-DOTATOC-PET/CT the primary small bowel NET is more frequently detected.[18]

The appendix is the site of GEP- NETs in about 20% of cases, and up to 70% of cases are discovered at appendectomy.[41] These lesions are small and metastases to regional lymph nodes are uncommon, therefore, rarely detected on the basis of imaging findings.[41]

Colorectal NET

Neuroendocrine tumors of the colon are very rare. They involve more commonly the right colon and appear as large lesions (5 cm or more), already metastatic at the time of diagnosis.[36] Rectal NEN are more common than colonic NEN, representing about 11% of all GEP-NET.[36] They are usually small and generally from low to intermediate grade.[19] Typically, rectal NET are single, sub-mucosal tumors, smaller than 1 cm. Metastases occur in tumors larger than 2 cm.[22] EUS evaluates the depth of tumor invasion in the rectal wall and regional

lymph nodes.[42] MR examination is increasingly used to assess local tumor spread and nodes involvement, and to guide surgical management for lesion larger than 1 cm.[19,43] For lesion larger than 2 cm or those with rectal wall invasion on EUS, the spread of disease should be assessed using CT. SRS is not routinely recommended in rectal NETs smaller than 2 cm without invasion of the muscularis propria.[43]

Pancreatic NET

PNETs are the second most common pancreatic cancer, exhibiting a heterogeneous spectrum of clinical symptoms and behaviors.[44] Between 60% and 90% of p-NETs are non-functional and are generally diagnosed at more advanced stages.[4] Imaging is fundamental during the work-up of these patients, for the detection of the primary tumor, its characterization and prognosis determination, for the local and distant assessment, as well as for the evaluation of treatment.[44] Functioning PNETs are generally small (1–2 cm) and manifest as well-defined, hypervascular lesions, owing to their rich capillary network. Non-functioning tumors are larger in size (4 cm) at the time of detection, often well defined, encapsulated and show a heterogeneous enhancement. Rarely, they can be completely cystic, with a hypervascular rim in up to 90% of cases. Malignant tumors often show local invasion into the retroperitoneum and metastases (regional nodes and liver), and they can rarely involve the main pancreatic duct.[22] According to ENETS guideline, PET/CT with 68Ga-labelled somatostatin analogs DOTA-TOC/TATE/NOC is now the method of choice to localize and stage the disease in non-insulinoma P-NETs patients.[4] In addition, functional imaging plays a role in targeted therapy selection.[22] In case of rapid tumor growth in earlier diagnosed G1-G2 tumors, 18-FDG-PET/CT may be considered for the assessement of tumor burden and prognosis.[4] In a small percentage of patients with insulinomas (<5–10%) all conventional imaging studies are negative. Receptor scintigraphy with radio-labelled Glucagon-like peptide-1 (GLP-1) receptor's analogues is a sensitive method to detect insulinomas as they frequently overexpresses this receptor.[4] Unfortunately this method is not routinely available anywhere and it has been mainlyused in research applications. The preoperative imaging assessment of p-NET may establish the anatomical position of the lesion, its relation to the pancreatic duct and the main bile duct, as well as, encasement of the hepatic, splenic and mesenteric artery and vein and the portal vein. When MRI is performed, MR cholangiopancreatography should be included (Figure 6).[45]

EUS is the most advantageous imaging technique to detect pNETs with a sensitivity mean of the 90% (range 77–100%). For insulinomas, the sensitivity is less (84%).[4] Some researches showed that EUS improves sensitivity for the detection of small tumours and multiple lesions in MEN1 or VHL syndromes compared to CT or MRI.[46,47] The primary aims of EUS are to guide a biopsy in order to obtain a tissue sample and also to guide the decision-making process between an enucleation and a Whipple's procedure.[48]

CT is the first-line imaging modality employed in the evaluation of patients with suspected PNETs, allowing the study of the pancreas as well as the assessment of the disease extension. The study protocol should consist of a multiphase imaging, including unenhanced, arterial/pancreatic, venous and delayed phase. The late arterial (30 s) or pancreatic phase (40 s) is mandatory in order to increase the detection of small functioning PNET, in particular insulinoma. Moreover, it also increases the detection of hepatic metastases and assesses the encasement of the hepatic, splenic and mesenteric artery. The venous phase allows to assess the hepatic parenchyma and the encasement of mesenteric and portal vain. The delayed phase is complementary of the all other phases, allowing the detection of delayed enhancement presented by some fibrous tumors.[44] PNETs are expected to be hypervascular, and benign tumours show a homogenous hypervascular pattern followed by early wash-out in the venous phase.[49] Progression towards malignancy is associated with derangement in vessel architecture and function. Although these tumours remain hypervascular, their anarchic vasculature reflects into their less homogenous CEP; delayed contrast enhancement may be considered as a sign of malignancy in pNETs.[50,51] Cappelli *et al.*[49] showed that CEP might preoperatively suggest the behavior of pNETs. Even Takumi *et al.*[52] assessed the relation between contrast-enhanced computed tomography features and tumour aggressiveness, showing that non-hyperattenuating P-NETs during the venous phase were suggestive of G2. In the quantitative analysis, tumor contrast enhancement and tumor-to-pancreas contrast during the venous phase were significantly higher in G1 than in G2 tumors.[52] To improve the conspicuity of pancreatic tumor and reduce radiation dose, Marin *et al.*[53] assessed the low-tube-voltage, high-tube-current CT technique, demonstrating that it improves the enhancement

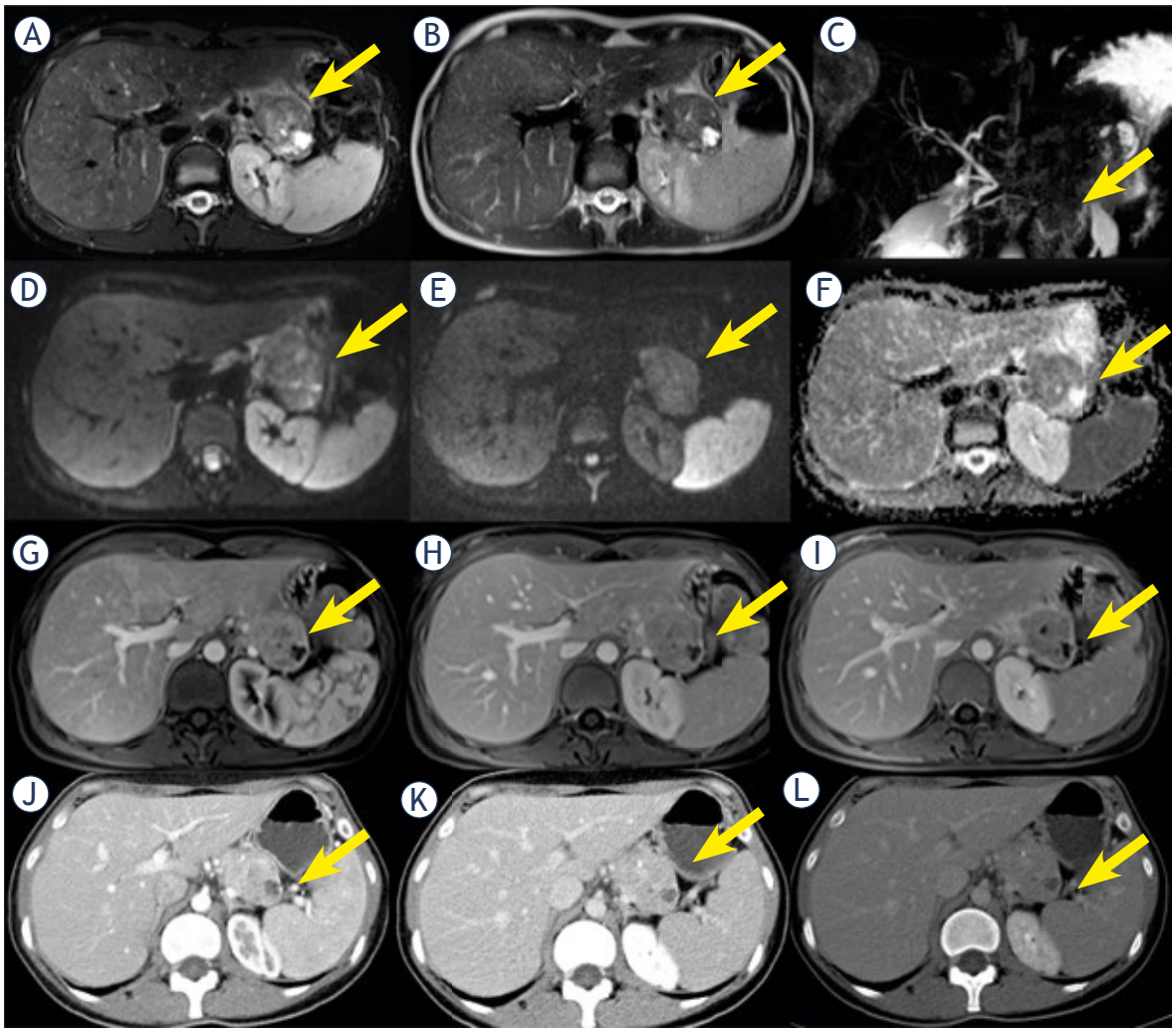

FIGURE 6. A 29 yrs old female with p-Net of pancreatic tail. The lesion shows inhomogeneous signal with cystic component (arrow) on T2-W sequences **(A, B)**. MR cholangiopancreatography **(C)** sequence show its relation to the pancreatic duct and the main bile duct (arrow). The lesion shows restricted diffusion **(D, E, F)** and inhomogeneous contrast enhancement during arterial **(G, J)**, venus **(H, K)** and late **(I, L)** phase as in MR as in CT (arrow).

of the pancreas and peripancreatic vasculature, increasing tumor conspicuity and reducing patient's radiation dose. The use of dual energy CT (DECT) has potential clinical implications for pancreas imaging.[54] However, there are limited data assessing the utility of DECT for other pancreatic masses excluding adenocarcinomas.[55] Potential benefits include the evaluation of enhancement in neuroendocrine tumours. DECT has shown a higher sensitivity for the detection of pancreatic insulinomas compared to conventional CT (95.7 *vs.* 68.8%).[56]

MRI shows higher diagnostic accuracy than CT. For MRI the sensitivity is 93% (range 85–100%) and specificity 88% (range 75–100%).[57] In a recent study, the sensitivity of MRI was similar to that of EUS 95%.[58] The advantages of MRI over CT are:the lack of ionizing radiation and the utilization of gadolinium chelate contrast agents, which have a better safety profile in terms of allergic reactions. Moreover, MRI provides functional data extracted by DWI to evaluate the distribution of water molecules in the interstial space and the blood motion in the capillaries.[59] MR imaging protocol should include: T1-Weigthed (T1-W) and T2-Weigthed (T2-W) sequences, dynamic three-dimensional (3D) sequences before and after cm multi arterial, venous and delayed (> 5 min) acquisitions, DWI and cholangiopancreatic sequences.[44,58] DWI increases the sensitivity for detection of the lesion as well as of the liver metastases. The Apparent Diffusion Coefficient (ADC) value has been recently identified as biomarker of tumor aggressiveness related

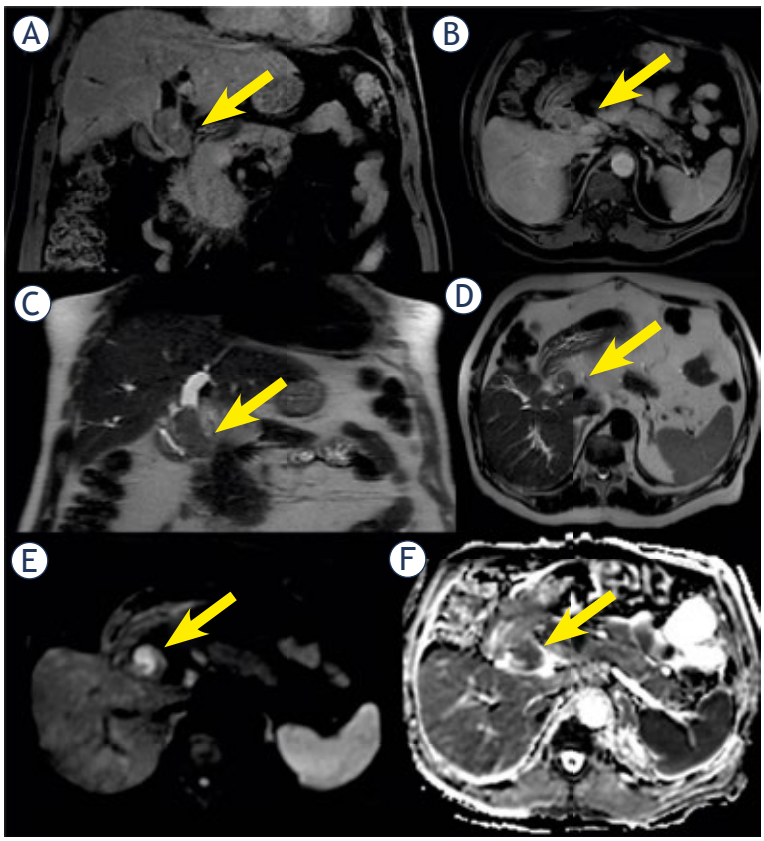

FIGURE 7. A 58 yrs old male wih primitive NET of biliary tree. The lesion shows hypointense signal (arrow) during portal phase of contrast study **(A, B)**, hyperintense signal (arrow) on T2-W sequences **(C, D)** and restricted diffusion (arrow) on DW sequences **(E, F)**.

to the histological grade of PNET: low ADC is a strong predictor of high tumor grade.[44,58] MR cholangiopancreatography, assessing the involvement of the biliary and pancreatic ducts, is useful in the surgical planning and should always precede resection of a pancreatic NET.[58] Hypervascular tumors (typically insulinomas) are often better depicted in T2W with fat suppression sequences, whereas hypovascular tumors are better depicted in T1-W sequences during the arterial phase.[22] Wang *et al.* assessed an inverse correlation between tumor's Ki-67 index on pathology and ADC values, supporting the role of DWI in predicting tumor biology.[60] DCE-MRI should be used to assess microvascular structures.[61,62] The DCE-MRI can be assessed semi-quantitatively or quantitatively. Bol *et al.*[63] evaluated the role of DCE-MRI to assess the therapy in a murine model, showing that DCE-MRI-derived parameters predict peptide uptake better than the "contrast amount-related" parameters. Consequently, DCE-MRI elucidates the correlation between vascular characteristics, peptide delivery and therapy efficacy, and may predict targeting efficiency.[63] Huh *et al.*[64] tested, in a clinical study, DCE-MRI for pancreatic lesions, showing that between pancreatic adenocarcinomas and neuroendocrine tumours, there were significant differences in the Ktrans (0.073 ± 0.058 *vs.* 0.308 ± 0.062, respectively; $p = 0.007$) that represent the contrast rate between the vascular space and the extracellular extravascular space and initial area under time intesitu curve (iAUC) (1.501 ± 0.828 *vs.* 3.378 ± 0.378, respectively; $p = 0.045$).[64] Furthermore, the quantitative values of Ktrans and the contrast rate between the extracellular extravascular space and the vascular space (kep), are helpful for differentiating G2 NET from G1 ones.[65]

Recently, the term of "Radiomics" has been introduced to define a mathematical process to extract innumerable quantitative features from medical images (including each diagnostic technique) with high-throughput computing for diagnosis and prediction.[66] Compared to traditional visual interpretation of medical images, the deep mining of medical images by computer technology from radiomics makes features uptake more efficient, relatively objective and rich in features types. Radiomics is promising for tumor screening, early diagnosis, accurate grading and staging, treatment and prognosis, molecular characteristics and so on.[66,67] De Robertis *et al.* assessed MRI derived whole-tumour histogram analysis parameters in predicting pNEN grade and aggressiveness.[68] They showed that whole-tumour histogram analysis of ADC maps might be helpful in predicting tumour grade, vascular involvement, nodal and liver metastases in panNENs. $ADC_{entropy}$ and $ADC_{kurtosis}$ are the most accurate parameters for identification of panNENs with malignant behaviour.[68]

According to ENETs Consensus Guidelines, CEUS is the suggested technique for the diagnosis of neuroendocrine neoplasms.[4] Although CEUS is not indicated for the detection of focal solid or cystic pancreatic lesions, it improves the characterization of nodules detected on US.[69] So that,according to recommendation 26 of EFSUMB Guidelines, CEUS can be used to distinguish between pancreatic ductal adenocarcinomas and neuroendocrine tumors (Figure 1).[69]

Liver involvement

Primary hepatic NET

Primary hepatic NETS (PHNETs) are extremely rare. When a NET is detected in the liver, great care must be taken to exclude metastasis from an extra-

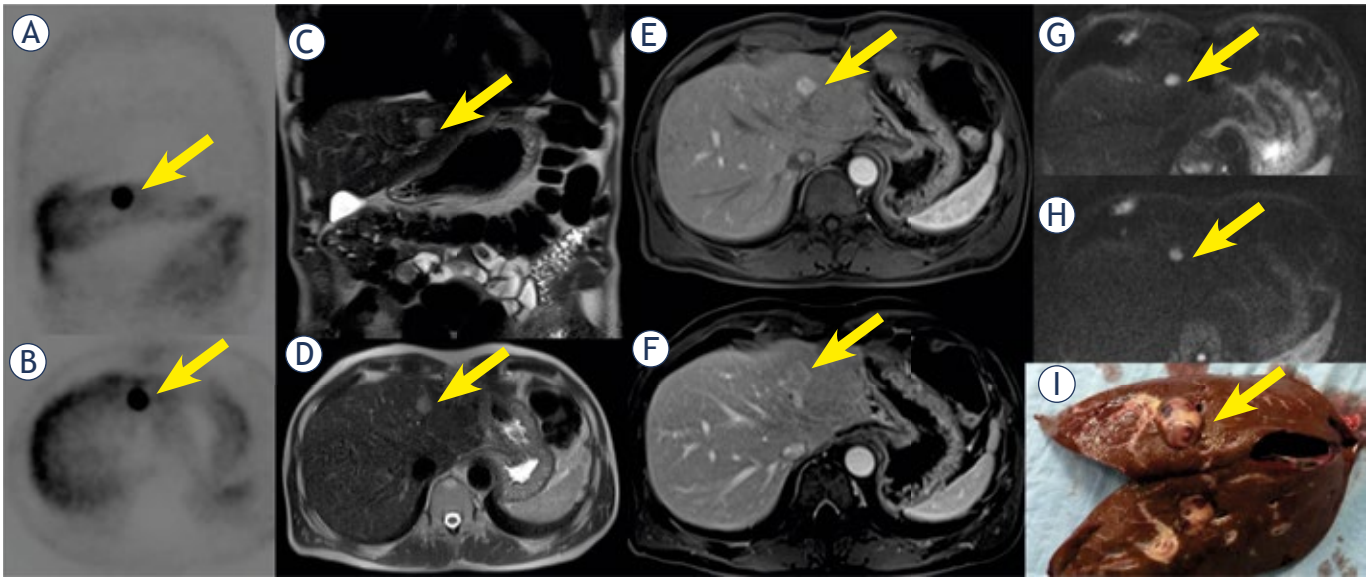

FIGURE 8. A 63 yrs old male with solitary liver lesion. The nodule is detected (arrow) by 68Ga-DOTATOC-PET/CT **(A, B)**, showing hyperintense signal (arrow) in T2-W sequences **(C, D)**. The lesion shows hypervascular appearance (arrow) during arterial phase **(E)** and "target" appearance (arrow) during portal phase **(F)** of contrast study, with restricted diffusion **(G, H)**. In **(I)** it is shown speciemen.

hepatic unknown site.[70] The clinical features and treatment outcomes of PHNETs are still unclear.[70] This tumour occurrs in middle-aged patients and it is more common in women.[71-73] More than 80% of the NETs found in the liver are metastatic and fewer than 150 cases of PHNET have been reported in the literature.[74] Even rarer is the biliary tree involvement (Figure 7).[74-76] The radiologic findings of PHNETs have not been well defined, but the cases reported show that the lesions are typically solid with necrotic components.[71] The cross-sectional imaging features usually consist of a solitary hepatic mass with a diameter of up to 25 cm (Figure 8). The lesion may be solid (60% of cases), partially solid with cystic areas (25% of cases), or mainly cystic and may demonstrate peripheral enhancement after the administration of an iodinated CM. PHNETs have low signal intensity on T1-W and high signal intensity on T2-W and their enhancement characteristics at MR imaging are similar to those at contrast-enhanced CT.[70]

Liver metastases

Approximately 30–80% of GEP-NET will develop synchronous or metachronous liver metastases (NELM).[77] NELM is the most important prognostic factor of GEP-NETs, in fact liver failure is the most common cause of death, followed by bowel obstruction and ischemia, with 5-year overall survival rates are around 50% for those with liver involvement, compared to 70–80% for those without it.[77] Surgery is the most effective approach for the majority of well-differentiated NELM. Due to frequently bilobar and multifocal manifestation of NELM, not more than 20–30% of patients may be candidates for resection with curative intent (Figure 9). Liver transplantation is a therapeutic option in selected patients with unresectable metastases. Moreover, ablative therapies, in addition to surgical resection, can offer improved survival and quality of life at 5 years as compared with patients who do not undergo surgery (70%–90% *vs.* 50%).[78] In this scenario, it is therefore important to identify the exact number, anatomical side and size of NELM, their proximity to vascular and biliary structures, and the volume of the future liver remnant.[77-78] According to Ronot *et al.* MRI is the most accurate imaging modality for NELM detection and characterization. DWI is more sensitive in detecting NELM than T2-W while dynamic gadolinium-enhanced MR sequences should be systematically performed. Gadoxetic acid-enhanced MRI ismore sensitive for detecting liver metastases than conventional MR sequences.[77] Flechsig *et al.* assessed the role of MRI in NELM compared to CT and ^{68}Ga-DOTATOC PET, showing that contrast-enhanced (CE) MRI using Gd-EOB-DTPA in combination with DWI was superior to non-contrast MR-sequences and arterial- and portal-venous phase CT in lesion conspicuity, likewise CE-MRI

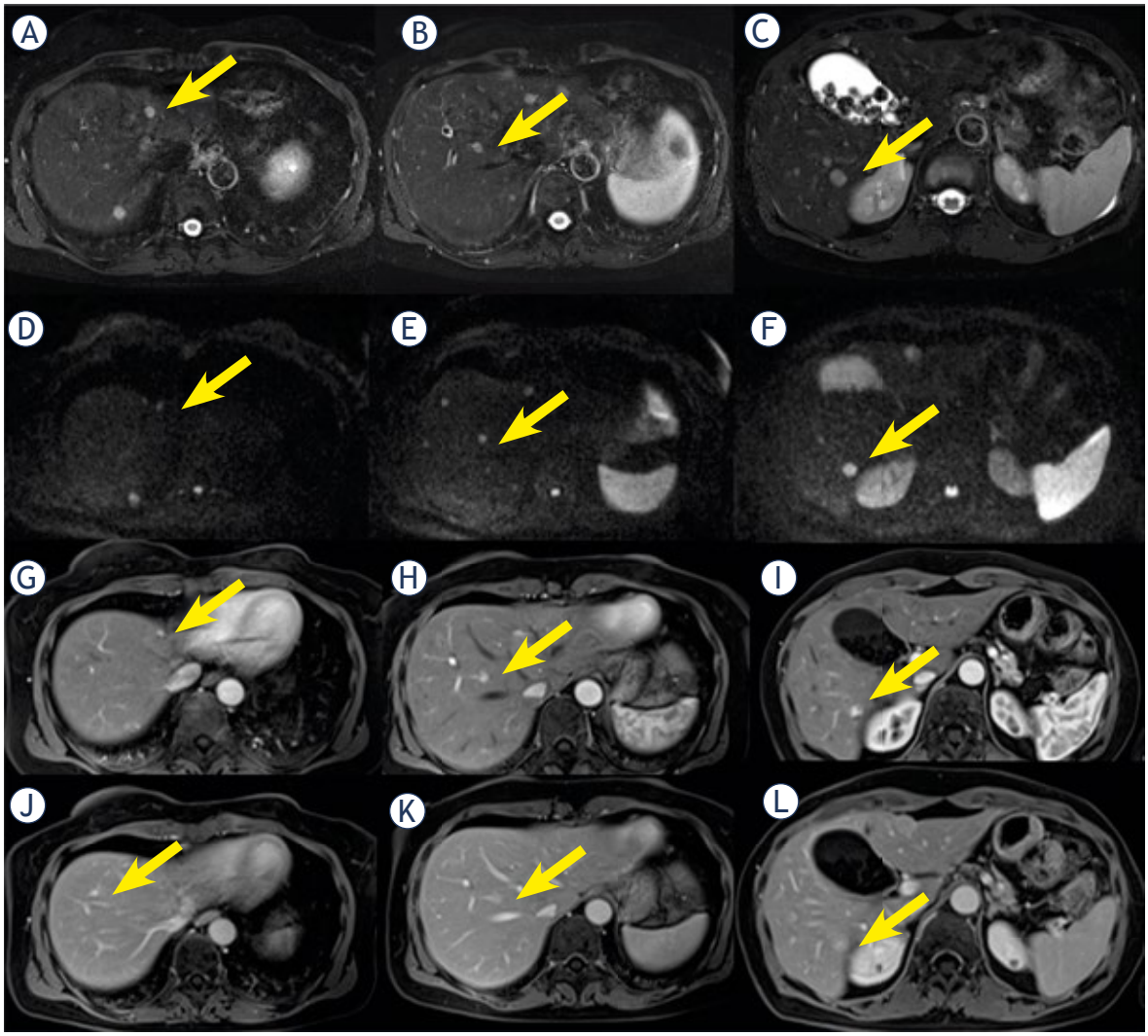

FIGURE 9. A 46 yrs old female with p-Net and bilobar liver metastases. The metastases show hyperintense signal (arrow) in T2-W sequences **(A, B ,C)**, restricted diffusion (arrow) in DW sequences **(D, E, F)**, hypervascular appearance (arrow) during arterial phase of contrast study **(G, H, I)** and hyperintense signal (arrow) during portal phase of contrast study **(J, K, L)**.

was superior to all other modalities concerning detectability of lesions.[78] Therefore, the researchers think that in the future PET/MR might replace the current standards of PET/CT or octeriotide scintigraphy/SPECT in liver metastasis detection of GEP-NET patients.[78] Up to the present, the best modality to detect vascular and biliary invasion is still unclear (Figure 10). CT and MRI should be considered the best imaging modalities in preoperatively detecting of vascular and biliary invasion.[77] According to Granata *et al.*, in the work-up of patients with liver colorectal metastases, the different phases should be considered by the radiologist; the same should be evaluated in the work-up of NELM.[26] In particular, in the preoperative setting, the radiologist should assess the functionality of the future liver remnant[26]; MRI with EOB may be a promising tool to assess this parameter, in order to avoid hepatic failure post surgery or ablative therapies.[26]

Treatment and follow-up

The aim of treatment should be curative when possible. The extention of the tumour, its metastases, histological grade and functional profile should be assessed before planning treatment**.** In fact**,** the choice of the therapy is related to symptoms, stage of disease, degree of uptake of radionuclide and histological features of NEN.[21]

According to ENETS guidelines, surgery with curative intent and/or locoregional or ablative

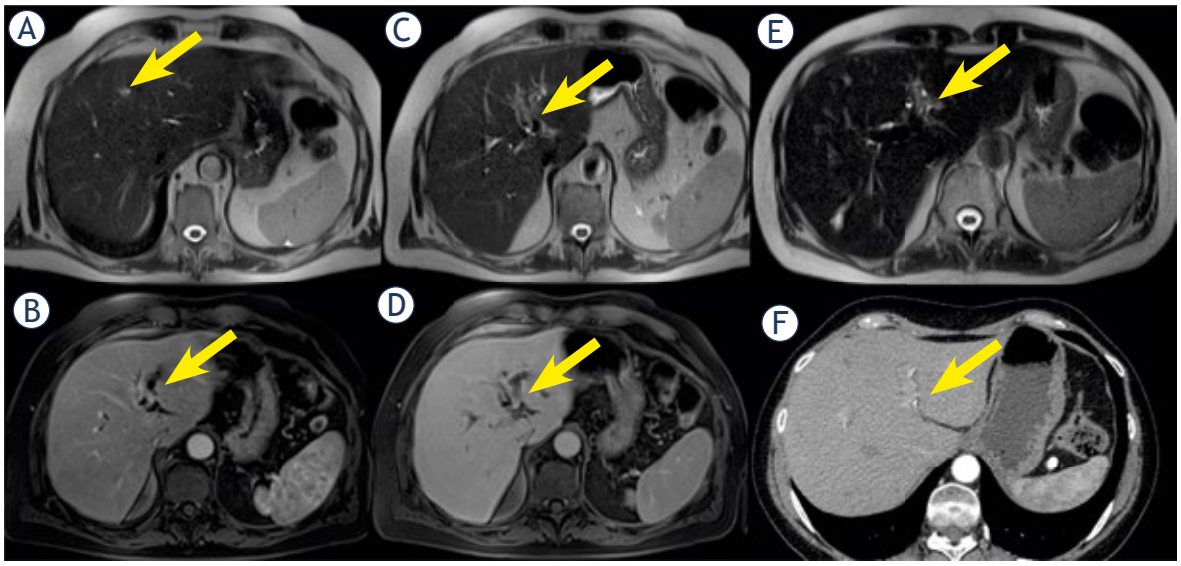

FIGURE 10. Man 51 y with p-Net and peribiliary metastasis. The lesion is hyperintense (arrow) in T2-W sequences **(A, C, E)** with progressive contrast enhancement (arrow) during contrast study **(B, D, F)** both in MR and in CT.

therapies should be considered at initial diagnosis and during the course of disease as an alternative approach to systemic therapies. Debulking surgery is indicated in patients with functional lesion with predominant liver disease for syndrome control. Liver transplantation is indicated in highly selected patients, with functional syndromes demonstrating early resistance to medical therapy. SSA, octreotide and lanreotide, are effective drugs for syndrome control in functional NET. SSA is recommended as a first-line therapy in midgut NET and can be considered in pancreatic NET as a first-line therapy (up to a Ki-67 of 10%). IFN-alpha is an established and approved therapy for syndrome control, and primarily used as second-line therapy in refractory carcinoid syndrome or functional pancreatic NET. Everolimus and sunitinib are approved antiproliferative therapies in progressive pancreatic NET, and they are one of the different options next to SSA and systemic chemotherapy. In G3 NEC, platinum-based chemotherapy is recommended as a first-line therapy. PRRT is recommended after failure of medical therapy.[4] There is no consensus on the optimal follow-up for completely resected gastroenteropancreatic neuroendocrine tumors. Published guidelines for follow-up are complex and emphasize closer surveillance in the first 3 years after resection. Neuroendocrine tumors have a different pattern and timescale of recurrence, and thus require more practical and tailored follow-up.[80,81] According to ENETS guidelines, in the follow-up of patients the pathological grade should be considered; for Grade1:US, CT, or MRI at 6 and 12 month (mo), then yearly or longer; octreoscan (or gallium-68–based PET) at baseline and every 2 y. Grade 2-3: US, CT, or MRI every 3 mo indefinitely; octreoscan (or gallium-68–based PET) at 3 mo and yearly.[80,81] Anyway, follow-up for NETs requires a multidisciplinary approach. CT or MR imaging plays a central role in long-term assessment after surgery. The follow-up protocol includes imaging studies every 6 months for the 1st year and then at yearly intervals if negative. The follow-up interval is shorter (3 months) for intermediate- and high-grade NETs and in patients undergoing chemotherapy or biologic therapies.[21] During follow-up, CT is the standard imaging method, to detect recurrent disease after surgery and locally ablative procedures, and to monitor systemic therapy. In young patients, MRI is generally preferred to CT.[45] RECIST (Response Evaluation Criteria In Solid Tumours) are utilized for therapy monitoring in general oncology and rely on morphological imaging to measure the longest diameter of a set of chosen target lesions.[82] The currently used criteria (RECIST 1.1) state that a maximum of two lesions per organ and five in total should be measured.[82] Some issues still remain in the application of RECIST to monitor NETs' therapy due to the fact that tumours have generally slow-growth, can have cystic components and that the various available therapies, especially the new targeted agents, such as everolimus and sunitinib, generally do not result in tumour shrinkage

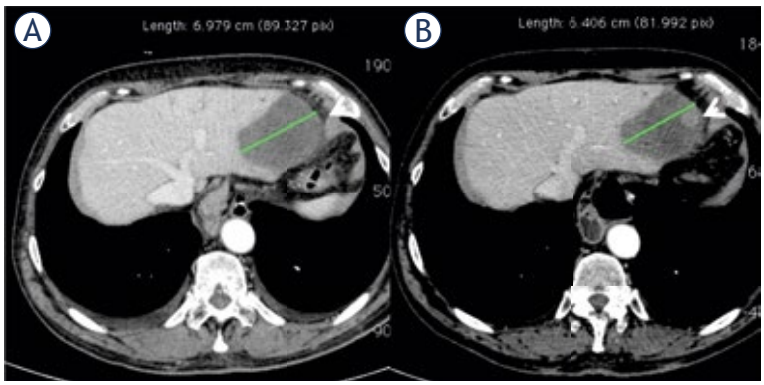

FIGURE 11. Nodule in nodule appearance (arrow) during follow-up of p-NET, indicating progressive disease.

but rather in stabilization of the disease. RECIST is, therefore, less suited for therapy monitoring of NETs than the one of other cancers.[45] Therefore, the radiologists should be aware of patients therapy in order to evaluate the real efficacy of the treatment. They should consider that the common and expected imaging response pattern of metastatic GEP-NETs to somatostatin analogues is a stable disease with no changes in tumor size. The typical imaging response pattern to targeted agents (Sunitinib and everolimus) is a decrease in tumor attenuation and enhancement and a stable to mild decrease in tumor size. Sometimes tumors have decreased density suggestive of response to treatment but show an increased size, which may lead to a misinterpretation of tumor progression according to size criteria (Figure 11). Sometimes target therapies cause intratumoral hemorrhage, which can result in an increase of density with a variable size change. If tumor size and density are increased by hemorrhage, an accurate interpretation of treatment response is difficult and may be confused with progression, even when new criteria, such as the Choi criteria and mRECIST, are used.[83]

Conclusions

NETs are a considerable diagnostic challenge since their clinical presentation is protean, nonspecific and usually late, often when hepatic metastases are already evident. An effective diagnosis requires a multimodal approach that combines evaluation of clinical symptoms, hormone levels, radiological and nuclear imaging, and histological confirmation.

The radiologists are important members of the multidisciplinary NET team both in the assessment of tumor staging and in the treatment follow up. In diagnostic work-up of NETs two critical issues are present: firstly the need to identify tumor presence and secondly to define the primary site and to assess regional and distant metastases. The most appropriate imaging technique depends on the type of neuroendocrine tumour.

The role of somatostatin receptor-based ^{68}Ga-PET–CT imaging is well established and is recommended for diagnosis and follow-up of NETs. MRI of the liver with hepatocyte-specific contrast media and DWI areused to detect liver metastases with high sensitivity. MRI of the liver is highly recommended before any liver surgery and for monitoring liver metastases. Enteroclysis-CT or MR is mandatory to assess small bowel in patients with NET. PET/CT with 68Ga-labelled somatostatin analogs DOTA-TOC/TATE/NOC is the method of choice to fully stage and localize the extent of disease in patients with non-insulinoma P-NETs. The preoperative imaging assessment of p-NET needs to establish the anatomical position of the lesion, its relation to the pancreatic duct and the main bile duct, as well as the encasement of the hepatic, splenic and mesenteric artery and vein and the portal vein. The treatment follow-up requires a multidisciplinary approach, including biochemical (chromogranin A, hormones, vasoactive amines), radiologic, and histologic investigations and an important role is assumed by radiologist. CT or MR imaging plays a central role in long-term assessment after surgery. RECIST is less suited for therapy monitoring of NETs than of other cancers.

References

1. Fraenkel M, Kim MK, Faggiano A, Valk GD. Epidemiology of gastroenteropancreatic neuroendocrine tumours. *Best Pract Res Clin Gastroenterol* 2012; **26:** 691-703. doi: 10.1016/j.bpg.2013.01.006

2. Oberg K, Akerström G, Rindi G, Jelic S; ESMO Guidelines Working Group. Neuroendocrine gastroenteropancreatic tumours: ESMO Clinical Practice Guidelines for diagnosis, treatment and follow-up. *Ann Oncol* 2010; **21 (Suppl 5):** v223-7. doi: 10.1093/annonc/mdq192

3. Modlin IM, Moss SF, Chung DC, Jensen RT, Snyderwine E. Priorities for improving the management of gastroenteropancreatic neuroendocrine tumors. *J Natl Cancer Inst* 2008; **100:** 1282-9. doi: 10.1093/jnci/djn275

4. Falconi M, Eriksson B, Kaltsas G, Bartsch DK, Capdevila J, Caplin M, et al. ENETS Consensus guidelines update for the management of patients with functional pancreatic neuroendocrine tumors and non-functional pancreatic neuroendocrine Tumors. *Neuroendocrinology* 2016; **103:** 153-71. doi: 10.1159/000443171

5. Pavel M, O'Toole D, Costa F, Capdevila J, Gross D, Kianmanesh R, et al. ENETS Consensus guidelines update for the management of distant metastatic disease of intestinal, pancreatic, bronchial neuroendocrine neoplasms (NEN) and NEN of unknown primary site. *Neuroendocrinology* 2016; **103:** 172-85. doi: 10.1159/000443167

6. Sundin A. Radiological and nuclear medicine imaging of gastroenteropancreatic neuroendocrine tumours. *Best Pract Res Clin Gastroenterol* 2012; **26:** 803-18. doi: 10.1016/j.bpg.2012.12.004

7. Yu R, Wachsman A. Imaging of neuroendocrine tumors: indications, interpretations, limits, and pitfalls. *Endocrinol Metab Clin North Am* 2017; **46:** 795-814. doi: 10.1016/j.ecl.2017.04.008

8. Rockall AG, Reznek RH. Imaging of neuroendocrine tumours (CT/MR/US). *Best Pract Res Clin Endocrinol Metab* 2007; **21:** 43-68. doi: 10.1016/j.beem.2007.01.003

9. Gatto F, Hofland LJ. The role of somatostatin and dopamine D2 receptors in endocrine tumors. *Endocr Relat Cancer* 2011; **18:** R233-R251. doi: 10.1530/ERC-10-0334

10. Rust E, Hubele F, Marzano E, Goichot B, Pessaux P, Kurtz JE, et al. Nuclear medicine imaging of gastro-entero-pancreatic neuroendocrnne tumors. The key role of cellular differentiation and tumor grade: from theory to clinical practice. *Cancer Imaging* 2012; **12:** 173-84. doi: 10.1102/1470-7330.2012.0026

11. Auernhammer CJ, Spitzweg C, Angele MK, Boeck S, Grossman A, Nölting S, et al. Advanced neuroendocrine tumours of the small intestine and pancreas: clinical developments, controversies, and future strategies. *Lancet Diabetes Endocrinol* 2018; **6:** 404-15. doi: 10.1016/S2213-8587(17)30401-1

12. Bodei L, Sundin A, Kidd M, Prasad V, Modlin IM. The status of neuroendocrine tumor imaging: from darkness to light? *Neuroendocrinology* 2015; **101:** 1-17. doi: 10.1159/000367850.

13. Sundin A, Arnold R, Baudin E, Cwikla JB, Eriksson B, Fanti S, et al. ENETS Consensus guidelines for the standards of care in neuroendocrine tumors: radiological, nuclear medicine & hybrid imaging. *Neuroendocrinology* 2017; **105:** 212-44. doi: 10.1159/000471879

14. Delle Fave G, O'Toole D, Sundin A, Taal B, Ferolla P, Ramage JK, et al; Vienna Consensus conference participants. ENETS consensus guidelines update for gastroduodenal neuroendocrine neoplasms. *Neuroendocrinology* 2016; **103:** 119-24. doi: 10.1159/000443168

15. Garcia-Carbonero R, Sorbye H, Baudin E, Raymond E, Wiedenmann B, Niederle B, et al. ENETS consensus guidelines for high-grade gastroenteropancreatic neuroendocrine zumors and neuroendocrine carcinomas. *Neuroendocrinology* 2016; **103:** 186-94. doi: 10.1159/000443172

16. Klöppel G, Couvelard A, Perren A, Komminoth P, McNicol AM, Nilsson O, et al. Mallorca consensus conference participants; European Neuroendocrine Tumor Society. ENETS consensus guidelines for the standards of care in neuroendocrine tumors: towards a standardized approach to the diagnosis of gastroenteropancreatic neuroendocrine tumors and their prognostic stratification. *Neuroendocrinology* 2009; **90:** 162-6. doi: 10.1159/000182196

17. O'Toole D, Kianmanesh R, Caplin M. ENETS 2016 consensus guidelines for the management of patients with digestive neuroendocrine tumors: an update. *Neuroendocrinology* 2016; **103:** 117-8. doi: 10.1159/000443169

18. Niederle B, Pape UF, Costa F, Gross D, Kelestimur F, Knigge U, et al. ENETS consensus guidelines update for neuroendocrine neoplasms of the jejunum and ileum. *Neuroendocrinology* 2016; **103:** 125-38. doi: 10.1159/000443170

19. Ramage JK, De Herder WW, Delle Fave G, Ferolla P, Ferone D, Ito T, et al. ENETS consensus guidelines update for colorectal neuroendocrine neoplasms. *Neuroendocrinology* 2016; **103:** 139-43. doi: 10.1159/000443166

20. Etchebehere EC, de Oliveira Santos A, Gumz B, Vicente A, Hoff PG, Corradi G, et al. 68Ga-DOTATATE PET/CT, 99mTc-HYNIC-octreotide SPECT/CT, and whole-body MR imaging in detection of neuroendocrine tumors: a prospective trial. *J Nucl Med* 2014; **55:** 1598-604. doi: 10.2967/jnumed.114.144543

21. Sahani DV, Bonaffini PA, Fernández-Del Castillo C, Blake MA. Gastroenteropancreatic neuroendocrine tumors: role of imaging in diagnosis and management. *Radiology* 2013; **266:** 38-61. doi: 10.1148/radiol.12112512

22. Baumann T, Rottenburger C, Nicolas G, Wild D. Gastroenteropancreatic neuroendocrine tumours (GEP-NET) - Imaging and staging. *Best Pract Res Clin Endocrinol Metab* 2016; **30:** 45-57. doi: 10.1016/j.beem.2016.01.003

23. Kamaoui I, De-Luca V, Ficarelli S, Mennesson N, Lombard-Bohas C, Pilleul F. Value of CT enteroclysis in suspected small-bowel carcinoid tumors. *AJR Am J Roentgenol* 2010; **194:** 629-33. doi: 10.2214/AJR.09.2760

24. Tan EH, Tan CH. Imaging of gastroentero- pancreatic neuroendocrine tumors. *World J Clin Oncol* 2011; **2:** 28-43. doi: 10.5306/wjco.v2.i1.28

25. Woodard PK, Feldman JM, Paine SS, Baker ME. Midgut carcinoid tumors: CT findings and biochemical profiles. *J Comput Assist Tomogr* 1995; **19:** 400-5.

26. Granata V, Fusco R, Avallone A, Catalano O, Piccirillo M, Palaia R, et al. A radiologist's point of view in the presurgical and intraoperative setting of colorectal liver metastases. *Future Oncol* 2018; **14:** 2189-206. doi: 10.2217/fon-2018-0080

27. Granata V, Fusco R, Catalano O, Avallone A, Palaia R, Botti G, et al. Diagnostic accuracy of magnetic resonance, computed tomography and contrast enhanced ultrasound in radiological multimodality assessment of peribiliary liver metastases. *PLoS One* 2017; **12:** e0179951. doi: 10.1371/journal.pone.0179951

28. Granata V, Fusco R, Catalano O, Avallone A, Leongito M, Izzo F, et al. Peribiliary liver metastases MR findings. *Med Oncol* 2017; **34:** 124. doi: 10.1007/s12032-017-0981-7

29. Granata V, Fusco R, Catalano O, Filice S, Avallone A, Piccirillo M, et al. Uncommon neoplasms of the biliary tract: radiological findings. *Br J Radiol* 2017; **90:** 20160561. doi: 10.1259/bjr.20160561

30. Granata V, Cascella M, Fusco R, dell'Aprovitola N, Catalano O, Filice S, et al. Immediate adverse reactions to Gadolinium-Based MR contrast media: A retrospective analysis on 10,608 examinations. *Biomed Res Int* 2016; **2016:** 3918292. doi: 10.1155/2016/3918292

31. Kulke MH, Anthony LB, Bushnell DL, de Herder WW, Goldsmith SJ, Klimstra DS, et al. NANETS treatment guidelines: well-differentiated neuroendocrine tumors of the stomach and pancreas. *Pancreas* 2010; **39:** 735-52. doi: 10.1097/MPA.0b013e3181ebb168

32. Cambruzzi E, Azeredo AM, Kronhart A, Foltz KM, Zettler CG, Pêgas KL. The presence of metastases in regional lymph nodes is associated with tumor size and depth of invasion in sporadic gastric adenocarcinoma. *Arq Bras Cir Dig* 2014; **27:** 18-21. doi: 10.1590/S0102-67202014000100005

33. Scherübl H, Jensen RT, Cadiot G, Stölzel U, Klöppel G. Neuroendocrine tumors of the small bowels are on the rise: Early as- pects and management. *World J Gastroin- test Endosc* 2010; **2:** 325-34. doi: 10.4253/wjge.v2.i10.325

34. Oberg K, Castellano D. Current knowledge on diagnosis and staging of neuroendocrine tumors. *Cancer Metastasis Rev* 2011; **30 (Suppl 1):** 3-7. doi: 10.1007/s10555-011-9292-1

35. Turaga KK, Kvols LK. Recent progress in the understanding, diagnosis, and treatment of gastroenteropancreatic neuroendocrine tumors. *CA Cancer J Clin* 2011; **61:** 113-32. doi: 10.3322/caac.20097

36. Chang S, Choi D, Lee SJ, Lee WJ, Park MH, Kim SW, et al. Neuro-endocrine neoplasms of the gastrointestinal tract: classification, pathologic basis, and imaging features. *RadioGraphics* 2007; **27:** 1667-79. doi: 10.1148/rg.276075001

37. Modlin IM, Lye KD, Kidd M. A 5-decade analysis of 13,715 carcinoid tumors. *Cancer* 2003; **97:** 934-59. doi: 10.1002/cncr.11105

38. Masselli G, Polettini E, Casciani E, Bertini L, Vecchioli A, Gualdi G. Small-bowel neo- plasms: prospective evaluation of MR en- teroclysis. *Radiology* 2009; **251:** 743-50. doi: 10.1148/radiol.2513081819

39. Van Weyenberg SJ, Meijerink MR, Jacobs MA, Van der Peet DL, Van Kuijk C, Mulder CJ, et al. MR enteroclysis in the diagno- sis of small-bowel neoplasms. *Radiology* 2010; **254:** 765-73. doi: 10.1148/radiol.09090828

40. Claudon M, Dietrich CF, Choi BI, Cosgrove DO, Kudo M, Nolsøe CP, et al. World Federation for Ultrasound in Medicine; European Federation of Societies for Ultrasound. Guidelines and good clinical practice recommendations for Contrast Enhanced Ultrasound (CEUS) in the liver - update 2012: A WFUMB-EFSUMB initiative in cooperation with representatives of AFSUMB, AIUM, ASUM, FLAUS and ICUS. *Ultrasound Med Biol* 2013; **39:** 187-210. doi: 10.1016/j.ultrasmedbio.2012.09.002

41. Shapiro R, Eldar S, Sadot E, Papa MZ, Zip- pel DB. Appendiceal carcinoid at a large tertiary center: pathologic findings and long-term follow-up evaluation. *Am J Surg* 2011; **201:** 805-8. doi: 10.1016/j.amjsurg.2010.04.016

42. Kobayashi K, Katsumata T, Yoshizawa S, Sada M, Igarashi M, Saigenji K, et al. Indications of endoscopic polypectomy for rectal carcinoid tumors and clinical use- fulness of endoscopic ultrasonography. *Dis Colon Rectum* 2005; **48:** 285-91. doi: 10.1007/s10350-004-0765-y

43. Anthony LB, Strosberg JR, Klimstra DS, Maples WJ, O'Dorisio TM, Warner RR, et al. The NANETS consensus guidelines for the diagnosis and management of gastro- intestinal neuroendocrine tumors (nets): well-differentiated nets of the distal colon and rectum. *Pancreas* 2010; **39:** 767-74. doi: 10.1097/MPA.0b013e3181ec1261

44. Dromain C, Déandréis D, Scoazec JY, Goere D, Ducreux M, Baudin E, et al. Imaging of neuroendocrine tumors of the pancreas. *Diagn Interv Imaging* 2016; **97:** 1241-57. doi: 10.1016/j.diii.2016.07.012

45. van Essen M, Sundin A, Krenning EP, Kwekkeboom DJ. Neuroendocrine tumours: the role of imaging for diagnosis and therapy. *Nat Rev Endocrinol* 2014; **10:** 102-14.

46. Ueno N, Tomiyama T, Tano S, Wada S, Aizawa T, Kimura K, et al. Utility of endoscopic ultrasonography with color Doppler function for the diagnosis of islet cell tumor. *Am J Gastroenterol* 1996; **91:** 772e6. doi: 10.1038/nrendo.2013.246

47. Rösch T, Braig C, Gain T, Feuerbach S, Siewert JR, Schusdziarra V, et al. Staging of pancreatic and ampullary carcinoma by endoscopic ultrasonography. Comparison with conventional sonography, computed tomography, and angiography. *Gastroenterology* 1992; **102:** 188e99. doi: 10.1016/0016-5085(92)91800-j

48. Ramage JK, Ahmed A, Ardill J, Bax N, Breen DJ, Caplin ME, et al. Guidelines for the management of gastroenteropancreatic neuroendocrine (including carcinoid) tumours (NETs). *Gut* 2012; **61:** 6-32. doi: 10.1136/gutjnl-2011-300831

49. Cappelli C, Boggi U, Mazzeo S, Cervelli R, Campani D, Funel N, et al. Contrast enhancement pattern on multidetector CT predicts malignancy in pancreatic endocrine tumours. *Eur Radiol* 2015; **25:** 751-9. doi: 10.1007/s00330-014-3485-2

50. Bergers G, Benjamin LE. Tumorigenesis and the angiogenic switch. *Nat Rev Cancer* 2003; **3:** 401-10. doi: 10.1038/nrc1093

51. Koito K, Namieno T, Nagakawa T, Morita K. Delayed enhancement of islet cell carcinoma on dynamic computed tomography: a sign of its malignancy. *Abdom Imaging* 1997; **22:** 304-6.

52. Takumi K, Fukukura Y, Higashi M, Ideue J, Umanodan T, Hakamada H, et al. Pancreatic neuroendocrine tumors: Correlation between the contrast-enhanced computed tomography features and the pathological tumor grade. *Eur J Radiol* 2015; **84:** 1436-43. doi: 10.1016/j.ejrad.2015.05.005

53. Marin D, Nelson RC, Barnhart H, Schindera ST, Ho LM, Jaffe TA, et al. Detection of pancreatic tumors, image quality, and radiation dose during the pancreatic parenchymal phase: effect of a low-tube-voltage, high-tube-current CT technique-preliminary results. *Radiology* 2010; **256:** 450-9. doi: 10.1148/radiol.10091819

54. Granata V, Fusco R, Catalano O, Setola SV, de Lutio di Castelguidone E, Piccirillo M, et al. Multidetector computer tomography in the pancreatic adenocarcinoma assessment: an update. *Infect Agent Cancer* 2016; **11:** 57. doi: 10.1186/s13027-016-0105-6

55. George E, Wortman JR, Fulwadhva UP, Uyeda JW, Sodickson AD. Dual energy CT applications in pancreatic pathologies. *Br J Radiol* 2017; **90:** 20170411. doi: 10.1259/bjr.20170411

56. Lin XZ, Wu ZY, Tao R, Guo Y, Li JY, Zhang J, et al. Dual energy spectral CT imaging of insulinoma-Value in preoperative diagnosis compared with conventional multi-detector CT. *Eur J Radiol* 2012; **81:** 2487-94. doi: 10.1016/j.ejrad.2011.10.028

57. Van Binnebeek S, Vanbilloen B, Baete K, Terwinghe C, Koole M, Mottaghy FM, et al. Comparison of diagnostic accuracy of (111)In-pentetreotide SPECT and (68)Ga-DOTATOC PET/CT: a lesion-by-lesion analysis in patients with metastatic neuroendocrine tumours. *Eur Radiol* 2016; **26:** 900-9. doi: 10.1007/s00330-015-3882-1

58. Caramella C, Dromain C, De Baere T, Boulet B, Schlumberger M, Ducreux M, et al. Endocrine pancreatic tumours: which are the most useful MRI sequences? *Eur Radiol* 2010; **20:** 2618-27. doi: 10.1007/s00330-010-1840-5

59. Oberg KE, Reubi JC, Kwekkeboom DJ, Krenning EP. Role of somatostatins in gastroenteropancreatic neuroendocrine tumor development and therapy. *Gastroenterology* 2010; **139:** 742-53, 753.e1. doi: 10.1053/j.gastro.2010.07.002

60. Wang Y, Chen ZE, Yaghmai V, Nikolaidis P, McCarthy RJ, Merrick L, et al. Diffusion-weighted MR imaging in pancreatic endocrine tumors correlated with histopathologic characteristics. *J Magn Reson Imaging* 2011; **33:** 1071-9. doi: 10.1002/jmri.22541

61. Devries AF, Griebel J, Kremser C, Judmaier W, Gneiting T, Kreczy A, Ofner D, Pfeiffer KP, Brix G, Lukas P. Tumor microcirculation evaluated by dynamic magnetic resonance imaging predicts therapy outcome for primary rectal carcinoma. *Cancer Res* 2001; **61:** 2513-6.

62. DeVries AF, Kremser C, Hein PA, Griebel J, Krezcy A, Ofner D, et al. Tumor microcirculation and diffusion predict therapy outcome for primary rectal carcinoma. *Int J Radiat Oncol Biol Phys* 2003; **56:** 958-65. doi: 10.1016/s0360-3016(03)00208-6

63. Bol K, Haeck JC, Groen HC, Niessen WJ, Bernsen MR, de Jong M, et al. Can DCE-MRI explain the heterogeneity in radiopeptide uptake imaged by SPECT in a pancreatic neuroendocrine tumor model? *PLoS One* 2013; **8:** e77076. doi: 10.1371/journal.pone.0077076

64. Huh J, Choi Y, Woo DC, Seo N, Kim B, Lee CK, et al. Feasibility of test-bolus DCE-MRI using CAIPIRINHA-VIBE for the evaluation of pancreatic malignancies. *Eur Radiol* 2016; **26:** 3949-56. doi: 10.1007/s00330-016-4209-6

65. Zhao W, Quan Z, Huang X, Ren J, Wen D, Zhang G, et al. Grading of pancreatic neuroendocrine neoplasms using pharmacokinetic parameters derived from dynamic contrast-enhanced MRI. *Oncol Lett* 2018; **15:** 8349-56. doi: 10.3892/ol.2018.8384

66. Li Q, Ye ZX. [Radiomics: the process and applications in tumor research]. *Zhonghua Zhong Liu Za Zhi* 2018; **40:** 801-4. doi: 10.3760/cma.j.issn.0253-3766.2018.11.001

67. Napel S, Mu W, Jardim-Perassi BV, Aerts HJWL, Gillies RJ. Quantitative imaging of cancer in the postgenomic era: Radio(geno)mics, deep learning, and habitats. *Cancer* 2018; **124:** 4633-49. doi: 10.1002/cncr.31630

68. De Robertis R, Maris B, Cardobi N, Tinazzi Martini P, Gobbo S, Capelli P, et al. Can histogram analysis of MR images predict aggressiveness in pancreatic neuroendocrine tumors? *Eur Radiol* 2018; **28:** 2582-91. doi: 10.1007/s00330-017-5236-7

69. Sidhu PS, Cantisani V, Dietrich CF, Gilja OH, Saftoiu A, Bartels E, et al. The EFSUMB guidelines and recommendations for the clinical practice of Contrast-Enhanced Ultrasound (CEUS) in Non-c hepatic applications: Update 2017 (Long Version). *Ultraschall Med* 2018; **39:** e2-e44. doi: 10.1055/s-0044-101254

70. Wang LX, Liu K, Lin GW, Jiang T. Primary hepatic neuroendocrine tumors: comparing CT and MRI features with pathology. *Cancer Imaging* 2015; **15:** 13. doi: 10.1186/s40644-015-0046-0

71. Tan Y, Xiao EH. Rare hepatic malignant tumors: dynamic CT, MRI, and clinicopathologic features: with analysis of 54 cases and review of the literature. *Abdom Imaging* 2013; **38:** 511-26. doi: 10.1007/s00261-012-9918-y

72. Rückert RI, Rückert JC, Dörffel Y, Rudolph B, Müller JM. Primary hepatic neuroendocrine tumor: successful hepatectomy in two cases and review of the literature. *Digestion* 1999; **60:** 110-6. doi: 10.1159/000007635

73. Iwao M, Nakamuta M, Enjoji M, Kubo H, Fukutomi T, Tanabe Y, et al. Primary hepatic carcinoid tumor: case report and review of 53 cases. *Med Sci Monit* 2001; **7:** 746-50.

74. Li W, Zhuang BW, Wang Z, Liao B, Hong LY, Xu M, et al. Case report of contrast-enhanced ultrasound features of primary hepatic neuroendocrine tumor: A CARE-Compliant Article. *Medicine (Baltimore)* 2016; **95:** e 3450. doi: 10.1097/MD.0000000000003450

75. Iimuro Y, Deguchi Y, Ueda Y, Tanaka A, Iwasa Y, Ishihara M, et al. Primary hepatic carcinoid tumor with metachronous lymph node metastasis after long-term follow up. *J Gastroenterol Hepatol* 2002; **17:**1119-24. doi: 10.1046/j.1440-1746.2002.02663.x

76. Abdel Wahab M, Fathy O, Elghwalby N, Sultan A, Mostafa M, El-Baz M, et al. Primary hepatic carcinoid tumor: one Egyptian center experience. *Hepatogastroenterology* 2006*;* **53:** 33-8.

77. Ronot M, Clift AK, Baum RP, Singh A, Kulkarni HR, Frilling A, Vilgrain V. Morphological and functional imaging for detecting and assessing the resectability of neuroendocrine liver metastases. *Neuroendocrinology* 2018; **106:** 74-88. doi: 10.1159/000479293

78. Veenendaal LM, Borel Rinkes IH, Lips CJ, van Hillegersberg R. Liver metastases of neuroendocrine tumours; early reduction of tumour load to improve life expectancy. *World J Surg Oncol* 2006; **4:** 35. doi: 10.1186/1477-7819-4-35

79. Flechsig P, Zechmann CM, Schreiweis J, Kratochwil C, Rath D, Schwartz LH, et al. Qualitative and quantitative image analysis of CT and MR imaging in patients with neuroendocrine liver metastases in comparison to ^{68}Ga-DOTATOC PET. *Eur J Radiol* 2015; **84:** 1593-600. doi: 10.1016/j.ejrad.2015.04.009

80. Knigge U, Capdevila J, Bartsch DK, Baudin E, Falkerby J, Kianmanesh R, et al. ENETS consensus recommendations for the standards of care in neuroendocrine neoplasms: follow-up and documentation. *Neuroendocrinology* 2017; **105:** 310-9. doi: 10.1159/000458155

81. Singh S, Moody L, Chan DL, Metz DC, Strosberg J, Asmis T, et al. Follow-up recommendations for completely resected gastroenteropancreatic neuroendocrine tumors. *JAMA Oncol* 2018; **4:** 1597-604. doi: 10.1001/jamaoncol.2018.2428

82. Eisenhauer EA, Therasse P, Bogaerts J, Schwartz LH, Sargent D, Ford R, et al. New response evaluation criteria in solid tumours: revised RECIST guideline (version 1.1). *Eur J Cancer* 2009; **45:** 228-47. doi: 10.1016/j.ejca.2008.10.026

83. Kim KW, Krajewski KM, Nishino M, Jagannathan JP, Shinagare AB, Tirumani SH, et al. Update on the management of gastroenteropancreatic neuroendocrine tumors with emphasis on the role of imaging. *AJR Am J Roentgenol* 2013; **201:** 811-24. doi: 10.2214/AJR.12.10240

review

Advances in the management of craniopharyngioma in children and adults

Mojca Jensterle[1,2], Soncka Jazbinsek[2,3], Roman Bosnjak[2,4], Mara Popovic[2,5] , Lorna Zadravec Zaletel[2,6], Tina Vipotnik Vesnaver[2,7], Barbara Faganel Kotnik[2,8], Primoz Kotnik[2,3]

[1] Department of Endocrinology, Diabetes and Metabolism, University Medical Centre Ljubljana, Ljubljana, Slovenia
[2] Medical Faculty, University of Ljubljana, Ljubljana, Slovenia
[3] Department of Endocrinology, Diabetes and Metabolism, University Children's Hospital, University Medical Centre Ljubljana, Ljubljana, Slovenia
[4] Department of Neurosurgery, University Medical Centre Ljubljana, Ljubljana, Slovenia
[5] Institute of Pathology, Medical Faculty, University of Ljubljana, Ljubljana, Slovenia
[6] Department of Radiotherapy, Institute of Oncology Ljubljana, Ljubljana, Slovenia
[7] Clinical Institute of Radiology, University Medical Centre Ljubljana, Ljubljana, Slovenia
[8] Department of Hematology and Oncology, University Children's Hospital, University Medical Centre Ljubljana, Ljubljana, Slovenia

Radiol Oncol 2019; 53(4): 388-396.

Received 21 June 2019
Accepted 11 July 2019

Correspondence to: Asst. Prof. Primož Kotnik, M.D., Ph.D., Department of Endocrinology, Diabetes and Metabolism, University Children's Hospital, University Medical Center Ljubljana, Bohoričeva 20, SI-1000 Ljubljana, Slovenia. Department of Pediatrics, Faculty of Medicine, University of Ljubljana, Bohoričeva 20, SI-1000 Ljubljana, Slovenia. E-mail: primoz.kotnik@mf.uni-lj.si

Disclosure: No potential conflicts of interest were disclosed.

Background. Childhood and adult-onset craniopharyngioma is a rare embryogenic tumor of the sellar, suprasellar, and parasellar region. Survival rates are high; however, tumor location and treatment sequalae including endocrine deficits, visual impairment, metabolic complications, cognitive and psychosocial deficits can significantly impair patient's quality of life. There is considerable controversy regarding the optimal management of craniopharyngiomas. Subtotal resection of the tumor followed by targeted irradiation to avoid further hypothalamic damage is currently indicated. Novel insights in the tumor's molecular pathology present the possibility for targeted therapy possibly decreasing the rate and severity of treatment-associated morbidity.

Conclusions. Craniopharyngioma should be seen as a chronic disease. To achieve optimal outcomes a multidisciplinary team of specialized neurosurgeons, neuro-radiologists, neuro-oncologists, pathologists and endocrinologists should be involved in the diagnosis, planning of the surgery, irradiation and long-term follow-up.

Key words: craniopharyngioma; hypopituitarism; metabolic syndrome; proton beam therapy; *CTNNB1* gene; MAPK/ERK pathway

Introduction

Craniopharyngioma (CP) is a rare epithelial tumor of the sellar and parasellar region, histologically of low-grade (WHO grade I). They represent approximately 1% of all primary intracranial neoplasms in adults and 1.2–4% in children, making them the most common sellar tumors in the latter. The overall incidence of CP is 1.24–1.46 per million/year with no difference between gender and race.[1-5]

In 1904, Austrian pathologist Jakob Erdheim first reported that CP arises from squamous cell rests occurring in the region of the remnant hypophyseal/pharyngeal duct, most frequently originating around the infundibulum. Rarely CP arises in less typical locations along the remnants of the primitive craniopharyngeal duct including the nasopharynx, sphenoid bone, or as primary intraventricular lesions.[6,7]

The growth of CP is slow, but their location enables them to be large at the time of diagnosis, extending supero-posteriorly into the third ventricle and hypothalamus, compressing supero-anteriorly the optic pathways and inferiorly the pituitary gland, impairing their functions. Adherence to these critical structures often limits the ability of the surgeon to completely resect the lesion, exposing patients to a high risk of recurrence. The overall 5-year survival rate is high (ranging from 91–98%). Unfortunately, the morbidity rate is equally high with severe neuroendocrine sequelae, impaired social and physical functionality and a negative impact on quality of life (QoL) in all patients. Because of this, strict follow up by a specialized multidisciplinary team is paramount.[8-13]

High morbidity rates following aggressive complete surgical removal were reported, therefore a change in the paradigm towards a subtotal removal of the tumor mass has now been proposed. As CP is known to recur frequently, postoperative irradiation has become a part of the standard treatment.[14-16] The first reports after the introduction of proton beam therapy show a decrease in adjuvant therapy induced morbidity, but long-term follow up data is still needed to evaluate its role in CP treatment.[17]

Despite all these recent improvements, we still observe high morbidity rates, especially panhypopituitarism, visual and neurological deficits, hypothalamic obesity (HO), increased cardiovascular issues and reduced quality of life, inciting the demand for alternative therapies to surgery.[8,18-22] Novel insights into the molecular pathogenesis of adamantinomatous craniopharyngioma (ACP) and papillary craniopharyngioma (PCP) have offered the possibility of pharmaceutical therapy targeting pathogenic pathways, which could decrease the chance of recurrence and possibly the initial tumor size.[23,24]

The aim of the present review is to accumulate up-to-date data to help in the development of national guidelines for the management of subjects with CP and the national registry of these patients. The review is presented on behalf of the national multidisciplinary craniopharyngioma working group.

Clinical presentation

Initial symptoms of CP are frequently unspecific, and the diagnosis can be made relatively late. According to the data from HIT Endo and Craniopharyngioma 2000 study data the most frequent symptoms before the diagnosis in children are headache (68%), followed by visual impairment (55%), growth failure (36%), nausea (34%) neurologic deficits (23%), polydipsia/polyuria (19%) and weight gain (16%).[25] In adults, the most common presenting symptoms are visual impairment (40–84%), headache (56%), menstrual irregularities in women (57%), loss of energy (32–48%) nausea and vomiting (26%), lethargy (26%), and weight gain (13–15%).[13,26,27] The period from initial symptoms to the diagnosis does not correlate with tumor size, hypothalamic involvement, functional capacity or survival.[26] It is however emphasized that weight gain and growth retardation are early signs of CP in children that should lead the investigator to further diagnostic workup. Raised intracranial pressure and/or acute vision loss because of tumor obstructing CSF pathways leading to obstructive hydrocephalus can also be the first manifestation, according to Mortini *et al.* more often identified in children.[26] In these patients, urgent surgical decompression is required and their presenting symptoms are the only ones connected with lower 10-year overall survival.[25]

Imaging and treatment

There is evidence that adequate presurgical imaging and assessment of hypothalamic involvement of CP is extremely important in estimating prognosis and long-term quality of life. Initial tumor involvement of the third ventricular floor, mammillary bodies and/or posterior hypothalamus on imaging are associated with a worse long-term prognosis due to hypothalamic obesity, regardless of chosen treatment strategies.[28-32] Magnetic resonance imaging (MRI) is the standard imaging modality in CP, but reliable discrimination between ACP and PCP based on neuroradiological criteria is not possible.[33] In addition, computer tomography (CT) limited to the sellar area and excluding orbital areas for better determinations of calcifications within the tumor is recommended. Papillary CP namely lacks calcifications and can be misdiagnosed as another type of a suprasellar tumor (Figure 1).[34]

A preoperative radiological grading system has been developed for pediatric patients.[35] Using this grading, the treatment of choice for CP without hypothalamic involvement (HI) (type 0 – no HI on MRI scan and type 1 – distorts or elevates the hypothalamus) is an attempt of complete resection

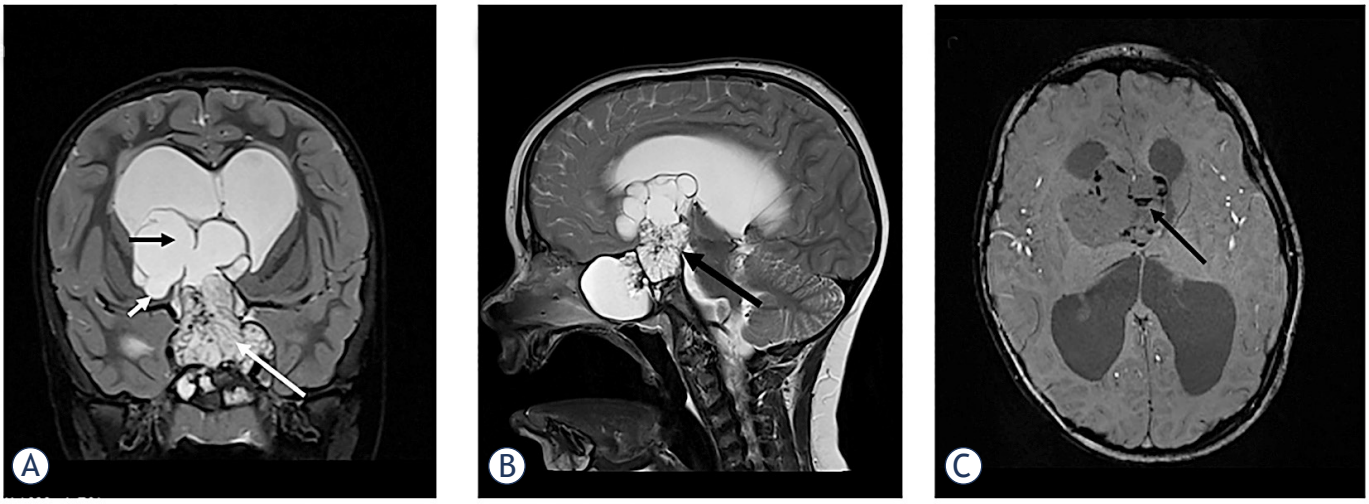

FIGURE 1. Large, partially solid, partially multicystic adamantinomatous craniopharyngioma in a 5-year old boy. **(A)** Coronal T2 sequence through sellar region; solid part of the tumor (white arrow) involves enlarged sella turcica, parasellar regions, occupies the suprasellar cistern and the third ventricle. The cystic portion of the tumor (black arrow) extends into the lateral ventricles and on the right side it infiltrates the adjacent brain parenchym (small arrow). Lateral ventricles are enlarged with a band of periventricular transependimal edema as a sign of acute hydrocephalus. **(B)** Sagital T2 sequence through the sellar region; Hypothalamus and mammillary bodies are not visible (arrow). **(C)** SWI sequence through the multicystic portion of the tumor shows multiple calcifications in the cyst walls (arrow).

(gross total resection - GTR), with preservation of visual, pituitary and hypothalamic function. For tumors located unfavourably (type 2 – hypothalamus not visible on MRI scan) GTR is not recommended. For prevention of severe morbidity, a subtotal resection (STR) should be performed, followed by adjuvant therapy.[28,35,36]

The optimal therapeutic strategy for CP is however still controversial. Surgical treatment of these lesions remains among the most challenging for neurosurgeons because of their complex and highly variable topographical relationships with crucial neural and vascular structures such as the optic chiasm, hypothalamus, third ventricle, and vessels of the circle of Willis. So far, no single best treatment paradigm exists, and the extent of surgical resection or adjuvant therapy should be considered on a case-to-case basis.

Previous studies show that the most significant factor associated with recurrence is the extent of surgical resection regardless of the histological subtype, but attempts of GTR in patients with tumor invading the hypothalamus results in significant morbidity in terms of hypothalamic dysfunction.[16,37,38] Therefore, the treatment focus is on prevention of additional hypothalamic injury. Precise presurgical imaging for defining the type based on location (primary third ventricle CP or primary suprasellar CP) and topography is essential.[30,32] Functional MRI of the infundibulum, tuber cinereum, mammillary bodies, and hypothalamus, although not currently feasible, may be helpful in distinguishing precise topography of CPs and planning the surgical approach.[39]

No significant difference was observed in 5- and 10-year overall survival (OS) and progression-free survival between GTR and STR followed by adjuvant therapy. STR without adjuvant therapy is associated with worse OS than STR with adjuvant therapy, with unacceptably high recurrent rates up to 63%.[15,40,41]

In patients that underwent STR postoperative external beam radiotherapy (RT) is presently standard of care to achieve an optimal progression-free survival.[13,41-44] In most studies, attention has been paid to radiation fibrosis syndrome while the impact of RT on QoL has been studied to a much lesser extent. Kiehna and Merchant reported results of meta-analysis of studies on pediatric CPs. They found out that more than two-thirds of patients treated with surgery and radiation therapy in childhood have favorable outcomes, and this rate is even higher in the modern era.[43] The most recent advances in the treatment of craniopharyngioma have focused on minimizing treatment-related toxicity. These advances include endoscopic surgery and precision radiotherapy. In the last decades radiation therapy technology has improved dose conformality and provided decreased doses to adjacent critical structures (hypothalamus, optic tract, pituitary gland, carotid

arteries, medial temporal lobe structures, etc.) with the goal of reducing long-term sequelae, especially endocrinologic and visual ones. Conformal RT enables a better coverage of the tumor while preserving surrounding tissue therefore decreasing the risk of adverse effects. Current techniques include fractionated three-dimension conformal RT, intensity modulated radiotherapy (IMRT), fractionated stereotactic radiotherapy (FSRT) or recently proton beam therapy (PBT). Tumor control between 80 and in access of 90% can be achieved.[45] Greenfield *et al.* published the first work on the use of IMRT in children with CPs and found this technique promising.[46] Harrabi *et al.* with colleagues reported that FSRT leads to excellent results in patients with CP regarding local control, overall survival and preservation of organ function.[47] Lately, in order to lessen adverse effects of radiation, PBT is increasingly used for the treatment of CPs in children. The major advantage of proton therapy is the high degree of dose conformity to the target. Beltran *et al.* retrospectively evaluated proton treatment plans with IMRT plan. He concluded that compared with photon IMRT proton therapy has the potential to significantly reduce whole brain and body irradiation. Result of that is lower collateral damage to critical structures thus reducing the risk of complications and secondary cancers.[48]

Regine and Kramer reported that a total dose of > 54 Gy is recommended for external radiation using conventional techniques with excessively rising recurrence rates for doses < 54 Gy. However, limitations are posed by the tolerance doses of vital organs in the vicinity. Therefore, commonly doses between 50–55.8 Gy, delivered in 1.5- to 2.0 Gy fractions, 5 days per week for a period of 6 weeks are used.[45,49]

If a cystic component in a tumor is present, careful monitoring during radiotherapy is necessary. Namely, dynamic cyst changes can occur throughout the 6 weeks of RT, recommending weekly MRIs during treatment to identify these changes, and to adapt RT plan according to changes in tumor volume.[13,46,50]

Stereotactic radiosurgery is an alternative to fractionated treatments in patients with craniopharyngioma harboring smaller lesions, but caution is needed because high dose applied in single fraction can carry higher risk for damage of vital structures.[45,51]

With the future development of targeted therapy, we should strive towards more personalized risk-adapted treatment strategy, taking the histological type of tumor and its mutations into consideration.

Molecular pathology

There are two main histological CP subtypes – adamantinomatous craniopharyngioma (ACP) and papillary craniopharyngioma (PCP). ACPs are more common and can be diagnosed at any age but are predominantly observed in the pediatric population. The average age of diagnosis of this subtype shows an asymmetric bimodal distribution, with a larger peak at 5–14 years and a smaller at 50–74 years.[1] PCPs account for approximately 11–14% of CPs and mainly occur in adults. The average age of diagnosis for this subtype is 44 ± 15 years.[27] PCPs have higher 5-year survival rates and less aggressive disease progression. PCPs are solid, more well circumscribed, while ACPs adhere to the surrounding, consist of a mixture of cysts and nodules and changes like fibrosis, calcifications and hemorrhages are seen.[52,53]

Important advances were made lately regarding the determination of the genes involved in the pathogenesis of the tumor that could have an important effect on the treatment modalities. ACPs are mainly caused by activating mutations of the Wingless pathway (WNT pathway) gene *CTNNB1,* encoding the β-catenin. Activating mutations in the gene are determined in more than two-thirds of CPs in recent studies.[54] They increase the resistance of β-catenin to proteasomal degradation resulting in its intranuclear accumulation. These clusters are pathologically unique for human ACP and are not present in any other pituitary tumour.[55,56] In one third of ACP the *CTNNB1* mutation is not identified, suggesting other genetic/epigenetic events might also be the cause of WNT activation.[54] Recently involvement of MAPK/ERK pathway in the tumorigenesis of ACP has been determined, which opens novel therapeutic opportunities by suppression of this pathway with chemical agents as is MEK inhibitor trametinib.[57]

In PCP subgroup *BRAF* V600E mutations were detected in about 90% and appear to be the critical event in the pathogenesis.[54,56] The same mutation is present in 7% of human cancers.[58] *BRAF* is a proto-oncogene encoding serine-threonine kinase and is involved in growth factor signaling and regulation. Its mutation results in a constitutively active form promoting cell proliferation and tumor growth. Although rarely, a coexistence of both mutations may occur.[59] Previous studies did not show larger chromosomal aberrations in any type of CP.[60]

While agents that target WNT signaling remain in development, the availability of BRAF inhibitors such as vemurafenib and dabrafenib suggests that

patients with papillary craniopharyngiomas could immediately benefit from such targeted therapeutics.[23,24,61-63] Vemurafenib and dabrafenib are already used as targeted therapy in other types of tumors with the same mutation. One of the most recent studies with the longest follow-up period, Himes BT *et al.*, demonstrated reduction of the tumor size using dabrafenib as a monotherapy for the treatment of recurrence of PCP. Patients remained symptom-free 1 year after administration and there was no radiographic evidence of tumor progression.[24] Recently a successful combination therapy with a dabrafenib and trametinib in reducing PCP in a subject with *BRAF* V600E mutation was published.[23]

Prieto and Pascual published a comprehensive overview about tissue biomarkers being currently used as predictors of tumour recurrence and aggressiveness of their behaviour, stressing that their precise impact still needs to be closely evaluated in conjunction with the degree of tumor removal, the tumor topography, the pattern of tumor attachment, and the histological variant observed in each case. Their early identification could also improve patient outcome, but so far tumor remnant after initial surgery remains the only well-established factor for recurrence.[54]

Long term consequences and prognosis

The long-term morbidity of craniopharyngiomas is associated with damage to critical neuronal structures by the primary or recurrent tumor combined with the adverse effects of the therapeutic interventions. Despite the improvements in the last decades, the outcome is still rather unfavorable. Patients with childhood-onset CP experience significantly more panhypopituitarism, morbid obesity, epilepsy and psychiatric conditions in comparison to patients with adult-onset disease.[8,11,14,19,64] Long term outcomes were shown to be particularly worse in the case of hypothalamic involvement, reducing 20-year OS rate and quality of life of these patients.[9,10,25] In this section, we will try to focus on differences in sequela between adult and childhood population.

Endocrine consequences

Hypotalamo-pituitary hormone deficiencies are determined in 40–87% of children at the time of childhood-onset CP and 73% adults present with at least one deficient hypothalamic-pituitary axis.[8,13,21,35,65,66] As shown in Table 1, after initial treatment the prevalence of endocrine deficits ranging from single hormone insufficiency to panhypopituitarism increases and it is seen in almost all patients, requiring lifelong follow-up by an endocrinologist.

In children with CP growth hormone deficiency is most frequently seen, occurring in up to 96%, adrenocorticotropic (ACTH), gonadotropin, thyroid stimulating hormone (TSH) deficiency follow in decreasing order. Central diabetes insipidus resulting from anti-diuretic hormone (ADH) deficiency occurs almost twice more frequently in children than in adults, can be transient after the procedure and it persists in 65–96% of childhood-onset CP subjects.[8,18,21] Substitution therapy with hr-GH is safe, effective and does not affect relapse and progression rates.[67] In patients with GH substitution, a better QoL has been reported.[11] In children after the surgery, despite their GH deficiency, a normal or accelerated growth pattern has been observed. Activation of IGF-1 by hypothalamic hyperphagia/obesity induced hyperinsulinism is suggested to explain this growth pattern.[68]

Sixty-one % of adults have panhypopituitarism after treatment for CP, most commonly affecting gonadotropin axis.[8] Post-surgical onset of central diabetes insipidus was observed in up to 69.6% of the patients.[33] Adequate timing and dosing of glucocorticoids, thyroxine, sex steroid and ADH is essential. Concerning GH substitution, observational studies suggest that GH replacement in adult-onset CP does not increase the risk of tumor recurrence. Lifelong surveillance by an endocrinologist is required.[33]

Metabolic consequences

Damage of the posterior hypothalamic region results in hypothalamic obesity (HO), which occurs in 40–66% of patients with childhood-onset CP and has a major impact on the outcome.[9] Especially preoperative lesions that include the dorsal hypothalamic area and dorsomedial nucleus in the posterior hypothalamus are at very high risk for rapid and pathological weight gain during the first year following surgery, sometimes beginning in the months prior to surgery. Postsurgical diabetes insipidus was found to be an endocrine marker for the development of HO.[29]

The major mechanisms that reinforce HO are vagally mediated hyperinsulinemia, disrupted

TABLE 1. Comparison of pediatric and adult-onset craniopharyngioma characteristics

	Pediatric-onset	Adult-onset
Age at presentation	30–50 % of all CPs Peak at 5–14 years[1]	Peak at 40–44 years[2]
Gender distribution (m/f)	Equal[8,21]	Equal[8,27]
Most frequent presentation	Headache (68–85%) Visual impairment (36– 55%) Growth failure (7–36%)[9,35,66]	Visual impairment (40–84%) Menstrual irregularities (57%) Headache (42–56%)[13,26,27]
Pathohistological type	Adamantinomatous 99% Papillary extremely rare*	Papillary 14–50%[33]
Initial hypothalamic involvement	42–66%[8,9,35]	42%[18]
Endocrine deficits at diagnosis		
Any	40–87%[8,13,21,35,65,66]	41–73%[8]
GH	41–75%[8,13,21,35,65,66]	18–86%[8,13]
FSH/LH	20–56%[8,13,21,35,65,66]	29–74%[8,13]
ACTH	8–68%[8,13,21,35,65,66]	35–58%[8,13]
TSH	15–32%[8,13,21,35,65,66]	35–56%[8,13]
ADH	7–17%[8,13,21,35,65,66]	6–17%[8,13]
Pituitary hormone deficiencies after treatment		
Any	64–100%[8,64]	48–97%[8,64]
GH	93–96%[8,18,21]	52–68%[8,18]
FSH/LH	59–95%[8,18,21]	70–94%[8,18]
ACTH	78–100%[8,18,21]	74–88%[8,18]
TSH	86–100%[8,18,21]	81–92%[8,18]
ADH	65–96%[8,18,21]	43–70%[8,18]
Panhypopituitarism***	43–100%[8,18,64]	59–74%[8,18,64]
Obesity**	44–64%[8,9,19,64]	41–47%[8,19,64]

* Only 23 identified cases since 1995.[83]

** Obesity was defined with BMI > 30 kg/m^2 in adults and BMI >95. percentile for their age in children.

*** Panhypopituitarism was defined as present when 3 anterior pituitary deficiencies were diagnosed in one patient (growth hormone deficiency, thyroid-stimulating hormone deficiency, adrenocorticotropic hormone deficiency, and late puberty in children or hypogonadism in adults).

ACTH = adrenocorticotropic hormone; ADH = vasopressin (antidiuretic hormone); FSH/LH = follicle stimulating hormone/luteinizing hormone; GH = growth hormone; TSH = thyroid stimulating hormone

or impaired sensitivity to feeding-related signals for leptin, insulin, and ghrelin, altered energy expenditure, reduced melatonin levels, increased daytime sleepiness and reduced physical activity. CNS stimulating agents, somatostatin analogs, a supraphysiological dosage of thyroid hormone, GLP-1 RAs in patients with intact hypothalamus and hindbrain and bariatric surgery have been considered as a potential treatment strategy in adult population based on some individual-level experiences or serial case reports.[69] Early involvement of a dietician, psychologist and physiotherapist by providing individual lifestyle and dietary advice may decrease aggravation of HO. Regular visits to the outpatient clinic should be offered to closely monitor weight development and to support patients. Unfortunately, no treatment options for HO have been proven to be effective so far.[69]

In 178 patients with CP Wijnen *et al*. reported the prevalence of metabolic syndrome (MetS) in almost half of the patients with HI (48% with childhood onset and 45% with adult-onset CP). Obesity and reduced HDL cholesterol were more prevalent in childhood-onset patients, whereas hypertension and elevated triglycerides were more prevalent in adults. MetS, regardless of the age of onset, was more frequent in female patients than in male patients (54% vs 40%) and in patients not treated for their GH deficiency (57% *vs*. 43%).[19] Non-alcoholic fatty liver disease occurs in about 50% of childhood-

onset CP patients with HI, especially in patients treated with stimulants for their daytime sleepiness and severe fatigue.[70,71] Increased mortality due to cardiovascular disease in hypopituitarism is already known and it is 3 to 19-fold higher in this specific subgroup of patients with CP. In women with CP, an even higher risk is reported.[10,72-75]

Visual impairment

Defoort *et al*. reported the presence of visual disturbances in up to 96% of patients at the diagnosis in pediatric CP cohort of twenty-nine patients. Typical manifestations are the loss of visual acuity, visual field defects, strabismus, papilledema or optic nerve atrophy. In children, the loss of visual acuity was most frequently observed, with post-surgical improvement in 46-66%.[76] The risk of post-surgical visual impairment increases with the initial pre-surgical severe visual defect and localization of the tumor in pre-chiasmatic area.[66] Wijnen *et al*. reports visual acuity disorder and visual field defect 63–66% of pediatric and adult patients after surgery.[8]

Cognitive and psychosocial deficits

Memory, attention, impulse control, motivation and socialization deficits are present in CP patients.[77,78] They cannot be fully explained by a lesion in the hypothalamus alone.

In patients with childhood-onset CP, the most consistent findings in the cognitive domain are impairments in learning and episodic memory. There is also evidence that hypothalamic tumor involvement reduces gray and white matter volumes in fronto-limbic areas, outside the area of tumor growth. Focal hypothalamic lesions may trigger distal changes in connected brain areas, which then contribute to the above-mentioned impairments, not explicable by a hypothalamic lesion alone.[79]

There is no published data on cognitive and social deficits in patients with adult-onset CP to the best of our knowledge.

Quality of life

Patients with childhood onset CP rated their social and emotional functioning lower than their healthy controls. The most frequent problems reported were difficulties with learning, inability to control emotions, unsatisfactory peer relationships and concerns regarding their physical appearance. Impairment in QoL was rather psychosocial than physical.[80] Patient's parents asses their QoL worse than patients themselves.[12]

Adult-onset CP patients score worse than the previous group, but on the contrary, they describe impairments in QoL mainly due to general and physical fatigue, psychical condition and physical mobility. Younger adults reported also social isolation and difficulties in social functioning. Adult-onset patients also performed worse on the depression score than childhood-onset patients. The main independent predictors for decreased QoL were visual field defects, female gender, repeated surgery and HO.[81,82]

Conclusions

CP is a low grade tumor with locally aggressive behaviour resulting in high morbidity in both children and adults. A multidisciplinary team of neurosurgeons, neuro-radiologists, neuro-oncologists pathologists and endocrinologists should be involved in the diagnosis, treatment planning and lifelong follow-up of these patients to achieve the best outcomes. The development of a national registry increases the quality of management. At present subtotal resection of the tumor with localized irradiation is the treatment of choice to prevent further complications associated with the hypothalamic damage. Careful pituitary hormone replacement in addition to individualized nutritional intake and regular physical activity planning is essential to decrease the morbidity associated with endocrine and metabolic consequences of the tumor and its management, especially if the hypothalamic region has been significantly damaged. Further studies of the signalling pathways involved in the pathogenesis of the tumor will hopefully give rise to novel treatment modalities, enabling a less aggressive surgical and radiation therapy and possibly better neuroendocrine and metabolic outcomes.

References

1. Bunin GR, Surawicz TS, Witman PA, Preston-Martin S, Davis F, Bruner JM. The descriptive epidemiology of craniopharyngioma. J Neurosurg 1998; **89:** 547-51. doi: 10.3171/jns.1998.89.4.0547

2. Nielsen EH, Feldt-Rasmussen U, Poulsgaard L, Kristensen LO, Astrup J, Jorgensen JO, et al. Incidence of craniopharyngioma in Denmark (n = 189) and estimated world incidence of craniopharyngioma in children and adults. *J Neurooncol* 2011; **104:** 755-63. doi: 10.1007/s11060-011-0540-6

3. Ostrom QT, Gittleman H, Liao P, Vecchione Koval T, Wolinsky Y, Kruchko C, et al. CBTRUS Statistical Report: primary brain and other central nervous system tumors diagnosed in the United States in 2010–2014. *Neuro Oncol* 2017; **19(Suppl. 5):** 1-88. doi: 10.1093/neuonc/nox158
4. Ostrom QT, Gittleman H, Xu J, Kromer C, Wolinsky Y, Kruchko C, et al. CBTRUS statistical report: Primary brain and other central nervous system tumors diagnosed in the United States in 2009-2013. *Neuro Oncol* 2016; **18:** 1-75. doi: 10.1093/neuonc/now207
5. Thapar K, Kovacs K. Neoplasms of the sellar region. Russell and Rubinstein's Pathology of tumors of the nervous system., 6th edition. McLendon RE, Rosenblum MK, Bigner DD, editors. Bica Raton, Florida: CRC Press Taylor & Francis Group; 1998. p. 629-80.
6. Zada G, Lin N, Ojerholm E, Ramkissoon S, Laws ER. Craniopharyngioma and other cystic epithelial lesions of the sellar region: a review of clinical, imaging, and histopathological relationships. *Neurosurg Focus* 2010; **28:** E4. doi: 10.3171/2010.2.FOCUS09318
7. Pascual JM, Prieto R, Rosdolsky M, Strauss S, Castro I, Verena D. Cystic tumors of the pituitary infundibulum: seminal autopsy specimens (1899 to 1904) that allowed clinical-pathological craniopharyngioma characterization. *Pituitary* 2018; **21:** 393-405. doi: 10.1007/s11102-018-0889-z
8. Wijnen M, Van Den Heuvel-Eibrink MM, Janssen JAMJL, Catsman-Berrevoets CE, Michiels EMC, Van Veelen-Vincent MLC, et al. Very long-term sequelae of craniopharyngioma. *Eur J Endocrinol* 2017; **176:** 755-67. doi: 10.1530/EJE-17-0044
9. Sterkenburg AS, Hoffmann A, Gebhardt U, Warmuth-Metz M, Daubenbüchel AMM, Müller HL. Survival, hypothalamic obesity, and neuropsychological/psychosocial status after childhood-onset craniopharyngioma: Newly reported long-term outcomes. *Neuro Oncol* 2015; **17:** 1029-38. doi: 10.1093/neuonc/nov044
10. Erfurth EM, Holmer H, Fjalldal SB. Mortality and morbidity in adult craniopharyngioma. *Pituitary* 2013; **16:** 46-55. doi: 10.1007/s11102-012-0428-2
11. Müller HL, Merchant TE, Puget S, Martinez-Barbera JP. New outlook on the diagnosis, treatment and follow-up of childhood-onset craniopharyngioma. *Nat Rev Endocrinol 2*017; **13:** 299-312. doi: 10.1038/nrendo.2016.217
12. Heinks K, Boekhoff S, Hoffmann A, Warmuth-Metz M, Eveslage M, Peng J, et al. Quality of life and growth after childhood craniopharyngioma: results of the multinational trial KRANIOPHARYNGEOM 2007. *Endocrine* 2018; **59:** 364-72. doi: 10.1007/s12020-017-1489-9
13. Karavitaki N, Brufani C, Warner JT, Adams CBT, Richards P, Ansorge O, et al. Craniopharyngiomas in children and adults: systematic analysis of 121 cases with long-term follow-up. *Clin Endocrinol (Oxf)* 2005; **62:** 397-409. doi: 10.1111/j.1365-2265.2005.02231.x
14. Muller HL. Craniopharyngeoma - a chronic disease. *Swiss Med Wkly* 2018; **148:** w14548. doi: 10.4414/smw.2017.14548
15. Schoenfeld A, Pekmezci M, Barnes MJ, Tihan T, Gupta N, Lamborn KR, et al. The superiority of conservative resection and adjuvant radiation for craniopharyngiomas. *J Neurooncol* 2012; **8:** 133-9. doi: 10.1007/s11060-012-0806-7
16. Hoffmann A, Warmuth-Metz M, Gebhardt U, Müller H. Childhood craniopharyngioma – changes of treatment strategies in the trials KRANIOPHARYNGEOM 2000/2007. *Klin Padiatr* 2014; **226:** 161-8. doi: 10.1055/s-0034-1368785
17. Ajithkumar T, Mazhari AL, Stickan-Verfürth M, Kramer PH, Fuentes CS, Lambert J, et al. Proton therapy for craniopharyngioma - an early report from a single European centre. *Clin Oncol* 2018; **30:** 307-16. doi: 10.1016/j.clon.2018.01.012
18. Kendall-Taylor P, Jönsson PJ, Abs R, Erfurth EM, Koltowska-Häggström M, Price DA, et al. The clinical, metabolic and endocrine features and the quality of life in adults with childhood-onset craniopharyngioma compared with adult-onset craniopharyngioma. *Eur J Endocrinol* 2005; **152:** 557-67. doi: 10.1530/eje.1.01877
19. Wijnen M, Olsson DS, Van Den Heuvel-Eibrink MM, Hammarstrand C, Janssen JAMJL, Van Der Lely AJ, et al. The metabolic syndrome and its components in 178 patients treated for craniopharyngioma after 16 years of follow-up. *Eur J Endocrinol* 2018; **178:** 11-22. doi: 10.1530/EJE-17-0387
20. Andereggen L, Hess B, Andres RH, El-Koussy M, Mariani L, Raabe A, et al. A ten-year follow-up study of treatment outcome of craniopharyngiomas. *Swiss Med Wkly* 2018; **148:** 1-8. doi: 10.4414/smw.2017.14521
21. Tan TSE, Patel L, Gopal-Kothandapani JS, Ehtisham S, Ikazoboh EC, Hayward R, et al. The neuroendocrine sequelae of paediatric craniopharyngioma: a 40-year meta-data analysis of 185 cases from three UK centres. *Eur J Endocrinol* 2017; **176:** 359-69. doi: 10.1530/EJE-16-0812
22. Bosnjak R, Benedicic M, Vittori A. Early outcome in endoscopic extended endonasal approach for removal of supradiaphragmatic craniopharyngiomas: a case series and a comprehensive review. *Radiol Oncol* 2013; **47:** 266-79. doi: 10.2478/raon-2013-0036
23. Brastianos PK, Shankar GM, Gill CM, Taylor-Weiner A, Nayyar N, Panka, DJ, et al. Dramatic response of BRAF V600E mutant papillary craniopharyngioma to targeted therapy. *J Natl Cancer Inst* 2016; **108:** 1-5. doi: 10.1093/jnci/djv310
24. Himes BT, Ruff MW, Gompel JJ Van, Park SS, Galanis E, Kaufmann TJ, et al. Recurrent papillary craniopharyngioma with dabrafenib: case report. *J Neurosurg* 2018; **1:** 1-5. doi: 10.3171/2017.11.JNS172373
25. Hoffmann A, Boekhoff S, Gebhardt U, Sterkenburg AS, Daubenbüchel AMM, Eveslage M, et al. History before diagnosis in childhood craniopharyngioma: Associations with initial presentation and long-term prognosis. *Eur J Endocrinol* 2015; **173:** 853-62. doi: 10.1530/EJE-15-0709
26. Mortini P, Losa M, Pozzobon G, Barzaghi R, Riva M, Acerno S, et al. Neurosurgical treatment of craniopharyngioma in adults and children: early and long-term results in a large case series. *J Neurosurg* 2011; **114:** 1350-9. doi: 10.3171/2010.11.JNS10670
27. Crotty TB, Scheithauer BW, Young WF, Davis DH, Shaw EG, Miller GM, et al. Papillary craniopharyngioma: a clinicopathological study of 48 cases. *J Neurosurg* 1995; **83:** 206-14. doi: 10.3171/jns.1995.83.2.0206
28. Müller HL. Hypothalamic involvement in craniopharyngioma—Implications for surgical, radiooncological, and molecularly targeted treatment strategies. *Pediatr Blood Cancer* 2018; **65:** e26936. doi: 10.1002/pbc.26936
29. Roth CL, Eslamy H, Werny D, Elfers C, Shaffer ML, Pihoker C, et al. Semiquantitative analysis of hypothalamic damage on MRI predicts risk for hypothalamic obesity. *Obesity* 2015; **23:** 1226-33. doi: 10.1002/oby.21067
30. Mortini P, Gagliardi F, Bailo M, Spina A, Parlangeli A, Falini A, et al. Magnetic resonance imaging as predictor of functional outcome in craniopharyngiomas. *Endocrine* 2016; **51:** 148-62. doi: 10.1007/s12020-015-0683-x
31. Müller HL. Craniopharyngioma and hypothalamic injury: latest insights into consequent eating disorders and obesity. *Curr Opin Endocrinol Diabetes Obes* 2016; **23:** 81-9. doi: 10.1097/MED.0000000000000214
32. Pascual JM, Prieto R, Carrasco R, Barrios L. Displacement of mammillary bodies by craniopharyngiomas involving the third ventricle: surgical-MRI correlation and use in topographical diagnosis. *J Neurosurg* 2013; **119:** 381-405. doi: 10.3171/2013.1.JNS111722
33. Zoicas F, Schöfl C. Craniopharyngioma in adults. *Front Endocrinol (Lausanne)* 2012; **3:** 46. doi: 10.3389/fendo.2012.00046
34. Amelot A, Borha A, Calmon R, Barbet P, Puget S. Child dermoid cyst mimicking a craniopharyngioma: the benefit of MRI T2-weighted diffusion sequence. *Child's Nerv Syst* 2018; **34:** 359-62. doi: 10.1007/s00381-017-3602-z
35. Puget S, Garnett M, Wray A, Grill J, Habrand JL, Bodaert N, et al. Pediatric craniopharyngiomas: classification and treatment according to the degree of hypothalamic involvement. *J Neurosurg Pediatr* 2007; **106:** 3-12. doi: 10.3171/ped.2007.106.1.3
36. Elowe-Gruau E, Beltrand J, Brauner R, Pinto G, Samara-Boustani D, Thalassinos C, et al. Childhood craniopharyngioma: hypothalamus-sparing surgery decreases the risk of obesity. *J Clin Endocrinol Metab* 2013; **98:** 2376-82. doi: 10.1210/jc.2012-3928
37. Weiner HL, Wisoff JH, Rosenberg ME, Kupersmith MJ, Cohen H, Zagzag D, et al. Craniopharyngiomas: a clinicopathological analysis of factors predictive of recurrence and functional outcome. *Neurosurgery* 1994; **35:** 1001-11. http://dx.doi.org/10.1227/00006123-199412000-00001.
38. Müller HL, Gebhardt U, Teske C, Faldum A, Zwiener I, Warmuth-Metz M, et al. Post-operative hypothalamic lesions and obesity in childhood craniopharyngioma: results of the multinational prospective trial KRANIOPHARYNGEOM 2000 after 3-year follow-up. *Eur J Endocrinol* 2011; **165:** 17-24. doi: 10.1530/EJE-11-0158
39. Gu Y, Zhang X. Letter to the Editor: mammillary body angle and craniopharyngioma. *J Neurosurg* 2014; **120:** 1241-5. doi: 10.3171/2013.11.JNS132343
40. Coury JR, Davis BN, Koumas CP, Manzano GS, Dehdashti AR. Histopathological and molecular predictors of growth patterns and recurrence in craniopharyngiomas: a systematic review. *Neurosurg Rev* 2018. doi: 10.1007/s10143-018-0978-5
41. Karavitaki N, Cudlip S, Adams CB, and Wass JA. Craniopharyngiomas. *Endocr Rev* 2006; **27:** 371-97. doi: 10.1210/er.2006-0002
42. Clark AJ, Cage TA, Aranda D, Parsa AT, Sun PP, Auguste KI, et al. A systematic review of the results of surgery and radiotherapy on tumor control for pediatric craniopharyngioma. *Child's Nerv Syst* 2013; **29:** 231-8. doi: 10.1007/s00381-012-1926-2

43. Kiehna EN, Merchant TE. Radiation therapy for pediatric craniopharyngioma. *Neurosurg Focus* 2010; **28:** E10. doi: 10.3171/2010.1.FOCUS09297

44. O'steen L, Indelicato DJ. Advances in the management of craniopharyngioma. *F1000Research* 2018; **7:** 1632. doi:10.12688/f1000research.15834.1

45. Kortmann RD. Different Approaches in Radiation Therapy of Craniopharyngioma. *Front Endocrinol (Lausanne)* 2011; **2:** 100. doi: 10.3389/fendo.2011.00100

46. Bishop AJ, Greenfield B, Mahajan A, Paulino AC, Okcu MF, Allen, PK, et al. Proton beam therapy versus conformal photon radiation therapy for childhood craniopharyngioma: Multi-institutional analysis of outcomes, cyst dynamics, and toxicity. *Int J Radiat Oncol Biol Phys* 2014; **90:** 354-61. doi: 10.1016/j.ijrobp.2014.05.051

47. Harrabi SB, Adeberg S, Welzel T, Rieken S, Habermehl D, Debus J, et al. Long term results after fractionated stereotactic radiotherapy (FSRT) in patients with craniopharyngioma: maximal tumor control with minimal side effects. *Radiat Oncol* 2014; **9:** 203. doi: 10.1186/1748-717X-9-203

48. Beltran C, Roca M, Merchant TE. On the Benefits and Risks of Proton Therapy in Pediatric Craniopharyngioma. *Int J Radiat Oncol* 2012; **82:** 281-7. doi: 10.1016/j.ijrobp.2011.01.005

49. Regine WF, Kramer S. Pediatric craniopharyngiomas: Long term results of combined treatment with surgery and radiation. *Int J Radiat Oncol* 1992; **24:** 611-17. doi: 10.1016/0360-3016(92)90705-M

50. Winkfield KM, Linsenmeier C, Yock TI, Grant PE, Yeap BY, Butler WE, et al. Surveillance of Craniopharyngioma Cyst Growth in Children Treated With Proton *Radiotherapy Int J Radiat Oncol* 2009; **73:** 716-21. doi: https://doi.org/10.1016/j.ijrobp.2008.05.010

51. Losa M, Pieri V, Bailo M, Gagliardi F, Barzaghi LR, Gioia L, et al. Single fraction and multisession Gamma Knife radiosurgery for craniopharyngioma. *Pituitary* 2018; **21:** 499-506. doi: 10.1007/s11102-018-0903-5

52. Buslei R, Nolde M, Hofmann B, Meissner S, Eyupoglu IY, Siebzehnrübl F, et al. Common mutations of β-catenin in adamantinomatous craniopharyngiomas but not in other tumours originating from the sellar region. *Acta Neuropathol* 2005; **109:** 589-97. doi: 10.1007/s00401-005-1004-x

53. Pekmezci M, Louie J, Gupta N, Bloomer MM, Tihan T. Clinicopathological characteristics of adamantinomatous and papillary craniopharyngiomas: University of California, San Francisco experience 1985-2005. *Neurosurgery* 2010; **67:** 1341-9. doi: 10.1227/NEU.0b013e3181f2b583

54. Prieto R, Pascual JM. Can tissue biomarkers reliably predict the biological behavior of craniopharyngiomas? A comprehensive overview. *Pituitary* 2018; **21:** 431-42. doi: 10.1007/s11102-018-0890-6

55. Apps JR, Martinez-Barbera JP. Molecular pathology of adamantinomatous craniopharyngioma: review and opportunities for practice. *Neurosurg Focus* 2016; **41:** E4. doi: 10.3171/2016.8.FOCUS16307

56. Brastianos PK, Taylor-Weiner A, Manley PE, Robert T, Dias-Santagata D, Thorner AR, et al. Exome sequencing identifies BRAF mutations in papillary craniopharyngiomas. *Nat Genet* 2014; **46:** 161-5. doi: 10.1038/ng.2868

57. Apps JR, Carreno G, Gonzalez-Meljem JM, Haston S, Guiho R, Cooper JE, et al. Tumour compartment transcriptomics demonstrates the activation of inflammatory and odontogenic programmes in human adamantinomatous craniopharyngioma and identifies the MAPK/ERK pathway as a novel therapeutic target. *Acta Neuropathol* 2018; **135:** 757-77. doi: 10.1007/s00401-018-1830-2

58. Davies H, Bignell GR, Cox C, Stephens P, Edkins S, Clegg S, et al. Mutations of the BRAF gene in human cancer. *Nature* 2002; **417:** 949. doi: 10.1038/nature00766

59. Larkin SJ, Preda V, Karavitaki N, Grossman A, Ansorge O. BRAF V600E mutations are characteristic for papillary craniopharyngioma and may coexist with CTNNB1-mutated adamantinomatous craniopharyngioma. *Acta Neuropathol* 2014; **127:** 927-9. doi: 10.1007/s00401-014-1270-6

60. Bi WL, Larsen AG, Dunn IF. Genomic Alterations in Sporadic Pituitary Tumors. *Curr Neurol Neurosci Rep* 2018; **18:** 4. doi: 10.1007/s11910-018-0811-0

61. Aylwin SJB, Bodi I, Beaney R. Pronounced response of papillary craniopharyngioma to treatment with vemurafenib, a BRAF inhibitor. *Pituitary* 2016; **19:** 544-6. doi: 10.1007/s11102-015-0663-4

62. Roque A, Odia Y. BRAF-V600E mutant papillary craniopharyngioma dramatically responds to combination BRAF and MEK inhibitors. *CNS Oncol* 2017; **6:** 95-9. doi: 10.2217/cns-2016-0034

63. Rostami E, Witt Nyström P, Libard S, Wikström J, Casar-Borota O, Gudjonsson O. Recurrent papillary craniopharyngioma with BRAFV600E mutation treated with neoadjuvant-targeted therapy. *Acta Neurochir (Wien)* 2017; **159:** 2217-21. doi: 10.1007/s00701-017-3311-0

64. Caldarelli M, Massimi L, Tamburrini G, Cappa M, Di Rocco C. Long-term results of the surgical treatment of craniopharyngioma: the experience at the Policlinico Gemelli, Catholic University, Rome. *Child's Nerv Syst* 2005; **21:** 747-57. doi: 10.1007/s00381-005-1186-5

65. Müller HL. Childhood craniopharyngioma. *Pituitary* 2013; **16:** 56-67. doi: 10.1007/s11102-012-0401-0

66. Boekhoff S, Bogusz A, Sterkenburg AS, Eveslage M, Müller HL. Long-term effects of growth hormone replacement therapy in childhood-onset craniopharyngioma: results of the German Craniopharyngioma Registry (HIT-Endo). *Eur J Endocrinol* 2018; **179:** 331-41. doi: 10.1530/EJE-18-0505.

67. Geffner ME. The growth without growth hormone syndrome. *Endocrinol Metab Clin* 1996; **25:** 649-63. doi: 10.1016/S0889-8529(05)70345-5

68. Holmer H, Pozarek G, Wirfält E, Popovic V, Ekman B, Björk J, et al. Reduced energy expenditure and impaired feeding-related signals but not high energy intake reinforces hypothalamic obesity in adults with childhood onset craniopharyngioma. *J Clin Endocrinol Metab* 2010; **95:** 5395-402. doi: 10.1210/jc.2010-0993

69. Bereket A, Kiess W, Lustig RH, Müller HL, Goldstone AP, Weiss R, et al. Hypothalamic obesity in children. *Obes Rev* 2012; **13:** 780-98. doi: 10.1111/j.1467-789X.2012.01004

70. Hoffmann A, Bootsveld K, Gebhardt U, Daubenbüchel AMM, Sterkenburg AS, Müller HL. Nonalcoholic fatty liver disease and fatigue in long-term survivors of childhood-onset craniopharyngioma. *Eur J Endocrinol* 2015; **173:** 389-97. doi: 10.1530/EJE-15-0422

71. Tomlinson JW, Holden N, Hills RK, Wheatley K, Clayton RN, Bates AS, et al. Association between premature mortality and hypopituitarism. *Lancet* 2001; **357:** 425-31. doi: 10.1016/S0140-6736(00)04006-X

72. Rosén T, Bengtsson BA. Premature mortality due to cardiovascular disease in hypopituitarism. Lancet 1990; **336:** 285-8. doi: 10.1016/0140-6736(90)91812-O

73. Bülow B, Attewell R, Hagmar L, Malmström P, Nordström CH, Erfurth EM. Postoperative prognosis in craniopharyngioma with respect to cardiovascular mortality, survival, and tumor recurrence. *J Clin Endocrinol Metab* 1998; **83:** 3897-904. doi: 10.1210/jc.83.11.3897

74. Holmer H, Ekman B, Björk J, Nordstöm CH, Popovic V, Siversson AB, et al. Hypothalamic involvement predicts cardiovascular risk in adults with childhood onset craniopharyngioma on long-term GH therapy. *Eur J Endocrinol* 2009; **161:** 671-9. doi: 10.1530/EJE-09-0449

75. Defoort-Dhellemmes S, Moritz F, Bouacha I, Vinchon M. Craniopharyngioma: ophthalmological aspects at diagnosis. *J Pediatr Endocrinol Metab* 2006; **19(Suppl 1):** 321-4. http://europepmc.org/abstract/MED/16700306

76. Pierre-Kahn A, Recassens C, Pinto G, Thalassinos C, Chokron S, Soubervielle JC, et al. Social and psycho-intellectual outcome following radical removal of craniopharyngiomas in childhood. A prospective series. *Child's Nerv Syst* 2005; **21:** 817-24. doi: 10.1007/s00381-005-1205-6

77. Riva D, Pantaleoni C, Devoti M, Saletti V, Nichelli F, Giorgi C. Late neuropsychological and behavioural outcome of children surgically treated for craniopharyngioma. *Child's Nerv Syst* 1998; **14:** 179-84. doi: 10.1007/s003810050207

78. Özyurt J, Müller HL, Warmuth-Metz M, Thiel CM. Hypothalamic tumors impact gray and white matter volumes in fronto-limbic brain areas. *Cortex* 2017; **89:** 98-110. doi: 10.1016/j.cortex.2017.01.017

79. Poretti A, Grotzer MA, Ribi K, Schonle E, Boltshauser E. Outcome of craniopharyngioma in complications and quality of life. *Dev Med Child Neurol* 2004; **46:** 220-9. doi: 10.1111/j.1469-8749.2004.tb00476.x

80. Dekkers OM, Biermasz NR, Smith JWA, Groot LE, Roelfsema F, Romijn, JA, et al. Quality of life in treated adult craniopharyngioma patients. *Eur J Endocrinol* 2006; **154:** 483-9. doi: 10.1530/eje.1.02114

81. Gautier A, Godbout A, Grosheny C, Tejedor I, Coudert M, Courtillot C, et al. Markers of recurrence and long-term morbidity in craniopharyngioma: a systematic analysis of 171 patients. *J Clin Endocrinol Metab* 2012; **97:** 1258-67. doi: 10.1210/jc.2011-2817

82. van Iersel L, Meijneke RWH, Schouten-van Meeteren AYN, Reneman L, de Win MM, van Trotsenburg ASP, et al. The development of hypothalamic obesity in craniopharyngioma patients: a risk factor analysis in a well-defined cohort. *Pediatr Blood Cancer* 2018; **65:** e26911. doi: 10.1002/pbc.26911

83. Borrill R, Cheesman E, Stivaros S, Kamaly-Asl ID, Gnanalingham K, Kilday J-P. Papillary craniopharyngioma in a 4-year-old girl with BRAF V600E mutation: a case report and review of the literature. *Child's Nerv Syst* 2019; **35:** 169-73. doi:10.1007/s00381-018-3925-4.

review

Cytokine CCL5 and receptor CCR5 axis in glioblastoma multiforme

Miha Koprivnikar Kranjc[1], Metka Novak[1], Richard G. Pestell[2], Tamara T. Lah[1,3]

[1] Department of Genetic Toxicology and Cancer Biology, National Institute of Biology, Ljubljana, Slovenia
[2] Pennsylvania Cancer and Regenerative Medicine Research Center, Baruch S. Blumberg Institute, Pennsylvania Biotechnology Center, Wynnewood, Pennsylvania, USA
[3] Faculty of Chemistry and Chemical Engineering, University of Ljubljana, Ljubljana, Slovenia

Radiol Oncol 2019; 53(4): 397-406.

Received 14 August 2019
Accepted 15 October 2019

Correspondence to: Prof. Tamara Lah Turnšek, Ph.D., Department of Genetic Toxicology and Cancer Biology, National Institute of Biology, Večna pot 111, SI-1000 Ljubljana, Slovenia. E-mail: tamara.lah@nib.si

Disclosure: No potential conflicts of interest were disclosed.

Background. Glioblastoma is the most frequent and aggressive brain tumour in humans with median survival from 12 to 15 months after the diagnosis. This is mostly due to therapy resistant glioblastoma stem cells in addition to intertumour heterogeneity that is due to infiltration of a plethora of host cells. Besides endothelial cells, mesenchymal stem cells and their differentiated progenies, immune cells of various differentiation states, including monocytes, comprise resident, brain tumour microenvironment. There are compelling evidence for CCL5/CCR5 in the invasive and metastatic behaviour of many cancer types. CCR5, a G-protein coupled receptor, known to function as an essential co-receptor for HIV entry, is now known to participate in driving tumour heterogeneity, the formation of cancer stem cells and the promotion of cancer invasion and metastasis. Clinical trials have recently opened targeting CCR5 using a humanized monoclonal antibody (leronlimab) for metastatic triple negative breast cancer (TNBC) or a small molecule inhibitor (maraviroc) for metastatic colon cancer. There are important CCL5 and CCR5 structure and signalling mechanisms in glioblastoma. In addition, the CCL5/CCR5 axis directs infiltration and interactions with monocytes/macrophages and mesenchymal stem cells, comprising glioblastoma stem cell niches.

Conclusions. CCR5 is highly expressed in glioblastoma and is associated with poor prognosis of patients. CCL5/CCR5 is suggested to be an excellent new target for glioblastoma therapy. The molecular mechanisms, by which chemoattractant and receptor respond within the complex tissue microenvironment to promote cancer stem cells and tumour heterogeneity, should be considered in forthcoming studies.

Key words: cytokines; CCL5-RANTES; glioblastoma; tumour microenvironment; mesenchymal stem cells; signalling

Introduction

Brain tumours originate from various types of cells, of which gliomas are most frequent. Recent epidemiological data in UK confirmed that glioblastoma (GB) is also the most common among glial tumours with 5–7 cases per 100.000 individuals yearly, and represents 50% of all gliomas.[1] The World Health Organisation (WHO) distinguishes four grades of glioma, of which GB is the most aggressive, invasive, and lethal among all types of brain tumours. According to the standard histological classification, GB originates from neoplastic glial cells, also called astrocytes, either *via* the *de novo* pathway without clinical or histologic evidence of a less malignant precursor lesions (primary glioblastoma) or *via* the progressive pathway through development from a low-grade astrocytoma, progressing to anaplastic astrocytoma into diffuse glioblastoma (secondary glioblastoma). The major marker of secondary glioblastoma is mutated isocitrate dehydrogenase (IDH1)[2], although also expressed in the proneural subtype of primary glioblastoma. Regardless of the origin,

GB is characterized by histological features, such as necrosis, vascular proliferation and pleomorphism.[3] Contrary to most tumour types, irradiation and chemotherapy have proven to be ineffective to impair GB progression in longer term, demonstrating its remarkable therapeutic resistance.[4] Commonly used chemotherapeutic is temozolomide (TMZ), showing the highest effectiveness in GB.[3,5] However, only in about 55–60% of patients with methylated, *i.e.* silenced gene coding for O^6-methylguanine deoxyribonucleic acid (DNA) methyltransferase (MGMT), thereby lowering the enzyme expression, the responsiveness to TMZ is more effective.[6] There is thus continuous search for new, adjuvant therapeutics, including kinase inhibitors, anti-angiogenic agents and recently also immunotherapeutics, to increase average survival of glioblastoma patients.

There are other reasons for GB therapy resistance, *i.e.* the presence of glioblastoma stem cells (GSCs), mostly due to their high DNA repair mechanisms expression.[7] The heterogeneity and plasticity of these cells that carry the genetic fingerprint of the developing glioma, has been recognised as one of the additional obstacles for their resistance. GSCs, similar to normal neural cells, which are precursors of glial and neural cells, express the characteristic stemness genes (e.*g.* CD133, Sox2, Nanog, Olig 4, Notch, etc.), in addition to selected oncogenes and tumour suppressor genes.[8] The initial transcriptome analyses by Philips *et al* [9] and Verhaak *et al.*[10], set the basis for the Cancer Genome Atlas (TCGA), defining four different glioblastoma subtypes: the proneural (PN), mesenchymal (MES), neural (N), and classical (CL) by their major genomic characteristics, which are: PDGFRA/IDH1 (in PN), NF1/TP53 (in MES) and epidermal growth factor receptor EGFR abnormalities *i.e.* amplification of the epidermal growth factor (EGF) (in N) and mutation in EGFRvIII/PTEN (in CL). These GB subtypes differ significantly in survival rate, being shorter in MES subtype. However, mixed subtypes are observed in the single tumour, giving rise to intra-tumour heterogeneity.[11]

Tumour microenvironment

Solid tumour progression is not only relaying on the genetic and epigenetic variations of cancerous cells acquired during their evolution, but also on how their homotypic and heterotypic interactions with the stromal cells of associated microenvironment are. The "tumour microenvironment" (TME) consists not only of local, resident cells being invaded by the tumour cells, but also of infiltrating host cells, e.g. bone-marrow and blood-derived mesenchymal stem cells (MSC) and haematopoietic stem cells (HSC) and their progenitors, e.g. mature lymphocytes, macrophages, etc. Very recently, Salmon *et al.*[12] reviewed specific determinants that might influence tumours development and argue that unrevealing these selective interactions, mediating for example tumour immunity should facilitate development of immunotherapeutic precision strategies for patients with cancer.

In glioblastoma in addition to their autonomous (inter-tumour) heterogeneity[11], the increasing attention is paid to their non-autonomous heterogeneity (intra-tumour heterogeneity), that is presenting an obstacle to a more informed treatment, as we still do not understand the ability of GB cells to manipulate and exploit these non-cancerous cells collectively termed "tumour stroma". As stated by Broekman *et al.*[13], almost all cell types in the GB stroma are affected: the tumour is able to stimulate angiogenesis and co-opt existing vasculature, suppress immune cell functions, disarm microglia and macrophages that should recognize and fight these "foreign elements" in the brain and coerce astrocytes into supporting tumour modification extracellular matrix (ECM) to facilitate invasion. GB cells recruit innate immune cells and change their phenotype to support tumour growth and suppress adaptive immune responses.[14] The increasing understanding of how T cells access the brain and how the tumour tricks the immune response, offers new strategies for mobilizing an anti-immune tumour response. For example, GB cells extensive cross-talk with microglia and infiltrating macrophages, through the release of cytokines (see below), extracellular vesicles exchange and connecting nanotubes and microtubules, results in their support to malignancy, as reviewed by Matias *et al*.[15] Among these cells, MSC homing to GB, have crucial effects on the microenvironment, either by their de-differentiation to other stromal cells, *via* paracrine effectors such as immunomodulatory cytokines[16], or by direct interactions with GB cells.[17]

Thus, GB cells spreading to the brain involve multiple modes of communication with stromal cells as extensively reviewed by Matias *et al.*[15] The aim of this review is to reveal the complex interactions of one of the most important cytokines, affecting glioblastoma progression i.e., chemokine (C-C motif) ligand 5 (CCL5) and its receptors.

Inflammatory chemokines & cytokines in cancer

As reviewed by Balkwill[18], chemokines are chemotactic cytokines that cause directed migration of stromal cells, such as leukocytes, that are induced by inflammatory cytokines. Chemokine signalling results in transcription of target genes that are involved in cell invasion, motility, interactions with the extracellular matrix (ECM) and cell survival. Chemokine signalling can coordinate cell movement during inflammation, as well as the homeostatic transport of HSCs, MSCs, myeloids cells lymphocytes, dendritic cells and neutrophils, as well as cancer-associated fibroblasts (CAFs).[19] Directed migration of cells that express the appropriate chemokine receptor, occurs along a chemical gradient of ligand - known as the chemokine-receptor axis — allowing cells to move towards high local concentrations of chemokines. More than 50 human chemokines and 20 chemokine receptors have been discovered so far. Cytokines, as pro-inflammatory mediators, when excessive, also play a role in causing chronic inflammation, for example induced by bacterial (e.g. by *H. pylori*) or after viral (Hepatitis B) infections, inducing immune suppression.[20] Various cancers have a specific complex chemokine network that influences the immune-cell recruitment of inflammatory cells to the tumour milieu, but being neutralised by cancer immune suppression, and providing an immunological privilege that enables neoplasia, i.*e.* tumour cell growth, survival and migration, angiogenesis and metastasis.[19,21]

CCL5 - RANTES and its receptors

The cytokine CCL5, also classified as C-C motif chemokine 5, has been initially termed RANTES ("Regulated upon Activation Normal T cell Expressed and Secreted"), and as a potent chemokine, attracting leukocytes.[22] Later, CCL5 was recognised as a versatile inflammatory mediator, expressed by breast cancer cells (BC), where along with CCL2 it promoted pro-malignant activities by attracting macrophages, T-cells and granulocytes, as well as mesenchymal stem cells and enhancing angiogenesis.[23] CCL5 has been suggested as potential therapeutic target to impair the disease progression. In immune cells, CCL5 was reported initially as a HIV-suppressive factor and expressed mainly by CD8+ T cells.[24] It binds to its cognate receptor C-C chemokine receptor type 5 (CCR5), which is (alongside C-X-C chemokine receptor type 4 (CXCR4)), an HIV entry co-receptor into CD4+ T cells.[25] The Food and Drug Administration approved the first CCR5-based entry inhibitor, now called maraviroc (MRV) in 2009, and based on this, new drugs that promote CCR5 and CXCR4 internalization, independent of canonical cellular signalling, provided clinical benefits for HIV patients with minor side effects.

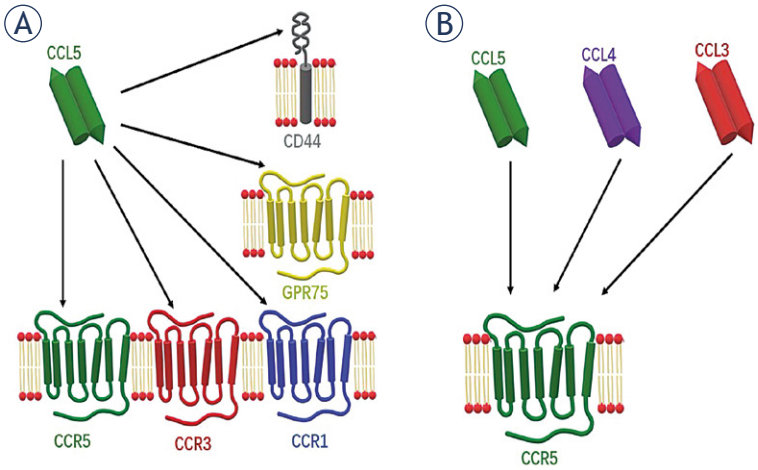

FIGURE 1. Chemokine CCL5 promiscuous binding to receptors. A variety of chemokine-receptors are interacting with CCL5/CCR5 in the signalling axis: **(A)** in addition to the cognate receptor CCR5, CCL5 binds also to CCR3 and CCR1. Non-conventional receptors are GPR75 and CD44. **(B)** The chemokines which bind to CCR5 are also CCL5, CCL4 and CCL3.

The mode of CCL5 action thus comprises binding not only to its cognate and the most studied interacting partner, the CCR5 membrane receptor, but also to other members of the G-protein coupled receptors (GPCR), such as C-C chemokine receptor type 1 (CCR1) and C-C chemokine receptor type 3 (CCR3). In addition to that, non-conventional or auxiliary receptors of CCL5 are CD44[26] and GPR75 (Figure 1A).[27] This is not unusual, as many chemokine receptors display promiscuous ligand binding, meaning they have more than one high-affinity ligand.[28] Such variety of CCL5 interactions causes the activation of multiple pathways and gives the ligand a diverse range of not only physiological, but also pathological functions, including in cancer.[29] In this vein, CCL5 has been shown to be highly expressed in a plethora of cancer types, such as colorectal[30], lung[31], prostate[32], breast[28,33,34] and cervical cancer.[35] In addition, tissue or plasma CCL5 also serve as a marker of poor prognosis, as it is the case in cervical[35], prostate[32], gastric[36], breast[37], pancreatic cancer[38], as well as in glioblastoma.[39] The cells that express and secrete CCL5 in cancer,

can either be cancerous cells themselves or stromal cells.[40]

The receptor CCR5, classified as C-C chemokine receptor 5, alternatively termed also CD195, is the main receptor through which CCL5 transduces signalisation.[41,42] Structurally, CCR5 is a GPCR, as are many other chemokine receptors.[41] This means that it has a N-terminal extracellular tail responsible for ligand binding, seven hydrophobic transmembrane regions, the six loops that connect them, and a C-terminal cytosolic tail. This is crucial for transducing the signal caused by ligand binding after its heterotrimeric G-proteins binding or through G-protein independent pathways.[41]

Similar to other chemokine receptors, CCR5 also acts redundantly for signalling pathways.[28] High affinity ligands that bind to CCR5 are CCL5, as well as chemokine (C-C motif) ligand 3 (CCL3) (also known as MIP-1α) and chemokine (C-C motif) ligand 4 (CCL4) (also known as MIP-1β) (Figure 1B).[42,43] As already mentioned, substantial research has been dedicated to the role of CCR5 in HIV infection; M-tropic or macrophage strain HIV-1 uses CD4 as its main receptor to bind to and enter CD4+ T cells, but for this it also needs co-receptors, CCR5 and CXCR4 acting as such. Small molecular inhibitors (maraviroc [MRV]) and the humanized monoclonal antibody (leronlimab)[44,45] are CCR5 antagonists that inhibit HIV-1 virus from entering the T-cells.[43] MRV binds to CCR5 and acts as an allosteric inverse agonist, locking CCR5 in an inactive conformation.[42] However, recent research has focused more on cancer, as similarly to CCL5, CCR5 is overexpressed in many types of cancers, including breast[28,33,34,46], prostate[32] and in particular glioblastoma.[47,48] Both maraviroc[49] and leronlimab[46] have been shown to potently block cancer metastasis in murine xenografts.

The impact of CCL5/CCR5 signalling in glioblastoma

The canonical (conventional) way of signalling is through a hepta-helical chemokine receptor and adjacent G proteins, more specifically their Gα subunit and G$\beta\gamma$ dimer.[41] Upon ligand binding, CCR5 activates G$\alpha\beta\gamma$ trimer by causing guanosine exchange (GDP à GTP) and the dissociation of the membrane-bound Gα subunit from the G$\beta\gamma$ dimer.[50] Activated Gα affects adenylyl cyclase, and subsequently cellular cyclic adenosine monophosphate (cAMP) levels that activates cytosolic protein kinase A (PKA). Gα together with G$\beta\gamma$ affect various targets (e.g. PLCβ), resulting in the production of secondary messengers, such as inositol-1,4,5-triphosphate (IP3), diacylglycerol (DAG) and increased cytosolic calcium concentration. Both Gα and G$\beta\gamma$ trigger calcium influx, therefore the direct interaction of chemokine and its receptor can be confirmed by a calcium mobilisation assay.[38] Influx of calcium activates calcium-dependant pathways (NF-κB), as well pathways independent of G-proteins, all favouring malignancy in one way or the other.[41]

The CCL5/CCR5 axis has been recently reported as a mechanism of tumour progression in pancreatic[38], gastric[20] and breast cancer.[33,34] Noteworthy, in cancer, the CCL5-receptors signalling can favour cancer progression directly by affecting proliferation, migration and cell survival of cancer cells, or indirectly, by affecting tumour microenvironment, *i.e.* by recruiting pro-tumour and/or anti-inflammatory effector cells.[20,51] The state of the art in affecting the key hallmarks of glioblastoma progression, first described by Kouno *et al.*[47] and recent reports on MES-GB subtypes[29] and glioblastoma stem cells[52,53], will be discussed below.

Direct impact on glioblastoma cells

Cancer cell proliferation is regulated by many pathways, one of them, most commonly mediated by CCL5/CCR5 signalling, is mammalian target of rapamycin mTOR) pathway. This pathway is convergent with the Phosphatidylinositol 3-kinase (PI3K) pathway, as they both activate the Akt (protein kinase B) pathway (Figure 2).[54]

The "mTOR is a kinase, encoded by mTOR gene *MTOR* and is the member of phosphatidylinositol 3 kinase (PI3K)-related kinase family that plays an important role in transcriptional activation, as it regulates the eukaryotic translation initiation factor 4E-binding protein 1 (4E-BP1). The role of 4E-BP1 is to sequester the eukaryotic translation initiation factor 4E (eIF4E), inhibiting translation. By inducing hyper phosphorylation of 4E-BP1, mTOR complex 1 (mTORC1) disables its eIF4E binding, enhancing the rate of translation.[51] Binding to CCR5, CCL5 has been proven to activate the mTOR/4E-BP1 pathway, inducing the translation of a specific subset of mRNAs that have a long and highly structured 5'-UTR region, coding for cell survival and growth related onco-proteins, such as cyclin D1, c-Myc, and Dad-1.[20] Indeed, CCL5/CCR5 signalling stimulated survival and

proliferation of MCF-7 breast cancer cells through the mTOR/4E-BP1 pathway.[55] Although similar has not directly been shown in glioblastoma, there are numerous reports on the role of the mTOR pathway in GB.[56] Moreover, Khan *et al*.[52] have shown that inhibition of mTOR complexes, mTORC1 and mTORC2, significantly increased the *in vitro* and *in vivo* sensitivity of glioblastoma stem cells to radiotherapy. The relevance of mTOR in GSCs, has been recently demonstrated by Mecca *et al*.[54], by inhibition of mTORC1/2 in glioblastoma, causing persistent and dramatic reduction in p-Akt levels, which inhibited GSCs' proliferation. Along these lines, Pan *et al*.[29], demonstrated that CCL5/CCL5-receptor signalling in GB cells created an autocrine signalling circuit, important for high-grade glioma growth. Interestingly, they found that increased CCL5 expression was restricted to both human and mouse MES-GB, subtype characterized by NF1 protein (neurofibromin). This protein negatively regulated CCL5 expression through suppression of AKT/mTOR signalling. Zhao *et al*.[56] also reported that GB cell proliferation is mediated through CCR5 signalling. Using BrdU incorporation *in vitro* in the GB cells U87 and U251, they determined that CCL5 stimulation significantly enhanced proliferation. In their experiments, CCL5/CCR5 axis activation triggered the PI3K/Akt pathway to promote proliferation, whereas PI3K inhibitors decreased Akt phosphorylation, which in turn decreased proliferation. However, both mTOR and PI3K are known to activate the Akt pathway, but the mutual relation of these two pathways is not clear. Further studies in GB are urgently needed due to the notions that most aggressive MES-GB and GSCs are affected by CCL5/CCR5 mediated treatment.

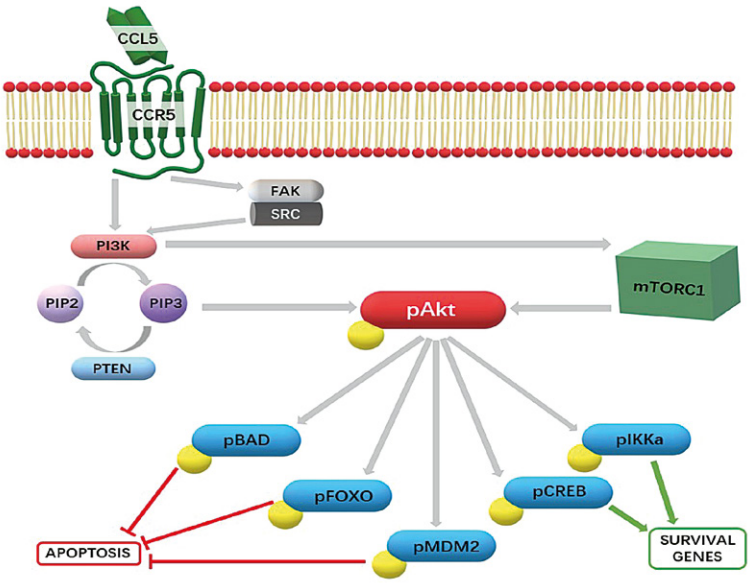

FIGURE 2. Phosphatidylinositol 3-kinase (PI3K)/pAkt-kinase pathway as a central CCL5/CCR5 signalling cascade in cancer cells. Upon CCL5 binding to its cognate receptor CCR5, primarily the PI3K/Akt pathway is triggered. This favours the phosphorylation of PIP2 to PIP3, a secondary messenger responsible for the activation of the Akt kinase, which in turn phosphorylates several downstream effectors. This causes the inhibition of pro-apoptotic effectors and the upregulation of survival genes. Another target of PI3K is the mammalian target of rapamycin complex 1 (mTORC1), which also activates the Akt kinase. However, it has also been shown that a secondary intracellular target, Focal Adhesion kinase (FAK) binding-SRC kinase complex can be activated, resulting in additional PI3K activation (in prostate cancer[62]).

Migration and invasion

Cell migration along or through 3D extracellular matrix (ECM) is fundamental to normal tissue formation and regeneration, stem cells and immune cells trafficking, and cancer cell invasion and metastasis.[57] As in various cancer cell types, migratory glioblastoma cell acquire mesenchymal type of movement[58], where invasion rates are governed by the capacity of cells to induce a proteolytic cascade. This includes metalloproteases (MMPs), plasminogen and its activators as well as cathepsins[59] and integrin- actomyosin mediated mechano-coupling. The process starts with cell polarisation of the actin cytoskeleton, enabling directional movement of the migrating cell. By forming frontal protrusions that activate integrin receptors, the cells are attached to the ECM integrins. Intracellularly, this triggers activity of small cytosolic GTPase proteins, RhoG, Cdc42 and Rac, which are essential in coordinating these processes[58] and thereby metastasis *in vivo*.[60] Monomeric G-actin polymerises into F-actin filaments, resulting in actomyosin contraction and subsequently migration, which is linked to FAK intracellular signalling and subsequent activation of PI3K at the leading edge.

Early studies showed the importance of CCR5 in the invasion of breast and prostate cancer cells.[61] In human lung cancer cells, CCL5/CCR5 activation augments the migratory ability by increasing their surface expression of $\alpha v\beta 3$ integrin[31] and phosphorylation of PI3K/Akt kinases. Further, the authors have shown that by PI3K/Akt inhibitors or transfection of the CCL5 treated cells by mutant PI3K and Akt, lead to a decrease in $\alpha v\beta 3$ integrin expression and migration. CCL5/CCR5 activation of PI3K/Akt signalling also activated IKKα/β and NF-κB, again enhancing $\alpha v\beta 3$ integrin expression and migration.[31] Presumably, the major mechanisms of CCL5 and other chemokines activation involves the PI3K-γ isoform through the G$\beta\gamma$ dimer of the

G-protein, which is coupled with the CCR5 receptor.[51]

Actin polymerisation as a result of CCL5 activation of CCR5 was observed also in pancreatic cancer[38] and recently in breast cancer epithelial cell lines[34], enhancing migration by a PI3K/Akt pathway. In GB cell lines U87 and U251, CCL5 stimulation enhanced their migratory ability.[56] After treatment of U87 cells with a PI3K inhibitor and CCR5 siRNA, inhibition of Akt phosphorylation was demonstrated in CCL5-treated cells and significant inhibition of growth was observed in U87 glioma xenografts in mouse model. Finally, high CCR5 expression in MES- GB was correlated with high p-Akt expression in patients' samples. We have shown that GB cell invasion is triggered by intracellular cathepsin B[62], followed by its activation of plasminogen system[63] and finally activating executive metalloproteases of which MMP-9 is directly degrading EMC, and the latter was also downregulated by downregulated CCR5-PI3K/Akt signalisation.[56] Wang *et al.*[64] reported that hypoxia, frequently found in GB, also induced CCR5 expression in U87 cells *in vitro.* This lead to an increase in matrix metalloproteinase-9 (MMP-9) expression and secretion and enhanced GB cancer cell invasion. The activation of CCR5 by hypoxia is undoubtedly one of the important mechanisms for enhancing cell migration *via* CCR5, but not the only one, as hypoxia simultaneously activates numerous signalling pathways.

Cell survival

Tumour's maintenance of cancer cell survival is a necessity for its progression. This is achieved by overexpression of DNA repair and/or by increasing the apoptotic threshold to avoid cancer cell death. CCR5 signalling promotes breast cancer cell survival in both ways[34], but in glioblastoma the CCL5/CCR5 activation mostly affects apoptosis. In human breast cancer, high CCR5 expression correlates with poor outcome, as recently reported by Jiao *et al*.[34] *In vitro*, reintroduction of CCR5 expression into CCR5-negative breast carcinoma BCa SUM-159 cells that were irradiated, lower level of DNA damage marker γH2AX was demonstrated, indicating an increased DNA repair *vs.* CCR5 negative cells. CCR5-expressing BCa raised more metastases in animal model. Single cell analysis revealed that CCR5 governs PI3K/Akt and cell survival signalling. The drug maraviroc dramatically enhanced cell killing effect, mediated by DNA-damaging chemotherapeutic agent doxorubicin. As CCR5 augments DNA repair, the CCR5 inhibitors may enhance the tumour-specific treatments, allowing for lower doses of standard chemotherapy and radiation.

In GB, Pan *et al*.[29] reported that GB cell survival also involves CCL5 signalling, although interestingly not by binding to CCR5, but to an auxiliary receptor CD44, and in an autocrine manner triggers signalisation that inhibits apoptosis. In the MES-GB subtype, CCL5 expression was shown to be increased and consistently with its role as a GB growth regulator, CCL5 knockdown in MES-GB cells reduced their survival *in vitro*, and increased mouse GB survival *in vivo*. Noteworthy, these authors demonstrated that CCL5 operates via CD44, activating the effector caspase-3 to inhibit apoptosis of MES-GB cells.

Impact on tumour microenvironment

Immunosuppression

Tumour-induced immunosuppression involves recruitment of different cells forming tumour microenvironment, such as tumour infiltrating lymphocytes (TIL), myeloid-derived suppressor cells (MDSCs), innate lymphoid cells, mesenchymal stem cells (MSC), immature dendritic cells (IDC) and tumour-associated macrophages (TAM), many of these cells expressing CCR5 and its ligand CCL5.[46,48,65] TAMs actually comprise as two ontogenetically distinct subsets, microglia and glioblastoma infiltrated macrophages (MDMs) derived from monocyte are representing about 30% of all cells in glioblastoma.[66,67] The difference between MDMs and microglia is also reflected in cytokine gene expression.[65] Microglia mediated immunosuppression dwells also on the CCL5/CCR5 and effect of CCR5 signalling on TAM activation (polarization) and GB progression has been investigated by Laudati *et al*.[48] The main finding reveals that the functional relationship exists between the chemokine-CCR5 system and microglia polarization. Overall, the pharmacological blockade of CCR5 prevents the occurrence of a M2 anti-inflammatory microglia state (Figure 3).

Furthermore, under conditions mimicking the late stage of glioma pathology, CCR5 blockade thus induces a prevailing M1 pro-inflammatory state. Such changes in microglia polarization profile are potentially associated with cytotoxic and anti-tumour properties, which leads to a potential reduction in tumour growth (Figure 3), as empha-

sised by Jiao *et al*.[46] Taken together, these changes suggest a possible clinical exploitation of CCR5 antagonists in the treatment of human GB. However, it has been shown *in vivo*, that the nature of microglia and TAM is not as simple binary as the M1/M2 paradigm predicts. TAM phenotypes are much more complex to distinguish in the context of human pathology, compared to *in vitro* experiments by immunosuppressive myeloid cells (IMC) of both monocytic and granulocytic lineages.[68] Ban *et al*.[69] demonstrated that the absence of the autocrine CCL5 abrogated the generation of granulocytic myeloid-derived suppressor cells and tumor-associated macrophages. In parallel, enhanced maturation of intra-tumoral neutrophils and macrophages occurred in spite of tumor-derived CCL5. Maraviroc was used to block the CCL5/CCR5 causing a reprograming of MDMs: initially they expressed anti-inflammatory effectors, but after maraviroc treatment they also underwent repolarisation and expressed significantly more pro-inflammatory mediators. Targeting the host CCL5 in bone marrow via nanoparticle-delivered expression silencing in combination with araviroc, resulted in robust immunities, suggesting that the myeloid CCL5/CCR5 axis is an excellent target for cancer immunotherapy.[69]

The concept of hierarchical tumour evolution from cancer stem cells is now widely accepted and proven also in GB.[7] GSCs and their progenies, represent the final obstacles for therapy failure, as these represent the most resistant cell phenotype in the GB. These cells, although a minority of total cancer cell populations, define the functional progression of GB by expressing a panel of stemless markers and cell damage resistance genes. Besides molecular set up of these cells' subpopulation, also the micro environmental cues contribute to their resistance by stromal cells' protection in the so-called tumour tissue niches. We have recently shown the cellular and functional features of GB niches around a fraction of arterioles by immunohistochemistry.[70] Besides the crucial endothelial-GSCs paracrine interactions, maintained mainly by CCL12-CXCR4 axis, other interactions with resident mesenchymal stem cells (MSCs) are plausible, and may be maintained by CCL5/CCR5 axis as shown on Figure 4 (unpublished data).

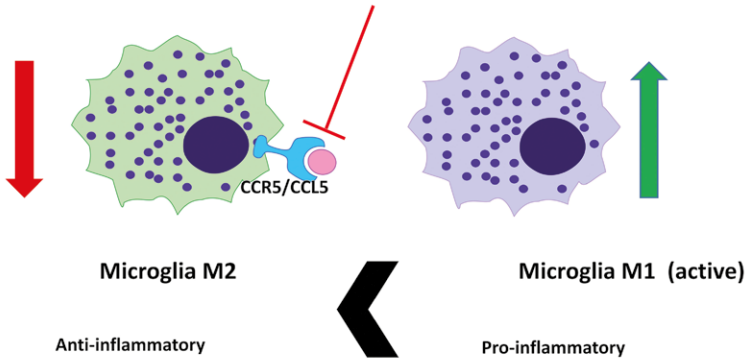

FIGURE 3. CCL5-CCR5 system and microglia polarization. The pharmacological blockade of CCR5 with maraviroc prevents the activity of glioblastoma-associated anti-inflammatory microglia M2 phenotype in and induces (green arrow) the conversion to prevailing pro-inflammatory M1 microglia phenotype.

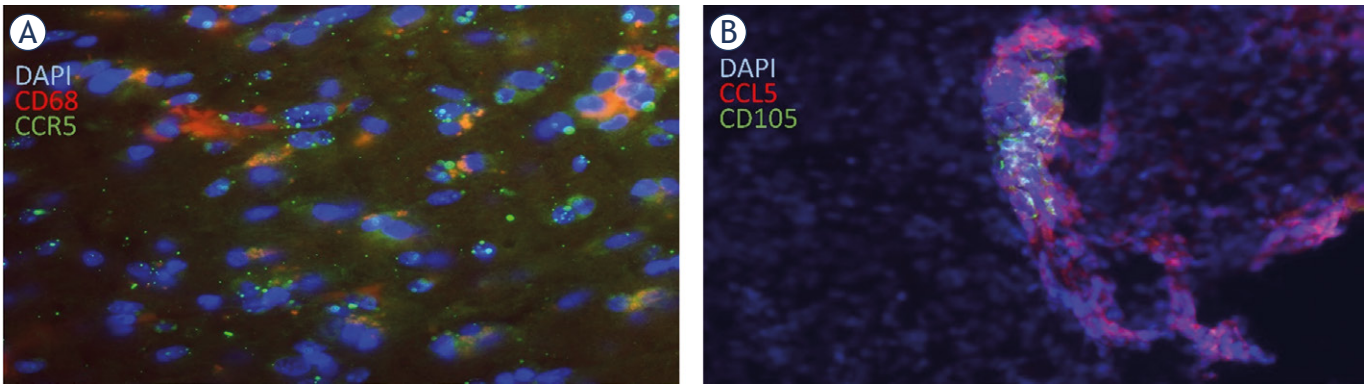

FIGURE 4. CCL5 and CCR5 in Glioblastoma microenvironment. **(A)** Fluorescence immunohistochemical labelling of CCR5 in glioblastoma associated macrophages. Macrophages in the tumour section were immuno-fluorescently labelled to detect antigen CD68 (marker for macrophages), as well as CCR5 expressions in glioblastoma tissue samples of glioblastoma patient. Nuclei were stained with DAPI (blue), CD68 with Alexa Fluor 546 (red) and CCR5 with Alexa Fluor 488 (green) dye. CCR5 is expressed in macrophages, shown in yellow in merged pictures. 40x magnification was used. **(B)** CCL5 is expressed in proximity to MSC on glioblastoma tissue slide. Immunofluorescence images of GB tissue slides, labelled for CD105 marker of Mesenchymal stem cells (green positive cells) and CCL5 (red). We observe selective localisation of CCL5 in glioblastoma cells and colonalization in the fraction of mesenchymal stem cells, expressing CCL5. This indicates the involvement of MSCs in the CCL5/CCR5 signalling in glioblastoma. CCL5 was also expressed in glioblastoma cells.

CCL5/CCR5 mediated cell-cross talk in glioblastoma

The basic question when investigating chemokine paracrine signalling is *what attracts what*, or when considering autocrine CCL5/CCR5 loop also, *what activates what*. Typical examples of the dilemma are numerous heterotypic interactions among heterogeneous glioblastoma cell subtypes, and stromal cells as listed above, microglia, infiltrating macrophages, lymphocytes, neutrophils, MSCs, neurons and neural stem cells, endothelial cells, etc. By categorically studying bilateral ligand and receptor expression by cell types, the mechanisms of individual cell types in CCL5/CCR5 signalling in GB may be elucidated. We are still far from being able to interpret complex multiple interactions under *in vivo* conditions. There are three types of situations, considering the trigger of signalling activation is the ligand CCL5.

External activation of receptor CCR5 expressing glioblastoma cells

The most commonly observed situation in CCL5/CCR5 signalling is activating host CCR5, expressed by differentiated glioblastoma cells, by stromal cells such as TAM, as discussed above and by Wang *et al*.[64] As GB cells highly express CCR5, being activated by adding macrophage conditioned media, containing CCL5, which was even overexpressed under hypoxic conditions[65], resulted in enhanced GB cell invasion. Another study[71] observed microglia specific activation of growth of Neurofibromatosis 1 glioma cells, presumably (MES-GB) expressing CCR5. RNA-sequencing of microglia cells revealed CCL5 to be highly expressed. Its functionality was determined by CCL5 neutralising antibodies that also reduced glioma growth in *in vivo* murine model. Taken together, stromal cells activation *via* tumour CCR5 is a common functional mode of the CCL5/CCR5 axis in GB and presents a potential therapy target.

Activating stroma by ligand CCL5 expressing glioblastoma cells

Another way of heterotypic cellular cross-talk in glioblastoma is via secreted CCL5 by GB cells. This ligand affects infiltrating or stromal cells that express CCR5, thus affecting their intracellular signalisation that results for example in the immunosuppression of the GB microenvironment, as has been discussed above in chapter *Immunosuppression*. Besides modifying macrophages, T-reg lymphocytes, expressing CCR5, are recruited effectors of GB, known to be important players in immunosuppression.[72] However, T-reg recruitment in GB in relation to CCL5/CCR5 signalling has been poorly studied so far. Similarly, as discussed above[48], host microglia express CCR5 and rely on tumour (GB) derived CCL5 to maintain anti-inflammatory properties and migrate to attracting GB tissues. These results confirm the hypothesis of Kouno J. *et al*. that CCR5 ligands are overexpressed in GB in order to attract effector cells that modulate local immunity.[47]

Autocrine activation of glioblastoma cells, expressing both CCL5 and CCR5

Another hypothesis by Kouno *et al.* was that the upregulation of CCR5 and its ligand in glioblastoma serves to facilitate an autocrine system that enhances GB proliferation.[47] This means that GB cells express both ligand and receptor, and thus activate the pathways downstream of CCR5 in a cell autonomous manner, as also suggested by Pan *et al*.[29] This cross-talk *via* CCL5/CCR5 in cancer is also known for other cancers, indeed expressing both, the receptor and the ligand. In osteosarcoma cells, Wang *et al*.[73], have shown that cells expressing both, CCL5/CCR5, regulate the VEGF expression, as a result of the autocrine CCL5/CCR5 activation attracts endothelial progenitor cells (EPC), contributing to tumour angiogenesis and subsequently, malignancy.

In MES-GB subtype, the autocrine CCL5/CCR5 activation loop has been examined as well by adding CCL5. Because no significant difference between wild-type tumours and those with additional stromal CCL5 was noticed, they concluded that CCL5 promotes survival and proliferation of the cells in a cell-autonomous and autocrine manner. Low grade gliomas seem to rely on stromal chemokine stimulation, whereas high grade gliomas (GB), establish autocrine chemokine stimulation. An interesting interpretation of this is that the ability of autocrine activation grants gliomas for relative stromal independency and this in turn causes the stromal cells to have less control over the regulation of the tumour leading in tumour malignancy.[29]

Acknowledgements

This work was supported by Slovenian Research Agency Programme P1-0245 (to T.T.L.) and by the

European Program of Cross-Border Cooperation for Slovenia-Italy Interreg TRANS-GLIOMA (T.T.L.).

References

1. Philips A, Henshaw DL, Lamburn G, O'Carroll MJ. Brain tumours: rise in glioblastoma multiforme incidence in England 1995-2015 suggests an adverse environmental or lifestyle factor. *J Environ Public Health*; **2018:** 2170208. doi: 10.1155/2018/7910754
2. Molenaar RJ, Maciejewski JP, Wilmink JW, Van Noorden CJF. Wild-type and mutated IDH1/2 enzymes and therapy responses. *Oncogene* 2018; **37:** 1949-60. doi: 10.1038/s41388-017-0077-z
3. Louis DN, Perry A, Reifenberger G, von Deimling A, Figarella-Branger D, Cavenee WK, et al. The 2016 World Health Organization classification of tumors of the central nervous system: a summary. *Acta Neuropathol* 2016; 131: 803-20. doi: 10.1007/s00401-016-1545-1
4. Stupp R, Hegi ME, Mason WP, van den Bent MJ, Taphoorn MJ, Janzer RC, et al. Effects of radiotherapy with concomitant and adjuvant temozolomide versus radiotherapy alone on survival in glioblastoma in a randomised phase III study: 5-year analysis of the EORTC-NCIC trial. *Lancet Oncol* 2009; **10:** 459-66. doi: 10.1016/S1470-2045(09)70025-7
5. Stupp R, Hegi ME, Gorlia T, Erridge SC, Perry J, Hong YK, et al. Cilengitide combined with standard treatment for patients with newly diagnosed glioblastoma with methylated MGMT promoter (CENTRIC EORTC 26071-22072 study): a multicentre, randomised, open-label, phase 3 trial. *Lancet Oncol* 2014; **15:** 1100-8. doi: 10.1016/S1470-2045(14)70379-1
6. Hegi ME, Genbrugge E, Gorlia T, Stupp R, Gilbert MR, Chinot OL, et al. MGMT promoter methylation cutoff with safety margin for selecting glioblastoma patients into trials omitting temozolomide: a pooled analysis of four clinical trials. *Clin Cancer Res* 2018; **25:** 1809-16. doi: 10.1158/1078-0432.ccr-18-3181
7. Lathia JD. Mack SC, Mulkearns-Hubert EE, Valentim CL, Rich JN. Cancer stem cells in glioblastoma. *Genes Dev* 2015; **29:** 1203-17. doi: 10.1101/gad.261982.115
8. Van Meir EG, Hadjipanayis CG, Norden AD, Shu HK, Wen PY, Olson JJ. Exciting new advances in neuro-oncology: the avenue to a cure for malignant glioma. *CA Cancer J Clin* 2010; **60:** 166-93. doi: 10.3322/caac.20069
9. Phillips HS, Kharbanda S, Chen R, Forrest WF, Soriano RH, Wu TD, et al. Molecular subclasses of high-grade glioma predict prognosis, delineate a pattern of disease progression, and resemble stages in neurogenesis. *Cancer Cell* 2006: **9:** 157-73. doi: 10.1016/j.ccr.2006.02.019
10. Verhaak RGW, Hoadley KA, Purdom E, Wang V, Qi Y, Wilkerson MD, et al. Integrated genomic analysis identifies clinically relevant subtypes of glioblastoma characterized by abnormalities in PDGFRA, IDH1, EGFR, and NF1. *Cancer Cell* 2010; **17:** 98-110. doi: 10.1016/j.ccr.2009.12.020
11. Teng J, da Hora CC, Kantar RS, Nakano I, Wakimoto H, Batchelor TT, et al. Dissecting inherent intratumor heterogeneity in patient-derived glioblastoma culture models. *Neuro Oncol* 2017; **19:** 820-32. doi: 10.1093/neuonc/now253
12. Salmon H, Remark R, Gnjatic S, Merad M. Host tissue determinants of tumour immunity. *Nat Rev Cancer* 2019; **19:** 215-27. doi: 10.1038/s41568-019-0125-9
13. Broekman ML, Maas SLN, Abels ER, Mempel TR, Krichevsky AM, Breakefield XO. Multidimensional communication in the microenvirons of glioblastoma. *Nat Rev Neurol* 2018; **14:** 482-95. doi: 10.1038/s41582-018-0025-8
14. Thorsson V, Gibbs DL, Brown SD, Wolf D, Bortone DS, Ou Yang TH, et al. The immune landscape of cancer. *Immunity* 2018; **48:** 812-30. e14. doi: 10.1016/j.immuni.2018.03.023
15. Matias D, Balça-Silva J, da Graça GC, Wanjiru CM, Macharia LW, Nascimento CP, et al. Microglia/astrocytes-glioblastoma crosstalk: crucial molecular mechanisms and microenvironmental factors. *Front Cell Neurosci* 2018; **12:** 1-22. doi: 10.3389/fncel.2018.00235
16. Motaln H, Koren A, Gruden K, Ramšak Ž, Schichor C, Lah TT. Heterogeneous glioblastoma cell cross-talk promotes phenotype alterations and enhanced drug resistance. *Oncotarget* 2015; **6:** 40998-1017. doi: 10.18632/oncotarget.5701
17. Oliveira MN, Pillat MM, Motaln H, Ulrich H, Lah TT. Kinin-B1 receptor stimulation promotes invasion and is involved in cell-cell interaction of co-cultured glioblastoma and mesenchymal stem cells. *Sci Rep* 2018; **8:** 1299. doi: 10.1038/s41598-018-19359-1
18. Balkwill F. Cancer and the chemokine network. *Nat Rev Cancer* 2004; **4:** 240-50. doi: 10.1038/nrc1388
19. Lazennec G, Richmond A. Chemokines and chemokine receptors: new insights into cancer-related inflammation. *Trends Mol Med* 2010; **16:** 133-44. doi: 10.1016/j.molmed.2010.01.003
20. Aldinucci D, Casagrande N. Inhibition of the CCL5/CCR5 axis against the progression of gastric cancer. *Int J Mol Sci* 2018; **19:** 1477. doi: 10.3390/ijms19051477
21. Ben-Baruch A. Inflammation-associated immune suppression in cancer: the roles played by cytokines, chemokines and additional mediators. *Sem Cancer Biology* 2006; **16:** 38-52. doi: 10.1016/j.semcancer.2005.07.006
22. Schall TJ, Bacon K, Toy KJ, Goeddel DV. Selective attraction of monocytes and T lymphocytes of the memory phenotype by cytokine RANTES. *Nature* 1990; **347:** 669-71. doi: 10.1038/347669a0
23. Soria G, Ben-Baruch A. The inflammatory chemokines CCL2 and CCL5 in breast cancer. *Cancer Lett* 2008; **267:** 271-85. doi: 10.1016/j.canlet.2008.03.018
24. Cocchi F, Tresoldi E, Björndal A, Fredriksson R, Colognesi C, Deng HK, et al. Identification of RANTES, MIP-1α, and MIP-1β as the major HIV-suppressive factors produced by CD8+T cells. *Science* 1995; **270:** 1811-5. doi: 10.1126/science.270.5243.1811
25. Alkhatib G. The biology of CCR5 and CXCR4. *Curr Opin HIV AIDS* 2009; **4:** 96-103. doi: 10.1097/COH.0b013e328324bbec
26. Roscic-Mrkic B, Fischer M, Leemann C, Manrique A, Gordon CJ, Moore JP, et al. RANTES (CCL5) uses the proteoglycan CD44 as an auxiliary receptor to mediate cellular activation signals and HIV-1 enhancement. *Blood* 2003; **102:** 1169-77. doi: 10.1182/blood-2003-02-0488
27. Liu B, Hassan Z, Amisten S, King AJ, Bowe JE, Huang GC, et al. The novel chemokine receptor, G-protein-coupled receptor 75, is expressed by islets and is coupled to stimulation of insulin secretion and improved glucose homeostasis. *Diabetologia* 2013; **56:** 2467-76. doi: 10.1007/s00125-013-3022-x
28. Velasco-Velazquez M, Xolalpa W, Pestell RG. The potential to target CCL5/CCR5 in breast cancer. *Expert Opin Ther Targets* 2014; **18:** 1-11. doi: 10.1517/14728222.2014.949238
29. Pan Y, Smithson LJ, Ma Y, Hambardzumyan D, Gutmann DH. Ccl5 establishes an autocrine high-grade glioma growth regulatory circuit critical for mesenchymal glioblastoma survival. *Oncotarget* 2017; **8:** 32977-89. doi: 10.18632/oncotarget.16516
30. Cambien B, Richard-Fiardo P, Karimdjee BF, Martini V, Ferrua B, Pitard B, et al. CCL5 neutralization restricts cancer growth and potentiates the targeting of PDGFRβ in colorectal carcinoma. *PLoS One* 2011; **6:** e28842. doi: 10.1371/journal.pone.0028842
31. Huang CY, Fong YC, Lee CY, Chen MY, Tsai HC, Hsu HC, et al. CCL5 increases lung cancer migration via PI3K, Akt and NF-κB pathways. *Biochem Pharmacol* 2009; **77:** 794-803. doi: 10.1016/j.bcp.2008.11.014
32. Vaday GG, Peehl DM, Kadam PA, Lawrence DM. Expression of CCL5 (RANTES) and CCR5 in prostate cancer. *Prostate* 2006; **66:** 124-34. doi: 10.1002/pros.20306
33. Pervaiz A, Zepp M, Mahmood S, Ali DM, Berger MR, Adwan H. CCR5 blockage by maraviroc: a potential therapeutic option for metastatic breast cancer. *Cellular Oncology* 2018; **42:** 93-106. doi: 10.1007/s13402-018-0415-3
34. Jiao X, Velasco-Velázquez MA, Wang M, Li Z, Rui H, Peck AR, et al. CCR5 Governs DNA damage repair and breast cancer stem cell expansion. *Cancer Res* 2018; **78:** 1657-71. doi: 10.1158/0008-5472.CAN-17-0915
35. Niwa Y, Akamatsu H, Niwa H, Sumi H, Ozaki Y, Abe A. Correlation of tissue and plasma RANTES levels with disease course in patients with breast or cervical cancer. *Clin Cancer Res* 2001; **7:** 285-9. doi: 10.1158/1078-0432.ccr-06-0074
36. Sugasawa H, Ichikura T, Kinoshita M, Ono S, Majima T, Tsujimoto H, et al. Gastric cancer cells exploit CD4+ cell-derived CCL5 for their growth and prevention of CD8+ cell-involved tumor elimination. *Int J Cancer* 2008; **122:** 2535-41. doi: 10.1002/ijc.23401 doi:10.1002/ijc.23401

37. Yaal-Hahoshen N, Shina S, Leider-Trejo L, Barnea I, Shabtai EL, Azenshtein E, et al. The chemokine CCL5 as a potential prognostic factor predicting disease progression in stage II breast cancer patients. *Clinical Cancer Res* 2006; **12:** 4474-80. doi: 10.1158/1078-0432.CCR-06-0074

38. Sushil KS, Mishra MK. CCR5/CCL5 axis interaction promotes migratory and invasiveness of pancreatic cancer cells. *Sci Rep* 2018; **8:** 1323. doi: 10.1038/s41598-018-19643-0

39. Pham K, Luo D, Liu C, Harrison JK. CCL5, CCR1 and CCR5 in murine glioblastoma: Immune cell infiltration and survival rates are not dependent on individual expression of either CCR1 or CCR5. *J Neuroimmunol* 2012; **246:** 10-7. doi: 10.1016/j.jneuroim.2012.02.009

40. Borsig L, Wolf MJ, Roblek M, Lorentzen A, Heikenwalder M. Inflammatory chemokines and metastasis-tracing the accessory. *Brit Dental J* 2014; **33:** 3217-24. doi: 10.1038/onc.2013.272

41. Oppermann M. Chemokine receptor CCR5: Insights into structure, function, and regulation. *Cellular Signalling* 2004; **16:** 1201-10. doi: 10.1016/j.cellsig.2004.04.007

42. Rosenbaum DM, Rasmussen SGF, Kobilka BK. The structure and function of G-protein-coupled receptors. *Nature* 2009; **459:** 356-63. doi: 10.1038/nature08144

43. Griffith JW, Sokol CL, Luster AD. Chemokines and chemokine receptors: Positioning cells for host defense and immunity. *Annu Rev Immunol* 2014; **32:** 659-702. doi: 10.1146/annurev-immunol-032713-120145

44. Kaplon H, Reichert JM. Antibodies to watch in 2019. *MAbs* 2019; **11:** 219-38. doi: 10.1080/19420862.2018.1556465

45. Dhody K, Pourhassan N, Kazempour K, Green D, Badri S, Mekonnen H, et al. PRO 140, a monoclonal antibody targeting CCR5, as a long-acting, single-agent maintenance therapy for HIV-1 infection. *HIV Clin Trials* 2018; **19:** 85-93. doi: 10.1080/15284336.2018.1452842

46. Jiao X, Nawab O, Patel T, Kossenkov AV, Halama N, Jaeger D, et al. Recent advances targeting CCR5 for cancer and its role in immuno-oncology. *Cancer Res Cancers* 2019; **179:** 4801-7. doi: 10.1158/0008-5472.CAN-19-1167

47. Kouno J, Nagai H, Nagahata T, Onda M, Yamaguchi H, Adachi K, et al. Up-regulation of CC chemokine, CCL3L1, and receptors, CCR3, CCR5 in human glioblastoma that promotes cell growth. *J Neurooncol* 2004; **70:** 301-7. doi: 10.1007/s11060-004-9165-3

48. Laudati E, Currò D, Navarra P, Lisi L. Blockade of CCR5 receptor prevents M2 microglia phenotype in a microglia-glioma paradigm. *Neurochem Int* 2017; **108:** 100-8. doi: 10.1016/j.neuint.2017.03.002

49. Velasco-Velazquez M, Jiao X, De La Fuente M, Pestell TG, Ertel A, Lisanti MP, et al. CCR5 antagonist blocks metastasis of basal breast cancer cells. *Cancer Res* 2012; **72:** 3839-50. doi: 10.1158/0008-5472.CAN-11-3917

50. Peng WT, Sun WY, Li XR, Sun JC, Du JJ, Wei W. Emerging roles of G protein-coupled receptors in hepatocellular carcinoma. *Int J Mol Sci* 2018; **19:** pii: E1366. doi: 10.3390/ijms19051366

51. Murooka TT, Rahbar R, Platanias LC, Fish EN. CCL5-mediated T-cell chemotaxis involves the initiation of mRNA translation through mTOR/4E-BPI. *Blood* 2008; **111:** 4892-901. doi: 10.1182/blood-2007-11-125039

52. Kahn J, Hayman TJ, Jamal M, Rath BH, Kramp T, Camphausen K, et al. The mTORC1/mTORC2 inhibitor AZD2014 enhances the radiosensitivity of glioblastoma stem-like cells. *Neuro Oncol* 2014; **16:** 29-37. doi: 10.1093/neuonc/not139

53. Mecca C, Giambanco I, Bruscoli S, Bereshchenko O, Fioretti B, Riccardi C, et al. PP242 counteracts glioblastoma cell proliferation, migration, invasiveness and stemness properties by inhibiting mTORC2/AKT. *Front Cell Neurosci* 2018; **10**: 12:99. doi: 10.3389/fncel.2018.00099

54. Mecca C, Giambanco I, Donato R, Arcuri C. Targeting mTOR in glioblastoma: rationale and preclinical/clinical evidence. *Dis Markers* 2018; **18:** 1-10. doi: 10.1155/2018/9230479

55. Murooka TT, Rahbar R, Fish EN. CCL5 promotes proliferation of MCF-7 cells through mTOR-dependent mRNA translation. *Biochem Biophys Res Commun* 2009; **387:** 381-6. doi: 10.1016/j.bbrc.2009.07.035

56. Zhao L, Wang Y, Xue Y, Lv W, Zhang Y, He S. Critical roles of chemokine receptor CCR5 in regulating glioblastoma proliferation and invasion. *Acta Biochim Biophys Sin* 2015; **47:** 890-8. doi: 10.1093/abbs/gmv095

57. Wolf K, Friedl P. Extracellular matrix determinants of proteolytic and non-proteolytic cell migration. *Trends Cell Biol* 2011; **21:** 746-8. doi: 10.1016/j.tcb.2011.09.006

58. Friedl P, Wolf K. Tumour-cell invasion and migration: Diversity and escape mechanisms. *Nat Rev Cancer* 2003; **3:** 362-74. doi: 10.1038/nrc1075

59. Lah TT, Duran Alonso MB, Van Noorden CJF. Antiprotease therapy in cancer: hot or not? *Expert Opin Biol Ther* 2006; **6:** 257-79. doi: 10.1517/14712598.6.3.257

60. Bouzahzah B, Albanese C, Ahmed F, Pixley F, Lisanti MP, Segall JD, et al. Rho family GTPases regulate mammary epithelium cell growth and metastasis through distinguishable pathways. *Mol Med* 2001; **7:** 816-30.

61. Sicoli D, Jiao X, Ju X, Velasco-Velazquez M, Ertel A, Addya S, et al. CCR5 receptor antagonists block metastasis to bone of v-Src oncogene-transformed metastatic prostate cancer cell lines. *Cancer Res* 2014; **74:** 7103-14. doi: 10.1158/0008-5472.CAN-14-0612

62. Gole B, Huszthy PC, Popović M, Jeruc J, Ardebili YS, Bjerkvig R, et al. The regulation of cysteine cathepsins and cystatins in human gliomas. *Int J Cancer* 2012; **131:** 1779-89. doi: 10.1002/ijc.27453

63. Colin C, Voutsinos-Porche B, Nanni I, Fina F, Metellus P, Intagliata D, et al. High expression of cathepsin B and plasminogen activator inhibitor type-1 are strong predictors of survival in glioblastomas. *Acta Neuropathol* 2009; **118:** 745-54. doi: 10.1007/s00401-009-0592-2

64. Wang Y, Liu T, Yang N Xu S, Li X, Wang D, et al. Hypoxia and macrophages promote glioblastoma invasion by the CCL4-CCR5 axis. *Oncol Rep* 2016; **36:** 3522-8. doi: 10.3892/or.2016.5171

65. Müller S, Kohanbash G, Liu SJ, Alvarado B, Carrera D, Bhaduri A, et al. Single-cell profiling of human gliomas reveals macrophage ontogeny as a basis for regional differences in macrophage activation in the tumor microenvironment. *Genome Biol* 2017; **18:** 234. doi: 10.1186/s13059-017-1362-4

66. Matias D, Balça-Silva J, da Graça GC, Wanjiru CM, Macharia LW, Nascimento CP, et al. Microglia/astrocytes-glioblastoma crosstalk: crucial molecular mechanisms and microenvironmental factors. *Front Cell Neurosci* 2018; **12:** 235. doi: 10.3389/fncel.2018.00235

67. Morisse MC, Jouannet S, Dominguez-Villar M, Sanson M, Idbaih A. Interactions between tumor-associated macrophages and tumor cells in glioblastoma: unraveling promising targeted therapies. *Expert Rev Neurother* 2018; **18:** 729-37. doi: 10.1080/14737175.2018.1510321

68. Ransohoff RM. A polarizing question: Do M1 and M2 microglia exist. *Nature Neuroscience* 2016; **19:** 987-91. doi: 10.1038/nn.4338

69. Ban Y, Mai J, Li X, Mitchell-Flack M, Zhang T, Zhang, L, et al. Targeting autocrine CCL5-CCR5 axis reprograms immunosuppressive myeloid cells and reinvigorates antitumor immunity. *Cancer Res* 2017; **77:** 2857-68. doi: 10.1158/0008-5472.CAN-16-2913

70. Hira VVV, Aderetti DA, van Noorden CJF. Glioma stem cell nichesn in human glioblastoma are periarteriolar. *J Histochem Cytochem* 2018; **66:** 349-58. doi: 10.1369/0022155417752676

71. Solga AC, Pong WW, Kim KY, Cimino PJ, Toonen JA, Walker J, et al. RNA sequencing of tumor-associated microglia reveals Ccl5 as a stromal chemokine critical for neurofibromatosis-1 glioma growth. *Neoplasia* 2015; **17:** 776-88. doi: 10.1016/j.neo.2015.10.002

72. Chakraborty R, Rooney C, Dotti G, Savoldo B. Changes in chemokine receptor expression of regulatory T cells after ex vivo culture. *J Immunother* 2012; **35:** 329-36. doi: 10.1097/CJI.0b013e318255adcc

73. Wang SW, Liu SC, Sun HL, Huang TY. CCL5/CCR5 axis induces vascular endothelial growth factor-mediated tumor angiogenesis in human osteosarcoma microenvironment. *Carcinogenesis* 2014; **36:** 104-14. doi: 10.1093/carcin/bgu218

research article

The "question-mark" MR anatomy of the cervico-thoracic ganglia complex: can it help to avoid mistaking it for a malignant lesion on ^{68}Ga-PSMA-11 PET/MR?

Ewa J. Bialek[1,2], Bogdan Malkowski[1,3]

[1] Department of Nuclear Medicine, The Franciszek Lukaszczyk Oncology Centre, Bydgoszcz, Poland
[2] Department of Nuclear Medicine, Military Institute of Medicine, Warsaw, Poland
[3] Department of Positron Emission Tomography and Molecular Diagnostics, Collegium Medicum of Nicolaus Copernicus University, Bydgoszcz, Poland

Radiol Oncol 2019; 53(4): 407-414.

Received 2 April 2019
Accepted 9 September 2019

Correspondence to: Bogdan Malkowski, Department of Nuclear Medicine, Oncology Centre, ul. dr I. Romanowskiej 2, 85-796 Bydgoszcz, Poland. E-mail: bmalkowski@mp.pl

Disclosure: No potential conflicts of interest were disclosed.

Background. Detectable uptake of ^{68}Ga-PSMA-ligands in sympathetic ganglia may potentially lead to mistaking them for malignant lesions. Our aim was to investigate the anatomy of cervico-thoracic-ganglia-complex (CTG-C) in the MR part of multimodal ^{68}Ga-PSMA-11 PET/MR imaging, in view of PET factors hindering its proper identification.

Patients and methods. In 106 patients, 212 sites of the CTG-C were retrospectively reviewed to assess the radiotracer uptake (SUV_{max}), size, shape, position, symmetry of location and visual uptake intensity. Asymmetry of PSMA-ligand uptake and increased uptake were regarded as risk factors of malignancy.

Results. In 66.0% left (L) and 53.8% right (R) CTG-C we noticed configurations, resembling the shape of an exclamation-mark, a question-mark, or its part (called "typical"). Tumor-like CTG-C shapes (oval, binodular or longitudinal) were detected in 28.3% L-CTG-C and in 40.6% R-CTG-C. When visual assessment of PET suggested malignancy, the recognition of "typical" shape of underlying CTG-C on MR generated a rise in the accuracy of their proper identification (from 34.4% to 75%, $\chi 2(1) = 70.4$; $p < 0.001$). Recognizing the shape of the CTG-C as "typical" in MR allowed us to classify as "not-suspicious" 61.9% of all CTG-C which were treated as "suspicious" after sole PET assessment.

Conclusions. The characteristic shape of cervico-thoracic-ganglia-complex (resembling a question-mark, or its part) helps in proper recognition of CTG-C on multimodal whole-body ^{68}Ga-PSMA-ligand PET/MR imaging, when detectable uptake might lead to considering pathology.

Key words: stellate ganglion; cervico-thocaracic ganglion; ^{68}Ga-PSMA; metastasis; lymph node; PET/MR; prostate; oncology

Introduction

Ganglia are consolidated parts of the sympathetic network located symmetrically along the spine. At the border of the chest and neck, the sympathetic inferior cervical ganglion (ICG) and the first thoracic ganglion (T1), may fuse to form a relatively large, variedly shaped, cervico-thoracic ganglion (CTG), called also the stellate ganglion (SG) (Figure 1A). Reported percentages of such fusions were scattered from 28% by Raveendran and Kamalamma[1] through about 82–83%[2,3]; up to 100% according to Hoffman.[4]

The exact location of CTG/SG had been studied in detail on cadavers[1-3,5-7] to find reliable anatomic landmarks for the needs of their therapeutic block

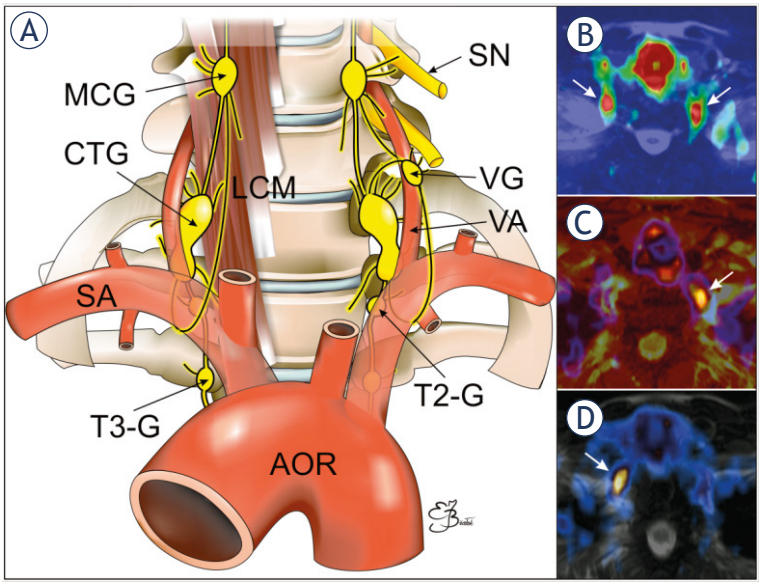

FIGURE 1. The scheme of the location of the sympathetic cervico-thoracic ganglia (CTG) and their surroundings **(A)** and examples of elevated PSMA-ligand uptake, potentially suggesting malignancy in both CTG complexes **(B)**, in the left CTG **(C)** and in the right CTG **(D)** on fused PET/MR T2-weighted images presented with application of different colour maps.

AOR = aortic arch; LCM = longus colli muscle; MCG = middle cervical sympathetic ganglion; SA = subclavian artery; SN = spinal nerve; T2-G = 2nd thoracic sympathetic ganglion; T3-G = 3rd thoracic sympathetic ganglion; VA = vertebral artery; VG = vertebral sympathetic ganglion

or ablation to relieve pain, in different diseases including cardio-vascular and post-traumatic stress disorder[8-10] or to assist avoiding their iatrogenic damage during surgery.

For a long time CTG/SG were not possible to be detected on any imaging because of their relatively small size. The first imaging study claims to be the magnetic resonance (MR) one, by Hogan and Ericson.[11] However, even when CTG/SG started to be visible on imaging, their proper classification was not essentially crucial from oncological point of view, as erroneous taking them for normal or benign lymph nodes did not generally cause any harm to the patient.

The circumstances changed after the introduction of a new radiotracer to multimodal positron emission tomography/computer tomography (PET/CT) imaging. The prostate specific membrane antigen (PSMA)-targeted radiotracers labelled with radioactive gallium (Ga-68) used for the primary staging and follow-up of prostate cancer patients, turned out to gather also in sympathetic ganglia, including CTG/SG.[12-15] In such circumstances, the relatively small size of CTG/SG does not exclude them from suspicion of malignancy, when they show the radiotracer uptake on PET, because ^{68}Ga-PSMA ligand (PET/CT) has the functional potential do detect micrometastases even in non-enlarged, and therefore missed on only morphological CT assessment, lymph nodes.[16,17]

Detection of uptake in CTG/SG on multimodal PET/CT imaging, causes the possibility of mistaking them for malignant lesions, primarily metastatic lymph nodes[12,13,15], which may lead to erroneous patient management and unnecessary treatment. The proposed hints for avoiding harmful misdiagnosis included the awareness of a possible pitfall, the anatomic location of CTG/SG[13], CTG/SG special shape, *i.e.* often met band- and tear-drop configuration, and significantly higher intensity of uptake than in prostate cancer metastatic lymph nodes.[15] However, the mentioned papers dealt with PET imaging combined with CT. In our study we have taken into consideration the MR-based multimodal PET imaging in order to check the shape of cervico-thoracic ganglia complex (CTG-C), in the view of PET factors hindering its proper identification (Figure 1B-D), including fused CTG/SG, not-fused CTG/SG and their connections with adjacent sympathetic ganglia if visible.

Patients and methods

The retrospective analysis of 212 sites of a CTG complex was undertaken in 106 patients undergoing whole body ^{68}Ga-PSMA-11 PET/MR examination. The retrospective study was performed in accordance with the principles of the 1964 Declaration of Helsinki and all subsequent revisions and with national regulations. All patients had provided routine written informed consent before each examination.

The patients were males (age range 40–78 years, mean 63.70 ± 6.86 years; weight range 59–115 kg, mean 86 ± 29 kg) referred for routine primary staging or follow-up of prostate cancer between November 2015 and February 2018. All exams were performed using a multimodal PET/MR system (Biograph mMR scanner, Siemens, Germany, based on the 3T MR platform). All patients underwent the whole body MR and the whole body PET imaging about 83.04±19.96 minutes (range, 50–143 minutes) after injection of 168.43 ± 17.69 MBq (range, 115–210 MBq) of ^{68}Ga-PSMA-11.

The procedure of ^{68}Ga-PSMA-11 preparation and the imaging protocol was the same as already described in Bialek and Malkowski.[18] ^{68}Ga-PSMA-11 was synthesized as follows. ^{68}Ge/^{68}Ga generator (Eckert & Ziegler Rdiopharma GmbH, Berlin, Germany) was eluted with 5ml of sterile, ul-

tra-pure 0.1M hydrochloric acid, in order to obtain sterile, endotoxin-free solution of Ga-68 chloride. For labelling a vial containing 20ug sterile and endotoxin-free lyophilisate of PSMA-11 (GMP) (ABX, Radeberg, Germany) and a vial containing 60 mg of sodium acetate was used. To the above set 2ml of Ga-68 chloride was added and mixed for 10-20s. to complete dissolution. Subsequently, the mixture was incubated for 10 min. at 95°C. The labelled tracer was purified on a column of Sep-Pak Light C18 (Waters) and filtered on a 0.22 μm pore size filter (MILLEX-GV, Merck). Radiochemical purity (≥95%) was confirmed by thin-layer chromatography, checked on iTLC-SG bands in ammonium acetate-methanol (1:1) solution.

To reduce patients discomfort during the long PET/MR examination time, the patient's arms were placed alongside the body. PET and MR imaging were performed simultaneously. MR sequences included: axial T2-wighted TSE fat-saturated 5mm-slice, 400mm field-of-view (FOV) images, respiratory gated in the region of the chest and abdomen, axial T1-weighted Vibe Dixon 3mm-slice, 430mm FOV images, breath-holded in the region of the chest and abdomen. Attenuation correction was calculated according to the manufacturer's protocol basing on a fast 3D FLASH based MR VIBE (volume interpolated breath-hold examination) sequence.

PET imaging was performed with an acquisition time of 5 min per bed position in caudocranial direction starting from the pelvis. Acquired PET sinograms were reconstructed with the HD-PET algorithm (point-spread function) using 3 iterations, 21 subsets, a Gaussian filter: the Full Width at Half Maximum (FWHM) 4.0 mm, an image matrix of 172. Performed separately, pelvis and lower limbs PET/MR imaging were not analyzed in the current study.

Image analysis

Retrospective analysis of ^{68}Ga-PSMA-11 PET/MR scans, fused and not-fused, included the estimation of the radiotracer uptake (SUV_{max} normalized by body weight) and morphologic features (the size, shape and position) of CTG complex, as well as the symmetry of their location and symmetry of visual uptake intensity. Analysis and quantification was performed on a Syngo.via Viewer workstation (Siemens, Germany).

We used the name "cervico-thoracic ganglia complex" (CTG-C) for the complex of ganglia located in the typical area (described in the discussion), because it is not possible to ascertain reliably on a whole-body MR part of a PET/MR scan if the detected ganglia structures are fused or not, as it is not possible to follow the whole sympathetic chain. The observed complex of ganglia connected by visible strands, possibly included sometimes a T2 sympathetic ganglion or a vertebral ganglion.

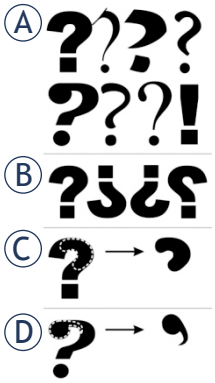

FIGURE 2. Schematic presentation of the discovered in current study "typical" cervico-thoracic ganglia complexes shapes resembling different forms of a question-mark or close to an exclamation-mark **(A)**, which may be configured in various orientations, for example normal, mirror, upside-down and reversed mirror **(B)** or represent a part of a question-mark similar to kidney **(C)** or comma **(D)**.

Asymmetry of PSMA-ligand uptake in CTG-C (in intensity, in the level of maximal intensity, or both), as well as increased uptake in visual assessment and independently, when SUV_{max} amounted at least 2, were regarded as risk factors of mistaking CTG-C for metastases or other malignant lesions. The background ^{68}Ga-PSMA-11 activity was measured in gluteal muscles (GM).

The analysis of the CTG-C shape consisted of two steps. First, the form of all CTG-C was characterized descriptively. Subsequently, the described configurations were reevaluated and categorized. When reviewing CTG complexes we noticed repeating configurations, not previously identified, resembling the shape of a question-mark (thinner or thicker, normal, reversed, mirror or upside-down, more or less straight including bludgeon-like shape), or a part of a question-mark similar to a kidney or comma, as well as exclamation-mark forms (Figure 2). These shapes were categorized as "typical".

The tumor-like shapes: oval, binodular or longitudinal, were regarded as "mistakable", potentially suspicious of malignancy, including lymph node metastasis.

The non-specific shapes (wavy with small nodules, bent or unreliable to be assessed), were named "other", and were also treated as not suspicious of malignancy.

TABLE 1. Dimensions of the right and left cervico-thoracic ganglia complex (CTG-C)

	thickness (mm)			width (mm)			length (mm)		
	Mean ± SD*	minimal	maximal	Mean ± SD	minimal	maximal	Mean ± SD	minimal	maximal
right CTG-C (n = 103)	4.31 ± 1.17	1.5	8	12.50 ± 5.30	4	28	12.7 ± 3.88	5	25
left CTG-C(n = 106)	4.35 ± 1.24	2	8	14.90±4.79	5	29	13.50 ± 3.53	7	25

* SD standard deviation

TABLE 2. ^{68}Ga-PSMA-11 uptake in the right and left cervico-thoracic ganglia complex (CTG-C)

	^{68}Ga-PSMA-11 uptake (SUV_{max})				
	mean	median	SD*	minimal	maximal
right CTG-C	2.54	2.45	0.82	1.06	6.23
left CTG-C	2.75	2.74	0.78	1.35	5.73

* SD standard deviation

Statistical analysis

Statistical calculations were performed using IBM SPSS Statistics for Windows, Version 23.0. Armonk, NY: IBM Corporation (Released 2015). Basic descriptive statistics was calculated and subsequently the Kolmogorov-Smirnov tests, the Pearson's r correlation and $\chi 2$ tests were performed. The significance level of $\alpha = 0.05$ ($p < 0.05$) was selected. The assessed variables included the patients' age (years), height (cm), weight (kg), radiotracer dose (MBq), uptake time (min), background in the GM (SUV_{max}), PSMA-ligand uptake in the right (R) CTG-C and the left (L) CTG-C (SUV_{max}), dimensions (thickness, width, length) of the R-CTG-C and L-CTG-C (mm) for basic descriptive statistics. Normality assumption was verified for variables intended for further correlations (*i.e.* the thickness and SUV_{max} values of CTG-C). Distributions of the thickness of the CTG-C, as well as SUV_{max} values of the right CTG-C and both CTG-C were not normal (differed from the Gaussian distribution). Therefore, verification of the level of skewness of these distributions was advised. The value of skewnees in all variables ranged from -2 to +2, meaning that the distributions were not highly asymmetrical. Therefore, if other assumptions were met, parametric analyses were performed. The correlation between thickness of CTG-C and SUV_{max} was investigated by means of a series of Pearson's r correlation analyses.

In order to check how recognizing the shape of CTG-C as not-suspicious, *i.e.* "typical" or "other", basing on MR, enhanced the accuracy of CTG-C proper identification in comparison with assessment based solely on PET, a series of $\chi 2$ analyses were performed. There were also additional calculations for "typical" shape carried out separately.

Results

On whole-body MR scans the CTG-C was identifiable in 100% on the left (L) side and in 97% (103/106) on the right (R) side, and were located symmetrically or partially symmetrically in 90% (95/106) of patients.

The mean thickness of the CTG-C, *i.e.* minimal transverse diameter, was 4.31 ± 1.20 mm (range, 1.5–8 mm), mean width, *i.e.* maximal diameter on a transverse MR plane, was 13.7 ± 5.18 mm (range, 4–29 mm) and mean length (in cranio-caudal orientation) was 13.1 ± 3.72 mm (range, 5–25 mm). Diameters with respect to the right and left side are presented in Table 1.

All identified CTG-C showed ^{68}Ga-PSMA-11 uptake, with mean SUV_{max} 2.65 ± 0.8 (range 1.06–6.23). Uptake values with respect to the right and left side are presented in Table 2.

With regard to the left CTG-C, there was a positive correlation of a medium size ($r = .318$; $p = .001$) between its thickness and SUV_{max}. Analysis regarding CTG-C of both sides taken together revealed a positive, statistically significant and small-size correlation with SUV_{max} ($r = .179$; $p = .01$). As for the right CTG-C, no correlation nor tendency was found between the thickness and SUV_{max} ($r = .028$; $p = .782$).

Noticeably increased, possible to be taken for malignant, ^{68}Ga-PSMA-11 uptake, $SUV_{max} \geq 2$, was detected in 87.7% (93/106) of the L-CTG-C and 74.5% (79/106) of the R-CTG-C (with respect to both sides see Figure 3); whereas the background in gluteal muscles presented mean SUV_{max} of 1.04 ± 0.32 (range, 0.46–1.81). In visual assessment, as routinely performed in clinical practice, suspicious of malignancy appearance of CTG-C was observed in

70.8% of the L-CTG-C (75/106) and 60.4% (64/106) of the R-CTG-C (with respect to both sides see Figure 3). The main criteria of possible malignancy on PET were the PSMA-ligand avidity and asymmetry of uptake (in the intensity, in the level of maximum intensity or both) in CTG-C (Figure 1B-D; Figure 3A,B; Figure 4A-D).

On MR part of the whole-body PET/MR, in the majority of patients (66.0% L-CTG-C, 70/106; 53.8% R-CTG-C, 57/106), the CTG complex presented the following shapes, reflecting their anatomic structure and connections: a question-mark (L-CTG-C: 23.6%, 25/106; R-CTG-C: 22.6%, 24/106), an exclamation-mark (L-CTG-C: 3.8%, 4/106; R-CTG-C: 2.8%, 3/106), or a part of a question-mark resembling kidney (L-CTG-C: 27.4%, 29/106; R-CTG-C: 12.3%, 13/106) or comma (L-CTG-C: 11.3%, 12/106; R-CTG-C: 16.0%, 17/106) (Figure 3E, F; Figure 5).

The tumor-like CTG-C shape, possible to be mistaken for malignancy, was detected in 28.3% (30/106) on the left side and in 40.6% (43/106) on the right side, probably due to MR artifacts obscuring finer linear elements of the CTG-C and not allowing for the tracing of the entire CTG-C tract (Figure 3C, D). The rest (L-CTG-C: 5.7%, 6/106; R-CTG-C: 5.7%, 6/106) of CTG-C presented non-specific shape.

In cases, where visual molecular assessment of PET revealed suspicious, potentially mistakable with malignancy, increased PSMA-ligand uptake in CTG-C, the recognition of a "typical" or an "other" shape of underlying CTG-C on MR part of the examination generated a rise in the accuracy of their proper identification. For the right CTG-C from 39.6% to 76.4%, $\chi2(1) = 29.46$; $p < .001$, for the left CTG-C from 29.2% to 77.4%, $\chi2(1) = 49.29$; $p < .001$, for both from 34.4% to 76.8%, $\chi2(1) = 77.41$; $p < .001$. The effect size was moderately large, with $V = .37$, $V = .48$ and $V = .43$ for the right, left and both CTG-C, respectively. Recognizing the shape of the CTG-C as a "typical" or an "other" in MR allowed us to classify as "not-suspicious" 60.9% of the right CTG-C, 68% of the left CTG-C and 64.7% of all CTG-C which were treated as "suspicious" after sole PET assessment.

In the separated evaluation of the "typical" MR CTG-C shape the rise in accuracy was from 39.6% to 76.4%, $\chi2(1) = 29.46$; $p < .001$ for the right CTG-C, from 29.2% to 73.6%, $\chi2(1) = 41.71$; $p < .001$ for the left CTG-C, from 34.4% to 75%, $\chi2(1) = 70.4$; $p < .001$ for both. The effect size was moderately large, with $V = .37$, $V = .44$ and $V = .41$ for the right, left and both CTG-C, respectively. Recognizing the shape of the CTG-C as "typical" in MR allowed us to classify as "not-suspicious" 60.9% of the right CTG-C, 62.67% of the left CTG-C and 61.9% of all CTG-C which were treated as "suspicious" after sole PET assessment.

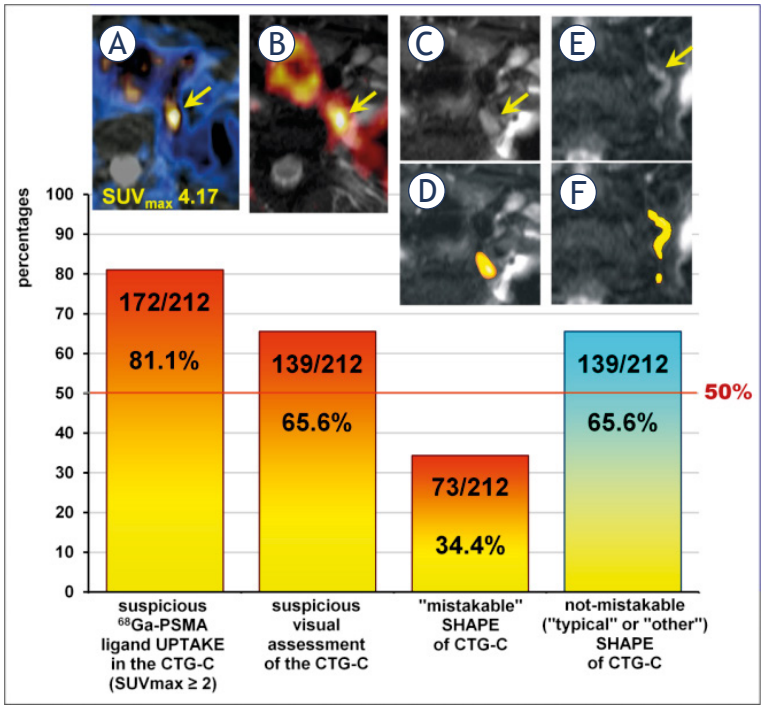

FIGURE 3. The chart comparing proportions of suspicious of malignancy PET presentation of cervico-thoracic ganglia complex (CTG-C) (arrow) in quantitative (SUV_{max} at least 2) and qualitative (visual) assessment with potentially "mistakable" and not-mistakable with malignancy underlying shape of CTG-C on MR part of the multimodal PET/MR. **(A, B)** Fused PET/MR scans of the left CTG-C potentially suspicious of malignancy in different patients. MR T2-weighted scans showing the mistakable (oval) shape **(C)** and not-mistakable (question-mark) shape **(E)** of the left CTG-C (arrow) with respective schemes **(D, F)**.

Discussion

The CTG/SG can be identified along the sympathetic chain on the border between the neck and thorax, anteriorly and slightly caudad to the head of the first rib[11,12], inferior and anterior to the transverse process of C7[12,19], lateral and posterior to the lateral edge of the longus colli muscle (at the level of T1)[11], inferior to the subclavian artery[12], medial, posterior, medial and anterior or medial and posterior to the vertebral artery[3,11]. Which was confirmed also in the current study.

In our study we have tracked down a configuration of the cervico-thoracic ganglia complex not categorized in previous MR study exploring CTG/SG.[11,19] The majority of CG-C in our work resem-

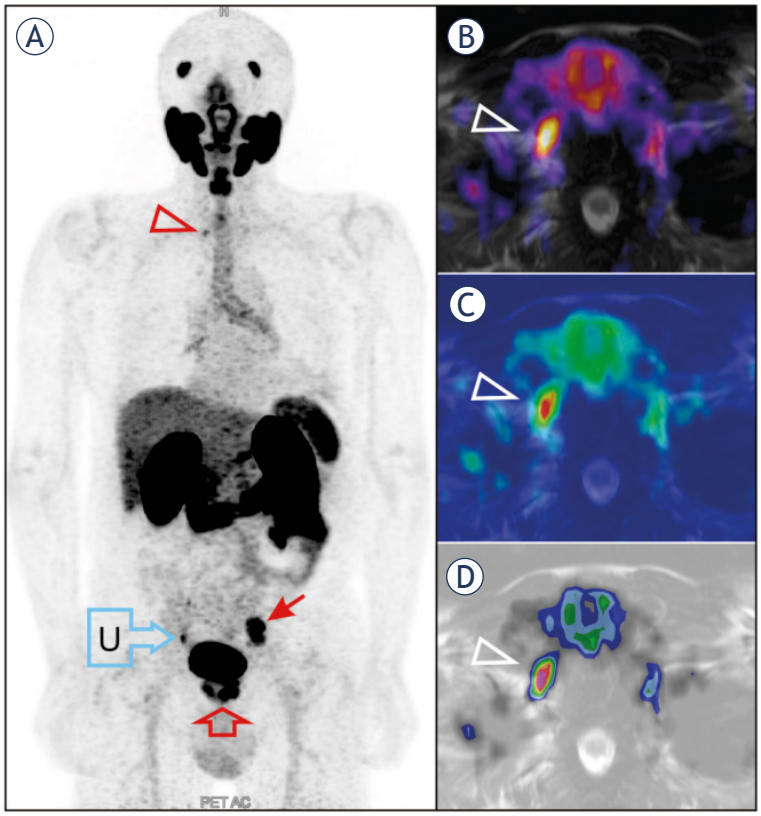

FIGURE 4. (A) Prostate cancer (empty block arrow) with lymph node metastases (arrow) on the maximum intensity projection (MIP) attenuation corrected (AC) PET image. Possibly suspected of metastasis asymmetric increased uptake in the right cervico-thoracic sympathetic ganglion (arrowhaed) is noticeable already on the MIP image **(A)** and more conspicuously on fused PET/MR T2-weighted images presented with application of different color maps **(B-D).**

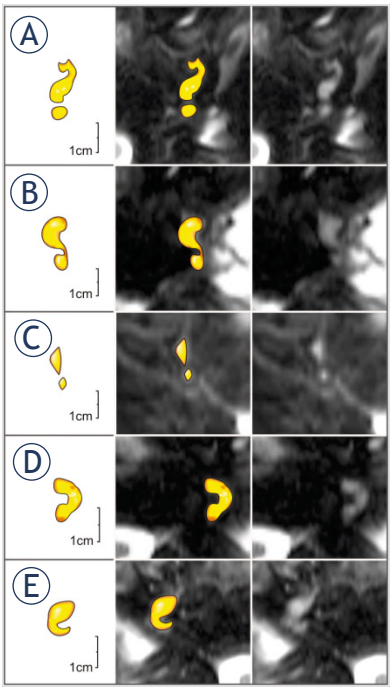

FIGURE 5. Schemes (two first columns) and original MR T2-weighted fat-saturated images (two last columns) depicting exemplary "typical" shapes of the cervico-thoracic ganglia complex (CTG-C): a question-mark shape **(A)**, a mirror question-mark shape **(B)**, an exclamation-mark shape **(C)**, a part of a question-mark resembling kidney **(D)**, a part of a question-mark resembling comma **(E)**.

bled a question-mark in various configurations: thinner or thicker, mirror, reversed or mirror and upside-down, more or less straight including bludgeon-like shape and an exclamation-mark, or a part of a question-mark: without a dot, resembling kidney or comma. Our "dot" in the question-mark or exclamation-mark sign might be T1 sympathetic ganglion (when CTG is not fused) or T2 ganglion (when CTG is fused) in case of a normal or a mirror shape, or a vertebral ganglion – in case of an upside-down appearance.

Even the oval, binodular or longitudinal shapes, classified as tumor-like, were usually partially surrounded by unsuccessful fat saturation artifacts, which probably obscured the finer sympathetic branches or chain and in more favorable conditions might let the recognition of a "typical" shape.

Many of presented in our work shapes or their parts correspond to the shapes described previously on CT or anatomical studies.[15]

On CT it is not possible to trace fine structures as nerves and their connections, therefore only thicker oval or longitudinal parts of a neuronal network are identifiable. That is the reason why MR-based multimodal PET/MR, which can depict strand of the sympathetic chain, may be more specific in identifying sympathetic ganglia. Nevertheless, the data available with PET/CT have been already proved to be entirely sufficient for correct interpretation of findings.[15]

The analysis of the CTG-C shape appears important in the context of potentially suggesting metastasis or other malignancy PSMA-ligand uptake on multimodal PET/MR, which was present in our study in 65.6% in visual assessment and in 81.1% when regarding abnormal SUV_{max} of at least 2. We have chosen the SUV_{max} 2, because it was used also in some previous papers as a cut-off value for prostate cancer metastases[16,20,21] and because it constitutes the reported lower range in lymph nodes metastases in prostate cancer[14,22], as well as it exceeded the upper range of the background SUV_{max} (1.81) in our study.

Elevated PSMA-ligand uptake in CTG/SG may be properly recognized as not alarming under a few conditions. The most important of them is awareness of the diagnostic reader that such a possibility exists, second is the typical location, subsequently – symmetry. The listed aspects were already underlined by authors of PET/CT studies.[13,15] Further aspects, including the likelihood on prostate cancer metastases on the level of the cervico-thoracic junction and the intensity of prostate cancer metastases[15] are discussed below.

We have observed, that morphological symmetry of CTG-C location (beginning and ending on the same or very similar level) did not necessarily overlap with the point of maximal PSMA-ligand uptake, therefore morphologically symmetric CTG-C seemed often to have asymmetric foci of maximal uptake when viewed on fused PET/MR images, facilitating a diagnostic mistake. Therefore, the additional observation of a specific underlying MR shape below the suspicious uptake on PET constitutes the additional useful tip aiding proper diagnosis. Reasons for asymmetry of CTG-C location on MR might include also, apart from true anatomic asymmetry, the asymmetric patient position resulting in the transverse MR plane not exactly perpendicular do the true long axis of the body.

Rischpler *et al.*[15] in the ample PET/CT study reported cervical sympathetic ganglia as having often a characteristic band-shaped (57.5%) and tear-drop (38.5%) configuration. The band-shape may reflect described in our current study elements of a question mark and a tear-drop may be close to our comma shape.

Shapes of SG described in MR-based study encompassed: fusiform, triangular, or globular but concerned only 9 volunteers.[11]

Shapes of SG described in anatomical cadaver studies included: spindle, dumbbell, and an inverted "L" shape (with the two latest demonstrating a definite "waist")[7], to which Marcer *et al.*[6] had added a perforated (by the vertebral artery usually at the superior portion) and a truncated form (where the vertebral artery created a shortened and flattened form of the ganglion). Kwon *et al.*[5] categorized SG shapes as fusiform-rounded, fusiform-elongated, and bilobed.

However, the shapes assessed basing on dissection studies may be deprived of their fine spacial arrangement visible on MR, but lost during preparation. The choice of the classification is subjective and may be free and depends on the imagination of the author. Comparing between pathology and imaging bears the burden of different condition of the organism at the time of examination, and therefore the results may be difficult to equate. The overall better tissue delineation on MR does not take the general diagnostic sufficiency away from CT.

The binodular shape in our study may reflect anatomically described dumbbell or bilobed form. The fusiform shape after dissection may lose its bent projection depicted on MR in the form of a question-mark. The truncated or "L" shape form probably might partially correspond to the kidney shape on MR. The association of CTG-C shape with the "question-mark" does not claim to be a novel discovery of that shape itself, but may better help an unexperienced reader to remember the problem.

Nevertheless, the results of previous papers prove, that data available with application of PET/CT are sufficient to correctly classify sympathetic ganglia on multimodal imaging with PSMA-ligands.[15] Especially that in case of prostate cancer, metastases as high as at the level of CTG-C are not so often and that prostate cancer metastases adjacent to ganglia show significantly more intense PSMA-ligand uptake[15], and we would like to stress the above conclusion.

The thickness range of CTG-C was in our study 1.5–8 mm, whereas Perlov and Vehe (1935) reported 3–10 mm for satellite ganglia. The mean thickness of CTG-C in our study (4.31 mm) was in close concordance with anatomical cadaver studies (4.5 mm by Marcer *et al.*[6]), but smaller than 8 mm reported by Jamieson *et al.*[2] The other diameters also differed in comparison with cadaver studies, the length was shorter, which was most probably caused by the different character of the study method: section – and imaging, and possibly because of different measurement policies and the measurement plane. Similarly, Hogan and Erickson[11] in MR study reported obtaining smaller cephalocaudal SG dimension than in previous dissection studies, of just over 1cm, which corresponded to our results of about 13 mm.

In our MR-based study mean SUV_{max} was similar, and only slightly higher (2.75 in the L-CTG-C and 2.54 in the R-CTG-C) than reported in CT-based multimodal PET studies: by Kanthan *et al.*[13]: 2.4 in the L-CTG-C and 2.2 in the R-CTG-C, and by Rischpler *et al.*[15]: 2.4.

The indisputable and undeniable, however unavoidable shortcoming of current study, identically to previous studies, is the impossibility of reliable confirmation of the true nature of studied ganglia, for obvious reasons of unattainable histopathological result. A few researches in previous works concerning celiac sympathetic ganglia tried to make a restitution for that by examining cadavers with CT or MRI and later performing the HP analysis.[14,23] Their conclusions confirmed the sufficiency of using anatomical landmarks for locating the ganglia.

To sum up, special properties of a novel PET PSMA-based radiotracer, physiologically accumulating also in anatomically normal sympathetic ganglia, including cervico-thoracic ones, impelled researchers to study meticulously all possible prop-

erties of these ganglia to avoid mistaking them for malignancy. In our study we associated discovered detailed anatomical CTG-C shapes with a form of a question-mark, exclamation-mark or a part of a question-mark to facilitate an unexperienced reader proper interpretation of the PSMA-ligand PET/MR examination.

Conclusions

The characteristic shape of the cervico-thoracic ganglia complex (resembling a question-mark or its part), reflecting CTG complex anatomy, helps in proper recognition of CTG-C on multimodal whole-body ^{68}Ga-PSMA-ligand PET/MR imaging, when detectable uptake might lead to considering pathology.

References

1. Raveendran VL, Kamalamma GK. Inferior cervical ganglion and stellate ganglion- concepts revisited. *J Evolution Med Dent Sci* 2018; **7:** 1653-8. doi: 10.14260/jemds/2018/373
2. Jamieson DW, Smith DB, Anson JB. The cervical sympathetic ganglia: an anatomical study of 100 cervicothoracic dissections. *Q Bull Northwest Univ Med Sch* 1952; **26:** 219-27. PMID: 14957979
3. Perlow S, Vehe KL. Variations in the gross anatomy of the stellate and lumbar sympathetic ganglia. *Am J Surg* 1935; **30:** 454-8
4. Hoffman HH. An analysis of the sympathetic trunk and rami in the cervical and upper thoracic regions in man. *Ann Surg* 1957; **145:** 94-103. doi: 10.1097/00000658-195701000-00010
5. Kwon OJ, Pendekanti S, Fox JN, Yanagawa J, Fishbein MC, Shivkumar K, et al. Morphological spectra of adult human stellate ganglia: Implications for thoracic sympathetic denervation. *Anat Rec (Hoboken)* 2018; **301:** 1244-50. doi: 10.1002/ar.23797
6. Marcer N, Bergmann M, Klie A, Moor B, Djonov V. An anatomical investigation of the cervicothoracic ganglion. *Clin Anat* 2012; **25:** 444-51. doi: 10.1002/ca.21266
7. Pather N, Partab P, Singh B, Satyapal KS. Cervico-thoracic ganglion: its clinical implications. *Clin Anat* 2006; **19:** 323-6. doi: 10.1002/ca.20214
8. Duong S, Bravo D, Todd KJ, Finlayson RJ, Tran DQ. Treatment of complex regional pain syndrome: an updated systematic review and narrative synthesis. *Can J Anaesth* 2018; **65:** 658-84. doi: 10.1007/s12630-018-1091-5
9. Przybylski A, Romanek J, Chlebuś M, Deręgowska B, Kuźniar J. Percutaneous stellate ganglion block as an adjunctive therapy in the treatment of incessant ventricular tachycardia. *Kardiol Pol* 2018; **76:** 1018-20. doi: 10.5603/KP.2018.0120
10. Summers MR, Nevin RL. Stellate ganglion block in the treatment of posttraumatic stress disorder: a review of historical and recent literature. *Pain Pract* 2017; **17:** 546-53. doi: 10.1111/papr.12503
11. Hogan QH, Erickson SJ. MR imaging of the stellate ganglion: normal appearance. *AJR Am J Roentgenol* 1992; **158:** 655-9. Erratum in: *AJR Am J Roentgenol* 1992; **158:** 1320. doi: 10.2214/ajr.158.3.1739014
12. Beheshti M, Rezaee A, Langsteger W. 68Ga-PSMA-HBED uptake on cervicothoracic (Stellate) ganglia, a common pitfall on PET/CT. *Clin Nucl Med* 2017; **42:** 195-6. doi: 10.1097/RLU.0000000000001518
13. Kanthan GL, Hsiao E, Vu D, Schembri GP. Uptake in sympathetic ganglia on 68Ga-PSMA-HBED PET/CT: a potential pitfall in scan interpretation. *J Med Imaging Radiat Oncol* 2017; **61:** 732-8. doi: 10.1111/1754-9485.12622
14. Krohn T, Verburg FA, Pufe T, Neuhuber W, Vogg A, Heinzel A, et al. [(68)Ga]PSMA-HBED uptake mimicking lymph node metastasis in coeliac ganglia: an important pitfall in clinical practice. *Eur J Nucl Med Mol Imaging* 2015; **42:** 210-4. doi: 10.1007/s00259-014-2915-3
15. Rischpler C, Beck TI, Okamoto S, Schlitter AM, Knorr K, Schwaiger M, et al. 68Ga-PSMA-HBED-CC uptake in cervical, coeliac and sacral ganglia as an important pitfall in prostate cancer PET imaging. *J Nucl Med* 2018; **59:** 1406-11. doi: 10.2967/jnumed.117.204677
16. Giesel FL, Fiedler H, Stefanova M, Sterzing F, Rius M, Kopka K, et al. PSMA PET/CT with Glu-urea-Lys-(Ahx)-[^{68}Ga(HBED-CC)] versus 3D CT volumetric lymph node assessment in recurrent prostate cancer. *Eur J Nucl Med Mol Imaging* 2015; **42:** 1794-800. doi: 10.1007/s00259-015-3106-6
17. Giesel FL, Kesch C, Yun M, Cardinale J, Haberkorn U, Kopka K, et al. 18F-PSMA-1007 PET/CT detects micrometastases in a patient with biochemically recurrent prostate cancer. *Clin Genitourin Cancer* 2017; **15:** e497-e9. doi: 10.1016/j.clgc.2016.12.029
18. Bialek EJ, Malkowski B. Celiac ganglia: can they be misinterpreted on multimodal 68Ga-PSMA-11 PET/MR? *Nucl Med Commun* 2019; **40:** 175-84. doi: 10.1097/MNM.0000000000000944
19. Chaudhry A, Kamali A, Herzka DA, Wang KC, Carrino JA, Blitz AM. Detection of the stellate and thoracic sympathetic chain ganglia with high-resolution 3D-CISS MR imaging. *AJNR Am J Neuroradiol* 2018; **39:** 1550-4. doi: 10.3174/ajnr.A5698
20. van Leeuwen PJ, Stricker P, Hruby G, Kneebone A, Ting F, Thompson B, et al. (68) Ga-PSMA has a high detection rate of prostate cancer recurrence outside the prostatic fossa in patients being considered for salvage radiation treatment. *BJU Int* 2016; **117:** 732-9. doi: 10.1111/bju.13397
21. Vinsensia M, Chyoke PL, Hadaschik B, Holland-Letz T, Moltz J, Kopka K, et al. 68Ga-PSMA PET/CT and volumetric morphology of PET-positive lymph nodes stratified by tumor differentiation of prostate cancer. *J Nucl Med* 2017; **58:** 1949-55. doi: 10.2967/jnumed.116.185033
22. Sahlmann CO, Meller B, Bouter C, Ritter CO, Ströbel P, Lotz J, et al. Biphasic ^{68}Ga-PSMA-HBED-CC-PET/CT in patients with recurrent and high-risk prostate carcinoma. *Eur J Nucl Med Mol Imaging* 2016; **43:** 898-905. doi: 10.1007/s00259-015-3251-y
23. Abtahi SM, Elmi A, Hedgire SS, Ho YC, Pourjabbar S, Singh S, et al. Depiction of celiac ganglia on positron emission tomography and computed tomography in patients with lung cancer. *Clin Imaging* 2014; **38:** 292-5. doi: 10.1016/j.clinimag.2013.12.017

research article

Radiological findings of porcine liver after electrochemotherapy with bleomycin

Maja Brloznik[1], Nina Boc[2], Gregor Sersa[2,3], Jan Zmuc[2], Gorana Gasljevic[2], Alenka Seliskar[1], Rok Dezman[4], Ibrahim Edhemovic[2], Nina Milevoj[1], Tanja Plavec[1,5], Vladimira Erjavec[1], Darja Pavlin[1], Masa Bosnjak[2], Erik Brecelj[2], Ursa Lampreht Tratar[2], Bor Kos[6], Jani Izlakar[2], Marina Stukelj[7], Damijan Miklavcic[6], Maja Cemazar[2,8]

[1] University of Ljubljana, Veterinary Faculty, Small Animal Clinic, Ljubljana, Slovenia
[2] Institute of Oncology Ljubljana, Ljubljana, Slovenia
[3] University of Ljubljana, Faculty of Health Sciences, Ljubljana, Slovenia
[4] University Medical Centre, Clinical Institute of Radiology, Ljubljana, Slovenia
[5] Small Animal Hospital Hofheim, Katharina-Kemmler-Strasse 7, Hofheim, Germany
[6] University of Ljubljana, Faculty of Electrical Engineering, Ljubljana, Slovenia
[7] University of Ljubljana, Veterinary Faculty, Clinic for Reproduction and Farm Animals, Clinic for Ruminants and Pigs, Ljubljana, Slovenia
[8] University of Primorska, Faculty of Health Sciences, Izola, Slovenia

Radiol Oncol 2019; 53(4): 415-426.

Received 15 August 2019
Accepted 12 September 2019

Correspondence to: Prof. Maja Čemažar, Ph.D., Institute of Oncology Ljubljana, Department of Experimental Oncology, Zaloška 2, Ljubljana, Slovenia. Phone: +386 1 587 94 34; E-mail: mcemazar@onko-i.si

Disclosure: D.M. is an inventor of several patents pending and granted. He is receiving royalties and is consulting for different companies and organizations, which are active in electroporation and electroporation-based technologies and therapies. The remaining authors report no conflicts of interest.

Background. Radiologic findings after electrochemotherapy of large hepatic blood vessels and healthy hepatic parenchyma have not yet been described.

Materials and methods. We performed a prospective animal model study with regulatory approval, including nine grower pigs. In each animal, four ultrasound-guided electroporated regions were created; in three regions, electrodes were inserted into the lumen of large hepatic vessels. Two types of electrodes were tested; variable linear- and fixed hexagonal-geometry electrodes. Ultrasonographic examinations were performed immediately and up to 20 minutes after the procedure. Dynamic computed tomography was performed before and at 60 to 90 minutes and one week after the procedure.

Results. Radiologic examinations of the treated areas showed intact vessel walls and patency; no hemorrhage or thrombi were noted. Ultrasonographic findings were dynamic and evolved from hyperechogenic microbubbles along electrode tracks to hypoechogenicity of treated parenchyma, diffusion of hyperechogenic microbubbles, and hypoechogenicity fading. Contrast-enhanced ultrasound showed decreased perfusion of the treated area. Dynamic computed tomography at 60 to 90 minutes after the procedure showed hypoenhancing areas. The total hypoenhancing area was smaller after treatment with fixed hexagonal electrodes than after treatment with variable linear geometry electrodes.

Conclusions. Radiologic findings of porcine liver after electrochemotherapy with bleomycin did not show clinically significant damage to the liver, even if a hazardous treatment strategy, such as large vessel intraluminal electrode insertion, was employed, and thus further support safety and clinical use of electrochemotherapy for treatment of hepatic neoplasia.

Key words: electrochemotherapy; pig; liver; hepatic vessels; ultrasound; computed tomography

Introduction

Surgical resection is the gold standard for the treatment of hepatic neoplasia. However, the majority of hepatic tumors are unresectable at the time of diagnosis. In these patients, alongside systemic chemotherapy, different local ablative techniques, such as radiofrequency and microwave ablation, are used.[1-3] However, these two techniques are not optimal for tumors located near major bile ducts and larger hepatic vessels due to the heat sink effect or potential damage to vital structures.[2-4] Hence, novel techniques, such as irreversible electroporation (IRE) ablation and electrochemotherapy (ECT), are advantageous for patients with unresectable hepatic neoplasia adjacent to major bile ducts and vessels.[1-3,5] ECT is a method for the delivery of chemotherapeutic drugs by reversible electroporation, which enables the entry of otherwise poorly or nonpermeant exogenous molecules into cells by the application of short high-intensity electric pulses that induce reversible cell membrane permeabilization.[6-8] ECT is nowadays widely used in European centers for the treatment of cutaneous tumors.[9,10]

Clinical studies have shown that ECT is safe and effective also for the treatment of liver metastases and hepatocellular carcinoma (HCC)[3,4,6,7,11–13], and also other deep-seated tumors like pancreatic carcinoma.[14-16] Potentially hazardous electrode insertion into the lumen of major hepatic vessels has been reported in a study with percutaneous ECT of portal vein tumor thrombosis in patients with HCC.[11] From ECT[3,4,6,7,11,12] and IRE[17-22] studies, it is assumed that ECT of large hepatic vessels is safe, but this assumption has not yet been demonstrated with early radiologic examinations, which could reveal possible intra-abdominal hemorrhage or thrombus formation that could prove fatal for the patient.

Radiologic findings after IRE of hepatic tissue have been thoroughly described and used to determine the area that was irreversibly electroporated[22-26], while there has only been one report of radiologic findings after ECT of liver, where ultrasonographic (US) changes in hepatic tumors were described as indicators of adequate electric field tumor coverage for effective ECT.[27] The effect of ECT on healthy hepatic parenchyma and large hepatic vessels has not been previously studied by diagnostic imaging methods. The aim of this study was to characterize radiologic findings after ECT of large hepatic vessels and hepatic parenchyma in a porcine model, and hence to confirm the safety of the procedure.

Materials and methods

Animals and ethics approval

In this prospective animal model study with regulatory approval issued by the National Ethics Committee at The Administration of the Republic of Slovenia for Food Safety, Veterinary, and Plant Protection (Approval number: U34401-1/2017/4, Approval date: 17.03.2017), nine female grower pigs, purchased from an authorized swine breeder (Globocnik, Sencur, Slovenia) 3–17 days before experiment, were included.[28] Experimental animals were reared according to the European Council directive for minimum standards for the protection of pigs (2008/120/EC). All procedures complied with relevant national and European legislation (2010/63/EU).

Animals were 12 weeks old, weighed 31 ± 2.5 kg, and their liver volume estimated from CT images was 865 ± 85 cm^3.

Electrochemotherapy

During open surgery, four US-guided electroporated regions were created.

Insertion of electrodes. Electrodes were inserted into the lumen of the caudal vena cava and surrounding hepatic parenchyma (region 1), into the left median hepatic vein and surrounding parenchyma (region 2), into the left portal vein and parenchyma (region 3), and in the hepatic parenchyma of the left liver lobe (region 4).

Bleomycin and control group. Two pigs served as a control group and received electric pulses (EP) only. In the remaining seven pigs, ECT was performed; bleomycin (Bleomycinum, Heinrich Mack Nachf. GmbH & CO. KG, Illertissen, Germany, 15.000 IE/m^2) was administered intravenously at 8 minutes before the first application of EP.

Types of electrodes. Two types of electrodes routinely used in clinical treatment were tested. Variable linear geometry electrodes consisted of two long needle electrodes (with a diameter of 1.2 mm and a 3 cm long active part), which were 2 cm apart (VG-1230T12, IGEA S.p.A., Carpi, Italy). These electrode were employed in five cases of ECT and the two cases of EP. Fixed hexagonal geometry electrodes consists of seven needle electrodes with a diameter of 0.7 mm that are hexagonally placed 0.73 cm apart in a round plastic holder (N-30-HG, IGEA). These electrodes were used in two cases of ECT.

Electric pulses. EP was delivered with an electric pulse generator (Cliniporator, IGEA), and the

number of pulses for linear and hexagonal geometry electrodes were 8 and 96, respectively (8 between each individual electrode pair). Each pulse was 100 microseconds long, and the voltage was set to 2000 V in the case of linear electrodes and 730 V in the case of hexagonal electrodes. The frequencies for the linear and hexagonal electrode geometries were 1 and 5000 Hz, respectively.

Numerical modeling of electric field distribution

The treated area electric field was calculated by the finite element method using the software package Comsol Multiphysics (COMSOL AB, Stockholm, Sweden) with MATLAB (Mathworks, Natick, MA, USA).[29,30] The electrical parameters and bleomycin dosage were consistent with the European standard operating procedures for the ECT protocol and ECT for colorectal liver metastases clinical trials.[3,31,32]

Study end-point

The animals were euthanized at two or seven days after ECT/EP using 3 ml/10 kg i.v. T61 euthanasia solution (Intervet, Boxmeer, Netherlands); the liver was explanted for histologic analyses, which were reported in a separate paper.[28]

Ultrasonography (US) and computed tomography (CT)

Ultrasonographic examinations (US) were performed immediately and up to 20 minutes after the procedure. Different US machines were used, as available: Resona 7 and/or M9 (Mindray, Shenzhen, China) and/or Logiq S7 Pro (GE, Milwaukee, WI, USA). US examinations included B-mode to provide information about echogenicity and echotexture changes, Doppler (color and pulse-wave) to examine vessel patency and contrast enhanced ultrasound (CEUS) to evaluate the perfusion of hepatic parenchyma. The region of CEUS investigation was chosen according to the available US machine. In the case of the Mindray machine, a linear probe was used and the near-field area was preferred, whereas with the GE machine, the far-field was chosen since contrast works only with a convex probe. CEUS was performed before and after EP/ECT. Low mechanical index (<0.1) was applied, and a transpulmonary contrast agent Sonovue (Bracco, Milan, Italy), based on sulfur hexafluoride microbubbles, was administered into the cephalic vein (2.4 ml), and then flushed with saline (2 ml). From the time of contrast application, a 90-second cine-clip was made for further image analysis.

CT of the liver was performed before and at 60 to 90 minutes after EP/ECT with a Somatom Scope CT scanner (Siemens, Erlangen, Germany) in seven pigs. In two pigs treated with ECT with variable linear geometry electrodes, CT was also performed at 1 week after ECT. The following CT parameters were used: referenced 170 mA, 110 kVp, 3.0 mm slice reconstruction thickness, 2.0 mm reconstruction increment, and beam pitch of 1.4. The dynamic study with the contrast medium iopromide (Ultravist; Bayer, Leverkusen, Germany, 0.5 ml/kg), which was administered intravenously with a Missouri dual chamber injector pump (Ulrich medical, Ulm, Germany) at a velocity of 3 ml/s, consisted of 5 phases: pre-contrast, arterial with bolus tracking in abdominal aorta, and 3 subsequent phases in 30-second intervals (at 30, 60 and 90 seconds after arterial phase).

Image analysis

All radiologic findings were interpreted in consensus by three radiologists (M.B., N.B., R.D.) with more than 10-years of experience in liver imaging.

CEUS perfusion curve, presenting the signal intensity, was analyzed with the US machine built-in software.

CT images were evaluated with a free and open source software program Horos (https://horosproject.org) and Impax 6 (Agfa HealthCare, Mortsel, Belgium). CT findings before and after EP/ECT were compared. Hepatic attenuation, contrast enhancement, vessel patency, diameter and possible extravasation were evaluated. In pre-contrast studies, hepatic attenuation has been evaluated subjectively for homogeneity of hepatic parenchyma and circular ROIs were used to measure the attenuation in Hounsfield units (HU). Vessel patency, diameter and possible extravasation were evaluated subjectively in contrast studies. Dynamic CT showed hypoenhancing areas, which were if compared to untreated areas most clearly seen at 30 or 60 seconds after arterial phase. In each animal, the phase with the most evident hypoenhancing regions was used for further evaluation. Attenuation of untreated hepatic parenchyma was measured with circular ROIs that did not include vessels. Since it was difficult to differentiate individual treatment regions, all hypoenhancing areas were measured; in each of the transverse CT images, all the hypoenhancing regions were carefully delineated (with manual ROIs) to measure the area (in mm^2) and attenuation (in

HU) of the region. The total area, mean area and attenuation of the total area were calculated for each animal. The latter was calculated by a mathematical formula *sum* (*area x attenuation* / *total area*). To exclude individual differences in contrast enhancement, attenuation of untreated hepatic parenchyma was also considered; the difference between the attenuation of untreated parenchyma and the attenuation of the total area was divided by the attenuation of untreated parenchyma and multiplied by 100.

Histology

Histologic examinations were performed by an experienced pathologist (G.G.) with more than 10-years of experience in surgical pathology. To provide a comparison of radiologic and histologic data, immediate core biopsies of ECT-treated and untreated areas were performed in two pigs treated with ECT using linear geometry electrodes. In the treated parenchyma, two biopsies located between and oriented parallel to the electrodes were collected: one adjacent to the electrode and one 1 cm away from the electrode to the middle of the treated area. Histologic samples were fixed overnight in 10% buffered formalin, embedded in paraffin, cut into 3- to 4-µm-thick sections and stained with hematoxylin and eosin (H&E).

Statistical analysis

Statistical package computer program SPSS (SPSS Inc., Chicago, Illinois, USA) was used. For analysis of hepatic parenchyma contrast enhancement, the Shapiro-Wilk test was utilized to test the normality. Since the variables were not normally distributed, the Mann-Whitney U test and the Kruskal Wallis H test were used. Statistical significance was defined as $P \leq 0.05$. For other data in this study, descriptive statistics were applied.

Results

Radiologic findings and numerical modeling of electric field distribution

US findings

EP were delivered only after US confirmation of electrode position (Figure 1A). Immediately after

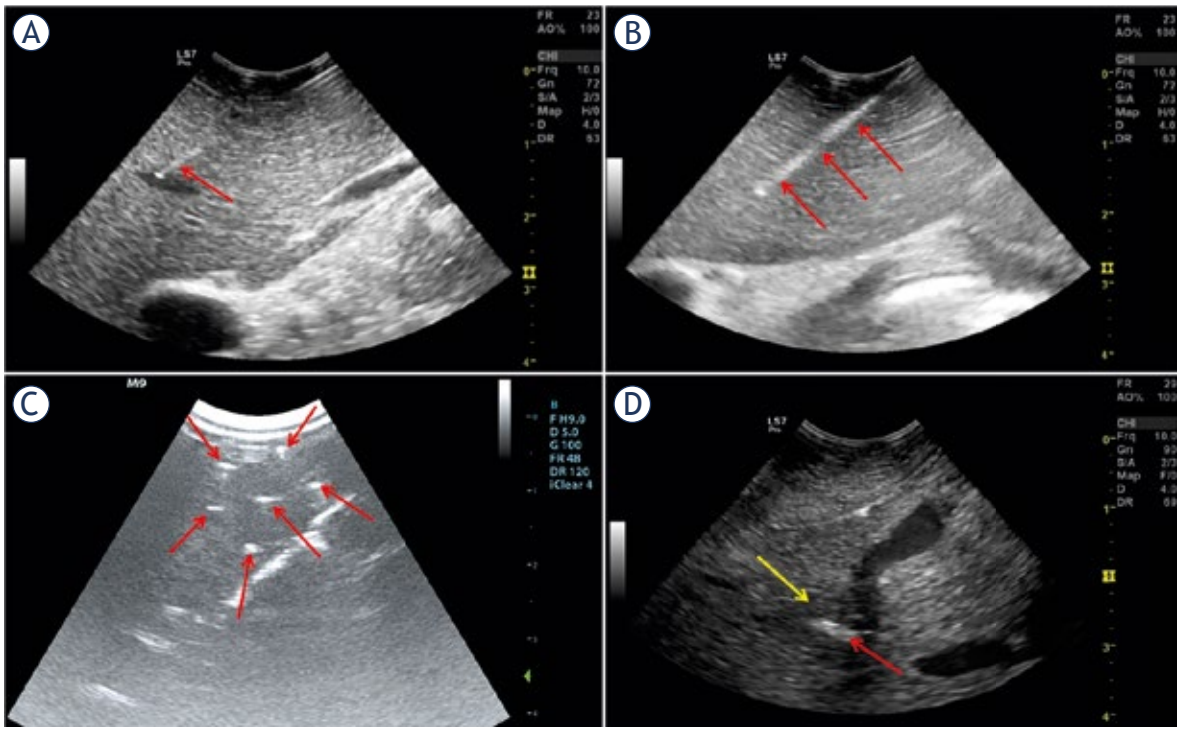

FIGURE 1. B-mode ultrasonography. **(A)** Position of the variable linear geometry electrode in the left middle hepatic vein (arrow). **(B)** Hyperechogenic microbubbles (arrows) observed immediately after electrochemotherapy (ECT) along the track of the linear electrode. **(C)** Hyperechogenic microbubbles observed immediately after ECT along the tracks of hexagonal geometry electrodes (arrows). **(D)** In the next minutes, the hepatic parenchyma of the treated area becomes hypoechogenic (yellow arrow), and hyperechogenic microbubbles (red arrow) start to diffuse.

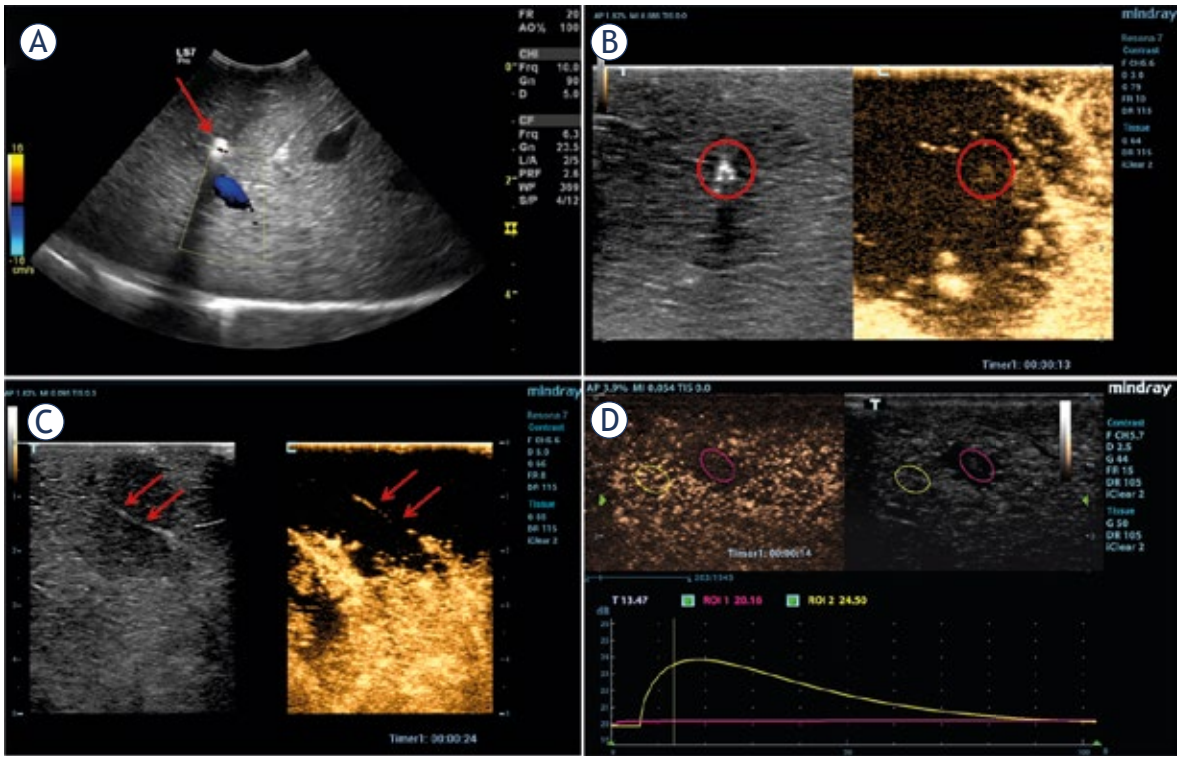

FIGURE 2. Doppler and contrast-enhanced ultrasonography. **(A)** Color Doppler in the left middle hepatic vein (blue) immediately after electrochemotherapy (ECT). Hyperechogenic microbubbles (arrow) can be noted. **(B)** Contrast enhanced ultrasound (CEUS) immediately after ECT and at 13 seconds after contrast administration; the position of the electrode is circled. **(C)** CEUS at 4 minutes after ECT and at 24 seconds after contrast; the larger vessel can be recognized (arrows). **(D)** CEUS at 5 minutes after ECT and at 14 seconds after contrast; a perfusion curve is shown.

the delivery of EP and removal of the electrodes, hyperechogenic microbubbles were observed along the electrode tracks (Figure 1B and C). In the next minutes, the treated parenchyma became hypoechogenic, and the hyperechogenic microbubbles started to diffuse (Figure 1D); the area of hypoechogenicity was larger than the area between the electrodes. In the next 5 to 10 minutes, the hyperechogenic microbubbles diffused through the treated area. There was no obvious difference between EP and ECT with variable linear geometry electrodes, while in the two cases of ECT with fixed hexagonal geometry electrodes, the hypoechogenicity was less evident compared to that with variable linear electrodes. After 10 minutes, the hypoechogenicity started to fade, and in the case of the treatment with hexagonal electrodes, it was no longer visible. The hypoechogenicity of the parenchyma was in contiguity to the treated vessel; however, the vessel wall appeared intact. There was no hemorrhage observed. Furthermore, the patency of the vessel was normal; there were no thrombi, stenotic lesions or extravasation noted, and the Doppler examination showed laminar flow (Figure 2A). CEUS showed that the perfusion of the treated area was significantly decreased (Figure 2B, C and D). The area of the hypoperfused parenchyma was larger than the area between the electrodes (Figure 2B), *i.e.* extending outside the borders of the area encompassed by the electrodes. In the case of the treatment with fixed hexagonal geometry electrodes, the decrease in perfusion was less pronounced compared to the treatment with variable linear geometry electrodes, which was consistent with computer simulation of the larger volume exposed to high strength electric fields in the variable linear geometry electrodes.

CT features

Dynamic contrast enhanced CT at 60 to 90 minutes after EP/ECT showed subtle hypoattenuating electrode tracks in the pre-contrast and arterial phases (Figure 3A and B), while in the 3 subsequent phases, hypoenhancing areas of treated hepatic parenchyma were noted (Figure 3C, D and E). These areas were most clearly observed at 30 or 60 seconds after the arterial phase, and the phase with

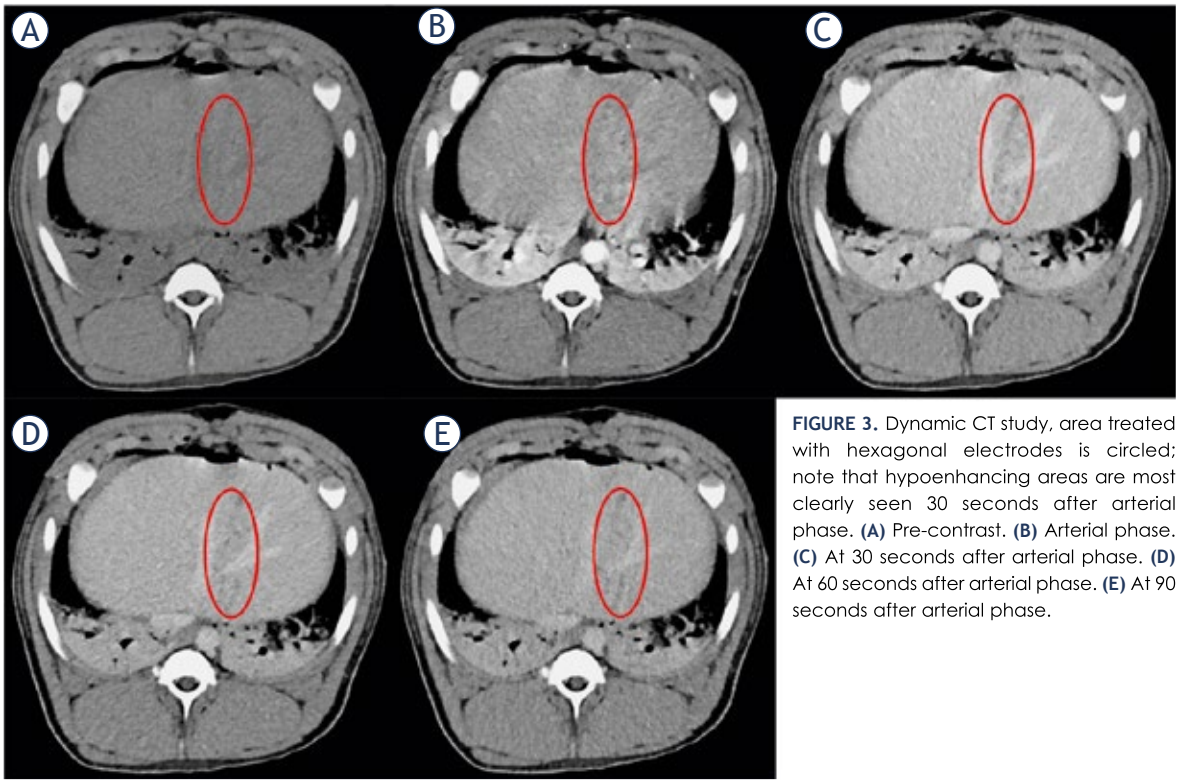

FIGURE 3. Dynamic CT study, area treated with hexagonal electrodes is circled; note that hypoenhancing areas are most clearly seen 30 seconds after arterial phase. **(A)** Pre-contrast. **(B)** Arterial phase. **(C)** At 30 seconds after arterial phase. **(D)** At 60 seconds after arterial phase. **(E)** At 90 seconds after arterial phase.

most evident hypoenhancing areas was used for further evaluation. As can be seen in Table 1, different number of hypoenhancing areas were measured in each animal. In the case of the treatment with linear geometry electrodes, the hypoenhancing regions were larger than those in the case of the treatment with hexagonal geometry electrodes (Figures 4A, B, 5A and 5B). An example of the multiplanar reconstruction (MPR) of one of the areas treated with variable linear geometry electrodes is presented in Figure 4C. All treated vessels were patent with no evidence of thrombosis (Figure 6A). Hypoenhancing areas were in contiguity with the treated vessels. There was no narrowing of the treated vessels, vessel wall and patency were not affected. No contrast extravasation was identified from large vessels in which the electrodes were inserted.

TABLE 1. Area and attenuation of hypoenhancing regions for each animal

		Number of measured hypo-enhancing regions	Total area (in mm²)	Median area (in mm²), IQR	A Attenuation of total area (in HU) ∑ ((area x attenuation) / total area)	B Attenuation of untreated parenchyma (in HU), ± SE 15 measurements in each animal	Difference in attenuation (B – A)	Corrected difference in attenuation (B–A)/B*100
Linear electrodes	ECT	48	8454	94.5, 46–168	72	118 ± 2	46	39
		66	3178	31.5, 19–53	86	114 ± 2	28	25
		91	5146	39, 25–75	82	123 ± 1	41	33
	EP	61	4538	51, 30–104	75	108 ± 1	33	30
		55	3563	32, 18–92	122	165 ± 3	43	26
Hexagonal electrodes	ECT	25	750*	21, 11.5–32*	98	124 ± 2	26	21
		46	2328*	39.5, 25–72*	80	101 ± 1	21*	21*
1 week after ECT with linear electrodes		11	99**	8, 5–11**	74	99 ± 1	24**	25**
		13	300**	19, 12–27.5**	76	101 ± 1	25**	25**

ECT = electrochemotherapy; EP = electroporation; HU = Hounsfield units; IQR = interquartile range; STD = standard deviation; *P < 0.01 compared to groups with variable linear geometry electrodes; **P < 0.01 compared to groups immediately after EP/EC

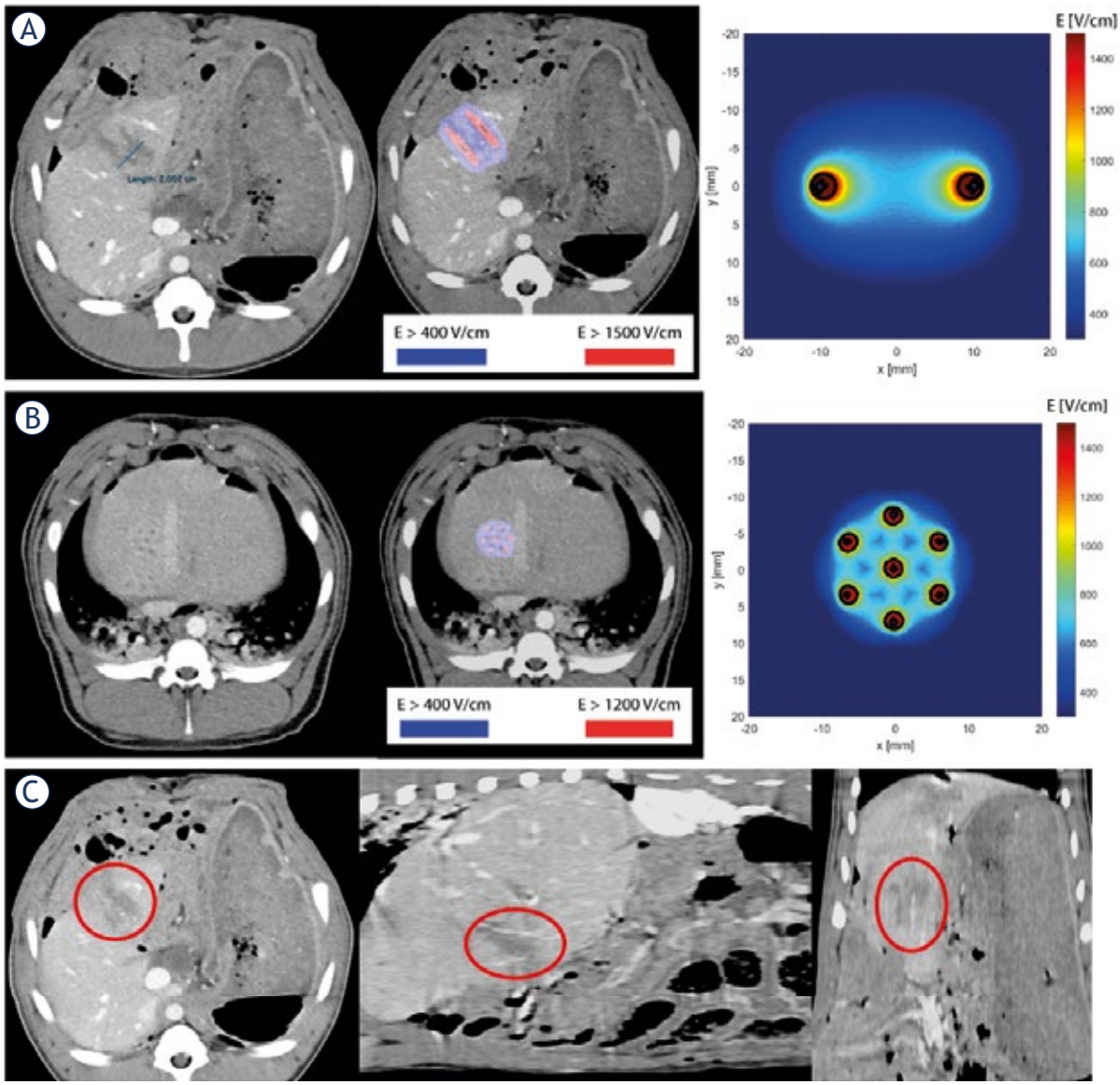

FIGURE 4. (A) Electrochemotherapy (ECT) of the liver with linear electrodes. Left figure is a CT image, where a distance between the hypoenhancing tracks of 2 cm can be noted. Right figure is numerical model of electric field distribution in linear electrodes. Middle figure shows electric field distribution superimposed on the CT image. **(B)** ECT of the liver with hexagonal electrodes. Left figure is a CT image and right figure is numerical model of electric field distribution in hexagonal electrodes. Middle image shows electric field distribution superimposed on the CT image. **(C)** Multiplanar reconstruction (MPR) of Figure 4A. The hypoenhancing area is circled. Note the larger vessel in the middle of the hypoenhancing area in coronal reconstruction.

After careful delineation of the hypoenhancing areas in each of the transverse CT images (Figure 6B), a statistically significant difference between attenuation of untreated parenchyma and attenuation of treated areas was observed in all animals. For each animal, CT measurements and calculations are presented in the Table 1. In the case of the treatment with hexagonal geometry electrodes, the total area of the hypoenhancing regions was smaller than that in the case of the treatment with linear electrodes ($P < 0.001$), which is in accordance with computer simulation. The results of the computer simulations are shown in Figure 4A and B, where the difference in the shape of the local electric field strength produced by the different electrodes is observed. Figure 4A shows that the treated volume produced by the variable linear geometry electrodes measures 30 mm in width and 20 mm in height (corresponding to the distance between the electrodes and the applied voltage) and

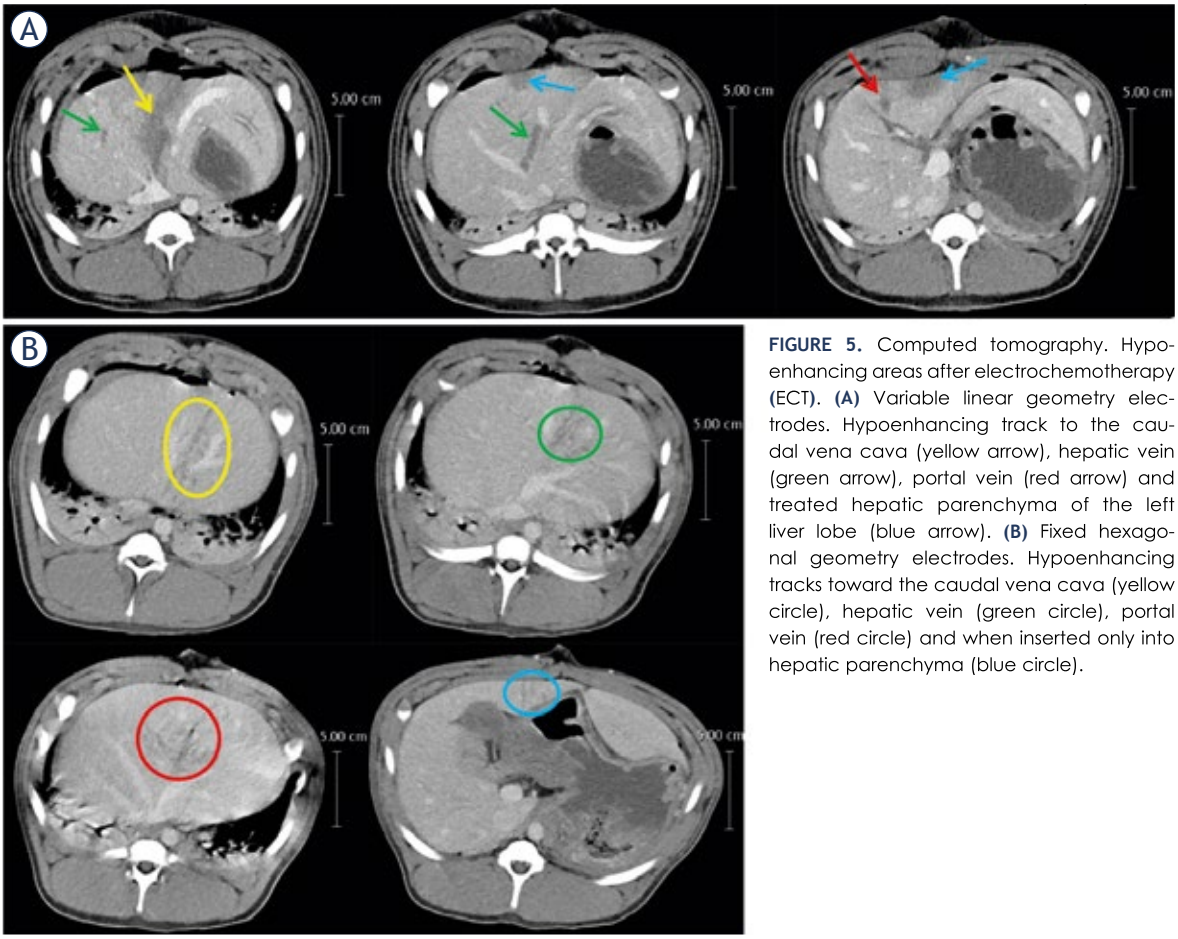

FIGURE 5. Computed tomography. Hypoenhancing areas after electrochemotherapy (ECT). **(A)** Variable linear geometry electrodes. Hypoenhancing track to the caudal vena cava (yellow arrow), hepatic vein (green arrow), portal vein (red arrow) and treated hepatic parenchyma of the left liver lobe (blue arrow). **(B)** Fixed hexagonal geometry electrodes. Hypoenhancing tracks toward the caudal vena cava (yellow circle), hepatic vein (green circle), portal vein (red circle) and when inserted only into hepatic parenchyma (blue circle).

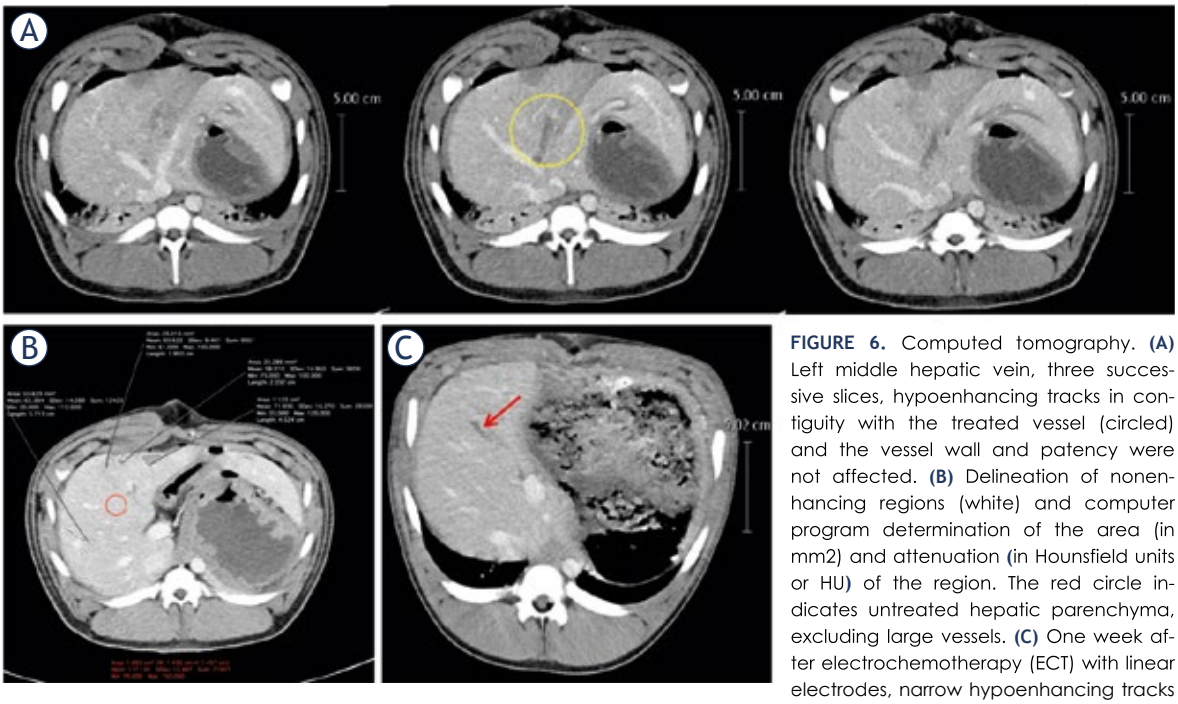

FIGURE 6. Computed tomography. **(A)** Left middle hepatic vein, three successive slices, hypoenhancing tracks in contiguity with the treated vessel (circled) and the vessel wall and patency were not affected. **(B)** Delineation of nonenhancing regions (white) and computer program determination of the area (in mm2) and attenuation (in Hounsfield units or HU) of the region. The red circle indicates untreated hepatic parenchyma, excluding large vessels. **(C)** One week after electrochemotherapy (ECT) with linear electrodes, narrow hypoenhancing tracks were observed (red arrow).

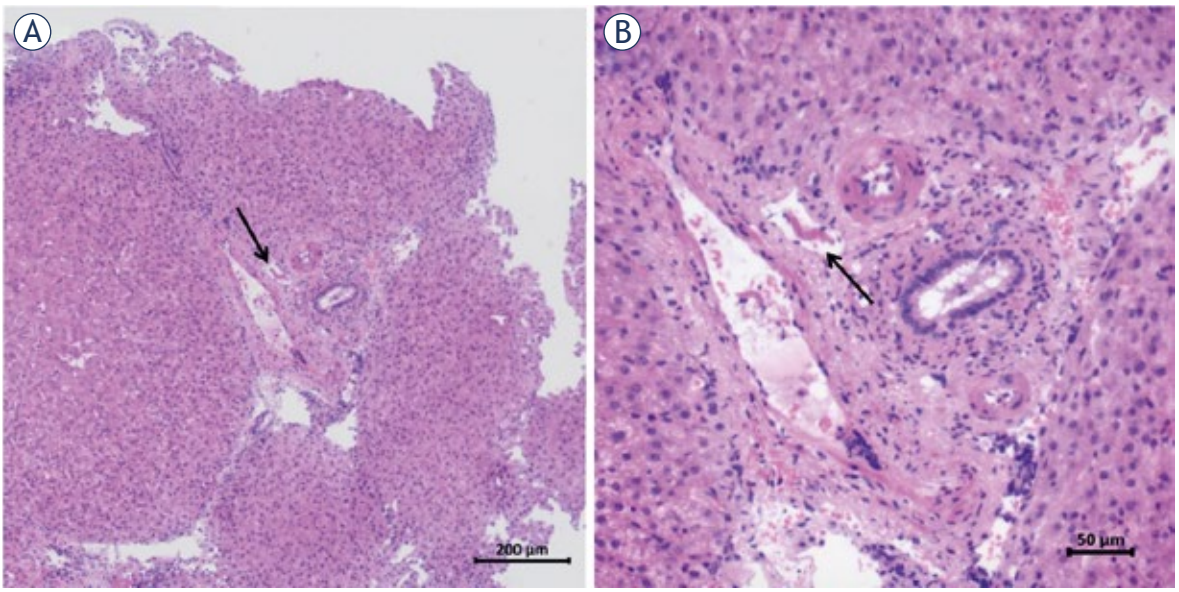

FIGURE 7. Histology of hepatic parenchyma immediately after electrochemotherapy (ECT). Fibrin thrombus in the lumen of a small venule (arrow). **(A)** H&E, 10x. **(B)** H&E, 20x.

is larger than the treated volume produced by the hexagonal electrodes, which is 20 mm by 20 mm (Figure 4B).

Furthermore, the difference and the corrected difference in attenuation were smaller after treatment with fixed hexagonal geometry electrodes than after treatment with variable linear electrodes ($P < 0.001$). There was no significant difference in the total area between the EP and ECT with linear electrodes ($P = 0.908$). In the CT findings at one week after ECT (Figure 6C), a regression of the ECT-induced changes was observed with only small hypoenhancing areas with diameters of up to 6 mm identified, which corresponds to the volume of irreversibly electroporated liver tissue determined by computer simulations, as shown in Figure 4A and B. The total area of the hypoenhancing regions was smaller than that observed immediately after the EP/ECT ($P < 0.001$). The difference and corrected difference in attenuation were both smaller after one week compared to those at 60 to 90 minutes after EP/ECT ($P < 0.001$, $P = 0.007$).

Histologic findings

Histologic findings of treated hepatic parenchyma immediately after ECT showed fibrin thrombi in small venules (Figure 7), with no other histologic changes of other vessels and bile ducts or the hepatic parenchyma.

Discussion

Radiologic findings after EP/ECT of large hepatic vessels and hepatic parenchyma were characterized in a porcine model, which was selected due to anatomical and physiological similarities with the human liver.[1,33] The results showed decreased perfusion in the treated area. This finding was an anticipated result since EP/ECT induces a local blood flow modifying effect or 'vascular lock' characterized by the vasoconstriction and increased wall permeabilization of small blood vessels. The effect on perfusion is shorter in EP compared to that in ECT and shorter in healthy compared to tumor tissue, which is known as the 'vascular disrupting effect'. Chemotherapeutic drugs are cytotoxic to endothelial cells, especially neoplastic endothelial cells, and this effect prolongs decreased perfusion.[34-41] In our case, there was no difference between EP and ECT, and no vascular disrupting effect was observed in healthy hepatic parenchyma[28], which confirms that bleomycin at the doses used has a negligible effect on healthy tissue.[34-36]

All radiologic modalities showed healthy vessel walls and patency, despite direct electrode insertion into the lumen of major hepatic vessels. These findings were consistent with previously published histologic results: no thrombosis was identified at two and seven days after EP/ECT in healthy liver.[28] This result was an expected finding considering

ECT[3,4,8,11-13] and IRE[17-22] clinical studies, where electrodes were inserted in the vicinity of[3,4,8,11-13,17-22] or into major hepatic vessels.[13] The absence of bleeding, even if needles are inserted deep into the hepatic parenchyma, is an important safety aspect of ECT due to the transient local hypoperfusion and possible electrocoagulation related to the high current density at the surface of needle electrodes.[29,35]

The US findings were dynamic. Hyperechogenic bubbles, which initially form around the electrodes, are a consequence of electrochemical reactions on the electrodes and electrocoagulation of the tissue.[27,29] The liberated gases are chlorine at the anode and hydrogen at the cathode.[42,43] Gas bubbles are formed in RFA[44] and IRE[18,45] ablations. Hypoechogenicity of the treated parenchyma indicates a structural change, which presumably occurs due to decreased perfusion caused by the vasoconstriction and increased wall permeability (edema) of small vessels.[34-37] The histologic findings of the treated hepatic parenchyma immediately after ECT showed fibrin thrombi in small venules, which is consistent with decreased perfusion due to vessel spasms.

Decreased perfusion of the treated areas was confirmed with CEUS and dynamic CT studies, the latter proving the decreased contrast enhancement of the treated areas at 30 to 90 seconds after arterial phase. The area of decreased perfusion was smaller after treatment with fixed hexagonal electrodes than after treatment with variable linear geometry electrodes. This effect is due to a larger distance between electrodes in the case of variable geometry electrodes where higher voltage must be applied to achieve same therapeutic effect, and is in accordance with computer simulation and histology.[28] The difference between the two geometry electrodes can be ascribed to a higher local electric field strength adjacent to the electrodes in the case of linear electrodes[46], as shown in Figure 4A and B. Despite the difference in size of hypoperfused hypoenhancing areas due to the higher local electric field, there is no difference in efficacy of electroporation between the variable linear- and fixed hexagonal-geometry electrodes.[29,46] In routine clinical practice hexagonal electrodes are used for smaller and superficial liver tumors, while linear electrodes are used for deep-seated and larger liver tumors.[47] The subtleness of the radiological changes of liver after EP/ECT agrees with laboratory and histologic findings that the procedure is safe, while on the contrary, it could indicate that CT findings might not be a good indicator of procedure efficacy in healthy liver. The vascular structures of the portal spaces as well as branches of the hepatic and portal veins in the liver parenchyma display different changes depending on their size and position in the ablated area: those situated in the central parts of the ablated areas and close to the electrodes show complete necrosis. Smaller structures are more sensitive to electroporation than larger structures with arterioles and bile canaliculi more resistant than venules.[12]

The CT studies at one week after ECT showed only small hypoenhancing areas, which is in accordance with histologic studies showing the existence of scar tissue.[12,28] Where electrodes punctured the wall of the large vessels, the architecture of the vessel wall was effaced with missing endothelium and no thrombosis present.[28]

Our study has several limitations. Due to the time limit of open surgery, there was limited time for US examinations, and the CT studies were performed in a range of 60 to 90 minutes after the EP/ECT. Performing radiologic examinations at different times was a major limitation because radiologic findings were dynamic and evolved in time. Another limitation of this study is the use of various US machines, which precluded numerical and statistical analyses of the US findings. Different heart rates and blood pressures of pigs influenced CEUS assessment of perfusion; therefore, comparisons among animals would be challenging. Another limitation of the study was that CT studies were only performed at 1 week after ECT with variable linear geometry electrodes. Furthermore, in CT studies, various treated areas could not always be differentiated from other areas. This limitation was overcome in the study with the percutaneous ECT of portal vein tumor thrombosis[13] and in a study with IRE of porcine liver[22] with a coaxial angiocatheter to define electrode orientation and position relative to the ablation zone. Only healthy liver was studied, further investigation of other tissues, particularly tumor tissue is required, because it is reasonable to expect that radiologic findings after ECT of hepatic neoplasia differ from radiologic findings after ECT of healthy liver due to differences in vascular and extracellular spaces. Furthermore, relatively small number of animals has been investigated, which prevented further statistical analyses and a better correlation between different groups.

Conclusions

Radiologic findings after EP/ECT of porcine liver did not show clinically significant damage to large

liver vessels and parenchyma; intact vessel walls and patency were observed, the hepatic parenchymal changes indicated by US hypoechogenicity and CT hypoenhancement were subtle. Histologic changes immediately after, and 2 and 7 days after treatment were in accordance with radiologic findings, and these results confirm that ECT is safe for the treatment of tumors that are adjacent to large hepatic vessels. Notably, radiologic features after EP/ECT are dynamic, and further studies are required to thoroughly investigate these features to provide definite answers, which, if any, are useful as indicators of adequate electric field distribution and as possible predictive factors that could guide decisions regarding the course of further treatment.

Acknowledgements

Authors acknowledge the staff of the Small Animal Clinic and Clinic for Ruminants and Pigs (Veterinary Faculty, University of Ljubljana) for their help with animal husbandry, surgery, radiologic examinations, and laboratory tests. Furthermore, we thank Mateja Nagode for the help with statistical analysis. Language editing services for this manuscript were provided by American Journal Experts. The authors acknowledge the financial support of the Slovenian Research Agency (research program No. P3-003, No. P4-0053 and No. P2-0249). The funder had no role in the study design, data collection and analysis, decision to publish, or preparation of the manuscript.

References

1. Ong SL, Gravante G, Metcalfe MS, Dennison AR. History, ethics, advantages and limitations of experimental models for hepatic ablation. *World J Gastroenterol* 2013; **19:** 147-54. doi: 10.3748/wjg.v19.i2.147
2. Au JT, Kingham TP, Jun K, Haddad D, Gholami S, Mojica K, et al. Irreversible electroporation ablation of the liver can be detected with ultrasound B-mode and elastography. *Surgery* 2013; **153:** 787-93. doi: 10.1016/j.surg.2012.11.022
3. Edhemovic I, Brecelj E, Gasljevic G, Music MM, Gorjup V, Mali B, et al. Intraoperative electrochemotherapy of colorectal liver metastases. *J Surg Oncol* 2014; **110:** 320-7. doi: 10.1002/jso.23625
4. Edhemovic I, Gadzijev EM, Brecelj E, Miklavcic D, Kos B, Zupanic A, et al. Electrochemotherapy: a new technological approach in treatment of metastases in the liver. *Technol Cancer Res Treat* 2011; **10:** 475-85. doi: 10.7785/tcrt.2012.500224
5. Kingham TP, Karkar AM, D'Angelica MI, Allen PJ, DeMatteo RP, Getrajdman GI, et al. Ablation of perivascular hepatic malignant tumors with irreversible electroporation. *J Am Coll Surg* 2012; **215:** 379-87. doi: 10.1016/j.jamcollsurg.2012.04.029
6. Colletti L, Battaglia V, De Simone P, Turturici L, Bartolozzi C, Filipponi F. Safety and feasibility of electrochemotherapy in patients with unresectable colorectal liver metastases: a pilot study. *Int J Surg* 2017; **44:** 26-32. doi: 10.1016/j.ijsu.2017.06.033
7. Tafuto S, von Arx C, De Divitiis, Maura CT, Palaia R, Albino V, et al. Electrochemotherapy as a new approach on pancreatic cancer and on liver metastases. *Int J Surg* 2015; **21:** S78-S82. doi: 10.1016/j.ijsu.2015.04.095
8. Miklavcic D, Mali B, Kos B, Heller R, Sersa G. Electrochemotherapy: from the drawing board into medical practice. *Biomed Eng Online* 2014; **13:** 29. doi: 10.1186/1475-925X-13-29
9. Campana LG, Clover JG, Valpione S, Quaglino P, Gehl J, Kunte C, et al. Recommendations for improving the quality of reporting clinical electrochemotherapy studies based on qualitative systematic review. *Radiol Oncol* 2016; **50:** 1-13. doi: 10.1515/raon-2016-0006
10. Campana LG, Marconato R, Valpione S, Galuppo S, Alaibac M, Rossi CR, et al. Basal cell carcinoma: 10-year experience with electrochemotherapy. *J Transl Med* 2017; **15:** 122. doi: 10.1186/s12967-017-1225-5
11. Djokic M, Cemazar M, Popovic P, Kos B, Dezman R, Bosnjak M, et al. Electrochemotherapy as treatment option for hepatocellular carcinoma, a prospective pilot study. *Eur J Surg Oncol* 2018; **44:** 651-7. doi: 10.1016/j.ejso.2018.01.090
12. Gasljevic G, Edhemovic I, Cemazar M, Brecelj E, Gadzijev EM, Music MM, et al. Histopathological findings in colorectal liver metastasis after electrochemotherapy. *PloS One* 2017; **12:** e0180709. doi: 10.1371/journal.pone.0180709
13. Tarantino L, Busto G, Nasto A, Fristachi R, Cacace L, Talamo M, et al. Percutaneous electrochemotherapy in the treatment of portal vein tumor thrombosis at hepatic hilum in patients with hepatocellular carcinoma in cirrhosis: a feasibility study. *World J Gastroenterol* 2017; **23:** 906-18. doi: 10.3748/wjg.v23.i5.906
14. Granata V, Fusco R, Piccirillo M, Palaia R, Petrillo A, Lastoria S, Izzo F. Electrochemotherapy in locally advanced pancreatic cancer: Preliminary results. *Int J Surg* 2015; **18:** 230-6. doi: 10.1016/j.ijsu.2015.04.055
15. Bimonte S, Leongito M, Granata V, Barbieri A, del Vecchio V, Falco M, et al. Electrochemotherapy in pancreatic adenocarcinoma treatment: preclinical and clinical studies. *Radiol Oncol* 2016; **50:** 14-20. doi: 10.1515/raon-2016-0003
16. Granata V, Fusco R, Setola SV, Palaia R, Albino V, Piccirillo M, et al. Diffusion kurtosis imaging and conventional diffusion weighted imaging to assess electrochemotherapy response in locally advanced pancreatic cancer. *Radiol Oncol* 2019; **53:** 415-24. doi: 10.2478/raon-2019-0004
17. Cannon R, Ellis S, Hayes D, Narayanan G, Martin RCG. Safety and early efficacy of irreversible electroporation for hepatic tumors in proximity to vital structures. *J Surg Oncol* 2013; **107:** 544-9. doi: 10.1002/jso.23280
18. Lee EW, Chen C, Prieto VE, Dry SM, Loh CT, Kee ST. Advanced hepatic ablation technique for creating complete cell death: irreversible electroporation. *Radiology* 2010; **255:** 426-33. doi: 10.1148/radiol.10090337
19. Lee YJ, Lu DS, Osuagwu F, Lassman C. Irreversible electroporation in porcine liver: short- and long-term effect on the hepatic veins and adjacent tissue by CT with pathological correlation. *Invest Radiol* 2012; **47:** 671-5. doi: 10.1097/RLI.0b013e318274b0df
20. Narayanan G, Bhatia S, Echenique A, Suthar R, Barbery K, Yrizarry J. Vessel patency post irreversible electroporation. *Cardiovasc Intervent Radiol* 2014; **37:** 1523-9. doi: 10.1007/s00270-014-0988-9
21. Kasivisvanathan V, Thapar A, Oskrochi Y, Picard J, Leen EL. Irreversible electroporation for focal ablation at the porta hepatis. *Cardiovasc Intervent Radiol* 2012; **35:** 1531-4. doi: 10.1007/s00270-012-0363–7
22. Lee YJ, Lu DS, Osuagwu F, Lassman C. Irreversible electroporation in porcine liver: acute computed tomography appearance of ablation zone with histopathologic correlation. *J Comput Assist Tomogr* 2013; **37:** 154-8. doi: 10.1097/RCT.0b013e31827dbf9b
23. Appelbaum L, Ben-David E, Sosna J, Nissenbaum Y, Goldberg SN. US findings after irreversible electroporation ablation: radiologic-pathologic correlation. *Radiology* 2012; **262:** 117-25. doi: 10.1148/radiol.11110475
24. Abdelsalam ME, Chetta JA, Harmoush S, Ensor J Jr, Javadi S, Dixon K, et al. CT findings after irreversible electroporation ablation in a porcine model: radiologic-pathologic correlation. *J Vasc Interv Radiol* 2013; **24:** S161. doi: 10.1016/j.jvir.2013.01.405
25. Charpentier KP, Wolf F, Noble L, Winn B, Resnick M, Dupuy DE. Irreversible electroporation of the liver and liver hilum in swine. *HPB (Oxford)* 2011; **13:** 168-73. doi: 10.1111/j.1477-2574.2010.00261.x

26. Chung DJ, Sung K, Osuagwu FC, Wu HH, Lassman C, Lu DS. Contrast enhancement patterns after irreversible electroporation: experimental study of CT perfusion correlated to histopathology in healthy porcine liver. *J Vasc Interv Radiol* 2016; **27:** 104-11. doi: 10.1016/j.jvir.2015.09.005

27. Boc N, Edhemovic I, Kos B, Music MM, Brecelj E, Trotovsek B, et al. Ultrasonographic changes in the liver tumors as indicators of adequate tumor coverage with electric field for effective electrochemotherapy. *Radiol Oncol* 2018; **52:** 383-91. doi: 10.2478/raon-2018-0041

28. Zmuc J, Gasljevic G, Sersa G, Edhemovic I, Boc N, Seliskar A, et al. Large liver blood vessels and bile ducts are not damaged by electrochemotherapy with bleomycin in pigs. *Sci Rep* 2019: **9:** 3649. doi: 10.1038/s41598-019-40395-y

29. Kos B, Voigt P, Miklavcic D, Moche M. Careful treatment planning enables safe ablation of liver tumors adjacent to major blood vessels by percutaneous irreversible electroporation (IRE). *Radiol Oncol* 2015; **49:** 234-41. doi: 10.1515/raon-2015-0031

30. Marčan M, Pavliha D, Kos B, Forjanič T, Miklavčič D. Web-based tool for visualization of electric field distribution in deep-seated body structures and planning of electroporation-based treatments. *Biomed Eng Online* 2015; **14 Suppl 3:** S4. doi: 10.1186/1475-925X-14-S3-S4

31. Marty M, Sersa G, Rémi Garbay J, Gehl J, Collins CG, Snoj M, et al. Electrochemotherapy – an easy, highly effective and safe treatment of cutaneous and subcutaneous metastases: results of ESOPE (European Standard Operating Procedures of Electrochemotherapy) study. *EJC Supplements* 2006; **4:** 3-13. doi: 10.1016/j.ejcsup.2006.08.002

32. Mir LM, Gehl J, Sersa G, Collins CG, Garbay JR, Billard V, et al. Standard operating procedures of the electrochemotherapy: instructions for the use of bleomycin or cisplatin administered either systemically or locally and electric pulses delivered by Cliniporator by means of invasive or non-invasive electrodes. *Eur J Cancer Suppl* 2006; **4:** 14-25. doi: 10.1016/j.ejcsup.2006.08.003

33. Nykonenko A, Vavra P, Zonca P. Anatomic peculiarities of pig and human liver. *Exp Clin Transplant* 2017; **15:** 21-6. doi: 10.6002/ect.2016.0099

34. Bellard E, Markelc B, Pelofy S, Le Guerroué, Sersa G, et al. Intravital microscopy at the single vessel level brings new insights of vascular modification mechanisms induced by electropermeabilization. *J Control Release* 2012; **163:** 396-403. doi: 10.1016/j.jconrel.2012.09.010

35. Jarm T, Cemazar M, Miklavcic D, Sersa G. Antivascular effects of electrochemotherapy: implications in treatment of bleeding metastases. *Expert Rev Anticancer Ther* 2010; **10:** 729-46. doi: 10.1586/era.10.43

36. Gehl J, Skovsgaard T, Mir LM. Vascular reactions to in vivo electroporation: characterization and consequences for drug and gene delivery. *Biochim Biophys Acta* 2002; **1569:** 51-8. doi: 10.1016/s0304-4165(01)00233-1

37. Markelc B, Bellard E, Sersa G, Jesenko T, Pelofy S, Teissié, et al. Increased permeability of blood vessels after reversible electroporation is facilitated by alterations in endothelial cell-to-cell junctions. *J Control Release* 2018; **276:** 30-41. doi: 10.1016/j.jconrel.2018.02.032

38. Ivanusa T, Beravs K, Cemazar M, Jevtic V, Demsar F, Sersa G. MRI macromolecular contrast agents as indicators of changed tumor blood flow. *Radiol Oncol* 2001; **35:** 139-47.

39. Sersa G, Cemazar M, Miklavcic D. Tumor blood flow modifying effects of electrochemotherapy: a potential vascular targeted mechanism. *Radiol Oncol* 2003; **37:** 43-8.

40. Sersa G, Cemazar M, Miklavcic D, Chaplin DJ. Tumor blood flow modifying effect of electrochemotherapy with bleomycin. *Anticancer Res* 1999; **19:** 4017-22.

41. Sersa G, Cemazar M, Parkins CS, Chaplin DJ. Tumour blood flow changes induced by application of electric pulses. *Eur J Cancer* 1999; **35:** 672-7. doi: 10.1016/s0959-8049(98)00426-2

42. Li K, Xin Y, Gu Y, Xu B, Fan D, Ni B. Effects of direct current on dog liver: possible mechanisms for tumor electrochemical treatment. *Bioelectromagnetics* 1997; **18:** 2-7. doi: 10.1002/(sici)1521-186x(1997)18:1<2::aid-bem2>3.0.co;2-6

43. Stehling MK, Guenther E, Mikus P, Klein N, Rubinsky L, Rubinsky B. Synergistic combination of electrolysis and electroporation for tissue ablation. *PloS One* 2016; **11:** e0148317. doi: 10.1371/journal.pone.0148317

44. Oei T, vanSonnenberg E, Shankar S, Morrison PR, Tuncali K, Silverman SG. Radiofrequency ablation of liver tumors: a new cause of benign portal venous gas. *Radiology* 2005; **237:** 709-17. doi: 10.1148/radiol.2372041295

45. Faroja M, Ahmed M, Appelbaum L, Ben-David E, Moussa M, Sosna J. Irreversible electroporation ablation: is all the damage non thermal? *Radiology* 2013; **266:** 462-70. doi: 10.1148/radiol.12120609

46. Miklavcic D, Semrov D, Mekid H, Mir LM. A validated model of in vivo electric field distribution in tissues for electrochemotherapy and for DNA electrotransfer for gene therapy. *Biochim Biophys Acta* 2000; **1523:** 73-83. doi: 10.1016/s0304-4165(00)00101-x

47. Miklavcic D, Sersa G, Brecelj E, Gehl J, Soden D, Bianchi G, et al. Electrochemotherapy: technological advancements for efficient electroporation-based treatment of internal tumors. *Med Biol Eng Comput* 2012; **50:** 1213-25. doi: 10.1007/s11517-012-0991-8

research article

Retrieved cerebral thrombi studied by T_2 and ADC mapping: preliminary results

Jernej Vidmar[1,2,3], Franci Bajd[4], Zoran V. Milosevic[3], Igor J. Kocijancic[3], Miran Jeromel[3,5], Igor Sersa[1,2]

[1] Institute of Physiology, Medical Faculty, University of Ljubljana, Slovenia
[2] Jožef Stefan Institute, Ljubljana, Slovenia
[3] Department of Diagnostic and Interventional Neuroradiology, Clinical Institute of Radiology, University Medical Centre Ljubljana, Slovenia
[4] Faculty of Mathematics and Physics, University of Ljubljana, Slovenia
[5] General Hospital Slovenj Gradec, Department of Diagnostic and Interventional Radiology, Slovenia

Radiol Oncol 2019; 53(4): 427-433.

Received 3 October 2019
Accepted 22 October 2019

Correspondence to: Igor Serša, Ph.D., Jožef Stefan Institute, Jamova cesta 39, SI-2000 Ljubljana, Slovenia, E-mail: igor.sersa@ijs.si

Disclosure: No potential conflicts of interest were disclosed.

Background. Recent advances in MRI technology makes it increasingly more competitive to CT also in the field of interventions. Multi-parametric MRI offers a significant amount of data relevant for characterization of human cerebral thrombi.

Patients and methods. Cerebral thrombi of 17 patients diagnosed with acute stroke were acquired by mechanical thrombectomy. The thrombi were subsequently scanned using a high spatial-resolution 3D T_1-weighted MRI to obtain morphological characteristics of the thrombi and also by apparent diffusion coefficient (ADC) and transversal nuclear magnetic resonance (NMR) relaxation time (T_2) mapping. The MRI results were analysed for possible correlations between thrombectomy procedure parameters (recanalization time and number of passes) and MR-measurable parameters (sample-mean ADC and T_2, within-sample coefficient of variation of ADC and T_2, and thrombus length).

Results. Both MRI mapping techniques enabled a good discrimination among thrombi regions of different water mobility and compaction. Within-sample coefficient of variation of ADC was found most sensitive for discrimination between the thrombi where thrombectomy procedure was performed in a single pass and those where is was performed in two or more passes ($p = 0.03$). Interestingly, negative correlation was found between the recanalization time and thrombus length ($\rho = -0.22$).

Conclusions. Preliminary results of presented study shows that pretreatment MRI assessment of thrombi in stroke patients could potentially ease stroke treatment planning. In this study it is shown that within-sample coefficient of variation of ADC could serve for prediction of possible complications during thrombectomy procedures.

Key words: stroke; mechanical thrombectomy; MR microscopy; ADC mapping; T_2 mapping

Introduction

Rates of death attributable to cardiovascular disease have declined, yet the burden of disease remains high.[1] The decline is among other factors also due to a significant improvement in treatment of large vessel occlusions in acute ischemic stroke. Early treatment of the stroke is usually based on recanalization approaches, namely, administration of thrombolytic agents[2] and/or mechanical removal of thrombi.[3] Occluding thrombi may stem from the heart or atherosclerotic lesions within or proximal to the affected vessel. Histological analysis alone is insufficient for determining the origin of occlusive thrombus since both thrombi etiologies, cardioembolic and arteriopathic, lead to a formation

of thrombi with complex histological patterns that overlap.[4] MRI was shown to have clinical potentials in thrombi localization and determination of its structure and composition.[5] Therefore, MRI can represent an interesting *in vivo* alternative to histology.

Microscopically, thrombi are composed of platelets and red blood cells (RBCs) interspersed within the fibrin meshwork. A fibrin meshwork by itself is a permeable porous structure; however, its permeability may be strongly influenced by the presence of platelets as well as of fibrin cross-linking which could considerably thicken the meshwork.[6,7] Entrapped RBCs in thrombi[8] reduce pore sizes within the meshwork and therefore also reduce the permeability of the thrombi.[9] Furthermore, distribution and proportion of the entrapped blood cells in thrombi (RBCs and platelets) influence their mechanical properties as well.[10] Therefore, overall susceptibility of thrombi to thrombolytic treatment (thrombolysis or mechanical thrombectomy) is strongly influenced by thrombi permeability and their mechanical properties.[11,12] An accurate assessment of the thrombi structure and composition could be helpful in treatment planning and prognosis of recanalization.[13,14]

Magnetic resonance imaging (MRI) is a sensitive tool for diagnosing ischemic stroke based on detecting water mobility in different tissue compartments. The detection is enabled by diffusion-weighted imaging (DWI) followed by a calculation of the apparent diffusion constant (ADC) map.[15] Another MRI mapping technique, namely the transversal nuclear magnetic resonance (NMR) relaxation time (T_2) mapping, can be used for characterization of thrombi structure and composition. NMR relaxation times are sensitive to molecular reorientation or tumbling and are therefore also associated with tissue structure and composition.[16] Differences in water mobility and NMR relaxation parameters between RBC-rich and platelet-rich regions were already found as an efficient discriminating factor for characterization of venous thrombi and assessment of their lytic outcome.[17] Specifically, ADC and T_2 mapping followed by the 2D histogram analysis confirmed large structural diversity of venous thrombi that differ by their origin and age.[18]

The aim of this study is fist to quantitatively characterize human cerebral thrombi using multiparametric MRI and second to find possible correlations between thrombectomy procedure parameters (recanalization time and number of passes) and MR-measurable parameters (sample-mean ADC and T_2, within-sample coefficient of variation of ADC and T_2, and thrombus length). Preliminary results of ongoing research are presented.

Patients and methods

Patients selected for the study (n = 17, mean age = 72 ± 12 years, 10 males and 7 females) were diagnosed with acute ischemic stroke due to occluded middle cerebral artery (MCA; M1 segment). The study design followed standard steps of acute ischemic stroke management in our tertiary centre. Urgent clinical evaluation by a neurologist was followed by an urgent multimodal CT imaging (native CT, CT perfusion imaging and CT agiography) to confirm the diagnosis of an ischemic stroke. The patients were then treated with the standard full dose of rt-PA (0.9 mg/kg, maximum 90 mg) and later, due to still presented clinical signs of large cerebral artery occlusion, underwent mechanical thrombectomy. All procedures were performed by the same skilled interventional neuroradiologist, using the same standard mechanical recanalization procedure with the same thrombectomy device (Trevo® stent retriever, 4 x 20 mm, Stryker Neurovascular, Kalamazoo, MI). For each thrombectomy, the recanalization time was registered as the time between the first contact of the thrombectomy device with the thrombus and the successful recanalization through the occluded artery with complete removal of the thrombus. In addition, for each procedure, number of passes with the thrombectomy device was registered as well.

The protocol of the study was approved by the Institutional Review Board and the Ethical Committee of the National Ministry of Health of the Republic of Slovenia, approval No. 118/04/14. The study was performed in agreement with the informed-consent policy.

MR imaging of the retrieved thrombi was performed within 24 hours on an experimental MRI scanner consisting of a 2.35 T horizontal-bore superconducting magnet (Oxford Instruments, Abingdon, United Kingdom) NMR/MRI spectrometer (Tecmag, Houston, TX, USA) and accessories for MR microscopy (Bruker, Ettlingen, Germany). Each thrombus sample was rinsed with isotonic saline of 0.9% w/v of NaCl, pH 7.4 and closed in Teflon tubes to prevent tissue desiccation during the MR scanning. The tube with the sample was then inserted into a 10 mm micro-imaging probe and then analyzed by a multi-parametric MRI protocol consisting of the 3D T_1-weighted MRI, fol-

lowed by diffusion-weighted imaging (DWI) for ADC mapping[19] and the multi-spin-echo imaging sequence for T_2 mapping.[20] The imaging parameters of the sequences are given in Table 1. During MRI scanning, the samples were held at a constant room temperature of 22°C.

To obtain five independent MR-measurable parameters of the thrombi (sample-mean ADC and T_2 values, their corresponding within-sample coefficients of variation CV_{ADC} and CV_{T2} and thrombus length) MR images were processed by using in-house written image-analysis software that was developed within the Matlab programming environment (MathWorks, Inc., Natick MA, USA). In the MR image processing software, ADC and T_2 values were calculated pixelwise from the masked diffusion-weighted and multi-spin-echo images of all slices through the entire thrombi volumes by fitting the corresponding exponential functions. For each thrombus in the study its sample-mean ADC and T_2 values and the corresponding within-sample coefficients of variation CV_{ADC} and CV_{T2} representing thrombus heterogeneity were calculated by analyzing the ADC and T_2 maps in all slices across the thrombus volume. Similarly, thrombus length (Length) of the thrombi were determined from the corresponding T_1-weighted images as the maximum length along the longitudinal direction.

MR-measurable parameters (ADC, T_2, CV_{ADC}, CV_{T2}, Length) of the thrombi in the study were then statistically analyzed for their correlations with the corresponding recanalization time (*RT*). Possible correlations were studied also between length of the thrombi and ADC, T_2, CV_{ADC}, CV_{T2}. In addition, the retrieved thrombi were also classified between a group with single pass retrieval, which was considered as thrombectomy non-problematic, and a group with multi-pass retrieval where the thrombectomy procedure was more difficult to perform. The two groups were subsequently statistically analyzed for significance of differences for different MR-measurable parameters using Student's t-test.

Results

Figure 1 depicts T_1-weighted images with the corresponding ADC and T_2 maps of two representative cerebral thrombi having a different structure and morphology. Comparison between ADC and T_2 maps of both samples in color-coded images shows a significant variability of ADC values across the thrombi for both samples, while their T_2 maps are more uniform. In ADC maps regions with high water mobility (yellow to white regions) can be well discriminated from compacted regions (blue to violet) where water mobility is much lower. T_2 maps can still discriminate between regions of different compactness/water (serum) content, however, not to the same extent.

Figure 2 shows graphs of correlation between the recanalization time and different MR-measurable thrombi parameters (ADC, T_2, CV_{ADC}, CV_{T2}, Length) as well as with number of passes with the thrombectomy device. Similarly, Figure 3 shows graphs of correlation between the thrombus length and structural and compositional parameters obtained from MR maps (ADC, T_2, CV_{ADC}, CV_{T2}). In

TABLE 1. MRI sequence parameters

Sequence parameter	MRI sequence		
	3D spin-echo	3D PGSE DWI	3D multi-echo
Field of view [mm³]	20 x 10 x 10	20 x 10 x 10	20 x 10 x 10
Imaging matrix	128 x 64 x 64	128 x 64 x 16	128 x 64 x 16
Spatial resolution [µm³]	156 x 156 x 156	156 x 156 x 625	156 x 156 x 625
Echo/inter-echo time [ms]	5	34	16
Repetition time [ms]	100	1035	1930
Signal averages	10	2	2
Number of echoes	1	1	8
b-values [s/mm²]	/	0, 260, 620, 1250	/
Scan time [h]	1	4.7	2.3

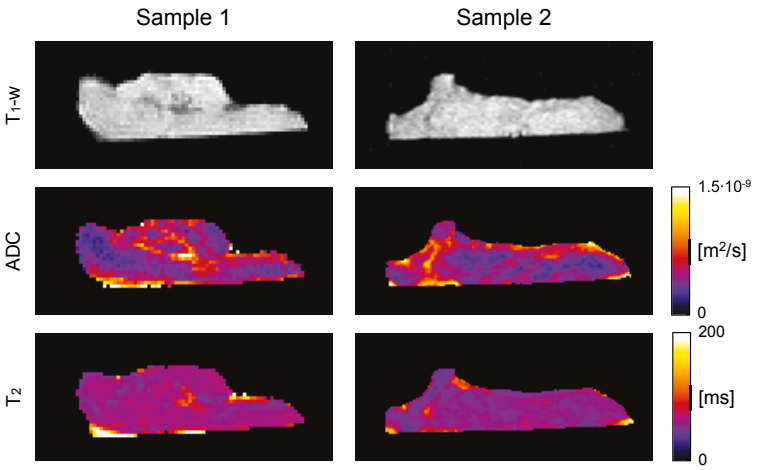

FIGURE 1. Two representative cerebral thrombi presented by central-slice T_1-weighetd images, ADC and T_2 maps. Low ADC and T_2 values, shown in dark blue, correspond to regions of higher compaction while brighter regions are less compact regions that are more susceptible to thrombolytic therapy. From the images can also be seen that variability of ADC values across the thrombi is considerably higher than that of T2 values.

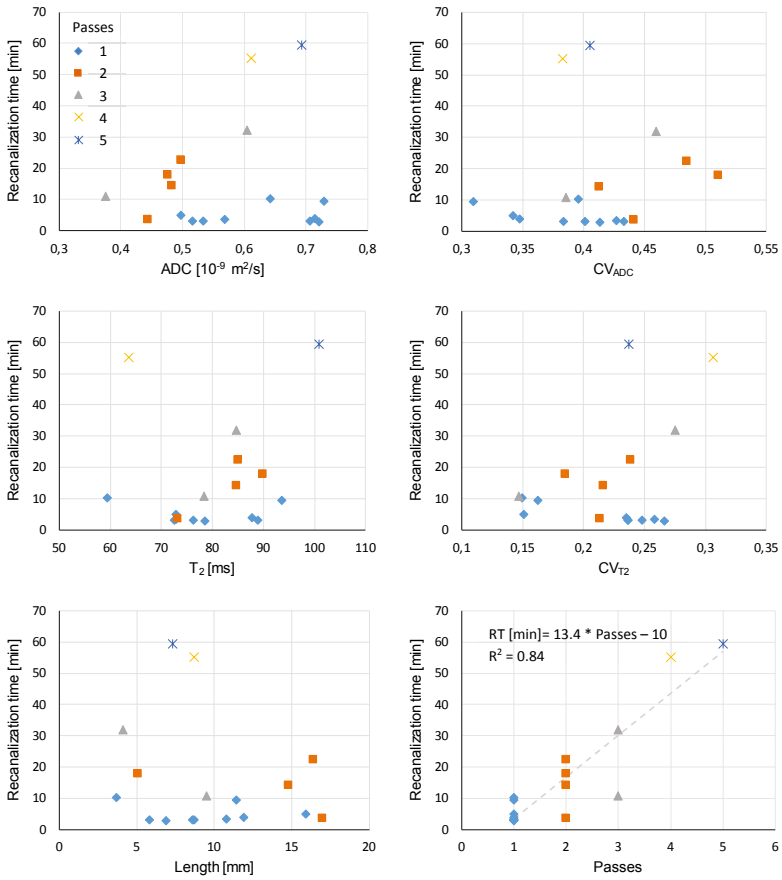

FIGURE 2. Graphs of correlation between the recanalization time (RT) of mechanical thrombectomy and different thrombi parameters: sample-mean apparent diffusion coefficient (ADC), within-sample coefficient of variation of apparent diffusion coefficient (CV_{ADC}), sample-mean spin-spin relaxation time (T_2), within-sample coefficient of variation of spin-spin relaxation time (CV_{T2}), thrombus length (Length), and number of thrombectomy procedure passes (Passes). Colour (symbol type) of experimental points indicates number of thrombectomy passes.

TABLE 2. Pearson correlation coefficient for different pairs of thrombi parameters. Correlation coefficients are sorted by their decreasing absolute values

Pair	ρ	Pair	ρ	Pair	ρ
Passes-RT	0.92	T_2-Passes	0.24	CV_{ADC}-Length	-0.14
ADC-CV_{ADC}	-0.43	Length-RT	-0.22	Length-Passes	-0.13
ADC-Length	-0.41	T_2-RT	0.21	ADC-T_2	0.13
CV_{T2}-RT	0.38	CV_{ADC}-Passes	0.19	CV_{ADC}-T_2	0.12
ADC-CV_{T2}	0.32	CV_{T2}-Length	-0.16	ADC-Passes	-0.09
CV_{ADC}-CV_{T2}	0.28	ADC-RT	0.15	T_2-Length	0.06
CV_{T2}-Passes	0.27	CV_{ADC}-RT	0.14	T_2-CV_{T2}	-0.01

ADC = apparent diffusion coefficient; CV_{ADC} = sample coefficient of variation CV_{ADC}; CV_{T2} = sample coefficient of variation CV_{T2}; Length = thrombus length; ρ = Pearson correlation coefficient; RT = recanalization time

the graphs, experimental points of different number of thrombectomy passes are colored differently and use different symbols. Correlation between different pairs of parameters given by the Pearson correlation coefficient is presented in Table 2. From the table it can be seen that correlation is the best between the recanalization time and the number of thrombectomy passes (ϱ = 0.92), which is expected. Each additional pass in average prolongs the recanalization time for 13 minutes. Other parameters do not correlate that well with the recanalization time. Among these, correlation was the best with CV_{T2} (ϱ = 0.38) and then with thrombus length (ϱ = -0.22), which is less than expected. Interesting is also that thrombus length correlates relatively well with ADC (ϱ = -0.41).

A closer inspection of correlation graphs in Figure 2 shows that distributions are significantly different for thrombi retrieved by a single pass of the thrombectomy device than for thrombi for which retrieval two or more passes were needed. In case of the single-pass thrombi group ADC and CV_{ADC} values are almost uniformly distributed over a wider range, while for the thrombi groups corresponding to multiple passes the values are more localized and are in average shifted to higher values for CV_{ADC} and to lower values for ADC. This observation is confirmed also with the t-test analysis of differences between the single-pass and multi-pass thrombi groups shown in Table 3. The test confirmed significance of difference between the groups for parameters ADC (p = 0.05) and CV_{ADC} (p = 0.03), while for other parameters (T_2, CV_{T2}, Length) the differences were not found significant.

Discussion

In the study it was shown that MR-measurable parameters of a thrombus and parameters of its retrieval by mechanical thrombectomy are correlated. While no significant correlation was found between the recanalization time and MR-measurable parameters, the parameter coefficient of variance of ADC was found efficient for discrimination between thrombi retrieved in a single pass of the thrombectomy device and those retrieved by multiple passes. This finding is supported by our previous observations of thrombi susceptibility to thrombolytic treatment.[17] In the study ADC was found more sensitive to structural and compositional changes in thrombi than T_2 and could therefore potentially serve for prediction of thrombolytic treatment outcome. Correlation between the re-

TABLE 3. Significance of differences between the single-pass (n = 9) and multi-pass (*n* = 8) thrombectomy groups for different parameters analysed by group-average values and by the t-test

Thrombectomy group / t-test	$ADC_{\_g}$ [10^{-9} m^2/s]	CV_{ADC_g}	T_{2_g} [ms]	CV_{T2_g}	$Length_{\_g}$ [mm]	$RT_{\_g}$ [min]
Single-pass	0.63 ± 0.1	0.38 ± 0.04	78 ± 10	0.22 ± 0.05	9.3 ± 3.7	4.8 ± 2.8
Multi-pass	0.52 ± 0.1	0.44 ± 0.05	82 ± 11	0.23 ± 0.05	10.4 ± 5.1	27 ± 20
p-value	0.05	0.03	0.41	0.64	0.62	0.006

ADC = apparent diffusion coefficient; $ADC_{\_g}$ = group-average of sample-mean ADC; CV_{ADC_g} = group-average of within sample coefficient of variation CV_{ADC}; CV_{T2_g} = group-average of within sample coefficient of variation CV_{T2}; $Length_{\_g}$ = group-average of thrombus length; p-value = result of the t-test analysis between single- and multi-pass thrombectomy groups; $RT_{\_g}$ = group-average of recanalization time; T_{2_g} = group-average of sample-mean T_2

canalization time and thrombus length of ϱ = -0.22, that was found in the present study, is somewhat surprising. Negative correlation between the two variables is a surprise, as one would expect that recanalization of longer thrombi should take longer[21] and that several passes of the thrombectomy device are need for retrieval of these. However, in our study, the thrombi with the longest recanalization time and with most passes of the thrombectomy device are of short to medium length (from 5 to 10 mm). This result indicates a strong influence of thrombi composition and compactness on the recanalization time. The recanalization time depends also on thrombus-vessel wall interactions.[22]

While thrombus length can be considered as a morphological parameter, the other four MR-measurable parameters are structural-dependent. ADC is a direct measure for water mobility in different tissue compartments of thrombi. It decreases due to an increased tortuosity and decreased porosity.[23] Relaxation time T_2 also depends on the thrombus microstructure. It is especially sensitive to changes in surface-to-volume ratio that when increased, can lead to an increased T_2 relaxation.[16] Specifically, in Figure 1, low ADC/T_2 values can be explained by the reduced mobility of water molecules due to an increased RBC compaction resulting in a significant reduction of the extracellular space. Another possible mechanism of the ADC/T_2 reduction is a high platelet-to-fibrin content that locally contracts fibrin meshwork resulting in a pore size reduction and extracellular serum expulsion.[7] From Figure 1 it can also be seen that ADC is more sensitive to structural changes in thrombi than relaxation time T_2. ADC maps have higher variability than T_2 maps, namely, they can better distinguish among regions of different compaction/water mobility than T_2 maps.

In the study thrombi were sorted into two groups, a single- and a multi-pass group, depending on the number of thrombectomy device passes performed for the retrieval of the thrombus. Classification of thrombi between the two groups enabled statistical analysis of differences among them using t-test of which results are shown in Table 3. The differences between the groups were found statistically significant ($p \leq 0.05$) for parameters CV_{ADC} and ADC, while they were not significant for CV_{T2}, T_2 and Length. Lack of significance for these three parameters could be due to too small number of samples analyzed (*n* = 17). With more samples included in the ongoing study the results of the study would be exacter. However, the current number of samples in the study, though low, was sufficient for demonstration of the expected trend between the MR-measurable and thrombectomy procedure pa-

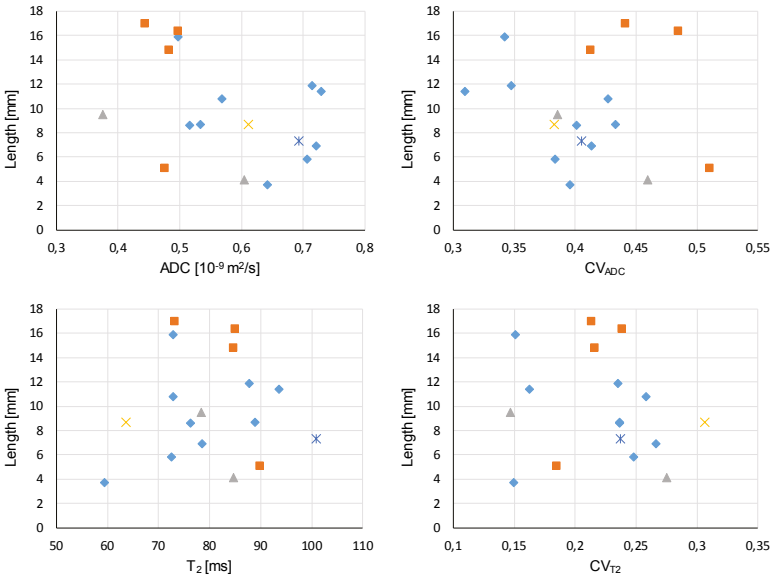

FIGURE 3. Graphs of correlation between the thrombus length (Length) and: sample-mean apparent diffusion coefficient (ADC), within-sample coefficient of variation of apparent diffusion coefficient (CV_{ADC}), sample-mean spin-spin relaxation time (T_2), and within-sample coefficient of variation of spin-spin relaxation time (CV_{T2}). Color (symbol type) of experimental points indicates number of thrombectomy passes as defined in Figure 2.

rameters. Another limitation of the study was its *ex vivo* design. Because of that some of the measured parameters differed from the corresponding values *in vivo*. This is especially true for diffusion-related parameters ADC and CV_{ADC}. Diffusion is slower at room temperature than at body temperature, while the relaxation time T_2 depends much less on temperature. Therefore, it is expected that T_2 values *ex vivo* are very similar to the corresponding *in vivo* values.[24] A special care was also taken to preserve tissue and structural integrity of the retrieved thrombi and therefore prevent possible mechanical sources for ADC and T_2 alternations. This was done during the thrombectomy procedure by minimizing possible thrombi fragmentation and after it by preventing tissue desiccation.

Ultimate goal of this research would be to perform MRI of thrombi *in vivo* on patients with acute ischemic stroke. Currently, MRI is too slow and does not provide sufficient resolution to compete with CT. Therefore, this application of MRI is ethically questionable. However, if thrombi would be analyzed *in vivo* only spectroscopically or imaged with very low resolution the scan time would be much shorter and information on the sample-mean ADC and sample-mean T_2 could still be obtained. Information on the thrombus length can in principle be obtained also from high-resolution CT images. Therefore, practically all the thrombus data of this study (apart from CV_{ADC} and CV_{T2}) could be obtained also *in vivo*. This information could ease decision making in stroke treatment. A proper selection of patients eligible for a treatment with mechanical recanalization is becoming extremely important since the window of thrombectomy for ischemic stroke patients was recently extended up to 24 hours.[25] Therefore, more patients are potential candidates for the procedure. A possibility of the procedure duration time prediction based on prior MR imaging of thrombi could significantly influence the decision about the thrombectomy in selected patients where an extended procedure duration time could present an increased risk of reperfusion related hemorrhage. Information about the composition of the thrombus could also in the future shift the treatment decision toward mechanical recanalization without pretreatment with the thrombolysis (prediction of failed thrombolysis). Finally, the information about the thrombus composition can also affect the decision making about the thrombectomy technique (choosing between stent retriever and aspiration device). Preliminary data from our study could also have an impact on further stent retriever design improvements. Namely, the design of the device could be tailored to different lengths of thrombi. Short thrombi may need a dedicated device, shorter in length but with much higher axial force. Alternatively, the aspiration technique may be used as a first modality of choice.

Conclusions

Preliminary results of our study shows that MRI can provide several parameters that are relevant for morphological and structural assessment of thrombi. With improvements of MRI technology, it can be expected that MRI scanning of patients with stroke could complement or even replace standard CT scanning in future. Therefore, MR-measurable parameters of thrombi, such as those presented in this study and perhaps some new ones, could in future, in combination with clinical and CT data help improving stroke treatment planning and easing treatment decisions. Results from this ongoing study my potentially influence further evolution of thrombectomy devices.

Acknowledgment

This study was financially supported by the Slovenian Research Agency grant J3-9288.

References

1. Roger VL, Go AS, Lloyd-Jones DM, Benjamin EJ, Berry JD, Borden WB, et al. Executive summary: heart disease and stroke statistics-2012 update: a report from the American Heart Association. *Circulation* 2012; **125:** 188-97. doi: 10.1161/CIR.0b013e31823ac046

2. Berkhemer OA, Fransen PSS, Beumer D, van den Berg LA, Lingsma HF, Yoo AJ, et al. A randomized trial of intraarterial treatment for acute ischemic stroke. *New Engl J Med* 2015; **372:** 11-20. doi: 10.1056/NEJMoa1411587

3. Xavier AR, Farkas J. Catheter-based recanalization techniques for acute ischemic stroke. *Neuroimag Clin N Am* 2005; **15:** 441-53. doi: 10.1016/j.nic.2005.06.007

4. Marder VJ, Chute DJ, Starkman S, Abolian AM, Kidwell C, Liebeskind D, et al. Analysis of thrombi retrieved from cerebral arteries of patients with acute ischemic stroke. *Stroke* 2006; **37:** 2086-93. doi: 10.1161/01.STR.0000230307.03438.94

5. Gasparian GG, Sanossian N, Shiroishi MS, Liebeskind DS. Imaging of occlusive thrombi in acute ischemic stroke. *Int J Stroke* 2015; **10:** 298-305. doi: 10.1111/ijs.12435

6. Bajd F, Vidmar J, Fabjan A, Blinc A, Kralj E, Bizjak N, et al. Impact of altered venous hemodynamic conditions on the formation of platelet layers in thromboemboli. *Thromb Res* 2012; **129:** 158-63. doi: 10.1016/j.thromres.2011.09.007

7. Weisel JW. Structure of fibrin: impact on clot stability. *J Thromb Haemost* 2007; **5:** 116-24. doi: 10.1111/j.1538-7836.2007.02504.x

8. Lipinski B, Pretorius E, Oberholzer HM, van der Spuy WJ. Interaction of fibrin with red blood cells: the role of iron. *Ultrastruct Pathol* 2012; **36:** 79-84. doi: 10.3109/01913123.2011.627491

9. Fang J, Tsui PH. Evaluation of thrombolysis by using ultrasonic imaging: an in vitro study. *Sci Rep* 2015; **5:** 11669. doi: 10.1038/srep11669.

10. Gennisson JL, Lerouge S, Cloutier G. Assessment by transient elastography of the viscoelastic properties of blood during clotting. *Ultrasound Med Biol* 2006; **32:** 1529-37. doi: 10.1016/j.ultrasmedbio.2006.06.008

11. Varin R, Mirshahi S, Mirshahi P, Klein C, Jamshedov J, Chidiac J, et al. Whole blood clots are more resistant to lysis than plasma clots - greater efficacy of rivaroxaban. *Thromb Res* 2013; **131:** E100-9. doi: 10.1016/j.thromres.2012.11.029

12. Wohner N, Sotonyi P, Machovich R, Szabo L, Tenekedjiev K, Silva MM, et al. Lytic resistance of fibrin containing red blood cells. *Arterioscl Throm Vasc Biol* 2011; **31:** 2306-13. doi: 10.1161/ATVBAHA.111.229088.

13. Yuki I, Kan I, Vinters HV, Kim RH, Golshan A, Vinuela FA, et al. The impact of thromboemboli histology on the performance of a mechanical thrombectomy device. *Am J Neuroradiol* 2012; **33:** 643-8. doi: 10.3174/ajnr.A2842

14. Mokin M, Morr S, Natarajan SK, Lin N, Snyder KV, Hopkins LN, et al. Thrombus density predicts successful recanalization with Solitaire stent retriever thrombectomy in acute ischemic stroke. *J Neurointerv Surg* 2015; **7:** 104-7. doi: 10.1136/neurintsurg-2013-011017.

15. van Everdingen KJ, van der Grond J, Kappelle LJ, Ramos LM, Mali WP. Diffusion-weighted magnetic resonance imaging in acute stroke. *Stroke* 1998; **29:** 1783-90. doi: 10.1161/01.str.29.9.1783

16. Brownstein KR, Tarr CE. Spin-lattice relaxation in a system governed by diffusion. *J Magn Reson (1969)* 1977; **26:** 17-24. doi: 10.1016/0022-2364(77)90230-X

17. Vidmar J, Blinc A, Sersa I. A comparison of the ADC and T-2 mapping in an assessment of blood-clot lysability. *Nmr Biomed* 2010; **23:** 34-40. doi: 10.1002/nbm.1422

18. Vidmar J, Kralj E, Bajd F, Sersa I. Multiparametric MRI in characterizing venous thrombi and pulmonary thromboemboli acquired from patients with pulmonary embolism. *J Magn Reson Imaging* 2015; **42:** 354-61. doi: 10.1002/jmri.24816

19. Stejskal EO, Tanner JE. Spin diffusion measurements: spin echoes in the presence of a time-dependent field gradient. *J Chem Phys* 1965; **42:** 288-92. doi: 10.1063/1.1695690

20. Carr HY, Purcell EM. Effects of diffusion on free precession in nuclear magnetic resonance experiments. *Phys Rev* 1954; **94:** 630-8. doi: 10.1103/PhysRev.94.630

21. Jindal G, Miller T, Shivashankar R, Mitchell J, Stern BJ, Yarbrough K, et al. Relationship of thrombus length to number of stent retrievals, revascularization, and outcomes in acute ischemic stroke. *J Vasc Interv Radiol* 2014; **25:** 1549-57. doi: 10.1016/j.jvir.2014.05.014

22. Yoo AJ, Andersson T. Thrombectomy in acute ischemic stroke: challenges to procedural success. *J Stroke* 2017; **19:** 121-30. doi: 10.5853/jos.2017.00752

23. Pisani L. Simple expression for the tortuosity of porous media. *Transport Porous Med* 2011; **88:** 193-203. doi: 10.1007/s11242-011-9734-9

24. Fan X, Macleod K, Mustafi D, Conzen SD, Markiewicz E, Zamora M, et al. Correlation of in vivo and ex vivo ADC and T2 of in situ and invasive murine mammary cancers. *Plos One* 2015; **10:** e0129212. doi: 10.1371/journal.pone.0129212

25. Powers WJ, Rabinstein AA, Ackerson T, Adeoye OM, Bambakidis NC, Becker K, et al. 2018 Guidelines for the early management of patients with acute ischemic stroke: a guideline for healthcare professionals from the American Heart Association/American Stroke Association. *Stroke* 2018; **49:** e46-e110. doi: 10.1161/STR.0000000000000158

research article

LncRNA NEAT1 promotes endometrial cancer cell proliferation, migration and invasion by regulating the miR-144-3p/EZH2 axis

Wei Wang[1], Liang Ge[2], Xiao-Juan Xu[1], Ting Yang[1], Yue Yuan[1], Xiao-Ling Ma[1], Xue-Hong Zhang[1]

[1] The Reproductive Medicine Special Hospital of the 1st Hospital of Lanzhou University, Key Laboratory for Reproductive Medicine and Embryo, Lanzhou, Gansu Province, P. R. China

[2] Department of Anesthesiology, Gansu Province Maternity and Child-care Hospital, Lanzhou, Gansu Province, P. R. China

Radiol Oncol 2019; 53(4): 434-442.

Received 22 May 2019
Accepted 21 September 2019

Correspondence to: Dr. Xue-Hong Zhang & Dr. Wei Wang, The Reproductive Medicine Special Hospital of the 1st Hospital of Lanzhou University, Key Laboratory for Reproductive Medicine and Embryo, No.1, Donggangxi Road, Chengguan District, Lanzhou 730000, Gansu Province, P. R. China. E-mail: zhangxueh@lzu.edu.cn and wangwei83819@163.com

Disclosure: No potential conflicts of interest were disclosed.

Background. Endometrial cancer (EC) is one of the most common gynaecological tumours in the worldwide. Long non-coding RNA (lncRNA) nuclear enriched abundant transcript 1 (NEAT1) promotes cell proliferation, migration and invasion in EC cells. However, the molecular mechanisms of NEAT1 in EC have not been fully clarified. We conducted this study to reveal the function of NEAT1 in EC tissues and cell lines.

Materials and methods. Cancer and adjacent tissues were collected from EC patients. HEC-1A and Ishikawa cells were cultured *in vitro*. NEAT1 expression was downregulated by transfecting small hairpin RNA (shRNA) and miR-144-3p was overexpressed by transfecting miR-144-3p mimics. Cell proliferation was detected by MTT assay and colony formation assay. Cell migration and invasion abilities were assessed by transwell assay. A dual-luciferase reporter assay was used to verify the relationship among NEAT1, EZH2, and miR-144-3p. The expression level of EZH2 was measured by Western blot and qPCR.

Results. NEAT1 was highly expressed in EC tissues and cells. Knockdown of NEAT1 inhibited the proliferation, migration and invasion of EC cells. Additionally, NEAT1 acted as a ceRNA of miR-144-3p, leading to EZH2 upregulation. Overexpression of miR-144-3p suppressed the proliferation and invasion of EC cells.

Conclusions. NEAT1 promotes EC cells proliferation and invasion by regulating the miR-144-3p/EZH2 axis.

Key words: endometrial cancer; NEAT1; miR-144-3p; EZH2

Introduction

Endometrial cancer (EC), one of the most common gynaecological tumours originating in the uterus, has increasing incidence rates, as shown by American Cancer Society statistics.[1] The relative 5-year survival relative rate for EC is only 77%, and approximately 11,350 women died of uterine cancer in 2016 in the U.S.[2] Consequently, determining the molecular mechanisms underlying the development of EC is of great importance.

Long non-coding RNAs (lncRNAs) are defined as the RNA transcripts, that are longer than 200 nucleotides but do not encode proteins. LncRNAs play unique regulatory roles in a variety of biological pathways, such as cardiovascular, reproductive, inflammatory, and metabolic functions and DNA repair processes.[3-5] Emerging evidence has confirmed the carcinogenic or anticancer effects of lncRNAs in cancer development.[6,7] LncRNA nuclear enriched abundant transcript 1 (NEAT1) is dysregulated in multiple types of malignancies, including bladder cancer, lung cancer, breast cancer and colorectal cancer.[8] It has been reported that overexpression of NEAT1 promotes cell proliferation, migration and invasion in EC and associates

with clinical progression.[9] In addition, NEAT1 can regulate the Wnt/β-catenin signalling pathway by targeting miR-214-3p or miR-146b-5p in EC.[10,11] The results mentioned above reveal the important roles of NEAT1 in EC progress. However, its mechanism in EC remains largely unknown.

The histone methyltransferase EZH2 has been identified as a clinically relevant biomarker associated with cancer. Dysregulation of EZH2 was found in various cancers. For example, EZH2 can promote tumour growth by increasing angiogenesis in pituitary adenoma.[12] EZH2 expressed is also dysregulated in EC and is related to high grade of EC.[13] It was demonstrated that EZH2 is the target of miR-144-3p in osteosarcoma cells and negatively correlates with the expression of miR-144-3p.[14] Whether miR-144-3p is involved in the progression of EC through EZH2 remains to be explored. In our previous work, we predicted that NEAT1 may target miR-144-3p. Thus, we speculated that NEAT1 might regulate EC cells proliferation, migration and invasion via the miR-144-3p/EZH2 axis.

In this study, we found that NEAT1 could bind to miR-144-3p to suppress its function and subsequently upregulate the expression of EZH2, leading to enhanced EC cells proliferation, migration, and invasion. Taken together, our findings reveal a mechanism in which the NEAT1-miR-144-3p-EZH2 axis regulates proliferation, migration and invasion in EC cells, suggesting that NEAT1 may serve as a potential target for EC treatment.

Materials and methods

Cell culture

The human endometrial cancer cell lines, HEC-1-A, HEC-1B, Ishikawa (type I), RL-95-2, and JEC and human normal endometrial stromal cells (hESCs) were maintained in DMEM (Gibco, USA) with 10% foetal bovine serum (FBS, Gibco, USA). The cells were cultured at 37ºC with 5% CO_2.

Cancer and adjacent tissue collection

All the EC and adjacent normal endometrial tissues were collected from EC patients at the First Hospital of Lanzhou University. The EC tissues (n = 36) and tumour adjacent tissues (n = 36) were collected during surgery and then rapidly frozen with liquid nitrogen and stored at -80°C. This study was approved by the Ethics Committee of the Reproductive Medicine Special Hospital of the First Hospital of Lanzhou University.

Quantitative real-time PCR (qRT-PCR)

Total RNA extraction was performed using Trizol reagent (Invitrogen USA), and a TaqMan Reverse Transcription Kit (Thermo Fisher, USA) was used for reverse transcription into cDNA according to the manufacturer's instructions. Real-time quantitative polymerase chain reaction (qPCR) was used to quantify the expression level of NEAT1 in cultured cells using an Applied Biosystems 7500 Fast Dx Real-Time PCR instrument (Thermo Fisher, USA). SYBR Green reagent was used for qPCR in this study. GAPDH was used as an internal reference to normalize NEAT1 and EZH2 values. U6 was used as an internal reference to normalize miR-144-3p values. The following primers were used for analysis:

NEAT1, 5′-TTGGGACAGTFFACGTGTGG-3′ (forward), and 5′-TCAAGTCCAGCAGAGCA-3′ (reverse);

miR-144-3p, 5′-GGCCGGCGTACAGTATAGATGA-3′ (forward), and 5′- GTGCAGGGTCCGAGGT-3′ (reverse);

EZH2, 5′-AAGCACAGTGCAACACCAAG-3′ (forward), and 5′-CAGATGGTGCCAGCAATAGA-3′ (reverse);

GAPDH, 5′-TGACGTGCCGCCTGGAGAAC-3′ (forward), and 5′-CCGGCATCGAAGGTGGAAGAG-3′ (reverse);

U6, 5′-CTCGCTTCGGCAGCACA-3′ (forward), and 5′- AACGCTTCACGAATTTGCGT-3′(reverse). Relative RNA levels were calculated using the $2^{-\Delta\Delta}$Ct method.

Cell transfection

Small hairpin RNA (shRNA) for NEAT1 or its respective negative control were designed, synthesized and cloned into the shRNA vector U6/GFP/Neo plasmid (GenePharma, Shanghai, China). A miR-144-3p mimic and its control were designed and synthesized by Sangon (Shanghai, China). The validated and purified reconstructed vectors were transfected into the indicated cells by Lipofectamine 3000 (Thermo Fisher, USA) according to the manufacturer's guidelines. Briefly, 0.2 μg indicated plasmid and 0.4 μL Lipofectamine 3000 were mixed with 5 μL Opti-MEM medium (Thermo Fisher, USA), and then, Opti-MEM medium containing plasmid was added to the other Opti-MEM medium containing Lipofectamine 3000. Subsequently, this mixture was added to cells whose density was approximately 70%.

Dual-luciferase reporter assay

To verify the binding ability of NEAT1 to miR-144-3p and miR-144-3p to EZH2, we performed a dual-luciferase reporter assay using a Promega dual-luciferase reporter assay kit (Madison, USA). Briefly, we constructed a pmiR-RB-REPORT™ (Ribobio) plasmid containing the exact sites for wild type NEAT1 and EZH2 3′-UTRs and the corresponding mutated sequences. The cells seeded in 96-well plates were co-transfected with the indicated plasmids and miR-144-3p mimic or NC duplex (Gene Pharma). After 48 h, the cells were harvested, and luciferase activity was measured using a dual-luciferase reporter assay kit (Promega Corporation) and a multi-plate reader (Synergy 2, Bio Tek).

MTT assay

An MTT assay was performed to measure cell proliferation. Cells were cultured in 96-well plates (1×10^4 per well). MTT (0.5 mg/mL, Gibco, USA) was added to the medium. Then, the plate was incubated at 37°C for 4 h and the supernatant was discarded. Next, 150 μL DMSO (Thermo Fisher, USA) was added to each well and the OD490 nm value was measured immediately using a microplate reader (3100, Thermo Fisher, USA).

Colony formation assay

A colony formation assay was used to determine cell proliferation. HEC-1-A and Ishikawa cells in logarithmic growth were digested by trypsin (Gibco, USA) and then resuspended in DMEM containing 10% FBS. Cells were seeded in culture dishes at a density of 500 cells per dish. Then, the cells were cultured at 37°C and 5% CO_2 until visible colonies were formed. The culture medium was discarded, and the cells were fixed using methanol and stained with a crystal violet solution (Gibco, USA). The number of colonies was counted.

Transwell assay

The migration and invasion assays were performed using transwells. For this assay, 24-well plates with 8-μm pore polycarbonate membranes (BD Biosciences, USA) were used. The upper side of the membranes was coated with Matrigel (20 μg/well, BD Biosciences, USA) and then air-dried for 1 h at 37°C. EC cells (2×10^5) in 200 μL of FBS-free medium were placed in the upper chamber, which was uncoated (migration assay) or coated (invasion assay). The lower chamber was filled with medium with 10% FBS as a chemoattractant. After 48 h of incubation, the cells on the upper surface of the membrane were removed by gentle scrubbing with a cotton swab. The membranes were fixed in a stationary liquid of 95% ethanol and 5% acetic acid for 30 min and stained with a crystal violet solution. The number of cells on the lower surface of the membrane in 5 random visual fields (magnification, ×200) was then counted using an Eclipse TE2000-U inverted microscope.

Western blot analysis

A protein detection kit (Thermo Fisher, USA) was used to measure the amount of protein. Equivalent amounts of protein samples were separated on 8-10% SDS-PAGE and transferred to polyvinylidene difluoride membranes (PVDF, Thermo Fisher, USA). After blocking with 0.1% Tween 20 and 5% skimmed milk, the protein-containing PVDF membranes were incubated for 12 h in solutions containing primary antibodies obtained from Abcam (anti-EZH2, ab186006; anti-GAPDH, ab9485) at 4°C. Then, secondary antibodies were incubated for 2 h. A western blotting kit (Thermo Fisher Scientific, USA) was used to detect the signals.

Statistical analysis

Statistical analysis was performed using GraphPad Prism. The continuous variables are shown as the

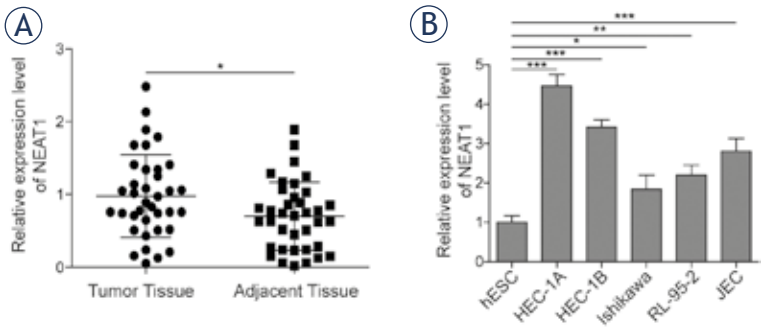

FIGURE 1. NEAT1 was highly expressed in EC tissues and cells. **(A)** NEAT1 was highly expressed in EC tissues. The transcription level of the *NEAT1* gene in EC tissues was measured by qRT-PCR. Cancer tissues and adjacent tissues were from human EC patients. **(B)** The transcription of NEAT1 was upregulated in various EC cell lines. qRT-PCR was used to examine the expression of *NEAT1* in various EC cell lines (HEC-1A, HEC-1B, Ishikawa, RL-95-2, and JEC), and hESCs, which were used as a control group.

* indicates $P < 0.05$; ** indicates $P < 0.01$; ***indicates $P < 0.001$. The Data are presented as the mean ± SD.

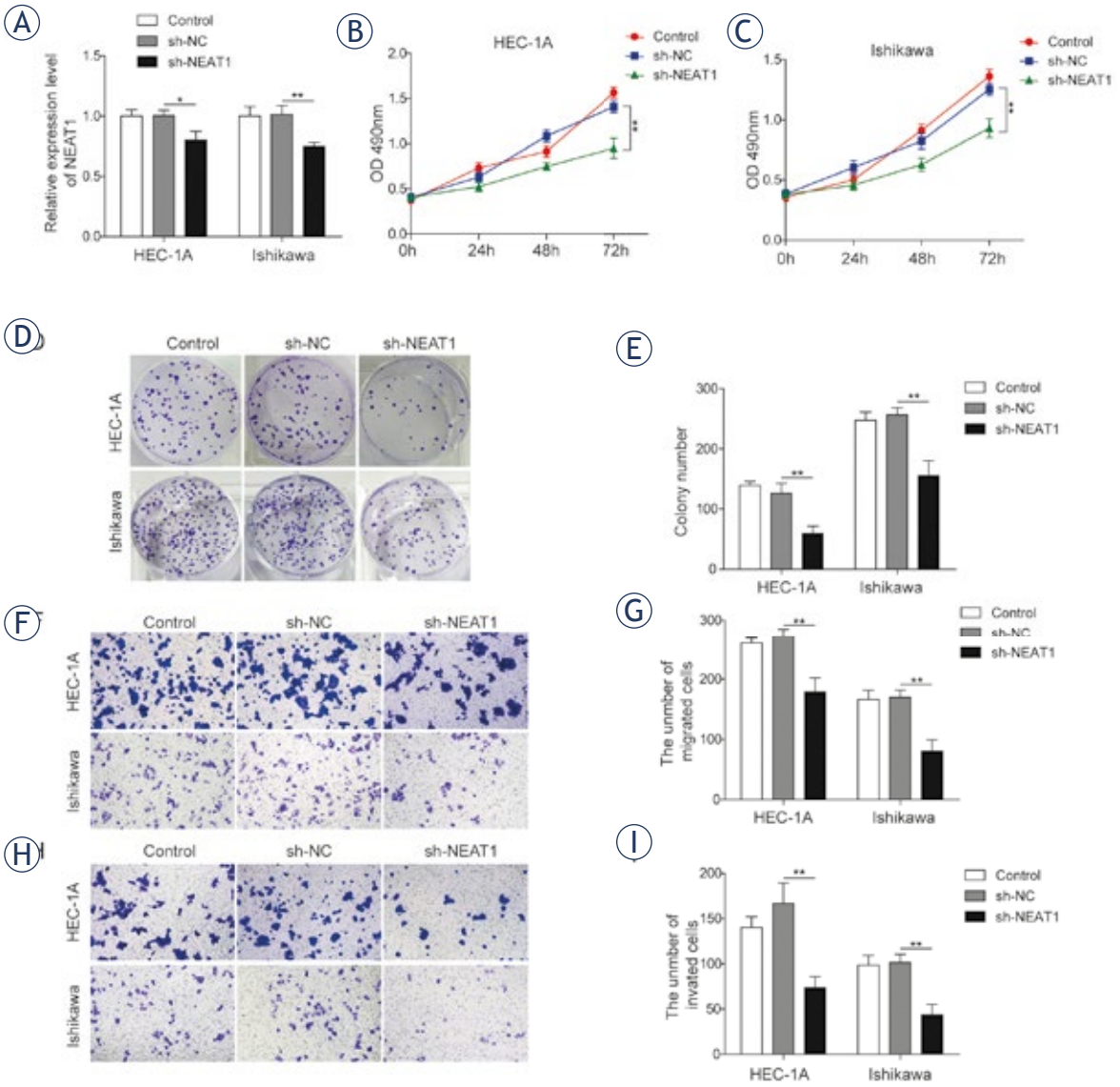

FIGURE 2. NEAT1 promoted EC cell proliferation, migration, and invasion. **(A)** Effects of NEAT1-shRNA on NEAT1 expression. The transcription of NEAT1 was measured by qRT-PCR after sh-NEAT1 and sh-NC were transfected into HEC-1A and Ishikawa cells for 48 h respectively. **(B, C)** Effects of NEAT1 knockdown on the proliferation of EC cells (HEC-1A and Ishikawa). The MTT assay results showed the effects on cell growth as measured by cell vitality on three consecutive days. **(D, E)** Effects of NEAT1 knockdown on the cell proliferation of EC cells. A colony formation assay was used to detect cell proliferation. Figure 2D is one representative result of the colony formation assay and Figure 2E shows one quantitative result repeated at least three times. **(F, G)** Effects of NEAT1 knockdown on the migration of EC cells. A transwell assay was used to measure the cell migration ability. Figure 2F is a representative result from the transwell assays, and Figure 2G shows one quantitative result with at least three replicates. **(H, I)** Effects of NEAT1 knockdown on the invasion of EC cells. A transwell assay was used to measure the cell invasion ability. Figure 2H is a representative result from the transwell assays and Figure 2I shows one quantitative result with at least three replicates.

* indicates $P < 0.05$; ** indicates $P < 0.01$. The data are presented as the mean ± SD.

mean ± standard deviation (SD), and their differences were analysed by Student's *t* test or ANOVA. *P* values less than 0.05 predicted the statistical significance of the results. Each assay was performed in triplicate.

Results

NEAT1 is highly expressed in EC tissues and cells

We first evaluated the expression of NEAT1 in cancer tissues and adjacent tissues derived from EC

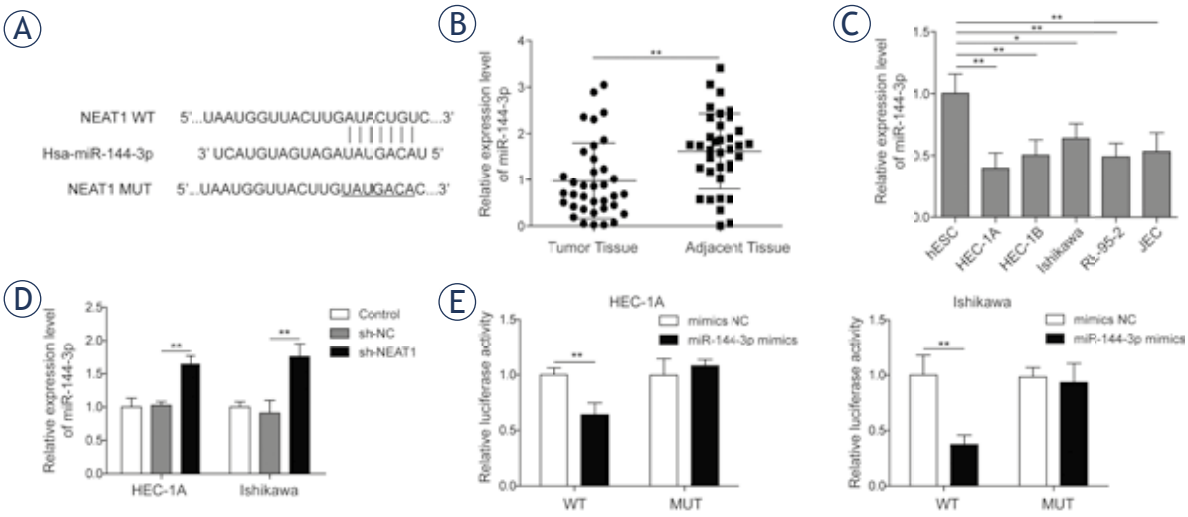

FIGURE 3. NEAT1 is a molecular sponge of miR-144-3p. **(A)** Sequences of miR-144-3p and wild-type NEAT1 **(**NEAT1 WT**)** and its mutant **(**NEAT1 MUT**)**. NEAT1 WT can target miR-144-3p, whereas NEAT1 MUT lost this ability. **(B)** miR-144-3p was downregulated in EC tissues. The transcription level of miR-144-3p in EC tissues was measured by qRT-PCR. Cancer tissues and adjacent tissues were from human EC patients. **(C)** The transcription of miR-144-3p was upregulated in various EC cell lines. qRT-PCR was used to examine the expression of miR-144-3p in various EC cell lines **(**HEC-1A, HEC-1B, Ishikawa, RL-95-2 and JEC**)**, and hESCs, which were used as a control group. **(D)** Effects of NEAT1 knockdown on miR-144-3p expression. The transcription of miR-144-3p was measured by qRT-PCR after sh-NEAT1 and sh-NC were transfected into HEC-1A and Ishikawa cells for 48 h. **(E)** NEAT1 targeted miR-144-3p. A dual luciferase activity assay was used to evaluate the binding ability of NEAT1 WT and NEAT1 MUT to miR-144-3p.

* indicates $P < 0.05$; ** indicates $P < 0.01$. The data are presented as the mean ± SD.

patients by qRT-PCR. As shown in Figure 1A, we found that the expression of NEAT1 was prominently higher in EC tissues than in adjacent tissues ($P<0.05$, indicated a significant difference). To determine whether NEAT1 is highly expressed in various EC-related cell lines, we performed qRT-PCR to detect its expression in hESCs and endometrial cancer cell lines. Interestingly, we found that the transcription levels of NEAT1 were significantly higher in EC cell lines, including HEC-1A, HEC-1B, Ishikawa, RL-95-2, and JEC, than in hESCs (Figure 1B). Among these cell lines, HEC-1A and Ishikawa cells had the highest and lowest expression of NEAT1, respectively, and they were selected for the following experiments.

NEAT1 promotes EC cell proliferation, migration, and invasion

To investigate whether endogenous NEAT1 plays a role in EC, we constructed a NEAT1-shRNA plasmid that efficiently downregulated NEAT1 expression after transfection into HEC-1A and Ishikawa cells (Figure 2A). MTT and colony formation assays were performed to measure the EC cell proliferation ability. According to the MTT assay, knockdown of NEAT1 significantly inhibited cell growth compared with the NC and control conditions in HEC-1A (Figure 2 B) and Ishikawa cells (Figure 2 C). Furthermore, colony formation assays indicated that the suppression of NEAT1 reduced colony formation in HEC-1A and Ishikawa cells (Figure 2 D, E). Taken together, the MTT assay and colony formation assays results indicated that knockdown of NEAT1 inhibited EC cell proliferation.

To determine whether endogenous NEAT1 affects EC cell migration and invasion, we performed a transwell assay to detect cell migration and invasion abilities. We found that knockdown of NEAT1 attenuated the migration of HEC-1A and Ishikawa cells (Figure 2 F, G). Consistently, we also found that knockdown of NEAT1 inhibited the invasion of HEC-1A and Ishikawa cells (Figure 2 H, I). Taken together, these data suggest that NEAT1 promotes EC cell proliferation, migration, and invasion.

NEAT1 is a molecular sponge of miR-144-3p

LncRNAs may act as sponges for direct binding to miRNA. In our previous work, we predicted that NEAT1 may target miR-144-3p using Starbase (http://starbase.sysu.edu.cn/) for bioinformatics prediction (Figure 3 A). The miR-144-3p level was much lower in EC tissues than in adjacent tissues according to qRT-PCR. MiR-144-3p was also ex-

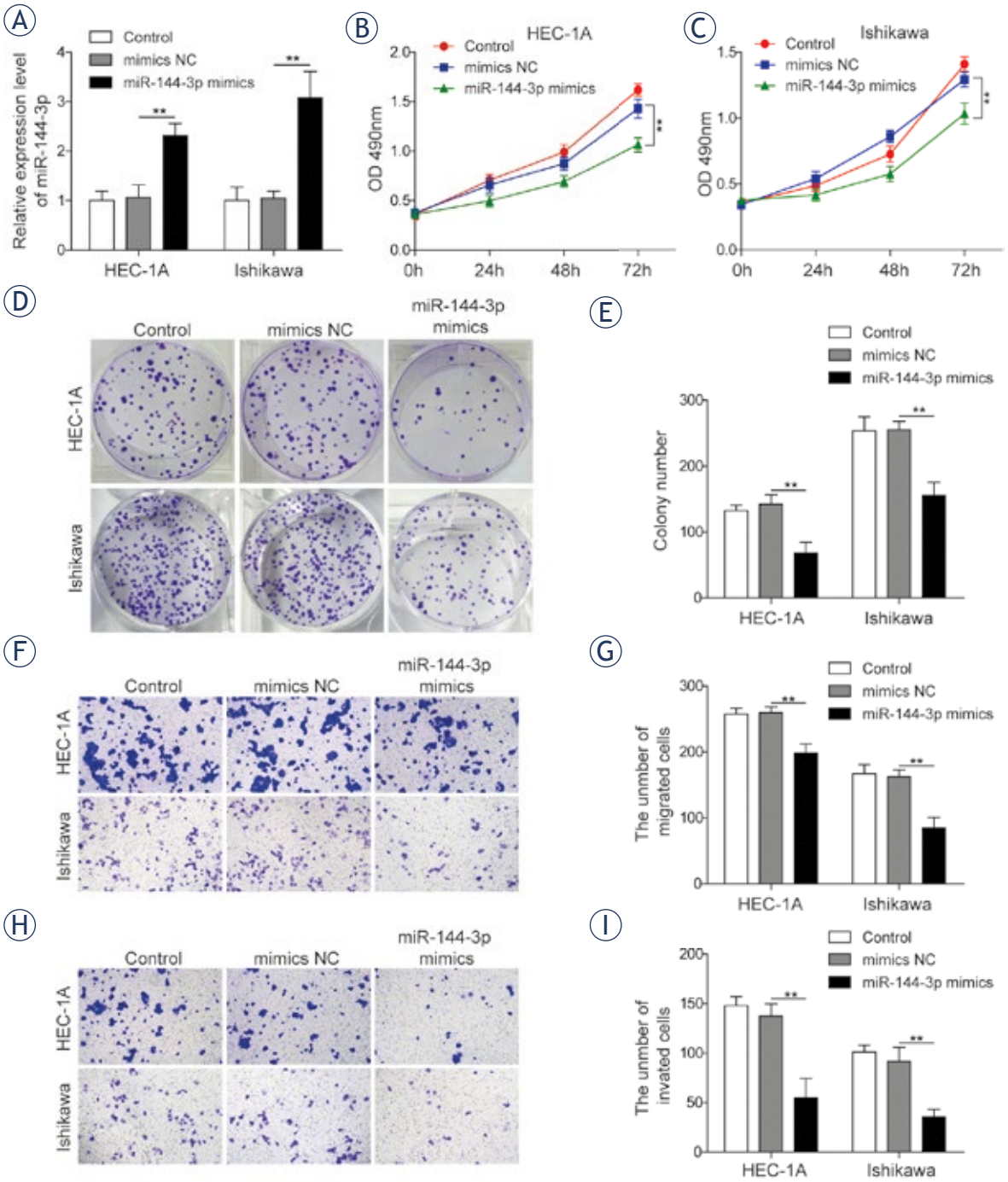

FIGURE 4. miR-144-3p inhibited EC cell proliferation, migration, and invasion. **(A)** Effects of the miR-144-3p mimic on miR-144-3p expression. The transcription of miR-144-3p was measured by qRT-PCR after miR-144-3p mimics or mimic NC transfection into HEC-1A and Ishikawa cells for 24 h. **(B, C)** Effects of the miR-144-3p mimic on the proliferation of EC cells. MTT assay results showed effects on cell growth as measured by cell vitality on three consecutive days. **(D, E)** Effects of the miR-144-3p mimic on the proliferation of EC cells. A colony formation assay was used to detect cell proliferation. Figure 4D is a representative result from the colony formation assay and Figure 4E shows one quantitative result repeated at least three times. **(F, G)** Effects of the miR-144-3p mimic on the migration of EC cells. A transwell assay was used to measure the cell migration ability. Figure 4F is a representative result from the transwell assays and Figure 4G shows one quantitative result with at least three replicates. **(H, I)** Effects of the miR-144-3p mimic on the invasion of EC cells. A transwell assay was used to measure the cell invasion ability. Figure 4H is a representative result from the transwell assays, and Figure 4I shows one quantitative result with at least three replicates.

** indicates $P < 0.01$. The data are presented as the mean ± SD.

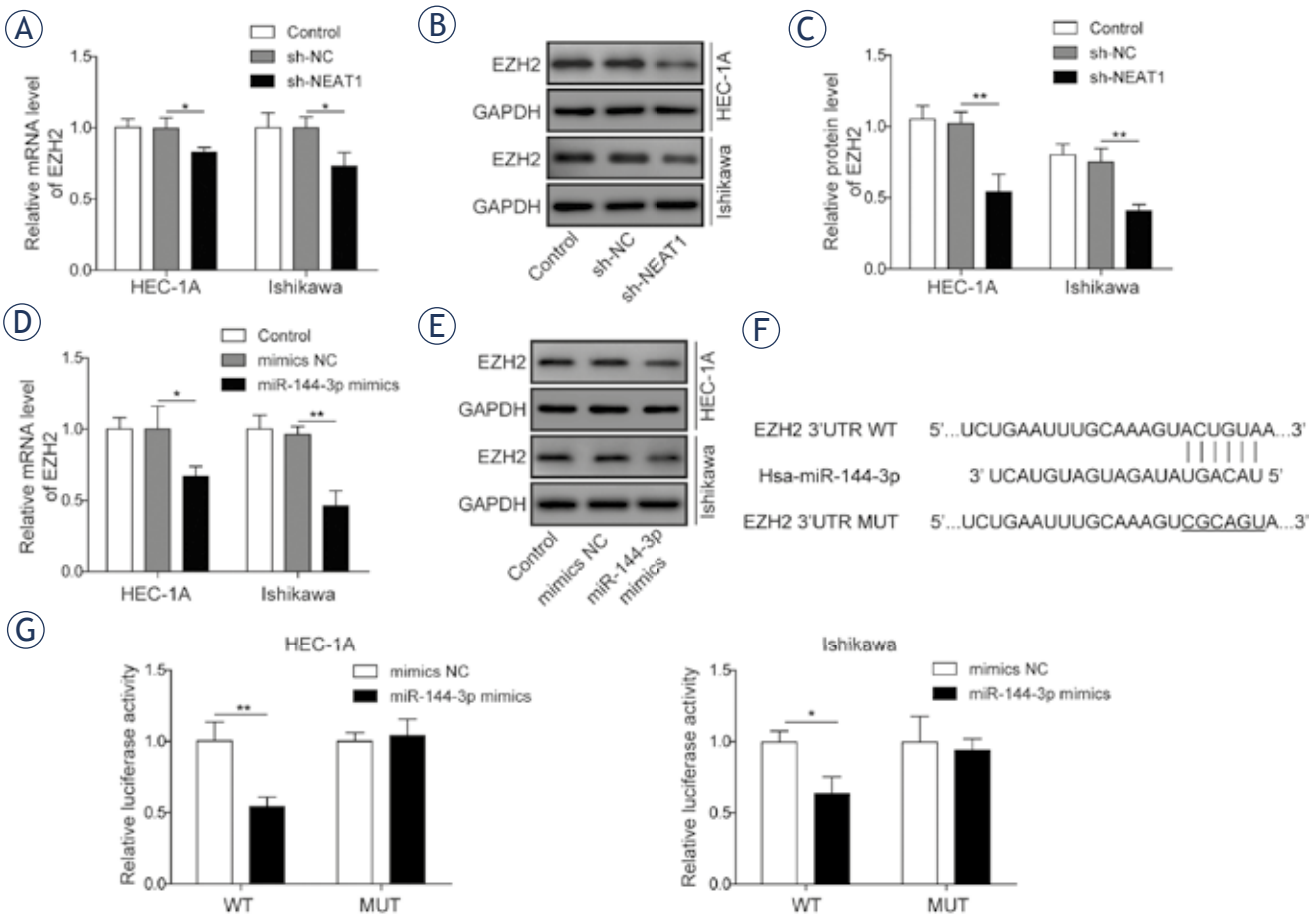

FIGURE 5. NEAT1 promoted the expression of EZH2 by miR-144-3p. **(A)** Effects of NEAT1 knockdown on the transcription of EZH2 in EC cells. The transcription of the EZH2 gene was measured by qRT-PCR after sh-NEAT1 and sh-NC were transfected into HEC-1A and Ishikawa cells for 48 h. **(B, C)** Effects of NEAT1 knockdown on the EZH2 protein level of in EC cells. The protein level of EZH2 was measured by Western blot after sh-NEAT1 and sh-NC transfection into HEC-1A and Ishikawa cells for 48 h. The indicated antibodies were used for Western blot analysis. Quantitative Western blot results are shown in Figure 5B with GAPDH as a control. Figure 4C shows one representative result and the right part shows one quantitative result repeated at least three times. **(D)** Effects of miR-144-3p mimic on the transcription of EZH2 in EC cells. The transcription of the EZH2 gene was measured by qPCR after miR-144-3p mimic and mimic NC transfection into HEC-1A and Ishikawa cells for 48 h. **(E)** Effects of the miR-144-3p mimic on the EZH2 protein level in EC cells. The EZH2 protein level was measured by Western blot after miR-144-3p mimics or mimic NC transfection into HEC-1A and Ishikawa cells for 48 h. The indicated antibodies were used for Western blot analysis. **(F)** Sequences of miR-144-3p and wild-type EZH2 (EZH2 3'-UTR WT) and its mutant (EZH2 3'-UTR MUT). EZH2 3'-UTR WT can be targeted by miR-144-3p, whereas miR-144-3p cannot bind to EZH2 3'-UTR MUT. **(G)** miR-144-3p directly targeted the 3'-UTR region of EZH2. A dual luciferase activity assay was used to evaluate the binding ability of miR-144-3p to EZH2 3'-UTR WT and EZH2 3'-UTR MUT.

* indicates $P < 0.05$, ** indicates $P < 0.01$. The data are presented as the mean ± SD.

pressed at lower level in EC cells than in hESCs (Figure 3 B, C). Next, we performed qRT-PCR to detect whether NEAT1 targets miR-144-3p to promote EC progression. As shown in Figure 3D, we found that knockdown of NEAT1 increased the level of miR-144-3p. To determine whether NEAT1 binds directly to miR-144-3p, we performed a dual luciferase activity assay to evaluate the binding ability by designing wild-type NEAT1 (WT-NEAT1) and a mutant (MUT-NEAT1). The luciferase signal will decrease when the lncRNA binds to its target miRNA. We found that the luciferase activity was decreased in the WT-NEAT1 and miR-144-3p mimic co-transfected group, while no significant difference was observed between the MUT-NEAT1 group and he mimic NC group (Figure 3E). These data suggested that NEAT1 could bind to miR-144-3p.

miR-144-3p inhibits EC cell proliferation, migration, and invasion

We designed experiments to reveal the function of miR-144-3p in EC cells. First, miR-144-3p was overexpressed in EC cell lines by miR-144-3p mimic transfection (Figure 4 A). Next, EC cell proliferation was examined via MTT and colony formation methods. In HEC-1A and Ishikawa cells, the MTT assay showed that cell proliferation was significantly inhibited in the miR-144-3p mimic group compared with that in the control and NC groups (Figure 4 B, C). Furthermore, colony formation assays showed that the miR-144-3p mimic markedly attenuated the cell proliferation of HEC-1A and Ishikawa cells compared with the control and NC groups (Figure 4 D, E). Finally, to determine whether miR-144-3p affects EC cell invasion and migration, we performed transwell assays to measure the migration and invasion abilities of EC cells. We found that the miR-144-3p mimic inhibited the migration of HEC-1A and Ishikawa cells (Figure 4 F, G). Consistently, we also found that the miR-144-3p mimic attenuated invasion of HEC-1A and Ishikawa cells (Figure 4 H, I). Taken together, these data indicated that miR-144-3p inhibited EC cell proliferation, migration, and invasion.

NEAT1 promotes the expression of EZH2 via miR-144-3p

We found that knockdown of NEAT1 suppressed the transcription of the EZH2 gene in HEC-1A and Ishikawa cells (Figure 5 A). Consistently, Western blot analysis showed that knockdown of NEAT1 decreased the expression of EZH2 in HEC-1A and Ishikawa cells (Figure 5 B, C). However, whether miR-144-3p regulates EZH2 in EC cells was unknown. To verify the relationship between miR-144-3p and EZH2 in EC cells, we overexpressed miR-144-3p in HEC-1A and Ishikawa cells by miR-144-3p mimic transfection and evaluated the expression of EZH2 by qRT-PCR and Western blotting. The qRT-PCR results showed that the transcription of the EZH2 gene was significantly lower in the miR-144-3p mimic group than in the control and NC groups in HEC-1A and Ishikawa cells (Figure 5 D). Consistently, Western blot analysis showed that the miR-144-3p mimic decreased the expression of EZH2 in HEC-1A and Ishikawa cells (Figure 5 E). To verify whether miR-144-3p decreases EZH2 expression by binding to its 3′-UTR site, we performed a dual luciferase activity assay to evaluate the binding ability and designed wild-type EZH2 (WT-EZH2) and its mutant (MUT-EZH2) sequences (Figure 5 F). The dual-luciferase activity assay results showed that the luciferase activity was lower in the miR-144-3p mimic group than in the NC WT-EZH2 group, while there was no difference in the MUT-EZH2 groups (Figure 5 G). Taken together, these data suggested that miR-144-3p could directly target the 3′-UTR region of EZH2. These data suggested that NEAT1 may act as a ceRNA of miR-144-3p, leading to increased the expression of EZH2 which is a target gene of miR-144-3p.

Discussion

It is well known that lncRNAs play critical roles in various biological functions and disease processes. In cancer, lncRNAs could regulate gene expression and mediate cell signalling pathways such as p53, NF-κB, PI3K/AKT and Notch signalling.[15]

NEAT1 is a novel lncRNA that is localized in nuclear paraspeckles. The gene that transcribes NEAT1 is located on the familial tumour syndrome multiple endocrine neoplasia type 1 locus.[16] In recent studies, high expression of NEAT1 has been found in various types of cancers, and it has been shown to serve as an oncogene. For examples, Chakravarty *et al.* found that NEAT1 is the most markedly overexpressed lncRNA in prostate cancer and that its expression is related to prostate cancer progression.[17] Dong *et al.* reported that the expression levels of NEAT1 are significantly increased in early-stage EC tissue samples, and high expression levels of NEAT1 predict a poor prognosis.[18] In this study, we found that NEAT1 was highly expressed in EC tissues and cell lines and that downregulation of NEAT1 in EC cells inhibited cancer cell proliferation, migration and invasion, which are consistent with of the results of Dong *et al.* These results suggested that NEAT1 may play carcinogenic roles in the progression of EC.

Acting as a competitive endogenous RNAs, lncRNAs regulate protein expression by binding to miRNAs. For example, NEAT1 inhibits glioma cell migration and invasion via modulating SOX2 by targeting miR-132.[19] In acute lymphoblastic leukaemia, NEAT1 can regulate miR-335-3p expression, and the dysregulation of miR-335-3p is associated with poor prognosis.[20] In colorectal cancer, NEAT1 could promote the tumourigenesis by sponging miR-193a-3p.[21] NEAT1 regulates the Wnt/β-catenin signalling pathway via the miR-214-3p-HMGA1 axis, leading to the promotion of cell growth, mi-

gration and invasion in EC cells.[11] In this study, we first revealed that NEAT1 directly targets miR-144-3p and that knockdown of NEAT1 promotes the expression of miR-144-3p. However, the function of miR-144-3p is still unknown. Through functional experiments, we found that overexpression of miR-144-3p can inhibit EC cell proliferation, migration and invasion. These results suggest that NEAT1 may act as an oncogene by targeting miR-144-3p in EC cells.

EZH2 participates in histone methylation, which regulates transcriptional repression.[22] Emerging evidence has shown that EZH2 is associated with EC cell proliferation. Eskander *et al.* found that inhibition of EZH2 expression in EC cells significantly attenuates cell proliferation, migration, and invasion by increasing the expression of the Wnt pathway inhibitors sFRP1 and DKK3.[23] Wang *et al.* reported that knockdown of EZH2 inhibits the proliferation of EC cells *in vitro* and induces apoptosis in EC cells via upregulating the expression of caspase 3/9 and downregulating the expression of Bcl-2.[24] Ihira *et al*. reported that knockdown of EZH2 suppresses EC progression via the miR-361/Twist axis.[25] In this study, we first confirmed that NEAT1 could upregulate the expression of EZH2 and promote the proliferation, migration and invasion of EC cells by targeting miR-144-3p, which further confirmed the function of EZH2 in the progression of EC.

In conclusion, we demonstrated that NEAT1, as an oncogene, regulates miR-144-3p-EZH2 axis, which promotes the proliferation, migration and invasion of EC cells, providing a promising therapeutic target for EC.

References

1. Siegel RL, Miller KD, Jemal A. Cancer statistics, 2017. *CA Cancer J Clin* 2017; **67:** 7-30. doi: 10.3322/caac.21387
2. Miller KD, Siegel RL, Lin CC, Mariotto AB, Kramer JL, Rowland JH, et al. Cancer treatment and survivorship statistics, 2016. *CA Cancer J Clin* 2016; **66:** 271-89. doi: 10.3322/caac.21349
3. Li J, Meng H, Bai Y, Wang K. Regulation of lncRNA and its role in cancer metastasis. *Oncol Res* 2016; **23:** 205-17. doi: 10.3727/096504016X14549667334007
4. Quinn JJ, Chang HY. Unique features of long non-coding RNA biogenesis and function. *Nat Rev Genet* 2016; **17:** 47-62. doi: 10.1038/nrg.2015.10
5. Sun W, Yang Y, Xu C, Guo J. Regulatory mechanisms of long noncoding RNAs on gene expression in cancers. *Cancer Genet* 2017; **216-217:** 105-10. doi: 10.1016/j.cancergen.2017.06.003
6. Jing N, Huang T, Guo H, Yang J, Li M, Chen Z, et al. LncRNA CASC15 promotes colon cancer cell proliferation and metastasis by regulating the miR4310/LGR5/Wnt/betacatenin signaling pathway. *Mol Med Rep* 2018; **18:** 2269-76. doi: 10.3892/mmr.2018.9191
7. Li S, Zhou J, Wang Z, Wang P, Gao X, Wang Y. Long noncoding RNA GAS5 suppresses triple negative breast cancer progression through inhibition of proliferation and invasion by competitively binding miR-196a-5p. *Biomed Pharmacother* 2018; **104:** 451-7. doi: 10.1016/j.biopha.2018.05.056
8. Ghafouri-Fard S, Taheri M. Nuclear enriched abundant transcript 1 (NEAT1): a long non-coding RNA with diverse functions in tumorigenesis. *Biomed Pharmacother* 2019; **111:** 51-9. doi: 10.1016/j.biopha.2018.12.070
9. Li Z, Wei D, Yang C, Sun H, Lu T, Kuang D. Overexpression of long noncoding RNA, NEAT1 promotes cell proliferation, invasion and migration in endometrial endometrioid adenocarcinoma. *Biomed Pharmacother* 2016; **84:** 244-51. doi: 10.1016/j.biopha.2016.09.008
10. Huang X, Zhong R, He X, Deng Q, Peng X, Li J, et al. Investigations on the mechanism of progesterone in inhibiting endometrial cancer cell cycle and viability via regulation of long noncoding RNA NEAT1/microRNA-146b-5p mediated Wnt/beta-catenin signaling. *IUBMB Life* 2019; **71:** 223-34. doi: 10.1002/iub.1959
11. Wang J, Zhao X, Guo Z, Ma X, Song Y, Guo Y. Regulation of NEAT1/miR-214-3p on the growth, migration and invasion of endometrial carcinoma cells. *Arch Gynecol Obstet* 2017; **295:** 1469-75. doi: 10.1007/s00404-017-4365-1
12. Liu B, Pang B, Wang Q, Yang S, Gao T, Ding Q, et al. EZH2 upregulation correlates with tumor invasiveness, proliferation, and angiogenesis in human pituitary adenomas. *Hum Pathol* 2017; **66:** 101-7. doi: 10.1016/j.humpath.2017.03.028
13. Zhou J, Roh JW, Bandyopadhyay S, Chen Z, Munkarah AR, Hussein Y, et al. Overexpression of enhancer of zeste homolog 2 (EZH2) and focal adhesion kinase (FAK) in high grade endometrial carcinoma. *Gynecol Oncol* 2013; **128:** 344-8. doi: 10.1016/j.ygyno.2012.07.128
14. Cao J, Han X, Qi X, Jin X, Li X. TUG1 promotes osteosarcoma tumorigenesis by upregulating EZH2 expression via miR-144-3p. *Int J Oncol* 2017; **51:** 1115-23. doi: 10.3892/ijo.2017.4110
15. Peng WX, Koirala P, Mo YY. LncRNA-mediated regulation of cell signaling in cancer. *Oncogene* 2017; **36:** 5661-7. doi: 10.1038/onc.2017.184
16. Zhang Q, Chen CY, Yedavalli VS, Jeang KT. NEAT1 long noncoding RNA and paraspeckle bodies modulate HIV-1 posttranscriptional expression. *MBio* 2013; **4:** *e00596-00512.* e00596-00512. doi: 10.1128/mBio.00596-12
17. Chakravarty D, Sboner A, Nair SS, Giannopoulou E, Li R, Hennig S, et al. The oestrogen receptor alpha-regulated lncRNA NEAT1 is a critical modulator of prostate cancer. *Nat Commun* 2014; **5:** 5383. doi: 10.1038/ncomms6383
18. Dong P, Xiong Y, Yue J, Xu D, Ihira K, Konno Y, et al. Long noncoding RNA NEAT1 drives aggressive endometrial cancer progression via miR-361-regulated networks involving STAT3 and tumor microenvironment-related genes. *J Exp Clin Cancer Res* 2019; **38:** 295. doi: 10.1186/s13046-019-1306-9
19. Zhou K, Zhang C, Yao H, Zhang X, Zhou Y, Che Y, et al. Knockdown of long non-coding RNA NEAT1 inhibits glioma cell migration and invasion via modulation of SOX2 targeted by miR-132. *Mol Cancer* 2018; **17:** 105. doi: 10.1186/s12943-018-0849-2
20. Pouyanrad S, Rahgozar S,& Ghodousi ES. Dysregulation of miR-335-3p, targeted by NEAT1 and MALAT1 long non-coding RNAs, is associated with poor prognosis in childhood acute lymphoblastic leukemia. *Gene* 2019; **692:** 35-43. doi: 10.1016/j.gene.2019.01.003
21. Yu HM, Wang C, Yuan Z, Chen GL, Ye T, Yang BW. LncRNA NEAT1 promotes the tumorigenesis of colorectal cancer by sponging miR-193a-3p. *Cell Prolif* 2019; **52:** e12526. doi:10.1111/cpr.12526
22. Vire E, Brenner C, Deplus R, Blanchon L, Fraga M, Didelot C, et al. The polycomb group protein EZH2 directly controls DNA methylation. *Nature* 2006; **439:** 871-4. doi: 10.1038/nature04431
23. Eskander RN, Ji T, Huynh B, Wardeh R, Randall LM, Hoang B. Inhibition of enhancer of zeste homolog 2 (EZH2) expression is associated with decreased tumor cell proliferation, migration, and invasion in endometrial cancer cell lines. *Int J Gynecol Cancer* 2013; **23:** 997-1005. doi: 10.1097/IGC.0b013e318296a265
24. Wang J, Ai Z, Chen J, Teng Y, Zhu J. Enhancer of zeste homolog 2 blockade by RNA interference is implicated with inhibited proliferation, invasion and promoted apoptosis in endometrial carcinoma. *Oncol Lett* 2018; **15:** 9429-35. doi: 10.3892/ol.2018.8518
25. Ihira K, Dong P, Xiong Y, Watari H, Konno Y, Hanley SJ, et al. EZH2 inhibition suppresses endometrial cancer progression via miR-361/Twist axis. *Oncotarget* 2017; **8:** 13509-20. doi: 10.18632/oncotarget.14586

research article

LncRNA PVT1 promotes proliferation and invasion through enhancing Smad3 expression by sponging miR-140-5p in cervical cancer

Qing-Qing Chang[1], Chun-Yan Chen[1], Zhao Chen[2], Shuai Chang[3]

[1] Department of Obstetrics and Gynecology, Hunan Provincial People's Hospital, Changsha, Hunan Province, China
[2] Department of Hematology, Hunan Provincial People's Hospital, Changsha, Hunan Province, China
[3] Changsha Medical University, Changsha, Hunan Province, China

Radiol Oncol 2019; 53(4): 443-452.

Received 23 May 2019
Accepted 21 August 2019

Correspondence to: Dr. Qing-Qing Chang, Department of Obstetrics and Gynecology, Hunan Provincial People's Hospital, No. 89, Guhan Road, Furong District, Changsha 410001, Hunan Province, P. R. China. E-mail: qingqingchangqqc@163.com

Disclosure: No potential conflicts of interest were disclosed.

Background. Cervical cancer is one of the most frequent malignancies among females worldwide. Increasing evidence have indicated the participation of long noncoding RNAs (lncRNAs) in the progression and metastasis of cervical cancer. Our present study was conducted to explore the effects of lncRNA plasmacytoma variant translocation 1 (PVT1) on the progression of cervical cancer and the underlying mechanisms.

Materials and methods. Expressions of PVT1, miR-140-5p and Smad3 in cervical cancer cell lines were detected by qRT-PCR and western blotting. Bioinformatics analysis and luciferase assays were used to elucidate the potential correlations between PVT1, miR-140-5p and Smad3. The roles of PVT1 on the progression of cervical cancer cells were determined by transfecting sh-RNA through series function assays such as colony formation assay, wound healing assay, transwell assay.

Results. PVT1 and Smad3 were upregulated, and miR-140-5p was downregulated in cervical cancer cells. PVT1 could bind directly with miR-140-5p, and Smad3 was a downstream target of miR-140-5p. Inhibition of PVT1 could enhance expression of miR-140-5p, inhibit the expression of Smad3, significantly inhibited the proliferation, migration, invasion in cervical cancer cells. While transfection of miR-140-5p inhibitor could partially reverse the above changes in cervical cancer cells.

Conclusions. The results revealed that PVT1 could promote the proliferation and metastasis via increasing the Smad3 expression by sponging miR-140-5p, which might be a promising prognostic and therapeutic target for cervical cancer.

Key words: cervical cancer; lncRNA PVT1; miR-140-5p; Smad3

Introduction

Cervical cancer is the second most frequent malignancy-affecting women worldwide, with approximately over 570000 new cases diagnosed and 310000 deaths each year. Nearly 85% of the cases occur in underdeveloped and developing countries.[1] Interactions between cervical cancer and the persistent infection of high-risk human papilloma virus (especially HPV16 and HPV18) have been indicated in epidemiological and molecular studies.[2-4] Despite the improvement of diagnostic approaches and treatment strategies have been made, the morbidity and mortality rates remain high as well as the poor prognosis. Therefore, there is an urgent need to clarify the underlying molecular mechanisms of cervical cancer, which could improve the development of therapeutic strategies against cervical cancer.

Long noncoding RNAs (lncRNAs) are a group of noncoding RNAs longer than 200 nucleotides that participate in numerous biological and physiologi-

cal processes including cell development, survival, differentiation and apoptosis.[5-7] Accumulating evidence also proved that lncRNAs have pivotal roles in the progression of cervical cancer. Yang *et al*.[8] showed that lncRNA CCHE1 could promote the proliferation of cervical cancer via upregulation the expression of PCNA. Han *et al*.[9] discovered that lncRNA NEAT1 could strengthen the resistance of cervical cancer against radiotherapy through the regulation of CCND1. Up to now, plasmacytoma variant translocation 1 (PVT1) has been recognized as an oncogenic lncRNA, which participates in the migration and invasion of many kinds of cancer cells and the development of cancers.[10, 11] Ding *et al.* found PVT1 was the most amplified gene in ovarian cancer patients, which was highly correlated with poor survival outcomes.[12] It was also proven that high PVT1 expression correlates with poorer outcome in cervical cancer patients.[13] However, the underlying mechanism on the effects of lncRNA PVT1 in cervical cancer remains for further investigation.

MicroRNAs (miRNAs) are another group of noncoding RNAs with length between 17-25 nucleotides that influence the pathogenesis of many human diseases including cancer.[14-16] MiRNAs are normally dysregulated in human cancers and could serve as either oncogenes or tumor suppressors.[17] Previous studies showed that expressions of miR-140-5p were downregulated in cancer tissues, which were negatively related to the prognosis of cancer[18-20], indicating the tumor-suppressor role of miR-140-5p in the progression of cancer formation. Li *et al*.[21] showed that miR-140-5p could inhibit the progression and invasion of colorectal cancer by targeting Smad3, indicating an interaction may exist between miR-140-5p and Smad3. However, whether miR-140-5p could regulate the metastasis of cervical cancer by targeting Smad3 remains to be determined. Bioinformatics analysis also revealed that targeted binding sites exist between lncRNA PVT1 and miR-140-5p. Therefore, we hypothesized that the elevated lncRNA PVT1 could upregulate the expression of Smad3 by targeting inhibition of miR-140-5p, thereby promoting the proliferation and migration of cervical cancer cells in cervical cancer.

In the present study, the role and the underlying molecular mechanism of lncRNA PVT1 in cervical cancer were illuminated. Our results showed that lncRNA PVT1 could promote the proliferation, migration and invasion through binding miR-140-5p, which may provide new insights into the therapeutic strategy against cervical cancer.

Materials and methods

Cell lines and cell culture

Human normal cervical epithelial cell line (End1/E6E7) and human cervical cell lines (HeLa and SiHa) were obtained from the Cell Bank of the Chinese Academy of Sciences (Shanghai, China). The cells were maintained in Dulbecco's minimal Eagle's medium (DMEM; Invitrogen, Carlsbad, CA, USA) containing 6% fetal bovine serum (FBS; Gibico, Grand Island, NY, USA) and 1% penicillin/streptomycin at 37°C in a humidified atmosphere containing 5% CO_2.

Dual luciferase reporter assay

A bioinformatics website (http://www.rna-society.org/raid2/index.html) was used to identify the binding sites for miR-140-5p, lncRNA PVT1 and Smad3, and obtain the fragment sequences containing action sites. The bioinformatics software was then applied to predict the binding sites between miR-140-5p and PVT1 as well as between miR-140-5p and Smad3. Then the wild-type PVT1 (PVT1-WT), mutant PVT1 (PVT1-MUT), wild-type Smad3 (Smad3-WT) and mutant Smad3 (Smad3-MUT) containing predicted miR-140-5 binding sites were synthesized and cloned into a pGL3 vector. Then, the above constructed vectors were transfected into cervical cancer cells in the presence of miR-NC or miR-140-5p inhibitor. Luciferase activity was detected using the Dual-Luciferase Reporter Assay System (Promega, Madison, USA).

Cell transfection

Sh-PVT1, negative control (sh-NC), miR-140-5p mimics and miR-140-5p inhibitor were synthesized by GenePharma (Shanghai, China). After reaching 60%-70% confluence, the cervical cancer cells were transfected by using Lipofectamine 2000 (Life Technologies, Carlsbad, CA) according to the manufacturer's instructions.

Cell colony formation assay

After transfection, cells were seeded in 6-well plates at a density of 1×10^3 cells/well. The cells were then fixed and stained with 0.1% crystal violet after incubation for 14 days. The numbers of colonies were counted under microscope. This assay was performed at least three times.

Wound healing assays

Cells were incubated in 6-well plates at a density of 1 × 10^6 cells/well. After transfection, the cells were cultured with serum-free medium for 24 h. Wounds were created by using a sterile plastic pipette tip to scratch the cell layer. Then the cells were incubated with medium containing 10% FBS for 48 h. Images were acquired by microscope. This assay was performed at least three times.

Transwell assays

The transwell assays were determined using transwell chambers (Corning, NY, USA) as previously described.[22] Briefly, transfected cells were suspended in serum-free medium and seeded into the upper chamber, while medium containing 10% FBS was added in the bottom chamber. After incubation at 37°C for 24 h, the cells that invaded through matrix membrane were fixed with 4% paraformaldehyde and stained with crystal violet. Then, stained cells were photographed and counted from five random fields per filter for analysis. This assay was performed at least three times.

RNA isolation and qRT-PCR

Total RNA was extracted from cell samples using Trizol reagents (Thermo Fisher Scientific, Waltham, MA, USA) from cell lines, and cDNA was synthesized using PrimeScript™ cDNA Kit (Takara, Dalian, China) according to the manufacture's protocols. qRT-PCR was determined using an ABI 7000 Prism Step One plus detection system (Life Technologies, USA). The relative expression was normalized using GAPDH as an internal reference gene, and U6 was used as the endogenous control of miR-140-5p. Fold changes were calculated using the formula $2^{-\Delta\Delta Ct}$. All qRT-PCR reactions were performed three times independently. The primer sequences used for qRT-PCR as follow.

PVT1 forward 5′-AAAACGGCAGCAGGAAATGT-3′ and reverse 5′-GGAGTCATGGGTGTCAGACA-3′.

miR-140-5p forward 5′-GGGCCAGTGGTTTTACCCTA-3′
and reverse 5′-GTCGTATCCAGTGCAGGGTCCGAGGTATTCGCACTGGATACGAC CTACCA-3′.

Smad3 forward 5′-CTCCAAACCTATCCCCGAAT-3′
and reverse 5′-CCTGTTGACATTGGAGAGCA-3′. U6 forward 5′-AAAGCAAATCATCGGACGACC-3′
and reverse 5′- GTACAACACATTGTTTCCTCGGA-3′.

GAPDH forward 5′-AGAAGGCTGGGGCTCATTTG -3′
and reverse 5′-AGGGGCCATCCACAGTCTTC-3′.

Western blotting

Cell samples were harvested and lysed using cell lysis buffer on ice. Total proteins were extracted and concentrations were detected using a BCA protein assay kit (Beyotime, China). Same amounts of protein samples were isolated by 12% SDS-PAGE gels and then transferred onto polyvinylidene fluoride (PVDF) membranes. The membranes were then blocked with TBS-T containing 5% nonfat milk powder for 2 h at RT and incubated with primary antibodies at 4°C overnight. The membranes were then incubated with secondary antibody for 1 h at RT. The images were visualized using an enhanced chemiluminescence system. Signals were quantified and analyzed using the Image-Pro Plus 6.0 software (Media Cybernetics, Sarasota, USA). The following primary antibodies were applied: anti-Smad3 (1:1000; #9513), anti-E-cadherin (1:1000; #14472), anti-vimentin (1:1000; #3932), anti-N-cadherin (1:1000; #4061) anti-Snail (1:1000; #3879) (All purchased from Cell signaling Technology). The corresponding HRP-conjugated antibody (1: 5000; Abcam, UK) was used as the secondary antibody.

Statistical analysis

Statistical analysis was performed using SPSS 22.0 software (IBM Corporation, NY, USA). All data were expressed as the mean ± standard deviation (SD). All experiments were performed triplicate independently. Comparisons were determined using one-way analysis of variance (ANOVA) or Student's *t*-test. $P < 0.05$ was considered significantly different.

Results

The expressions of lncRNA PVT1 and Smad3 were increased, while miR-140-5p was reduced in cervical cancer cell lines

To determine the roles of lncRNA PVT1, miR-140-5p and Smad3 in cervical cancer metastasis, expressions of lncRNA PVT1, miR-140-5p and Smad3 in cervical cancer cell lines (HeLa and SiHa) and human normal cervical cell line (End1/E6E7) were determined by qRT-PCR and western blotting. The results in Figure 1A and 1B show that lncRNA PVT1 expression was significantly upregulated in cervical cancer cell lines compared with that in the normal cervical cell line by over 1.6-fold ($P < 0.01$) and 1.3-fold ($P < 0.05$) respectively. While, the expression of miR-140-5p was remarkably downregulated in cervical cancer cell lines compared with the normal cervical epithelial cells as their respective reductions were 51.8% and 36.7% ($P < 0.01$). Furthermore, the mRNA and protein expressions of Smad3 were significantly increased in the cervical cancer cell lines compared with that in the normal cervical epithelial cells with 1.5-fold, 1.3-fold increase in mRNA levels and 3.8-fold, 3.3-fold increase in protein levels, respectively (Figure 1C and 1D, $P < 0.01$).

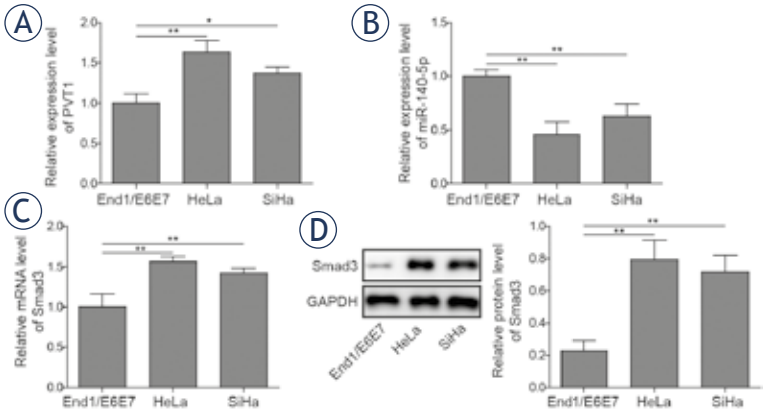

FIGURE 1. Expressions of PVT1, miR-140-5p and Smad3 in normal cervical epithelial cells and cervical cancer cell lines. Expression levels of PVT1 **(A)**, miR-140-5p **(B)** and Smad3 **(C)** were detected by qRT-PCR. **(D)** Protein expressions of Smad3 were detected by western blotting. The data are presented as means ± SD of three independent experiments. Statistical significance compared with the normal cervical epithelial cells is indicated by *$P < 0.05$ and **$P < 0.01$.

PVT1 directly sponged miR-140-5p and miR-140-5p directly targeted Smad3 in cervical cancer cells

Bioinformatics analysis showed that miR-140-5p might be a target of PVT1 (Figure 2A). Dual luciferase assay was further conducted to determine whether PVT1 could regulate miR-140-5p expression by acting as a molecular sponge, showing that miR-140-5p mimics could significantly inhibit the luciferase activity of PVT1-WT in both cancer cell lines, but had no significant effect on that of PVT1-MUT (Figure 2C and 2D). Furthermore, bioinformatics analysis revealed miR-140-5p can also bind directly to Smad3 (Figure 2B). The results of Figure 2E and 2F showed that miR-140-5p mimics could remarkably suppress the luciferase activity of Smad3-WT in both cervical cancer cell lines, and had no effect on that of Smad3-MUT.

Downregulation of lncRNA PVT1 inhibits proliferation, migration and invasion of cervical cancer cells

Since PVT1 was highly expressed in cervical cancer cells, revealing that lncRNA PVT1 could be a po-

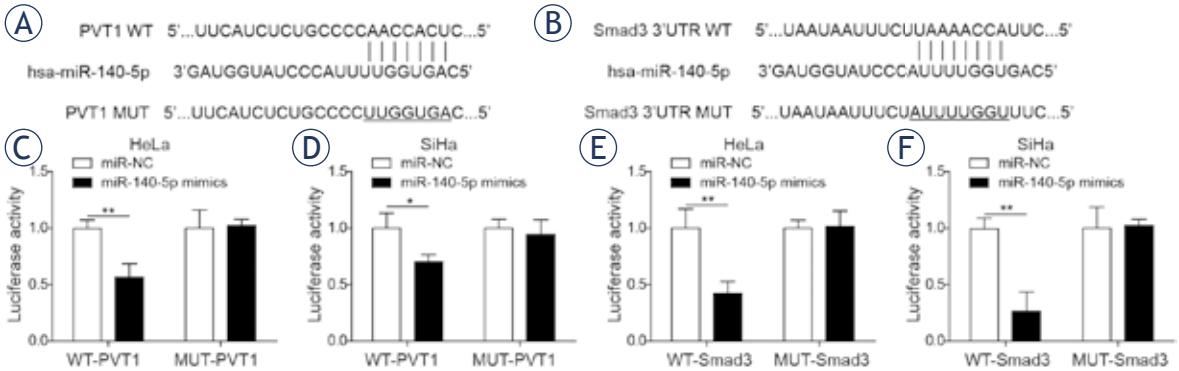

FIGURE 2. MiR-140-5p was a target of lncRNA PVT1 and Smad3 was a downstream target of miR-140-5p. **(A)** Binding sites between lncRNA PVT1 and miR-140-5p. **(B)** Binding sites between miR-140-5p and Smad3. Dual-luciferase assay was applied to explore the interaction between PVT1 and miR-140-5p in HeLa cells (**C**) and SiHa cells **(D)**. Dual-luciferase assay was applied to explore the interaction between miR-140-5p and Smad3 in HeLa cells **(E)** and SiHa cells **(F)**. The data are presented as means ± SD of three independent experiments. Statistical significance compared with miR-NC is indicated by *$P < 0.05$ and **$P < 0.01$.

tential oncogene during the progression of cervical cancer. To figure out the function of lncRNA PVT1 during the progression of cervical cancer cells, PVT1 specific sh-RNA was applied to knockdown the expression of PVT1. As shown in Figure 3A and 3B, the expressions of PVT1 were significantly downregulated in sh-PVT1 transfected cervical cancer cells compared with that in cells transfected with sh-NC and the control group as their respective reductions were 39.8% and 43.7% ($P < 0.01$). While, the expressions of miR-140-5p in sh-PVT1 transfected cervical cancer cells were significantly upregulated compared with cells transfected with sh-NC and the control group by over 1.4-fold ($P < 0.05$, Figure 3C) and 1.9-fold respectively ($P < 0.01$, Figure 3D). Meantime, the mRNA levels (Figure 3E and 3F) and protein levels (Figure 3G and 3H) of Smad3 were significantly decreased after transfecting with sh-PVT1 in cervical cancer cells with 25.3%, 38.5% reductions in mRNA levels and 57.2%, 62.3%

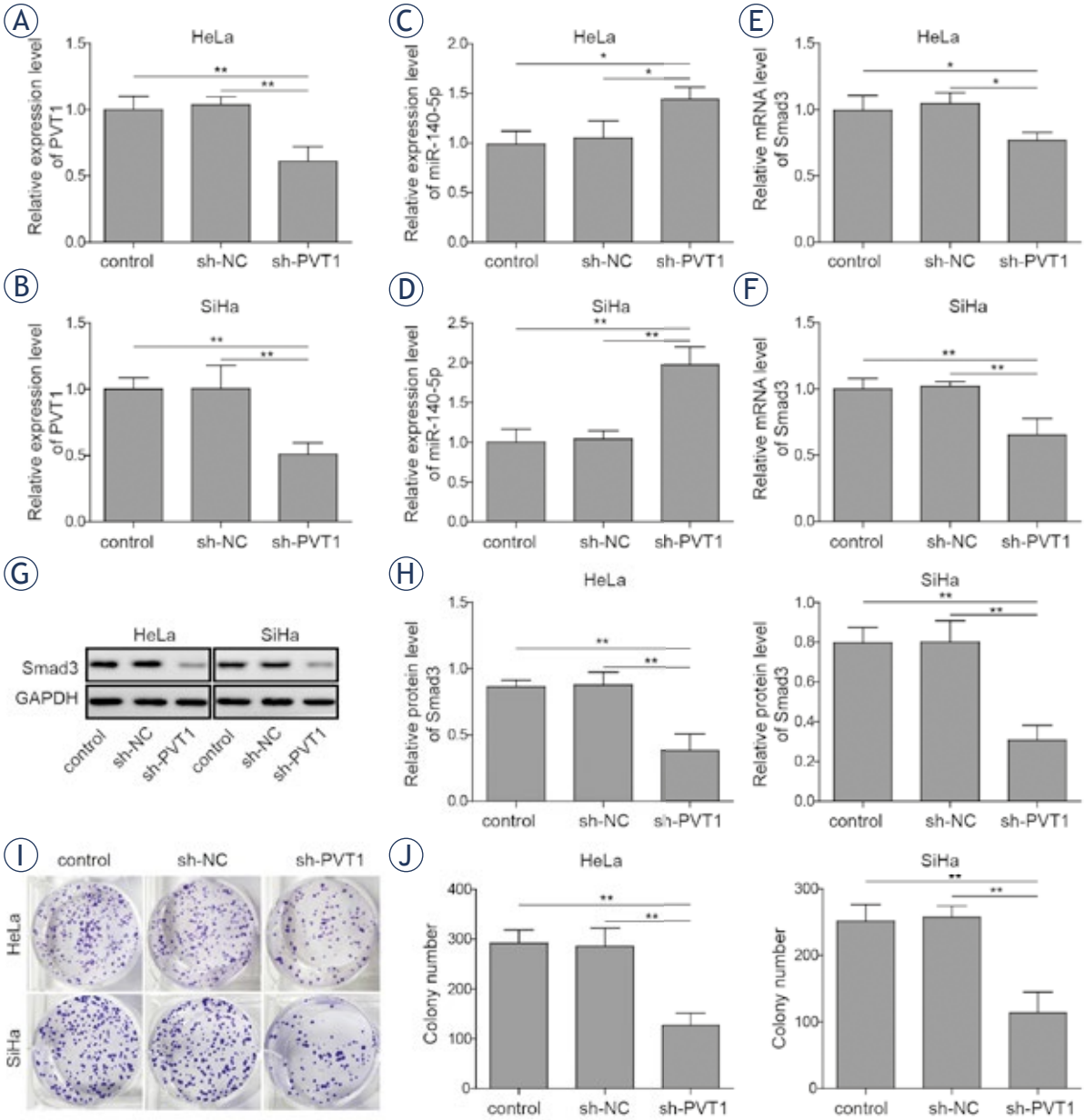

FIGURE 3. Silencing of lncRNA PVT1 inhibited proliferation of cervical cancer cells. Both HeLa and SiHa cells were transfected with sh-NC or sh-PVT1. Expressions of PVT1 **(A, B)** and miR-140-5p **(C, D)** were determined by qRT-PCR. (E-F) mRNA levels and **(G, H)** proteins levels of Smad3 were determined by qRT-PCR and western blotting respectively. **(I, J)** Colony formation assays were performed to evaluate the proliferation of both HeLa and SiHa cells. The data are presented as means ± SD of three independent experiments. Statistical significance compared with sh-NC is indicated by *$P < 0.05$ and **$P < 0.01$.

reductions in protein levels, respectively ($P < 0.01$). To explore the role of PVT1 in the proliferation of cervical cancer cells, colony formation assay was performed. As shown in Figure 3I and 3J, PVT1 knockdown significantly inhibit the proliferation of cervical cancer cells compared with the sh-NC group. Next, the migration activities of cervical cancer cells were detected by wound healing assay.

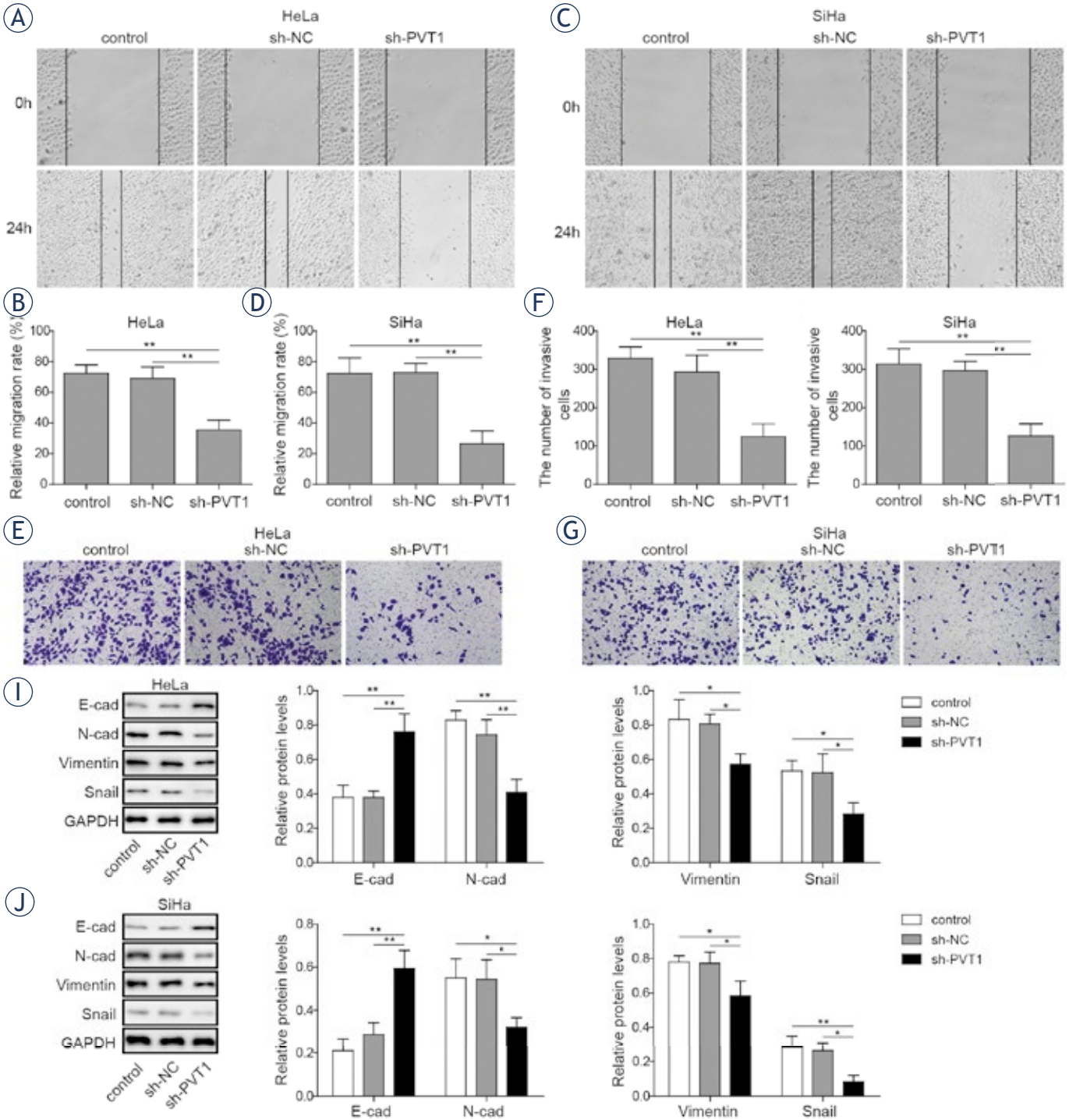

FIGURE 4. Silencing of lncRNA PVT1 suppressed the metastasis of cervical cancer cells. Both HeLa and SiHa cells were transfected with sh-NC or sh-PVT1. **(A-D)** Wound healing assay was conducted to evaluate the migration activities of HeLa and SiHa cells. **(E-H)** Transwell assay was conducted to evaluate the invasion activities of HeLa and SiHa cells. **(I, J)** Expressions of E-cadherin, N-cadherin, vimentin and Snail were determined by western blotting in both HeLa and SiHa cells. The data are presented as means ± SD of three independent experiments. Statistical significance compared with sh-NC is indicated by $*P < 0.05$ and $**P < 0.01$.

The results showed that PVT1 knockdown could significantly decrease the migration activities of cervical cancer cells compared with the sh-NC groups, with an inhibition rate of 51.2% and 61.3% in both cells lines respectively. (Figure 4A-4D, $P < 0.01$). Moreover, invasion capacity of cervical cancer cells was further determined by transwell assays. The results showed that PVT1 suppression could remarkably inhibit the invasion capacities of cervical cancer cells compared with the sh-NC groups, as their respective reductions were 59.2% and 61.2%, respectively (Figure 4E-4H, $P < 0.01$). Besides, expressions of E-cadherin, N-cadherin, vimentin and Snail were determined. The results showed that downregulation of PVT1 lead to significant increase in the expressions of E-cadherin (1.9-fold and 2.1-fold) and significant decrease in the expressions of N-cadherin (41.2% and 37.1%), vimentin (30.1% and 13.6%) and Snail (39.2% and 45%) compared with the sh-NC group (Figure 4I and 4J, $P < 0.05$). These data indicated that PVT1 could serve as an oncogenic lncRNA in the progression of cervical cancer.

LncRNA PVT1 promoted cervical cancer cells progression via modulating miR-140-5p

To determine whether miR-140-5p was implicated in the effect of lncRNA PVT1 on the progression of cervical cancer cells, sh-PVT1 transfected cervical cancer cells were transfected with or without miR-140-5p inhibitor. The results showed that miR-140-5p inhibitor could decline the PVT1 inhibition-mediated decreasing effect on the Smad3 expression in cervical cancer cells (Figure 5A-5D). Colony formation assay indicated that inhibition of miR-140-5p could reserve the inhibition effects of PVT1

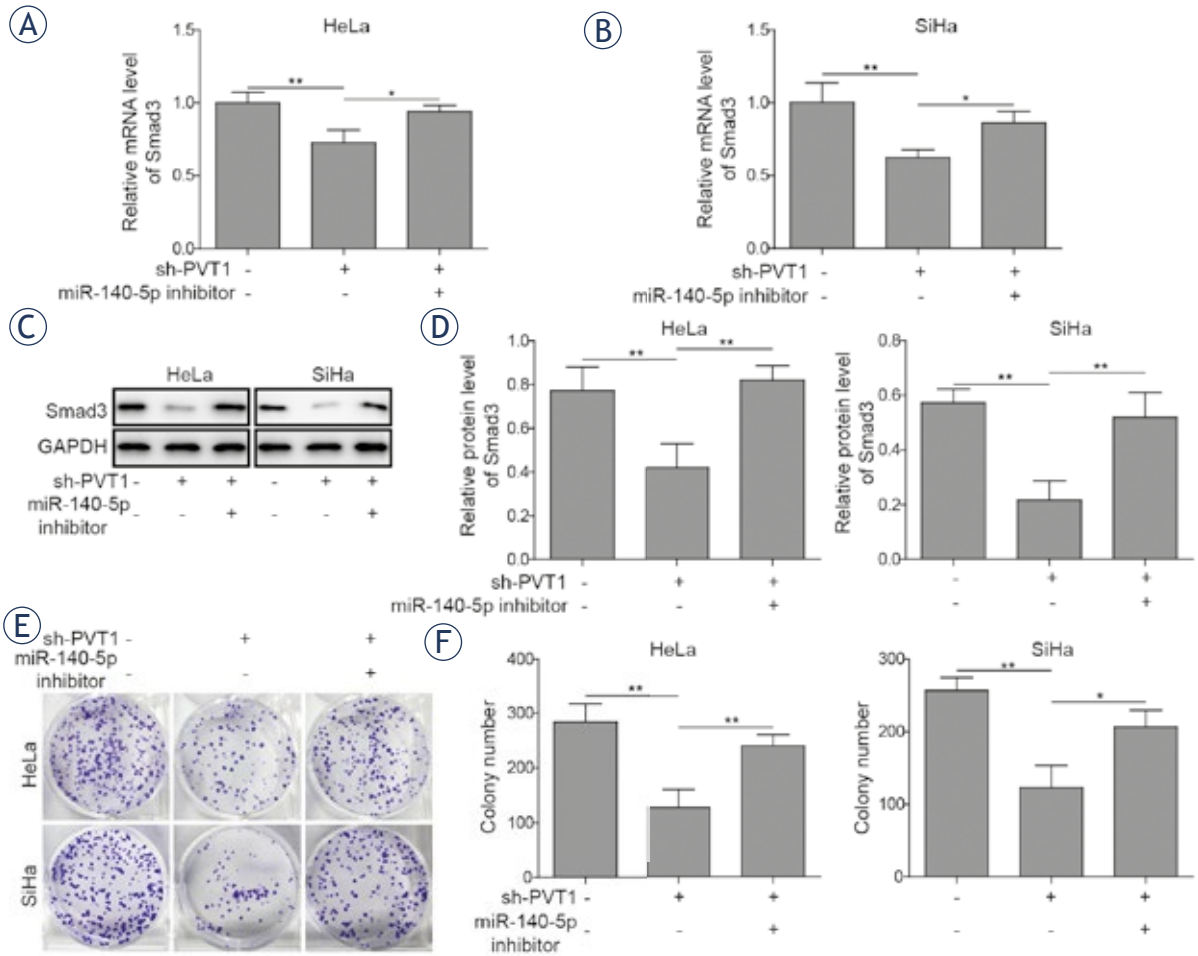

FIGURE 5. Silencing of miR-140-5p reversed the effects of PVT1 inhibition on the proliferation of cervical cancer cells. Both HeLa and SiHa cells were transfected with or without miR-140-5p inhibitor in the presence of sh-PVT1. **(A, B)** mRNA expressions and **(C, D)** protein expressions of Smad3 were determined by qRT-PCR and western blotting in both HeLa and SiHa cells. **(E, F)** Colony formation assays were performed to evaluate the proliferation of both HeLa and SiHa cells. The data are presented as means ± SD of three independent experiments. Statistical significance compared with sh-PVT1 is indicated by $*P < 0.05$ and $**P < 0.01$.

downregulation on proliferation of cervical cancer cells (Figure 5E and 5F). Similar results could also be observed in wound healing and transwell assays, that decreased migration and invasion abilities induced by PVT1 downregulation could be rescued by miR-140-5p inhibitor (Figure 6A-6H). Besides, treatment with miR-140-5p inhibitor could suppress sh-PVT1-induced upregulation of E-cadherin expression and reverse sh-PVT1-induced down-regulation of N-cadherin, vimentin

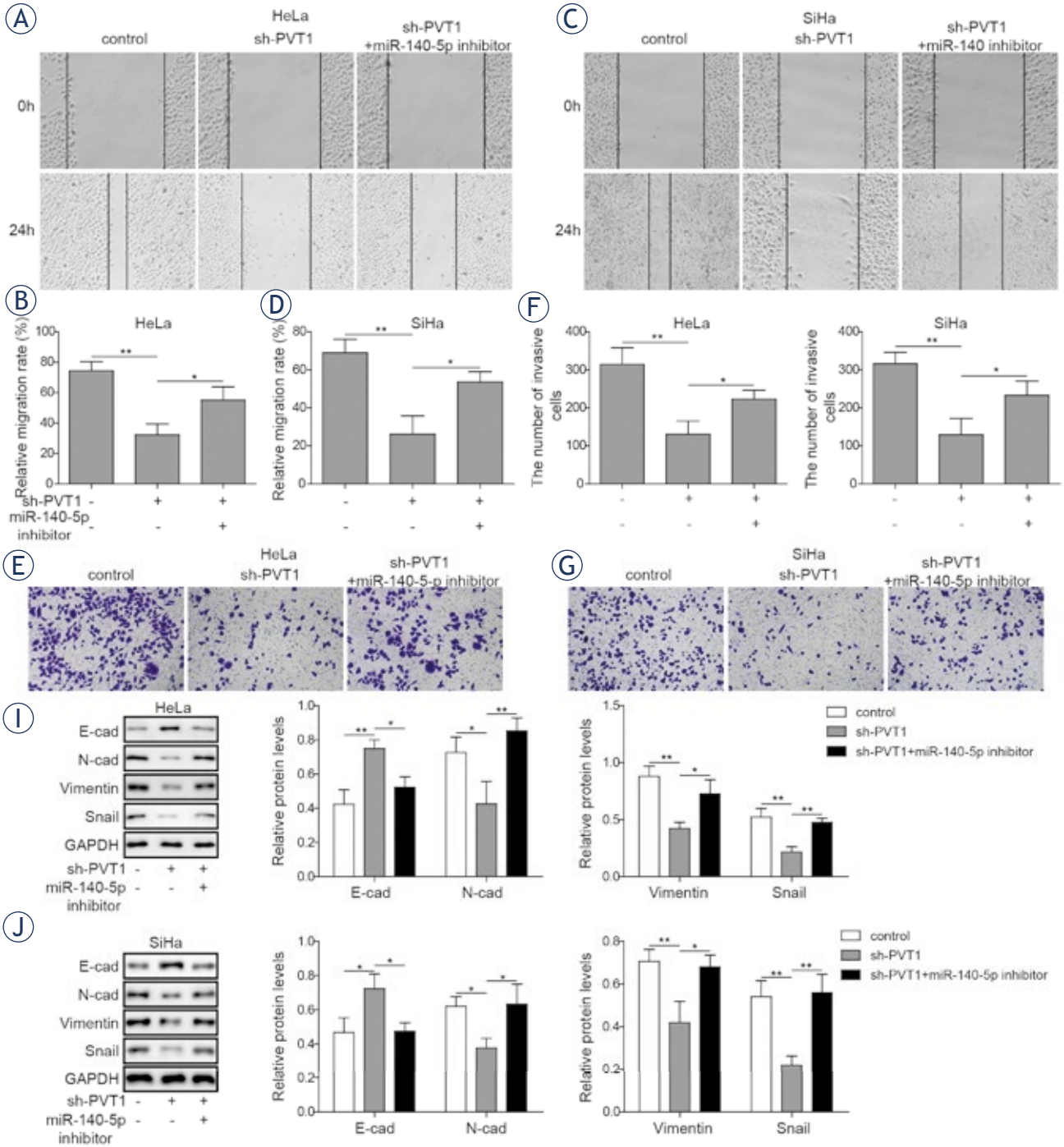

FIGURE 6. Silencing of miR-140-5p reversed the effects of PVT1 inhibition on the metastasis of cervical cancer cells. **(A-D)** Wound healing assay was conducted to evaluate the migration activities of HeLa and SiHa cells. **(E-H)** Transwell assay was conducted to evaluate the invasion activities of HeLa and SiHa cells. **(I, J)** Expressions of E-cadherin, N-cadherin, vimentin and Snail were determined by western blotting in both HeLa and SiHa cells. The data are presented as means ± SD of three independent experiments. Statistical significance compared with sh-PVT1 is indicated by $*P < 0.05$ and $**P < 0.01$.

and Snail expressions (Figure 6I-6J). These data indicated that PVT1 knockdown could suppress the progression of cervical cancer cells via miR-140-5p.

Discussion

Accumulating evidence has revealed that aberrantly expressed lncRNAs plays crucial role in tumor occurrence, invasion and metastasis including cervical cancer.[23] By far, PVT1 is recognized as an oncogene in many cancers, however, the role of PVT1 in the progression of cervical cancer and the potential underlying mechanism by which PVT1 participate in remains uncertain.

Recent studies have shown that PVT1 is upregulated in many kinds of cancers and serves as an oncogenic lncRNA. Zhang *et al*. have demonstrated that PVT1 could promote the proliferation and invasion by sponging miR-200a in glioma cells.[24] Zou *et al*.[25] showed that expressions of PVT1 were significantly elevated in ovarian cancer tissues and cells, and the progression of ovarian cancer cells promoted by PVT1 was mediated by the upregulation of SOX2. Our results also showed that PVT1 expressions were significantly upregulated in cervical cancer cells. Furthermore, knockdown of PVT1 could significantly decrease the proliferation, migration and invasion of cervical cancer cells. These findings showed that PVT1 might act as an oncogene in the progression of cervical cancer, which is in consistent with the previous researchers.[26,27]

Despite much progress have been made in the research of lncRNAs, the underlying mechanism remains unclear. Recently, interactions between lncRNAs and miRNAs have proposed that lncRNAs can serve as a sponge to bind miRNA and regulate the functions of miRNAs, which play a crucial role in the proliferation and tumorigenesis of many cancers.[28, 29] So, we further focused on miR-140-5p, due to its critical role in the progression of cervical cancer.[12, 13] Our data revealed that expressions of miR-140-5p were significantly downregulated in cervical cancer cells. Inhibition of PVT1 significantly increased the expressions of miR-140-5p in cervical cancer cells. In addition, luciferase assay was further applied to determine the correlation between PVT1 and miR-140-5p. Our results revealed that miR-140-5p upregulation could significantly inhibit the luciferase activities of PVT1-WT but did not affect that of PVT1-MUT, indicating that PVT1 binds to miR-140-5p and regulate its function. To further, clarify the interaction of PVT1 and miR-140-5p during the progression of cervical cancer cells. MiR-140-5p inhibitor were transfected into PVT1 knockdown cervical cancer cells then proliferation, migration and invasion assays of cervical cancer cells were performed. Zhang *et al*. showed that PVT1 could promote metastasis and proliferation of colon cancer via the inhibiting of miR-26.[30] Tian *et al*. reported that PVT1 could downregulate miR-31 to enhance CDK1 expression thus facilitating the progression of bladder cancer cells.[10] Our results illustrate the interaction between PVT1 and miR-140-5p in the progression of cervical cancer cells.

Normally, miRNAs could regulate tumorigenesis by targeting a variety of protein-coding genes.[31] Smad3 has been demonstrated increased and could act as an oncogenic role in the progression of many type of cancers. For instance, Yamazaki *et al*. showed that Smad3 could promote the invasion and migration of pancreatic cancer cells.[32] Fan *et al*. showed that activation of TGFA/Smad3 signal could induce the migration and invasion of cervical cancer cell lines, suggesting that Smad3 plays a vital role in cervical cancer metastasis.[33] Our present results also revealed that Smad3 expressions were significantly increased in cervical cancer cells. Besides, bioinformatics analysis showed that Smad3 might be downstream target of miR-140-5p. In addition, the luciferase assay displayed that miR-140-5p could target Smad3 directly. More importantly, our results corroborated that transfection of miR-140-5p inhibitor could partially reverse PVT1 knockdown-induced changes of Smad3 expressions in cervical cancer cells, indicating that miR-140-5p act as a tumor suppressor through the regulation of Smad3.

Collectively, we found that PVT1 is upregulated in cervical cancer cells, and PVT1 might serve as a prognostic indicator for cervical cancer patients.[34-36] Furthermore, PVT1 sponges directly to miR-140-5p and regulates its expression and function. In addition, Smad3 is also upregulated in cervical cancer cells and it is the downstream target of miR-140-5p. Moreover, PVT1 promotes the proliferation, migration and invasion of cervical cancer cells via regulating miR-140-5p and Smad3. Our findings provide new insights into the therapeutic strategy against cervical cancer.

Author contributions

QQC conceived and designed the experiments. CYC guaranteed the integrity of the whole research

and made the clinical studies. ZC defined intellectual content, SC did literature research, QQC made data analysis and CYC contributed statistical analysis. All authors were responsible for the editing of the manuscript. All authors read and approved the final manuscript.

References

1. Bray F, Ferlay J, Soerjomataram I, Siegel R L, Torre L A, Jemal A. Global cancer statistics 2018: GLOBOCAN estimates of incidence and mortality worldwide for 36 cancers in 185 countries. *CA Cancer J Clin* 2018; **68:** 394-424. doi: 10.3322/caac.21492
2. Pang T, Wang S, Gao M, Kang H, Zhao Y, Yao Y, et al. HPV18 E7 induces the over-transcription of eIF4E gene in cervical cancer. *Iran J Basic Med Sci* 2015; **18:** 684-90. PMID: 26351560
3. Moody CA, Laimins LA. Human papillomavirus oncoproteins: pathways to transformation. *Nat Rev Cancer* 2010; **10:** 550-60. doi: 10.1038/nrc2886
4. Santin A D, Zhan F, Bignotti E, Siegel E R, Cane S, Bellone S, et al. Gene expression profiles of primary HPV16- and HPV18-infected early stage cervical cancers and normal cervical epithelium: identification of novel candidate molecular markers for cervical cancer diagnosis and therapy. *Virology* 2005; **331:** 269-91. doi: 10.1016/j.virol.2004.09.045
5. Di Gesualdo F, Capaccioli S, Lulli M. A pathophysiological view of the long non-coding RNA world. *Oncotarget* 2014; **5:** 10976-96. doi: 10.18632/oncotarget.2770
6. Sun L, Luo H, Liao Q, Bu D, Zhao G, Liu C, et al. Systematic study of human long intergenic non-coding RNAs and their impact on cancer. *Sci China Life Sci* 2013; **56:** 324-34. doi: 10.1007/s11427-013-4460-x
7. Ching T, Peplowska K, Huang S, Zhu X, Shen Y, Molnar J, et al. Pan-cancer analyses reveal long intergenic non-coding RNAs relevant to tumor diagnosis, subtyping and prognosis. *EBioMedicine* 2016; **7:** 62-72. doi: 10.1016/j.ebiom.2016.03.023
8. Yang M, Zhai X, Xia B, Wang Y, Lou G. Long noncoding RNA CCHE1 promotes cervical cancer cell proliferation via upregulating PCNA. *Tumour Biol* 2015; **36:** 7615-22. doi: 10.1007/s13277-015-3465-4
9. Han D, Wang J, Cheng G. LncRNA NEAT1 enhances the radio-resistance of cervical cancer via miR-193b-3p/CCND1 axis. *Oncotarget* 2018; **9:** 2395-409. doi: 10.18632/oncotarget.23416
10. Tian Z, Cao S, Li C, Xu M, Wei H, Yang H, et al. LncRNA PVT1 regulates growth, migration, and invasion of bladder cancer by miR-31/ CDK1. *J Cell Physiol* 2019; **234:** 4799-481. doi: 10.1002/jcp.27279
11. Chen Y, Du H, Bao L, Liu W. LncRNA PVT1 promotes ovarian cancer progression by silencing miR-214. *Cancer Biol Med* 2018; **15:** 238-250. doi: 10.20892/j.issn.2095-3941.2017.0174
12. Ding Y, Fang Q, Li Y, Wang Y. Amplification of lncRNA PVT1 promotes ovarian cancer proliferation by binding to miR-140. *Mamm Genome 2019;* **30:** 217-25. doi: 10.1007/s00335-019-09808-1
13. Iden M, Fye S, Li K, Chowdhury T, Ramchandran R, Rader J S. The lncRNA PVT1 contributes to the cervical cancer phenotype and associates with poor patient prognosis. *PLoS One* 2016; **11:** e0156274. doi: 10.1371/journal.pone.0156274
14. Dong G, Liang X, Wang D, Gao H, Wang L, Wang L, et al. High expression of miR-21 in triple-negative breast cancers was correlated with a poor prognosis and promoted tumor cell in vitro proliferation. *Med Oncol* 2014; **31:** 57. doi: 10.1007/s12032-014-0057-x
15. Muhammad S, Tang Q, Wei L, Zhang Q, Wang G, Muhammad B U, et al. miRNA-30d serves a critical function in colorectal cancer initiation, progression and invasion via directly targeting the GNA13 gene. *Exp Ther Med* 2019; **17:** 260-72. doi: 10.3892/etm.2018.6902
16. Ma H P, Kong W X, Li X Y, Li W, Zhang Y, Wu Y. miRNA-223 is an anticancer gene in human non-small cell lung cancer through the PI3K/AKT pathway by targeting EGFR. *Oncol Rep* 2019; **41:** 1549-59. doi: 10.3892/or.2019.6983
17. Ventura A, Jacks T. MicroRNAs and cancer: short RNAs go a long way. *Cell* 2009; **136:** 586-91. doi: 10.1016/j.cell.2009.02.005
18. Fang Z, Yin S, Sun R, Zhang S, Fu M, Wu Y, et al. miR-140-5p suppresses the proliferation, migration and invasion of gastric cancer by regulating YES1. *Mol Cancer* 2017; **16:** 139. doi: 10.1186/s12943-017-0708-6
19. Lan H, Chen W, He G, Yang S. miR-140-5p inhibits ovarian cancer growth partially by repression of PDGFRA. *Biomed Pharmacother* 2015; **75:** 117-22. doi: 10.1016/j.biopha.2015.07.035
20. Zhang Y, Xu J. MiR-140-5p regulates hypoxia-mediated human pulmonary artery smooth muscle cell proliferation, apoptosis and differentiation by targeting Dnmt1 and promoting SOD2 expression. *Biochem Biophys Res Commun* 2016; **473:** 342-8. doi: 10.1016/j.bbrc.2016.03.116
21. Li J, Zou K, Yu L, Zhao W, Lu Y, Mao J, et al. MicroRNA-140 inhibits the epithelial-mesenchymal transition and metastasis in colorectal cancer. *Mol Ther Nucleic Acids* 2018; **10:** 426-37. doi: 10.1016/j.omtn.2017.12.022
22. Dong P, Xiong Y, Hanley S J B, Yue J, Watari H. Musashi-2, a novel oncoprotein promoting cervical cancer cell growth and invasion, is negatively regulated by p53-induced miR-143 and miR-107 activation. *J Exp Clin Cancer Res* 2017; **36:** 150. doi: 10.1186/s13046-017-0617-y
23. Dong J, Su M, Chang W, Zhang K, Wu S, Xu T. Long non-coding RNAs on the stage of cervical cancer. *Oncol Rep* 2017; **38:** 1923-31. doi: 10.3892/or.2017.5905
24. Zhang Y, Yang G, Luo Y. Long non-coding RNA PVT1 promotes glioma cell proliferation and invasion by targeting miR-200a. *Exp Ther Med* 2019; **17:** 1337-45. doi: 10.3892/etm.2018.7083
25. Zou M F, Ling J, Wu Q Y, Zhang C X. Long non-coding RNA PVT1 functions as an oncogene in ovarian cancer via upregulating SOX2. *Eur Rev Med Pharmacol Sci* 2018; **22:** 7183-8. doi: 10.26355/eurrev_201811_16251
26. Wan L, Sun M, Liu G J, Wei C C, Zhang E B, Kong R, et al. Long noncoding RNA PVT1 promotes non-small cell lung cancer cell proliferation through epigenetically regulating LATS2 expression. *Mol Cancer Ther* 2016; **15:** 1082-94. doi: 10.1158/1535-7163.MCT-15-0707
27. Ping G, Xiong W, Zhang L, Li Y, Zhang Y, Zhao Y. Silencing long noncoding RNA PVT1 inhibits tumorigenesis and cisplatin resistance of colorectal cancer. *Am J Transl Res* 2018; **10:** 138-49. PMID: 29423000
28. Shi X, Sun M, Liu H, Yao Y, Song Y. Long non-coding RNAs: a new frontier in the study of human diseases. *Cancer Lett* 2013; **339:** 159-66. doi: 10.1016/j.canlet.2013.06.013
29. Kim J, Piao H L, Kim B J, Yao F, Han Z, Wang Y, et al. Long noncoding RNA MALAT1 suppresses breast cancer metastasis. *Nat Genet* 2018; **50:** 1705-15. doi: 10.1038/s41588-018-0252-3
30. Zhang R, Li J, Yan X, Jin K, Li W, Liu X, et al. Long noncoding RNA plasmacytoma variant translocation 1 (PVT1) promotes colon cancer progression via endogenous sponging miR-26b. *Med Sci Monit* 2018; **24:** 8685-92. doi: 10.12659/MSM.910955
31. Huang V. Endogenous miRNAa: miRNA-mediated gene upregulation. *Adv Exp Med Biol* 2017; **983:** 65-79. doi: 10.1007/978-981-10-4310-9_5
32. Yamazaki K, Masugi Y, Effendi K, Tsujikawa H, Hiraoka N, Kitago M, et al. Upregulated SMAD3 promotes epithelial-mesenchymal transition and predicts poor prognosis in pancreatic ductal adenocarcinoma. *Lab Invest* 2014; **94:** 683-91. doi: 10.1038/labinvest.2014.53
33. Fan Q, Qiu M T, Zhu Z, Zhou J H, Chen L, Zhou Y, et al. Twist induces epithelial-mesenchymal transition in cervical carcinogenesis by regulating the TGF-beta/Smad3 signaling pathway. *Oncol Rep* 2015; **34:** 1787-94. doi: 10.3892/or.2015.4143
34. Chen X, Xiong D, Ye L, Wang K, Huang L, Mei S, et al. Up-regulated lncRNA XIST contributes to progression of cervical cancer via regulating miR-140-5p and ORC1. *Cancer Cell Int* 2019; **19:** 45. doi: 10.1186/s12935-019-0744-y
35. Su Y, Xiong J, Hu J, Wei X, Zhang X, Rao L. MicroRNA-140-5p targets insulin like growth factor 2 mRNA binding protein 1 (IGF2BP1) to suppress cervical cancer growth and metastasis. *Oncotarget* 2016; **7:** 68397-411. doi: 10.18632/oncotarget.11722
36. Yang J P, Yang X J, Xiao L, Wang Y. Long noncoding RNA PVT1 as a novel serum biomarker for detection of cervical cancer. *Eur Rev Med Pharmacol Sci* 2016; **20:** 3980-6.

research article

Incorporation of EGFR mutation status into M descriptor of new TNM classification influences survival curves in non-small cell lung cancer patients

Karmen Stanic[1], Nina Turnsek[2], Martina Vrankar[1]

[1] Department of Radiotherapy, Institute of Oncology Ljubljana
[2] Department of Medical Oncology, Institute of Oncology Ljubljana

Radiol Oncol 2019; 53(4): 453-458.

Received 1 August 2019
Accepted 30 August 2019

Correspondence to: Asst. Prof. Martina Vrankar, M.D., Ph.D., Institute of Oncology Ljubljana, Zaloška 2, SI-1000 Ljubljana, Slovenia.
E-mail: mvrankar@onko-i.si

Disclosure: No potential conflicts of interest were disclosed.

Data from this research have been partly presented as poster at 17th World Conference on Lung Cancer 2016 in Vienna. *J Thorac Oncol* 2017; **12(Suppl 1):** S302.

Background. The 8th edition of tumor node metastasis (TNM) staging system for lung cancer introduced a revision of M descriptor. The limitation of new classification to predict prognosis is its focus on anatomical extent of the disease only. Information on molecular status of the tumor significantly influences treatment response and survival; however, data addressing this issue is scarce. This report points to the impact of epidermal growth factor receptor (EGFR) mutation in non-small cell lung cancer (NSCLC) patients on survival in view of new M descriptors of TNM classification system.

Patients and methods. Medical records of 479 consecutive metastatic NSCLC patients treated between 2009 and 2011, all tested for EGFR mutations, were retrospectively reviewed. For 355 patients medical records included sufficient information to be appropriately categorized into one of the new subgroups according to the M descriptor in 8th TNM classification, of those 89 (25.1%) patients harboured EGFR mutations (EGFR-m).

Results. Median overall survival (mOS) of EGFR-m patients was significantly longer than mOS of patients without EGFR mutations (20.6 months *vs*. 8.3 months, $p < 0.001$). Patients with limited disease burden (M1b sub-group) had the longest mOS among EGFR wild type patients (EGFR-wt) and also among EGFR-m patients, 14.4 months and 39.2 month, respectively. In spite of widespread metastatic disease of M1c EGFR-m patients, their mOS (18.8 months) was longer than mOS of oligometastatic EGFR-wt patients (M1b), who had the lowest disease burden (14.4 months). Median follow up was 53.9 months.

Conclusions. Incorporation of EGFR mutation status in advanced NSCLC further differentiates survival curves of M categories in 8th TNM classification and more precisely predicts survival compared to number of metastasis or number of metastatic sites alone.

Key words: EGFR mutations; non-small cell lung cancer; survival; metastases; TNM

Introduction

The 8th edition of tumour-node-metastases (TNM) staging system for lung cancer came into practice in January 2018 and replaced 7th edition from 2007.[1-3] TNM classification is a coding system for the anatomic extent of the disease. By its definition it does not include tumour markers, genetic signatures, comorbidities etc., which are all known to influence the survival. Nevertheless, the authors of new TNM proposal pointed out improvement in survival curves as one of major reasons for the

change of classification. Several new diagnostic, imaging and treatment developments were introduced during the period in which patients were included, from 1990 to 2000. New imaging techniques such as PET/CT and MRI influence the stage migration, while the new treatment with targeted agents and immunotherapy influences the survival curves.[4-9] The majority of new improvements and developments in the last 15 years were implemented for metastatic patients and therefore affected mostly M descriptor. With new classification there are no changes of M1a category, while there is further sub-classification of M1b category into M1b (single distant metastatic lesion in single organ) and M1c (multiple metastases in one organ or in multiple distant metastatic sites).[10] There is growing evidence showing that information on molecular tumour status significantly affects treatment response and survival.[11-16] This report points on impact of epidermal growth factor receptor (EGFR) mutation on survival in view of new TNM classification system.

Patients and methods

Medical records of 479 consecutive metastatic non-small cell lung cancer (NSCLC) patients, treated between 2009 and 2011, all tested for EGFR mutations were retrospectively reviewed. They were categorized into sub-groups according to new M descriptors. For 355 out of 479 patients, among them 89 (25.1%) with EGFR mutations (EGFR-m), there was sufficient information in medical records

TABLE 1. Baseline characteristics of patients by EGFR mutation status

Characteristics	All n	EGFR-wt n	(%)	EGFR-m n	(%)	p
All patients	355	266	75	89	25	
Age (years)						
median	64.4	63.5	65.6	65.6		0.98
range	25-88	25–87	25–87	36–88		
Gender						
female	165	107	40.2	58	65.2	< 0.001
male	190	159	59.8	31	34.8	
Smoking status						< 0.001
current	142	132	49.6	10	11.2	
former	101	81	30.5	20	22.5	
never	95	40	15.0	55	61.8	
unknown	17	13	4.9	4	4.5	
Histology						
adenocarcinoma	309	232	87.2	77	86.2	0.86
non-small cell lungcancer, NOS	46	34	12.8	12	13.5	
Metastatic sites*						
Brain	86	61	22.9	25	28.1	0.33
Bone	151	104	39.1	47	52.8	0.02
Lung	157	106	39.8	51	57.3	0.01
Pleura	115	83	31.2	32	36.0	0.48
Liver	55	40	15.0	15	16.9	0.68
Adrenal gland	49	43	16.2	6	6.7	0.02
Distant lymph nodes	55	46	17.3	9	10.1	0.10
Other sites	40	34	12.8	6	6.7	0.11

* Sum of all metastasis is more than 355 as some patients had multiple metastases; EGFR-m = patients harboured EGFR mutations; EGFR-wt = EGFR wild type patients

that allowed appropriate new categorisation according to new TNM classification. Median overall survival was calculated from the date of diagnosis to the death or last follow up and estimated using Kaplan-Meier method.[17] The association between the EGFR mutation status and the clinico-pathological characteristics of patients were tested using the Mann-Whitney U (MW-U) or the Kruskal Wallis H (KW-H) test. Survival and prognosis was assessed using Cox proportional hazard regression analysis. All p values reported were based on the two-sided hypothesis. Data was calculated using SPSS v.20 statistical package.

This analysis is part of a retrospective study approved by Institutional Review Board Committee and National Ethics Committee (No.143/1/2011).

Results

Totally, 355 patients were included in final analysis, of those 89 (25.1%) were EGFR-m positive. Median age of all patients was 64.4 years (range 25-88). Majority were male, current or former smokers and had adenocarcinoma. Data on basic patients' characteristics are listed in Table 1.

The distribution of metastases according to EGFR mutation status differed between the two groups, with metastases to bones and lung being more frequent in EGFR-m patients compared to EGFR wild type (EGFR-wt) patients, while metastases to adrenal gland were less frequent in EGFR-m patients as compared to EGFR-wt patients.

Most of the patients with EGFR-m tumors were primary treated with EGFR tyrosine kinase inhibitors (TKIs) (71 cases, 79%). Chemotherapy (ChT) was applied to 10 patients as first-line systemic treatment while after progression to ChT treatment with TKI was the most common. Eight patients with EGFR-m tumors did not receive any form of systemic treatment. The reason could not be clearly established from the medical records.

For patients with EGFR-wt tumors, platinum based chemotherapy was the most common form of systemic treatment (150/266 cases, 56.4%). In 29 patients, TKIs were used for maintenance treatment. In the group of EGFR-wt patients, no systemic treatment was given to 87 patients (33%) due to bad performance status and comorbidities, while palliative irradiation of symptomatic sites was used in some patients in addition to best supportive care.

We compared mOS of patients with and without systemic therapy according to EGFR mutation status. As expected, EGFR-m patients treated with TKI had longer survival than EGFR-m patients on symptomatic treatment only (21.3 *vs*. 3.3 month), though the number of non-treated patients was too low to draw any firm conclusions. Similarly, EGFR-wt patients who received chemotherapy had longer mOS than those without treatment (12.4 *vs*. 2.8 months). EGFR-m patients receiving best supportive care only, showed trend to better survival compared to EGFR-wt on best supportive care, but additional analysis was futile due to small number of cases in subcategories.

Patients were first categorized according to 7th TNM classification and according to their EGFR mutation status. Secondly, patients with 7th M1b category were grouped to those who had single metastatic site/organ and those with multiple metastases, presented in Table 2.

Finally, we joined cases with multiple metastatic sites and those with multiple metastases in one

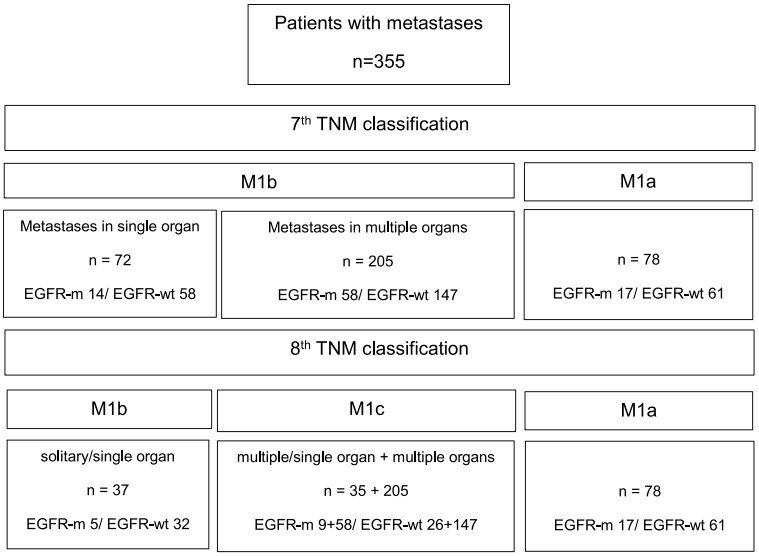

FIGURE 1. Diagram of division: From 7th to 8th TNM classification with incorporation of EGFR mutation status.

EGFR-m = patients harboured EGFR mutations; EGFR-wt = EGFR wild type patients

TABLE 2. Overall survival of EGFR-m compared to EGFR-wt patients based on the M1b status in 7th TNM classification for single and multiple metastatic sites/organs

Metastatic sites (old M1b only)	all	EGFR-m		EGFR-wt		p
	n	n	mOS	n	mOS	
Single organ	72	14	32.5	58	11.5	< 0.001
Multiple organs	205	58	17.4	147	6.1	< 0.001
All	277	77	20.5	205	7.8	< 0.001

EGFR-m = patients harboured EGFR mutations; EGFR-wt = EGFR wild type patients

TABLE 3. M descriptors for 7th and 8th TNM classification according to EGFR mutation status and their median overall survival (mOS) in months

7th TNM classification						
M descriptor		**EGFR-m**			**EGFR-wt**	
	n	n	mOS	n	mOS	p
M1a	78	17	22.4	61	10.7	0.025
M1b	252	72	18.8	205	7.9	< 0.001
All	355	89	20.6	266	8.3	< 0.001
8th TNM classification		**EGFR-m**			**EGFR-wt**	
M1a	78	17	22.4	61	10.7	0.025
M1b	37	5	39.2	32	14.4	0.082
M1c	240	67	18.8	173	6.6	< 0.001
All	355	89	20.6	266	8.3	< 0.001

EGFR-m = patients harboured EGFR mutations; EGFR-wt = EGFR wild type patients

TABLE 4. Site specific median overall survival (mOS) according to EGFR mutation status

Metastatic site	Patients	mOS			
	n	all	EGFR-m	EGFR-wt	p
Brain	86	8.1	14.9	7.1	**0.003**
Bone	151	9.4	21.3	6.7	**< 0.001**
Lung	157	11.9	20.2	8.3	**0.002**
Pleura	115	8.8	20.6	6.5	**< 0.001**
Liver	55	5.6	10.4	5.5	0.245
Adrenal gland	49	5.2	4.9	5.5	0.595
Distant lymph nodes	55	6.2	13.0	5.5	0.237
Other sites	40	8.9	14.9	8.4	0.156

EGFR-m = patients harboured EGFR mutations; EGFR-wt = EGFR wild type patients

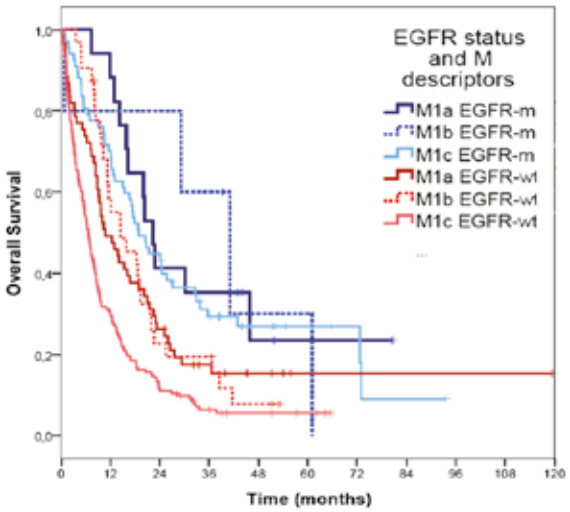

FIGURE 2. Survival curves of different M categories according to EGFR mutation status based on 8th TNM classification.

EGFR-m = patients harboured EGFR mutations; EGFR-wt = EGFR wild type patients

organ to form new M1c, incorporating also EGFR mutation status following the process shown in Figure 1.

Survival results show that mOS was better for all metastatic EGFR-m patients compared to metastatic EGFR-wt patients (20.6 *vs.* 8.3 months, p < 0.001). Detailed mOS for new versus old M descriptor is shown in Table 3.

Patients with metastases to single organ only had better survival than those who had metastases in multiple organs, irrespective of the presence of EGFR mutations (14.4 and 7.9 months, p = 0.006). Significantly better overall survival of EGFR-m patients compared to EGFR-wt patients was seen in group of patients with single organ metastases only as well as in group with metastases in multiple organs (p < 0.001).

Survival curves of different new M categories (TNM 8th edition) according to EGFR mutation status are presented in Figure 2.

Distribution of metastatic spread to different organs with regard to EGFR mutation status was also analysed. In EGFR-m patients multiple metastases were observed in all organs, the only exception being the adrenal gland where there was only one case with single metastases. On the contrary, EGFR-wt patients had more frequently either one or multiple metastases in single organ. Site specific mOS with regard to EGFR mutation status is shown in Table 4. EGFR-m patients with metastases to brain, bone, lung and pleura have significantly better survival than EGFR-wt patients, while no statistical difference was noted for other metastatic sites.

Discussion

Our retrospective review analyzed metastatic non-small cell lung cancer patients with objective to categorize them according to new M descriptor incorporating also the data on EGFR mutation status. In the proposal of new M descriptor 1059 metastatic cases were included into detailed survival analysis.[10] Since the patients were diagnosed between 1999 and 2012, not all could have had EGFR mutation testing, as this was not a routine procedure before the year 2004.[18] Their main purpose was analysis of expected change in survival curves due to stage migration, incorporating new diagnostic procedures (PET/CT) and new treatment options with local approaches, especially irradiation of oligometastatic sites as well as improvement in systemic treatment, mainly molecular targeted agents.[19] In

our single institution analysis 355 patients were included, which represent one third (35.5%) of cases published in a paper that is proposing and justifying the classification changes.

In further detailed analysis of distribution pattern of metastatic spread according to EGFR mutation status, we first divided patients by organ/site they metastasized to rather than number of metastasis in a single organ. As shown in this analysis and known also from clinical practice and previous studies, patients with single metastatic site (organ) have better prognosis than those with multiple metastatic sites.[20] Patients with low number of metastatic sites are known to have oligometastatic disease, though the definitions differ and current guidelines propose modified treatment.[21-23] The new M descriptor does not define oligometastatic disease in a way that would help clinicians make decision about the treatment. For example, treatment and prognosis of patients with one metastasis in the brain (M1b) might be the same as of three small metastases (M1c).[24] Similarly, treatment of one metastasis in the liver (M1b) will probably be the same as for multiple metastases (M1c). One special situation is metastasis to the adrenal gland. Therapeutic options for metastasis to the adrenal gland as a single metastatic site are local treatments, either irradiation or operation.[25,26] No cases with more than one metastasis in a single adrenal gland were observed in the current analysis. Patients with metastases in the adrenal gland, which are often affected on both sides, have bad prognosis and survival. According to our analysis, patients with metastases to adrenal gland have the worst survival regardless of EGFR-m status. In addition, other researchers noticed that patients with adrenal gland metastasis showed impaired survival.[10] However, based on their data they concluded that the site of metastasis is not prognostic for single or multiple lesions within the single organ. It is questionable whether one or more metastases in a single organ really influence survival. On the contrary, current analysis suggests that the number of metastatic sites might be more important prognostic factor than number of metastatic lesions in one organ.

Even though large number of patients was included in our series, only 5 patients with EGFR mutations were sub-classified into M1b category. It seems that once EGFR-m tumors metastasize they do it in aggressive and widespread way. For the first time we have shown that not only have EGFR-m patients better mOS than EGFR-wt patients but also better mOS in each sub-category of M descriptor. This analysis showed that in spite of widespread metastatic disease (M1c) and high tumor burden, EGFR-m patients treated with TKI had longer mOS (18.8 months) than EGFR-wt patients with only one metastasis (M1b) (14.4 months). Likely, EGFR-m status has greater impact on survival curves than different sub-categories of M descriptor.

We are aware of the need for simple and predictable system for classification in prognostic groups of patients with lung cancer. However, according to our survival data it seems that TNM classification is inadequate for relevant prediction of survival, because in some cases, as we show for EGFR mutations, molecular feature is more important than anatomical distribution of malignant disease. Maybe we should consider adding the new descriptor to TNM classification that labels molecular feature of tumor. Recently, investigators from University of California published an article on how integration of molecular prognostic classifier into TNM system might improve identification of high-risk patients and predict survival in non-metastatic NSCLC. They used 11 cancer-related target genes; however, they did not include current biomarkers such as EGFR, KRAS ALK, which was recognized as an important drawback of their study.[27]

There are some important limitations to the current analysis. It was not possible to find reliable metastatic information for about 25% of cases in our database, which could not be included in the analysis. It should be recognized that due to small number of series those might be the cases that could influence the results and represent the potential bias. There were also more patients with symptomatic treatment among EGFR-wt patients than EGFR-m patients, reflecting real clinical situation. However, this is not surprising as majority of EGFR-m patients are nonsmokers and have less comorbidities. Also, in contrast to EGFR-wt patients who can receive chemotherapy only in good performance status (PS) 0-2, EGFR-m patients may also receive TKI in poor PS (3-4). Due to retrospective nature of the study not all metastatic sites rather symptomatic ones were diagnosed and collected in routine clinical practice.

Conclusions

Number of metastatic sites might be more important predictive survival factor than number of metastatic lesions in single organ, though both fall into M1c category. Incorporation of EGFR mutation sta-

tus seem to predict survival more reliably than the number of metastasis or number of metastatic sites in NSCLC. Our results indicate that further analysis with incorporation of information on also other molecular status is warranted to further improve differentiation of survival curves in the future.

References

1. Brierly DJ, Gospodarowicz MK, Witekind C, editors. *TNM classification of malignant tumours.* 8th edition. Oxford: Wiley-Blackwell; 2017. p. 114-20.
2. Sobin LH, Gospodarowicz MK, Witekind C, editors. *TNM classification of malignant tumours.* 7th edition. Oxford: Wiley-Blackwell; 2009. p. 138-46.
3. Goldstraw P, Crowley J, Chansky K, Giroux DJ, Groome PA, Rami-Porta R, et al. The IASLC Lung Cancer Staging Project: proposals for the revision of the TNM stage groupings in the forthcoming (seventh) edition of the TNM classification of malignant tumours. *J Thorac Oncol* 2007; **2:** 706-14. doi: 10.1097/JTO.0b013e31812f3c1a
4. Kligerman S, Digumarthy S. Staging of non small cell lung cancer using integrated PET/CT. *AJR Am J Roentgenol* 2009; **193:**1203-11. doi: 10.2214/AJR.09.3193
5. Kim SY, Kim JS, Park HS, Cho MJ, Kim JO, Kim JW, et al. Screening of brain metastasis with limited magnetic resonance imaging (MRI): clinical implications of using limited brain MRI during initial staging for non-small cell lung cancer patients. *J Korean Med Sci* 2005; **20:** 121-6. doi: 10.3346/jkms.2005.20.1.121
6. Rami-Porta R, Asamura H, Goldstraw P. Predicting the prognosis of lung cancer: the evolution of tumor, node and metastasis in the molecular age-challenges and opportunities. *Transl Lung Cancer Res* 2015; **4:** 415-23. doi: 10.3978/j.issn.2218-6751.2015.07.11
7. Huang A, Li R, Zhao J, Wang X, Jin B, Niu Y, et al. Epidermal growth factor receptor (EGFR)-tyrosine kinase inhibitors combined with chemotherapy in first-line treatment in an advanced non-small cell lung cancer patient with EGFR sensitive mutation. *Thorac Cancer* 2016; **7:** 614-8. doi: 10.1111/1759-7714.12364
8. Park HJ, Oh HJ, Kim KH, Kim TO, Park CK, Shin HJ, et al. Quantification of epidermal growth factor receptor (EGFR) mutation may be a predictor of EGFR-tyrosine kinase inhibitor treatment response. *Thorac Cancer* 2016; **7:** 639-47. doi: 10.1111/1759-7714.12378
9. Reck M, Rodríguez-Abreu D, Robinson AG, Hui R, Csőszi T, Fülöp A, et al. Pembrolizumab versus chemotherapy for PD-L1-positive non-small-cell lung cancer. *N Engl J Med* 2016; **375:** 1823-33. doi: 10.1056/NEJMoa1606774
10. Eberhardt WEE, Mitchell A, Crowley J, Kondo H, Kim YT, Turrisi A 3rd, et al. The IASLC Lung Cancer Staging Project Proposals for the revision of the M descriptors in the forthcoming eighth edition of the TNM classification of lung cancer. *Thorac Oncol* 2015; **10:** 1515-22. doi: 10.1097/JTO.0000000000000673
11. Stanic K, Zwitter M, Hitij NT, Kern I, Sadikov A, Cufer T. Brain metastases in lung adenocarcinoma: impact of EGFR mutation status on incidence and survival. *Radiol Oncol* 2014; **48:** 173-83. doi: 10.2478/raon-2014-0016
12. Soria JC, Tan DSW, Chiari R, Wu YL, Paz-Ares L, Wolf J, et al. First-line ceritinib versus platinum-based chemotherapy in advanced ALK-rearranged non-small-cell lung cancer (ASCEND-4): a randomised, open-label, phase 3 study. *Lancet* 2017; **389:** 917-29. doi: 10.1016/S0140-6736(17)30123-X
13. Duruisseaux M, Besse B, Cadranel J, Pérol M, Mennecier B, Bigay-Game L, et al. Overall survival with crizotinib and next-generation ALK inhibitors in ALK-positive non-small-cell lung cancer (IFCT-1302 CLINALK): a French nationwide cohort retrospective study. *Oncotarget* 2017; **8:** 21903-17. doi: 10.18632/oncotarget.15746
14. Soria JC, Ohe Y, Vansteenkiste J, Reungwetwattana T, Chewaskulyong B, Lee KH, et al. Osimertinib in untreated EGFR-mutated advanced non-small-cell lung cancer. *N Engl J Med* 2018; **378:** 113-25. doi: 10.1056/NEJMoa1713137
15. Lee CK, Man J, Lord S, Cooper W4, Links M, Gebski V, et al. Clinical and molecular characteristics associated with survival among patients treated with checkpoint inhibitors for advanced non-small cell lung carcinoma: a systematic review and meta-analysis. *JAMA Oncol* 2018; **4:** 210-16. doi: 10.1001/jamaoncol.2017.4427
16. Kaderbhaï C, Tharin Z, Ghiringhelli F. The role of molecular profiling to predict the response to immune checkpoint inhibitors in lung cancer. *Cancers (Basel)* 2019; **11:** E201. doi: 10.3390/cancers11020201
17. Kaplan EL, Paul Meier. Nonparametric estimation from incomplete observations. *Journal of the American Statistical Association* 1958; **53:** 457-81.
18. Rami-Porta R, Goldstraw P. Strength and weakness of the new TNM classification for lung cancer. *Eur Respir J* 2010; **36:** 237-9. doi: 10.1183/09031936.00016210
19. Doroshow DB, Herbst RS. Treatment of advanced non-small cell lung cancer in 2018. *JAMA Oncol* 2018; **4:** 569-70. doi: 10.1001/jamaoncol.2017.5190
20. Hendriks LE, Derks JL, Postmus PE, Damhuis RA, Houben RM, Troost EG, et al. Single organ metastatic disease and local disease status, prognostic factors for overall survival in stage IV non-small cell lung cancer: results from a population-based study. *Eur J Cancer* 2015; **51:** 2534-44. doi: 10.1016/j.ejca.2015.08.008
21. National Comprehensive CancerNetwork. Non-small cell lung cancer. National Comprehensive Cancer Network Guidelinese. v.5. 2018. [cited 2018 Jul 25]. Available at: http://www.nccn.org/professionals/physician_gls/pdf/nscl.pdf
22. Novello S, Barlesi F, Califano R, Cufer T, Ekman S, Levra MG, et al. Metastatic non-small-cell lung cancer: ESMO Clinical Practice Guidelines for diagnosis, treatment and follow-up. *Ann Oncol* 2016; **27(Suppl 5):** v1-27, 2016. doi: 10.1093/annonc/mdw326
23. Folkert MR, Timmerman R. Review of treatment options for oligometastatic non-small cell lung cancer. *Clin Adv Hematol Oncol* 2015; **13:**186-93. PMID: 26352427
24. Sperduto PW, Yang TJ, Beal K, Pan H, Brown PD, Bangdiwala A, et al. Estimating survival in patients with lung cancer and brain metastases: an update of the graded prognostic assessment for lung cancer using molecular markers (Lung-molGPA). *JAMA Oncol* 2017; **3:** 827-31. doi: 10.1001/jamaoncol.2016.3834
25. Miyaji N, Miki T, Itoh Y, Shimada J, Takeshita T, Churei H, et al. Radiotherapy for adrenal gland metastasis from lung cancer: report of three cases. *Radiat Med* 1999; **17:** 71-5. PMID: 10378656
26. Pardo Aranda F, Larrañaga Blanc I, Rivero Déniz JR, Trujillo JC, Rada Palomino A, García-Olivares E, et al. Surgical treatment of lung cancer with synchronous adrenal metastases: adrenalectomy first. *Cir Esp* 2017; **95:** 97101. doi: 10.1016/j.ciresp.2017.01.003
27. Kratz JR, Haro GJ, Cook NR, He J, Van Den Eeden SK, Woodard GA, et al. Incorporation of a molecular prognostic classifier improves conventional non-small cell lung cancer staging. *J Thorac Oncol* 2019; **14:** 1223-32. doi: 10.1016/j.jtho.2019.03.015

research article

Factors affecting voice quality in early glottic cancer before and after radiotherapy

Jana Mekis[1], Primoz Strojan[1,2], Irena Hocevar Boltezar[1,3]

[1] Faculty of Medicine, University of Ljubljana, Ljubljana, Slovenia
[2] Institute of Oncology Ljubljana, Ljubljana, Slovenia
[3] University Department of Otorhinolaryngology and Cervicofacial Surgery, University Medical Centre, Ljubljana, Slovenia

Radiol Oncol 2019; 53(4): 459-464.

Received 25 August 2019
Accepted 17 September 2019

Correspondence to: Prof. Irena Hočevar Boltežar, M.D., Ph.D., University Department of Otorhinolaryngology and Cervicofacial Surgery, Zaloška cesta 2, 1000 Ljubljana, Slovenia; Phone: +386 41 958 336; Fax: +386 1 522 41 08; E-mail: boltezar.irena@gmail.com or irena.hocevar-boltezar@mf.uni-lj.si

Disclosure: No potential conflicts of interest were disclosed.

Background. Radiotherapy (RT) is a successful mode of treatment for early glottic cancer. The aim of the study was to assess voice quality both before and 3 months after successful RT using multimodal methods while also identifying the factors affecting it.

Patients and methods. In 50 patients with T1 glottic carcinoma, the subjective (patients' assessment of voice quality [VAS], Voice Handicap Index [VHI] questionnaire, phoniatricians' assessment using the grade/roughness/breathiness [GRB] scale), and objective assessments (fundamental laryngeal frequency [F_0], jitter, shimmer, maximum phonation time [MPT]) of voice quality were performed before RT and 3 months post-RT. The data on gender, age, extent of the tumors, biopsy types, smoking, local findings, and RT were obtained from the medical documentation.

Results. Three months after the treatment, VAS, VHI, G and R scores, F_0, and MPT significantly improved in comparison with their assessment prior to treatment. Before the treatment, the involvement of the anterior commissure significantly deteriorated jitter ($p = 0.044$) and the involvement of both vocal folds deteriorated jitter ($p = 0.003$) and shimmer ($p = 0.007$). After the RT, F_0 was significantly higher in the patients with repeated biopsy than in the others ($p = 0.047$). In patients with post-RT changes, the B score was significantly higher than in those without post-RT changes ($p = 0.029$).

Conclusions. Voice quality already significantly improved three months after the treatment of glottic cancer. The main reason for the decreased voice quality prior to treatment is the tumor's extent. Post-RT laryngeal changes and repeated biopsies caused more scarring on vocal folds adversely influencing voice quality after the treatment.

Key words: glottic cancer; radiotherapy; subjective assessment; acoustic analysis; aerodynamic measurement

Introduction

Radiotherapy (RT) and transoral endoscopic laser surgery are the treatments of choice for early (T1N0M0) glottic cancer.[1,2] In these cases, the aim of treatment is not only the eradication of the tumor, but also the preservation of larynx functions.[3] The choice between the two treatment options should be adjusted for each patient based on tumor characteristics, her/his medical condition and personal preferences, anticipated treatment morbidity with their quality of voice as the priority, and, additionally, based on costs.[2] Even though the studies showed that RT is more expensive than endoscopic laser surgery, RT still remains the preferred treatment modality in many oncological centres due to the presumably better voice quality outcome.[1,4,5] Voice quality has a significant effect on patients' quality of life as it plays an important role in patients' communication with others.[6] It also defines the time when the patient is unable to work, especially for those who use their voice in their profession. Therefore, it is important for them to have good voice quality as soon as possible following treatment.

There are several factors that influence the voice outcome following the RT treatment. Such factors include smoking during and after the treatment, talking during the treatment, the type and extent of the biopsy, extent and depth of the invasion of the tumor, the patient's age, total radiation dose and its distribution in the larynx, RT fractionation pattern, and also RT-related side effects such as oedema and fibrosis.[7-10] Different subjective and objective methods are available for the assessment of voice quality.[3] There are almost no studies focusing on the early improvement of one's voice following RT treatment.

The aims of the present study were: (i) to assess changes in voice quality three months after RT using subjective and objective methods of evaluation; (ii) to identify possible factors influencing voice quality before and after the treatment of early glottic cancer.

Patients and methods

Patients

In the prospective study, 77 consecutive patients who had been diagnosed at a tertiary centre between 2006–2012 with glottic squamous cell carcinoma of stage T1N0M0 and who had been treated with curative-intent RT were included. All patients signed written informed consent after receiving detailed information concerning the study and related examinations. In three patients, a local recurrence was diagnosed during a follow-up, and 24 patients did not attend all planned follow-up visits. Therefore, the study group consisted of 50 patients.

The characteristics of patients with information about smoking, the extent of tumors in the glottis, vocal fold closure during phonation, biopsy types (punch mucosal biopsy or deep excisional biopsy, possible repeated biopsy), and RT details were collected from the medical documentation. After treatment, patients were followed-up at 3 months in order to assess the improvement of their voices and the handicaps related to their voice qualities.

Radiotherapy

All the patients were treated with RT in the supine position and immobilized with a thermoplastic mask. They were irradiated with a continuous-course irradiation using one daily fraction of 2.25 Gy up to the median total dose of 63 Gy (range, 58.5–65.25 Gy; all but 5 patients received 63 Gy), delivered over 36 to 49 days (median, 39 days; mean 39.82 ± 2.56 days). MV photon beams and computer-generated dosimetry were employed in all patients. The dose was prescribed to a planning target volume (PTV) encompassing involved vocal cord(s) with ipsilateral arytenoid(s), the parapharyngeal space, and anterior commissure, up to the most cranial extent of the arytenoid cartilage superiorly and 1–1.5 cm below the level of the true vocal cord inferiorly.

Evaluation of laryngeal function and voice quality

The examinations were performed before RT and 3 months after irradiation.

Subjective phoniatrician's and patient's evaluation

A perceptive analysis of voice quality during spontaneous speech by a phoniatrician was performed using the GRB score (grade [G], roughness [R], breathiness [B]; graded from 0 to 3 [0 = not present, 3 = severe disorder]) before and three months after the treatment.

Patients assessed their voice quality according to the visual analogue scale (VAS, from 0 to 100%). They also completed the Voice Handicap Index questionnaire (VHI), which is showing the influence of the patients' voice on their lives.[12] A score above 18 was considered characteristic for a clinical voice disorder.[13]

In order to evaluate the post-radiation mucosal changes (tissue defects, atrophy, fibrosis, oedema; graded from 0 to 3 [0 = no changes, 3 = severe changes]), closure between the vocal folds (complete, incomplete), and the mobility of the vocal folds (normal, impaired, immobile), a stroboscopy was performed 3 months after the RT.

Objective acoustic analysis of voice samples and aerodynamic measurement

An acoustic analysis of three samples of the vowel /a/ at the most comfortable pitch and volume, employing the Multi-Dimensional Voice Program (KayPentax®, USA), along with a measurement of the maximum phonation time (MPT) were performed. The mean values of fundamental frequency ($F_{0,}$ Hz), pitch perturbation (jitter, %) and amplitude perturbation (shimmer, %) of all three voice samples were used for further analysis.

Ethical consideration and statistics

The study protocol was in accordance with the Helsinki declaration and requirements accepted by the Republic of Slovenia National Medical Ethics Committee. Analyses were performed using the SPSS version 22.0 (SPSS Inc., Chicago, IL, USA). All statistical tests were two-sided and a p-value of ≤ 0.05 was considered statistically significant.

The results of the perceptive assessment of the patient's and phoniatrician's voice, VHI questionnaires, the acoustic analysis of voice samples, and MPT were compared both pretreatment and three months after RT. The normality testing of numerical data was done by the Shapiro-Wilk test, which was presented as mean ± standard deviation (SD) or as median (range). For a paired comparison of numerical data, the paired t-test or non-parametric Wilcoxon signed-rank test was employed. The relationship between certain factors (smoking before and after treatment, the extent of the tumor, involvement of anterior commissure, type of biopsy, repeated biopsy, post-radiation mucosal changes), the results of subjective evaluations (VAS, VHI, GRB scores), the objective measurements (F_0, jitter, shimmer, MPT), t-test or non-parametric Mann Whitney test, and the bivariate correlation (age) were used.

Results

In the study group, there were 44 men and 6 women, between 32 and 85 years of age. Ten patients were under 56 years of age and 21 subjects were under 61 years of age. The tumor was limited to one vocal fold in 40 patients. In seven cases, the anterior commissure was involved. Data on type of biopsy was not available for one patient. The patients' characteristics are shown in Table 1.

Before treatment, 30 patients were active smokers and 12 patients stopped smoking more than 6 months before the beginning of treatment. Four patients did not answer the question about smoking. See Table 1. After the treatment, only two patients were still smoking.

The patients' assessment of voice quality on VAS and the results of VHI were significantly improved three months after the treatment in comparison to their evaluations before treatment. Before treatment, all the patients had hoarse voices according to the phoniatrician's assessment (G > 0). After the treatment, the phoniatrician's assessment of G and R also showed significantly better voice quality (Table 2).

TABLE 1. Characteristics of the patients in the study (N = 50)

Patients' characteristic	Data
Gender (male/female)	44 / 6
Age (mean/standard deviation, years)	62.48 ± 9.99
Smoking (before treatment)	
- non-smokers	4
- smokers	30
- ex-smokers*	12
- unknown	4
Type of biopsy	
- punch biopsy	13
- excisional biopsy	36
- unknown	1
Repeated biopsy	15
Glottic cancer	
- one vocal fold	40
- both vocal folds	10
- anterior commissure involvement	7

* patients stopped smoking more than 6 months before the beginning of the treatment

TABLE 2. Comparison of the subjective and objective assessments of vocal fold function and voice quality (N = 50)

Parameter	Before treatment (mean / SD)	3 months after treatment (mean / SD)	P
Subjective phoniatrician's assessment			
- Grade Score	1.95 / 0.71	1.35 / 0.61	0.000
- Roughness Score	1.91 / 0.71	1.28 / 0.63	0.000
- Breathiness Score	0.05 / 0.21	0.02 / 0.15	0.324
Patient's assessment of voice quality (VAS; %)	44.67 / 22.37	70.54 / 24.22	0.000
Voice Handicap Index Score	49.67 / 30.09	22.46 / 23.56	0.000
Post-radiation mucosa changes			
- not present	/	2	
- slight	/	40	
- moderate	/	2	
- not assessed	/	6	
Vocal folds' mobility			
- normal	50	47	
- impaired		3	
Vocal fold closure			
- complete	1	8	
- incomplete	49	35	
- not assessed		7	0.036
F_0 (Hz)	187.63 / 80.38	152.71 / 32.46	0.000
Jitter (%)	3.79 / 3.47	2.84 / 4.11	0.148
Shimmer (%)	7.98 / 5.79	6.64 / 5.17	0.178
Maximum phonation time (s)	14.06 /7.21	18.98 / 7.8	0.032

F_0 = fundamental laryngeal frequency

At three months post-RT, the post-radiation mucosal changes of the vocal folds were seen in all but two patients (Figures 1 and 2). In six patients, an assessment of the vocal cords was not possible because of an adduction of the ventricular folds above them during phonation. The vocal fold closure became complete in 7 patients after the successful treatment of glottic cancer (Table 2).

After RT, the mean F_0 decreased to a more acceptable value regarding gender. The perturbation of pitch (jitter) and amplitude (shimmer) became lower, exhibiting less voice instability although, compared to pre-RT values, the difference was not significant. Also, MPT was found significantly longer after RT (Table 2).

Three months after the RT treatment, the patients expressed considerable satisfaction with their voices as 26 (52%) of them had VHI score less than 19 compared to only 9 (18%) patients with a VHI score less than 19 during their pre-RT evaluation (p = 0.000). Twenty (40%) patients assessed their voice quality as 80% of a normal voice or higher. On the other hand, the phoniatrician perceptively detected normal voice (G score = 0) in only 2 patients after therapy. In all patients, at least one of the objective parameters of voice quality (F_0, jitter, shimmer, MPT) remained abnormal.

The relationship between different factors with a possible impact on voice quality (i.e. gender, age, extent of the tumor, involvement of the anterior commissure, type of biopsy, repeated biopsy, smoking before and after therapy, post-radiation mucosal changes, impaired vocal fold mobility, incomplete vocal fold closure during vibration) and their influence on the subjective and objective parameters of voice assessment (VAS, VHI, GRB, F_0, jitter, shimmer, MPT) before and 3 months after RT were also analysed. Only the statistically significant differences are presented in Table 3. Age, type of biopsy, and smoking did not significantly affect the results of subjective and objective voice quality evaluations and laryngeal function.

TABLE 3. Significant associations between some factors possibly affecting voice quality and the results of the subjective and objective vocal quality assessment in patients with early glottis cancer (N = 50)

Parameter	Present (mean/ SD)	Not present (mean/ SD)	P
Gender			
- F_0 before therapy (male)	178.91 / 45.05		
- F_0 before therapy (female)		240.17 / 44.48	0.001
- F_0 after therapy (male)	145.00 / 25.20		
- F_0 before therapy (female)		209.80 / 21.41	0.000
Anterior commissure involvement			
- jitter before therapy	5.39 / 2.74	3.52 / 3.53	0.044
Tumor on both vocal folds			
- jitter before therapy	7.21 / 5.91	3.02 / 2.07	0.003
- shimmer before therapy	12.74 / 6.91	7.18 / 5.02	0.007
Repeated biopsy			
- F_0 after therapy	200.60 / 46.77	182.94 / 51.96	0.047
Post-radiation changes			
- maximum phonation time after therapy	18.39 / 7.55	30.00 / 2.82	0.039
- Breathiness score after therapy	0.02 / 0.15	0	0.029
Complete vocal fold closure during phonation			
- maximum phonation time after therapy	25.29 / 8.71	17.84 / 7.04	0.000

F_0 = fundamental laryngeal frequency

Discussion

In the present study, a significant improvement of voice quality was found three months after RT treatment for early glottic cancer when assessed subjectively by the patients (VAS, VHI) and by the phoniatrician (GR scale) or by objective methods (F0, MPT). After successful treatment, more than one half of the patients (52%) demonstrated VHI scores typical for subjects without voice problems. However, normal voice quality was only detected in two patients by the phoniatrician's perceptive evaluation.

We evaluated voice quality through several subjective and objective methods. The patient's subjective assessments showed more favourable results than the phoniatrician's and the objective ones. Still, the subjective evaluations showed more improvement than the objective ones. One of the reasons could be the methodology of acoustic analysis and aerodynamic measurements. In both cases, only voice samples are assessed, whereas the patient (or phoniatrician) evaluates voices during everyday communication and not just voice samples.

We noticed a significant improvement in the G and R components of the GRB evaluation recorded by the phoniatrician at three months post-RT. Marciscano *et al*. report a significant improvement in voice quality according to the GRBAS composite score across the first four months after the RT.[14] In our study, we only decided to carry out the assessment of the individual parameters, G, R, and B. Therefore, a complete comparison with Marciscano's study cannot be done as we can merely compare trends in the change of individual parameters. In any case, both studies are among a few, rare studies that assessed voice quality in the first months following the end of the RT.

According to the patients' assessment, voice quality on VAS significantly improved after RT.

40% of the patients assessed their voice as 80% of a normal voice or even better. The VHI after RT gave even better results. More than one half of the patients (52%) gained a score of 18 or lower. In a review paper of several translations of VHI in different languages, the values between 12 and 20 were found as cut-off points to distinguish between subjects with normal and pathological voices. The authors suggest that any VHI value above 18 is a sign of strong possibility of a clinical voice problem.[13] According to this recommendation, we decided to choose 19 points as the cut-off point. Despite favourable patient assessments of voice quality and its impact on their handicaps in their every-day lives, the phoniatrician detected normal voices in only two patients. We believe that the patients valuated their post-RT voice in comparison with the voice before the treatment. The phoniatrician tried to assess voices according to the accepted standards without being influenced by or without experience of the handicap of the pre-treatment voice quality.

The cause for a hoarse voice in a patient with early vocal fold cancer is the tumor itself. It disables normal vocal fold vibration and the completeness of the closure between them. Tumors affecting both vocal folds and/or anterior commissure cause more irregular vibrations of vocal folds and a less stable voice (increased jitter and shimmer). Following successful RT, the tumor disappears, which results in the scarring of the affected vocal fold; the mucosa of one or both vocal folds can become atrophic and/or swollen. The fibrotic transformation of tissues only at the site of the previous tumor or larger part/whole larynx with post radiation changes to the laryngeal joints, muscles, and nerves can result in the progressive impairment of mobility of one or both vocal folds.[15-17] In our study, videoendostroboscopies showed post-radiation changes in all but two patients and impaired mobility of the affected vocal fold(s) was detected in three patients. Other authors also reported changes in the vocal folds' mobility after RT for early glottis cancer. Marciscano *et al*. found a significant improvement in the mobility and vibration of the ipsilateral vocal cord and a significant worsening in the contralateral vocal cord more than four months after treatment.[14]

The vocal fold closure was only complete in one patient before therapy. After the tumor disappeared from the glottis, the closure became complete in eight patients. The mass of the vocal folds with tumors decreased and more regular and symmetrical vibration was possible. The phonation demanded less effort and less activation of the laryngeal muscles. These are likely the main reasons for the improvements in voice quality. The F_0 decreased as less tension in the laryngeal muscles was necessary for phonation. The perturbation of pitch and amplitude decreased but these changes did not reach a level of statistical significance. Nevertheless, the post-radiation changes (fibrosis, atrophy, oedema, decreased mobility) appeared in a high proportion of irradiated patients and negatively influenced voice quality. In those patients with repeated biopsies during the diagnostic phase, the scarring was even more prominent thus causing thinner vocal folds which vibrated with higher frequency (higher F_0). We expect that in these patients' post-radiation, changes will continue to influence voice quality over the following months.

In our group, before the treatment, the mean F_0 for men was higher (almost 179 Hz) than the reported normal range (80-160 Hz).[18] After treatment, it decreased to a normal range (145 Hz). In women, F_0 also decreased after RT but the values remained within normal range (i.e. before and after the treatment). On the contrary, Lombardo *et al*. reported no statistically significant difference in F_0 after RT treatment.[19] The impact of gender on F_0 before and after therapy is expected and related to anatomical characteristics of the larynx.[6]

In the present study, jitter and shimmer showed a pathological instability of the voice in all the patients with glottic cancer. After the successful treatment, the values remained above normal thresholds.[18] Van Gogh *et al*. objectively assessed the voice outcome in 39 patients with T1 glottic cancer before and up to 2 years after RT. Three months after the treatment, F_0 significantly decreased in comparison with the values before treatment and jitter and shimmer showed a significant improvement.[20] The exact values of jitter and shimmer cannot be compared between the two groups of patients because a different instrument was used in our study.

In addition, a significant improvement in the MPT was found in our patients 3 months after RT completion. The reason was the better closure of vocal folds during phonation. The breathy vocal characteristic was also a consequence of the incomplete vocal fold closure. Wagmare *et al*. also reported an improvement of MPT in patients after RT for early glottic cancer, but the observation time was significantly longer in his group than in ours.[8]

One fifth of our patients was under the age of 56 and one third under the age of 61. This means that they were still professionally active at the time of diagnosis and treatment. From the patients' point

of view, it is very important that their voices improve soon after the completion the treatment, allowing them to return to work. Three months after RT, more than one half of the patients had VHI below 19, a cut-point discriminating between normal and pathological voices. In any case, this also means that more than one half of the patients did not feel handicapped by their voice quality. Due to an abnormal voice quality in a great majority of the patients (according to G score) found by the phoniatrician, we suppose that performing professions with higher voice load or demands for higher voice quality would not be possible. We did not have information about the professional voice use of our patients.

The shortcomings of our study are that all of the instrumental examinations could not be performed on all included patients, although this was due to objective reasons. Still, we succeeded in completing them in at least 85% of the patients. Furthermore, we did not consider the role of RT-related parameters to the voice quality as the total dose and fractionation pattern were rather comparable in all patients. Having information concerning the profession of the patients would also have given us better insight in their capabilities to return to work three months after the RT treatment.

Conclusions

Voice disorders have an adverse impact on the social and professional life of patients and reduce the quality of their lives. The main reasons for a decrease in voice quality before treatment is the tumor mass affecting vocal fold mobility and causing the irregular free edge of the affected vocal fold. After successful treatment, the tumor disappears and enables more normal, regular and symmetrical vibrations, with more complete vocal fold closure as well as requiring less effort during phoniation. These are the reasons for significant improvements in voice quality three months after the completion of RT. Unfortunately, post-radiation scarring also affects the vocal folds' vibration and negatively influences the voice quality. However, more than one half of the patients in our study expressed minimal voice handicap three months after RT for early glottic cancer, which is particularly important for those patients who are still professionally active.

References

1. Peeters AJ, van Gogh CD, Goor KM, Verdonck-de Leeuw IM, Langendijk JA, Mahieu HF. Health status and voice outcome after treatment for T1a glottic carcinoma. *Eur Arch Otorhinolaryngol* 2004; **261:** 534-40. doi: 10.1007/s00405-003-0697-5
2. Mendenhall WM, Takes RP, Shah JP, Bradley PJ, Beitler JJ, Strojan P, et al. Current treatment of T1N0 squamous cell carcinoma of the glottic larynx. *Eur Arch Otorhinolaryngol* 2015; **272:** 1821-4. doi: 10.1007/s00405-014-3388-5
3. Agrawal N, Ha PK. Management of early-stage laryngeal cancer. *Otolaryngol Clin North Am* 2008; **41:** 757-69. doi: 10.1016/j.otc.2008.01.014
4. Huang G, Luo M, Zhang J, Liu H. The voice quality after laser surgery versus radiotherapy of T1a glottic carcinoma: systematic review and meta-analysis. *Onco Targets Ther* 2017; **10:** 2403-10. doi: 10.2147/OTT.S137210
5. Lee SH, Hong KH, Kim JS, Hong YT. Perceptual and acoustic outcomes of early-stage glottic cancer after laser surgery or radiotherapy. A meta-analysis. *Clin Exp Otorhinolaryngol* 2019; **12:** 241-8. doi: 10.21053/ceo.2018.00990
6. Aronson AE. *Clinical voice disorders. An interdisciplinary approach*. 3rd Edition. New York: Thieme Inc.; 1990.
7. Hocevar-Boltezar I, Zargi M, Strojan P. Risk factors for voice quality after radiotherapy for early glottic cancer. *Radiother Oncol* 2009; **93:** 524-9. doi: 10.1016/j.radonc.2009.09.014
8. Waghmare CM1, Agarwal J, Bachher GK. Quality of voice after radiotherapy in early vocal cord cancer. *Expert Rev Anticancer Ther* 2010; **10:** 1381-8. doi: 10.1586/era.10.126
9. Verdonck-de Leeuw IM, Hilgers FJ, Keus RB, Koopmans-van Beinum FJ, Greven AJ, de Jong JM, et al. Multidimensional assessment of voice characteristics after radiotherapy for early glottic cancer. *Laryngoscope* 1999; **109:** 241-8. doi: 10.1097/00005537-199902000-00014
10. Al-Mamgani A, van Rooij PH, Woutersen DP, Mehilal R, Tans L, Monserez D, et al. Radiotherapy for T1-2N0 glottic cancer: a multivariate analysis of predictive factors for the long-term outcome in 1050 patients and a prospective assessment of quality of life and voice handicap index in a subset of 233 patients. *Clin Otolaryngol* 2013; **38:** 306-12. doi: 10.1111/coa.12139
11. Barsties B, De Bodt M. Assessment of voice quality: Current state-of-the-art. *Auris Nasus Larynx* 2015; **42:** 183-8. doi: 10.1016/j.anl.2014.11.001
12. Jacobson BH, Johnson A, Grywalski C, Silbergleit A, Jacobson G, Benninger MS, et al. The voice handicap index (VHI): development and validation. *Am J Speech Lang Pathol* 1997; **6:** 66-70. doi: 10.1044/1058-0360.0603.66
13. Tafiadis D, Chronopoulos SK, Helidoni ME, Kosma EI, Voniati L, Papadopoulos P, et al. Checking for voice disorders without clinical intervention: The Greek and global VHI thresholds for voice disordered patients. *Sci Rep* 2019; **9:** 9366. doi: 10.1038/s41598-019-45758-z
14. Alexander FW. Micropathology of radiation reaction in the larynx. *Ann Otol Rhinol Laryngol* 1963; **72:** 831-41. doi: 10.1177/000348946307200316
15. Tedla M, Valach M, Carrau RL, Varga I, Profant M, Mráz P, et al. Impact of radiotherapy on laryngeal intrinsic muscles. *Eur Arch Otorhinolaryngol* 2012; **269:** 953-8. doi: 10.1007/s00405-011-1686-8
16. Rubin P, Casarett GW. *Clinical radiation pathology*. Philadelphia: W.B. Saunders Company; 1968. p. 36-61.
17. Marciscano AE, Charu V, Starmer HM, Best SR, Quon H, Hillel AT, et al. Evaluating post radiotherapy laryngeal function with laryngeal videostroboscopy in early stage glottic cancer. *Front Oncol* 2017; **7:** 124. doi: 10.3389/fonc.2017.00124
18. Colton RH, Casper JK. *Understanding voice prob*lems. A physiological perspective for diagnosis and treatment. Fourth Edition. Baltimore: Lippincott, Williams and Wilkins; 2006.
19. Lombardo N, Aragona T, Alsayyad S, Pelaia G, Terracciano R, Savino R. Objective and self-evaluation voice analysis after transoral laser cordectomy and radiotherapy in T1a-T1b glottic cancer. *Lasers Med Sci* 2018; **33:** 141-7. doi: 10.1007/s10103-017-2361-0
20. Van Gogh CD, Verdonck-de Leeuw IM, Wedler-Peeters J, Langedijk JA, Mahieu HF. Perspective evaluation of voice outcome during the first two years in male patients treated by radiotherapy or laser surgery for T1a glottis carcinoma. *Eur Arch Otorhinolaryngol* 2012; **269:** 1647-52. doi: 10.1007/s00405-012-1947-1

research article

Total neoadjuvant treatment of locally advanced rectal cancer with high risk factors in Slovenia

Mojca Tuta[1], Nina Boc[1], Erik Brecelj[2], Mirko Omejc[4], Franc Anderluh[3], Ajra Secerov Ermenc[3], Ana Jeromen Peressutti[3], Irena Oblak[3], Bojan Krebs[5], Vaneja Velenik[3]

[1] Division of Radiology, Institute of Oncology, Ljubljana, Slovenia
[2] Division of Surgery, Institute of Oncology, Ljubljana, Slovenia
[3] Division of Radiotherapy, Institute of Oncology, Ljubljana, Slovenia
[4] Division of Surgery, University Medical Centre Lubljana, Ljubljana, Slovenia
[5] Division of Surgery University Medical Centre Maribor, Maribor, Slovenia

Radiol Oncol 2019; 53(4): 465-472.

Received 1 July 2019
Accepted 13 August 2019

Correspondence to: Assoc. Prof. Vaneja Velenik, M.D., Ph.D., Institute of Oncology Ljubljana, Zaloška cesta 2, SI-1000 Ljubljana, Slovenia.
E-mail: vvelenik@onko-i.si

Disclosure: No potential conflicts of interest were disclosed.

Background. In the light of a high rate of distant recurrence and poor compliance of adjuvant chemotherapy in high risk rectal cancer patients the total neoadjuvant treatment was logical approach to gaining acceptance. We aimed to evaluate toxicity and efficiency of this treatment in patients with rectal cancer and high risk factors for local or distant recurrence.

Patients and methods. Patients with rectal cancer stage II and III and with at least one high risk factor: T4, presence of extramural vein invasion (EMVI), positive extramesorectal lymph nodes or mesorectal fascia (MRF) involvement were treated with four cycles of induction CAPOX/FOLFOX, followed by capecitabine-based radiochemotherapy (CRT) and two consolidation cycles of CAPOX/FOLFOX before the operation. Surgery was scheduled 8–10 weeks after completition of CRT.

Results. From November 2016 to July 2018 66 patients were evaluable. All patients had stage III disease, 24 (36.4%) had T4 tumors, in 46 (69.7%) EMVI was present and in 47 (71.2%) MRF was involved. After induction chemotherapy, which was completed by 61 (92.4%) of patients, radiologic downstaging of T, N, stage, absence of EMVI or MRF involvement was observed in 42.4%, 62.1%, 36.4%, 69.7% and 68.2%, respectively. All patients completed radiation and 54 (81.8%) patients received both cycles of consolidation chemotherapy. Grade 3 adverse events of neoadjuvant treatment was observed in 4 (6%) patients. Five patients rejected surgery, 3 of them with radiologic complete clinical remissions. One patient did not have definitive surgery of primary tumor due to unexpected cardiac arrest few days after sigmoid colostomy formation. Among 60 operated patients pathological complete response rate was 23.3%, the rate of near complete response was 20% and in 96.7% radical resection was achieved. Pathological T, N and stage downstaging was 65%, 96.7% and 83.4%, respectively. Grade ≥ 3 perioperative complications were anastomotic leakage in 3, pelvic abscess in 1 and paralytic ileus in 2 patients. The rate of pathologic complete response (pCR) in patients irradiated with 3D conformal technique was 12.1% while with IMRT and VMAT it was 37% ($p < 0.05$). Hypofractionation with larger dose per fraction and simultaneous integrated boost used in the latest two was the only factor associated with pCR.

Conclusions. Total neoadjuvant treatment of high risk rectal cancer is well tolerated and highly effective with excellent tumor and node regression rate and with low toxicity rate. Longer follow up will show if this strategy will improve distant disease control and survival.

Key words: total neoadjuvant treatment; radiochemotherapy; rectal cancer; capox

Introduction

More than half of the patients with rectal cancer present with locally advanced stage of disease and are treated with combination of preoperative chemoradiotherapy (CRT) followed by total mesorectal excision (TME) and adjuvant chemotherapy with 5-fluorouracil or capecitabine with or without oxaliplatin. With this approach decreased 5 year local recurrence rates to approximately 5–10% has been observed. However, good local control did not result in better survival due to high, more than 30% rate of distant recurrence, which remains the leading cause of rectal cancer-related death.[1,2] The reason probably lies in insufficient dose of chemotherapy (ChT) prior the operation and poor compliance of patients to recieve remaining postoperative ChT needed to influence on micrometastases and prevent distant spread of the disease. Randomised trials testing intensification of preoperative treatment by adding oxaliplatin to capecitabine based CRT failed to prove significant benefit over the gold standard. Oxaliplatin significantly decreased distant failure, but did not improve overall survival (OS), disease free survival (DFS) and local failure (LF) compared to 5-fluorouracyl CRT.[3]

In the light of these unfavorable facts shifting adjuvant ChT into preoperative setting, so called the total neoadjuvant treatment (TNT), was the next logical step. In comparison with standard treatment, TNT is more effective regarding tumor regression rate, the rate of radical resections, sphincter sparing proceadures, patological complete remissions (pCR) and offers a good platform for less radical surgery or potential non-operative management in selected patients. Further, more favorable compliance and lower toxicity rate if ChT is deliverd preoperatively, allows more patients to complete the treatment according to the protocol.[4-6] Currently, there are two slightly different TNT approaches in the treatment of locally advanced rectal cancer (LARC) with high risk of local recurrence. While American National Comprehensive Cancer Network (NCCN) guidelines recommend induction 5-fluorouracyl, leucovorin and oxaliplatin (FOLFOX) or capecitabine and oxaliplatin (CAPOX) ChT followed by CRT and operation, in the northern Europe the same ChT given after short course RT as a consolidation therapy before surgery, is more prefered treatment option according to the latest guidelines from European Socienty for Medical Oncology (ESMO).[7-9]

In Slovenia, the TNT was introduced in 2016. The treatment scheme consists of four induction cycles of FOLFOX/CAPOX, capecitabine or 5-FU-based CRT and two additional cycles of FOLFOX/CAPOX as a consolidation therapy before the TME surgery. With this regimen the interval between conclusion of CRT and surgery at 8–10 weeks is preserved. At first, only the patients with T4 tumors or with the presence of EMVI or extramesorectal lymph nodes involvement on magnetic resonance imaging (MRI) were considered candidates for TNT. Later on two more indications for this treatment selection were added: N2 disease and the distance £ 1 mm of tumor or lymph nodes from mesorectal fascia (MRF).

The main objective of the present study is to evaluate efficiency and toxicity of TNT treatment in LARC with high risk factors for local or distant recurrence in Slovenia.

Patients and methods

Patient selection

This prospective observational study included all patients with newly diagnosed LARC, treated with TNT from November 2016 to July 2018. Inclusion criteria for the treatment were as follows: histologically proven rectal adenocarcinoma situated up to 15 cm from the anal verge; locally advanced disease (T3/T4 or N+) confirmed by MRI; no evidence of distant metastases on pretreatment workout; the presence of at least one high risk factor: T4, extramural vascular invasion (EMVI), positive extramesorectal lymph nodes or MRF involvement. Patients with second primary or history of carcinoma other than nonmelanoma skin cancer or cervical carcinoma in situ, inflammatory bowel disease and malabsorbtion syndrome were excluded from the analysis. The study was performed with the approval of the Ethics Committee of the Institute of Oncology Ljubljana, number ERIDEK-0014/2019 and ERID-KSOPKR-0009/2019, the National Medical Ethics Committee of the Republic of Slovenia, number 0120-298/2019/5, and in accordance with the principles of the Declaration of Helsinki. All the patients signed informed consent form before treatment.

Pretreatment evaluation

Pretreatment evaluation included the patient's medical history, physical examination, laboratory test (complete blood count, serum biochemistry, carcinoembryonic antigen), colonoscopy with biopsy, computed tomography of the chest and

abdomen and MRI of the pelvis for local staging. All patients were evaluated on a multidisciplinary meeting.

Treatment regimen

All protocol-mandated preoperative treatment was delivered at the Institute of Oncology in Ljubljana. Induction chemotherapy consisted of four cycles of capecitabine (1000 mg/m2/12h per os on days 1-14) and oxaliplatin (oxaliplatin 130 mg/m2 IV over 2h on day 1) (CAPOX regimen) every three weeks or in patients with difficulties of swallowing pills 5-fluorouracil (400 mg/m2 IV bolus on day 1 then 1200 mg/m2/day for 2 days), oxaliplatin (85 mg/m2 IV over 2 h on day 1), and leucovorin (400 mg/m2 IV over 2 h on day 1) (mFOLFOX6 regimen) every 2 weeks.

Radiotherapy was scheduled 1 week after the completion of induction chemotherapy. CT simulation and treatment were performed with the patient in the supine position with full bladder protocol. Fusion with planning MRI carried out with the patient in the treatment position was used for contouring assistance when planning MRI was available. Three-dimensional conformal radiation therapy (3D-CRT), intensity-modulated radiotherapy using simultaneously integrated boost (IMRT SIB) or volumetric modulated arc therapy (VMAT SIB) were administered. 3D-CRT included 45 Gy to the pelvis in 25 fractions followed by the boost to the tumor to the dose 50.4 Gy for T3 and to 54 Gy for T4 tumors in 3–5 fractions. IMRT SIB or VMAT SIB included pelvic dose of 41.8 Gy with SIB to the tumor to the dose 46.2 Gy for T3 and 48.4 Gy for T4 tumors in 22 fractions.[10] Concomitant chemotherapy with capecitabine was administered from the first to the last day of the radiation treatment (including weekends) at a daily dose of 825 mg/m2/12 hours if IMRT/VMAT SIB technique was used and only on RT days in case of 3D conformal RT.

During radiotherapy the patients were evaluated weekly to check out acute toxicity according to the Common Toxicity Criteria for Adverse Events (CTCAE) version 4.0 and compliance with the intended treatment plan during CRT.[11] Two cycles of consolidation ChT with CAPOX were delivered after completion of CRT. Surgery was scheduled 8–10 weeks after the end of CRT. The choice between abdominoperineal and sphincter preserving surgery was at the surgeon's discretion. No additional treatment was administered after surgery.

Endpoints

The primary endpoint was pCR. The secondary endpoints included clinical and pathological downstaging, neoadjuvant rectal (NAR) score, toxicity profile, time to stoma closure and compliance during treatment. Pathologic stage was recorded according to the American Joint Committee on Cancer (AJCC) 7th edition.[12] Tumor regression grade was recorded according to the criteria by Dworak *et al.*[13] We defined pCR as ypT0N0 (Dworak tumor regression grade 4) – the absence of residual viable tumor cells in the surgical specimen.

Statistical analysis

The clinical tumor response was analyzed by comparison of the baseline clinical MRI stage with the one obtained on restaging before the CRT and 8 weeks from the end of CRT (if it was performed). For pathological tumor response the baseline MRI was compared with pathological record of surgical specimen. Each staging component (*T, N, stage, absence of EMVI or MRF involvement*) was analyzed separately. All pre- and postreatment MRI scans were reviewed independently by one radiologist.

Statistical analysis was performed using the Statistical Package for the Social Sciences, version 26.0. (SPSS Inc, Chicago, IL).[14] Descriptive statistics were used for presenting preoperative, surgical and pathological results. Possible associations between disease or treatment negative factors and pCR were determined with the Fisher exact test. All results with a p value of < 0.05 were considered statistically significant.

Results

Patient characteristics

Between November 2016 and July 2018, 66 patients with LARC with high risk factors (LARC-HR) were included. Table 1 describes patient's demographic and baseline clinical characteristics. Median age was 59 years (range 33–74), two thirds were men. All patients had stage III disease, 24 (36.4%) had T4 tumors, in 46 (69.7%) EMVI was present and in 47 (71.2%) MRF was involved.

Treatment delivery and toxicity

Figure 1 shows patients' progress through the treatment. Induction chemotherapy was com-

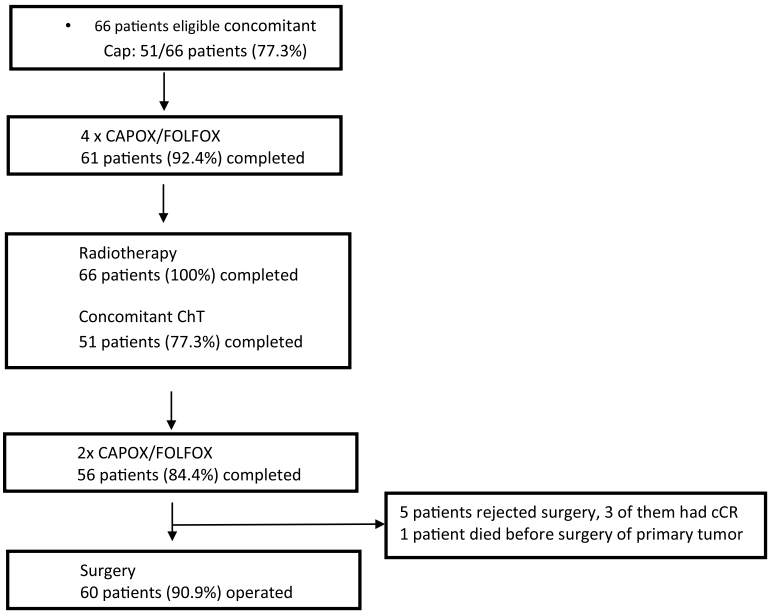

Cap = capecitabine; cCR = clinical coplete response; ChT = chemotherapy

FIGURE 1. Patients' progress through the treatment.

TABLE 1. Patient's demographic and baseline clinical characteristics (N = 66)

Characteristic	No. (66)	%
Gender		
Male	41	62.1
Female	25	37.9
Age, years		
Median, range	59, 33–74	
ECOG performance status		
0	50	75.8
1	16	24.2
Distance from the anal verge		
< 5 cm	25	37.9
5–10 cm	30	45.4
>10 cm	11	16.7
High risk factors		
cT4	24	36.4
EMVI+	46	69.7
Positive extramesorectal lgl	3	4.5
MRF+	47	71.2
cTN stage		
T2N2	1	1.5
T3N1	17	25.8
T3N2	24	36.4
T4N1	3	4.5
T4N2	21	31.8

c = clinical; ECOG = Eastern Cooperative Oncology Group; EMVI = ekstramesorectal vein invasion; MRF = mesorectal fascia; N = node; No. = number; T = tumor

TABLE 2. Acute toxicity during TNT

	Toxicity	Grade 1		Grade 2		Grade 3		Grade 5	
		N	%	N	%	N	%	N	%
During ChT	Thrombocytopenia	4	6.1	4	6.1				
	Anemia	8	12.1	2	3.0				
	Neutropenia	1	1.5	3	4.5				
	Diarrhea	4	6.1	3	4.5				
	Nausea	21	31.8	1	1.5				
	Vomiting	4	6.1	1	1.5				
	Hand-foot syndrome	7	10.6	1	1.5	1	1.5		
	Parasthesia	36	54.5	1	1.5				
During CRT	Thrombocytopenia	9	13.6	2	3.0				
	Anemia	5	7.6	3	4.5				
	Neutropenia	2	3.0	3	4.5				
	Diarrhea	22	33.3	4	6.1	1	1.5		
	Nausea	7	10.6						
	Cystitis	22	33.3	3	4.5				
	Proctitis	8	12.1	3	4.5				
	Dermatitis	5	7.6	5	7.6	2	3.0		
	Hand-foot syndrome	5	7.6	3	4.5				

ChT = chemotherapy; CRT = chemoradiotherapy

pleted by 61 (92.4%) of patients. All patients completed radiation and 77.3% received a full dose of concomitant capecitabine. In others the dose of capecitabine was modified, mainly due to hematological toxicities. Fifty-six (84.8%) patients received both cycles of consolidation chemotherapy. All 6 cycles of CAPOX/FOLFOX were given to 55 (83.3%) patients. Among them only 5/55 patients recevied ChT at modified dose. All planned doses of neoadjuvant ChT and TNT according to the protocol received 77.2% and 60.6% of patients, respectively.

Acute toxicity was assessed in all 66 patients. Data are shown in Table 2. During TNT, 22.7% of patients did not report any toxicity or it was not observed. The most frequent all-grade toxicities during induction and consolidation ChT were neurotoxicity and nausea, observed in 56% and 33.3% of patients, respectively. The most common haematological toxicity was anemia presented in 10 (15.1%) patients. Hematological and other gastrointestinal toxicities were mainly gradus 1. There was only one grade 3 toxicity, hand-foot syndrome.

All patients completed radiation therapy with the median interruption of 2 days due to hollidays and machine maintenance in 36 (54.5%) of them. The 3D conformal, IMRT SIB or VMAT SIB tech-

nique was used in 36 (54.5%), 17 (25.8%) and 13 (19.7%) patients, respectively. The most frequent all-grade CRT-related toxicities were diarrhea (39.4%) and radiation cystitis (37.8%). Similar to that observed during ChT period, gastrointestinal and hematological toxicities were mainly grade 1. Only three grade 3 toxicities were recorded (diarrhea in one and radiation dermatitis in two patients). During CRT thrombocytopenia (16.6%) was the most common adverse hematological event.

Surgery

Sixty (90.9%) patients underwent standard TME surgery or surgery beyond the TME planes. One patient underwent transanal TME, 40 patients underwent low anterior resection, 5 patients underwent anterior resection, 13 patients underwent abdominoperineal excision (APE) and 1 patient underwent total pelvic exenteration. Median time from the end of CRT to operation was 11 weeks (range 7–19). In 76.7% of them sphincter preserving procedure was performed. For the tumors in the lower third of rectum the rate of abdominoperineal amputations was 33%. Among 3 patients with clinically positive extramesorectal lymph nodes 1 patient, who underwent APE, had cancer cells present microscopically at the resection margin (R1), 1 patient who underwent anterior resection had pCR and 1 patient who underwent low anterior resection had pT3N2. One patient did not have definitive surgery of primary tumor due to unexpected cardiac arrest after one cycle of consolidation ChT and three days after sigmoid colostomy formation because of perineal infection in peripheral hospital. Five patients refused surgery, 3 of them with radiologic cCR of the tumor.

In 75% of patients no perioperative complications were noticed. The most common grade ≥ 3 perioperative complications were anastomotic leakage in 3, pelvic abscess in 1 and paralytic ileus in 2 patients. The most frequent all-grade-surgery-related toxicity was wound dehiscence (8.3%). Data on time to stoma closure was available for 29/37 patients with sphincter sparing procedure. Median time was 134 days (range 49–233). Time to stoma closure was nearly doubled in a female patient after TME with posterior vaginal wall excision because of the higher risk for delayed anastomotic-vagina fistula formation. The second longest delay to stoma closure of 200 days after surgery was in a female patients because of the chronic pelvic pain after low anterior resection without anastomotic leakage confirmation.

TABLE 3. Distribution of the initial clinical and pathologic stage, (N = 60)

Clinical stage	Pathological stage							
	pT0	pT1	pT2	pT3	pT4	pN0	pN1	pN2
cT2	1	/	/	/	/			
cT3	7	5	6	17	1			
cT4	6	0	6	8	3			
cN1						17	1	/
cN2						33	8	1

C = clinical; N = node; p = pathological; T = tumor

Efficacy of the treatment

After induction ChT radiologic (evaluation with MRI) downstaging of T, N, stage, absence of EMVI or MRF involvement was observed in 42.4%, 62.1%, 36.4%, 69.7% and 68.2% of patients, respectivelly. We recorded cCR in 6 (9%) patients.

MRI of pelvis after the consolidation ChT was performed in 27 patients, among them only 1 patient was operated outside our institution. Five more (7.6%) cCR were recorded.

Among 60 operated patients pCR rate was 23.3% (Dworak tumor regression grade 4), the rate of near complete response (Dworak tumor regression grade 3) was 20%. Radical resection rate was 96.7% and pathological T, N and stage downstaging was 65%, 96.7% and 83.4%, respectively (Table 3). Upstaging was observed in 1 patient after induction ChT (from T3N2 to T4N2), but after the TNT and surgery pCR has been reported. After operation was tumor upstaging observed in 1 patient (from T3N1 to pT4N0).

The mean neoadjuvant rectal (NAR) score was 10.7. It was low in 24 (40%), intermediate in 26 (43.3%) and high in 10 (16.7%) patients.

There was no association between pCR and disease stage, tumor grade, presence of EMVI, chemotherapy dose, treatment or chemotherapy interruption, total radiation dose received and time to operation on the Fisher exact test. Both radiotherapy techniques using hypofractionation (*i.e.* higher doses per fractions with concomitant boost) was the only variable associated with pCR. The rate of pCR in patients irradiated with 3D conformal technique and standard fractionation was 12.1% while with IMRT SIB and VMAT SIB and hypofractionation it was 37% ($p < 0.05$).

Discussion

Optimal therapy for patients with LARC is still controversial, but TNT is gaining acceptance in the treatment of a high risk group. The goal of the present analysis was to evaluate this approach for patients with LARC-HR in Slovenia. Compared to our previous study with intensified neoadjuvant capecitabine based treatment with one induction cycle of capecitabine before CRT and two consolidation cycles before the operation, TNT achieved better pCR (17.5% *vs.* 23.3%), T (55.5% *vs.* 65%) , N (77.7% *vs.* 96.7%) and stage (79.3% *vs.* 83.4%) downstaging with comparable toxicity and compliance of patients.[15] Direct comparison with the results of these near TNT study and other TNT studies is limited because in majority of them patients with stage II and III LARC were included. It is known that patients with clinical stage II tumors had higher response to treatment and pCR rate than patients with clinical stage III tumors.[6] Taking into account only the high risk group of patients in the study of Golo *et al.*, the greater efficacy of our TNT approach is even more prominent. The difference in pCR rate is 13.8% (10.5% *vs.* 23.3%).[15]

Another difficulty in comparison with other studies presents our scheme of TNT approach which is rather unique with combination of induction ChT before CRT and consolidation ChT after it. We found only one Chinese study reporting results on TNT in LARC-HR only with similar approach: 3 cycles of induction and 3 cycles of consolidation CAPOX, but even more intensified by oxaliplatin added to CRT.[16] Studies with different TNT schemes than our in LARC reported pCR rate ranging from 14% to 36%.[4-6,16,17] Our pCR rate of 23.3% is consistent with most of them. We achieved similar pCR than study from Chau *et al.* (24%) and slightly lower than Chinese study (31.7%).[4,16] Still, our downstaging data appear to be encouraging. We observed slightly higher proportion of low pathological T stage (ypT0-2; 51.7%) than in Chinese study (42.6%).[16] On the other side we observed slightly lower proportion of high pathological T stage (ypT3 and ypT4; 41.7% and 6.7%) than in Chinese study (ypT3 40.4%). In the only TNT-based randomized trial including both (II and III) stages of LARC T downstaging was observed in 43% of patients.[5]

We reported recently that preoperative IMRT-SIB can achieve a high rate of pCR and T or N downstaging.[18] Radiotherapy techniques used in the Chinese study were IMRT or VMAT[16] with standard fractionaction. The possible explanation for lower pCR rate in our study than in Chinese is that more than half of the patients were irradiated with 3D-CRT (54.5%) technique with standard fractionation. If we calculate CR (cCR+pCR) rate in subset of our patients (n = 30) who were irradiated with IMRT SIB or VMAT SIB with higher dose per fraction in shorter time (*i.e.* hypofractionation) with the biological equivalent total dose as with standard fractionation, we get an excellent CR rate of 36.7% (1 patient with cCR and 10 patients with pCR). The result is as good as the result of the Chinese study even without intensification of CRT with oxaliplatin and is better also for the subset of patients with HR in the study of But *et al.* in which pCR was 20%. Compared to this group we also achieved better N (85% *vs.* 96. 7%) downstaging.[18] Moreover, our results are comparable even to other studies involving also favorable stage II LARC.

Further, our interval from completion of CRT to surgery (mean and SD, 11.3 weeks ± 2.5 weeks) was shorter than in Chinese study (mean 20.1 weeks).[16] Time from completing neoadjuvant therapy to surgery is one of important determinant for achieving complete response.[19] Compared to the study from Cercek *et al.*, we had similar interval between completion of CRT and surgery but shorter time from completing neoadjuvant therapy to surgery (most frequent 2–4 weeks versus 8–12 weeks) due to different TNT regimens.[6] In the contrast with us, Cercek *et al.* reported higher rate of pCR (32.8%), but we also have to take into consideration that they reported result for LARC stage III with or without risk factors. To date, there is no consensus about optimal time for surgery after CRT. A lot of studies reported that long interval between preoperative radiotherapy and surgery was associated with a significantly better clinical tumor response and pathologic downstaging.[6,20,21] On the other side, longer interval to surgery was associated with increased risk of death and could have impact on surgical complication due to potential fibrosis development.[21] However, it is difficult to determine the point where the benefit is greater than the risk because time to surgery is not the only factors affecting pCR.

We also evaluated neoadjuvant rectal score (NAR). NAR was developed as a composite short-term endpoint for clinical trials involving neoadjuvant therapy for rectal cancer.[22] It's calculation is based on downstaging data (cT, pT, pN) and has greater predictive validity for overall survival than does ypCR.[23] In the NSABP R-04 randomised trial, the NAR score calculation was divided into three classes. Low (NAR < 8), intermediate (NAR = 8–16),

and high score (NAR > 16) were associated with 92%, 89% and 68% 5 year OS, respectively.[23] In our study 83.3% of patients had NAR in low and intermediate class. Direct comparison with other TNT studies was not possible as we did not find any reports on predictive NAR score. Taking into account the data from NSABP R-04 trial and from randomized trials with near TNT-based regimens for LARC reporting 5 year OS between 67–77%[5,24,25], we can consider results of current study as promising.

Compliance within TNT protocol in our study was in the range of 83% to 100% and is consistent with others who have studied TNT approach.[26] In the largest randomized study of the adjuvant ChT in rectal cancer poor adherence with all planned dose in only 43% of patients was reported.[27] The rates of compliance in TNT-based regimen are promising including our compliance rate for all planned dose ChT (60.6%).

Toxicities were acceptable with minimal life-threatening side effects. Grade 3 adverse event developed only in 6% of patients who recevied TNT and 1 unexplained death occured. Postoperative morbidity rate was 25% which is comparable to postoperative morbidity of TNT-based studies in which ranged from 13 to 51%.[26] In addition, most surgical complications were associated with operative wound healing and not with other serious complications. Compared to other TNT-based regimen in LARC-HR, no relevant differences in terms of treatment outcome and toxicity were observed.

One of the important factors in assessing the quality of life is also the time to temporary stoma closure and the presence of a temporary or permanent stoma due to negative impact on social functioning and gastrointestinal symptoms.[28] There is a lack of studies reporting the time to stoma closure. Cercek *et al.* reported that stoma closure was earlier in the TNT group (89 days in TNT group *vs.* 192 days in group with standard therapy).[6] There are two major reasons for prolonged interval in our study: first, complexity of surgery with prolonged recovery and second, too long waiting time to admission for stoma closure. As pointed out previously our result can not be compared with the control group or another group with similar characteristics, but in relation to the previously mentioned result we consider median time of 134 days in our study as acceptable.

Limitations of our study are lack of control arm and limited number of patients from a single institution. Further, long-term data for our TNT approach are not available yet. Moreover, it should be emphasized that the NAR calculation does not reflect direct clinical benefits but it predicts overall survival. All of the above mentioned facts will bet taken into consideration when designing future studies.

Conclusions

TNT of high risk LARC is well tolerated and highly effective with excellent tumor and node regression rate and with low toxicity rate. Treatment according to the protocol is achievable in a great proportion of patients. Regarding short term outcomes TNT seems to be better option for patients with LARC with high risk for local or systemic recurrence than standard preoperative CRT and adjuvant ChT. Longer follow up will show if this strategy will improve distant disease control and survival.

Reference

1. Peeters KC, Marijnen CA, Nagtegaal ID, Kranenbarg EK, Putter H, Wiggers T, et al. The TME trial after a median follow-up of 6 years: increased local control but no survival benefit in irradiated patients with resectable rectal carcinoma. *Ann Surg* 2007; **246:** 693-701. doi: 10.1097/01.sla.0000257358.56863.ce

2. Gollins S, Sebag-Montefiore D. Neoadjuvant treatment strategies for locally advanced rectal cancer. *Clin Oncol* 2016; **28:** 146-51. doi: 10.1016/j.clon.2015.11.003

3. De Felice F, Benevento I, Magnante AL, Musio D, Bulzonetti N, Caiazzo R, et al. Clinical benefit of adding oxaliplatin to standard neoadjuvant chemoradiotherapy in locally advanced rectal cancer: A meta-analysis. *BMC Cancer* 2017; **17:** 1-6. doi: 10.1186/s12885-017-3323-4

4. Chau I, Brown G, Cunningham D, Tait D, Wotherspoon A, Norman AR, et al. Neoadjuvant capecitabine and oxaliplatin followed by synchronous chemoradiation and total mesorectal excision in magnetic resonance imaging-defined poor-risk rectal cancer. *J Clin Oncol* 2006; **24:** 668-74. doi: 10.1200/JCO.2005.04.4875

5. Fernández-Martos C, Pericay C, Aparicio J, Salud A, Safont MJ, Massuti B, et al. Phase II, randomized study of concomitant chemoradiotherapy followed by surgery and adjuvant capecitabine plus oxaliplatin (CAPOX) compared with induction CAPOX followed by concomitant chemoradiotherapy and surgery in magnetic resonance imaging-defined. *J Clin Oncol* 2010; **28:** 859-65. doi: 10.1200/JCO.2009.25.8541

6. Cercek A, Roxburgh CSD, Strombom P, Smith JJ, Temple LKF, Nash GM, et al. Adoption of total neoadjuvant therapy for locally advanced rectal cancer. *JAMA Oncol* 2018; **4:** e180071. doi: 10.1001/jamaoncol.2018.0071

7. Benson AB 3rd, Venook AP, Al-Hawary MM, Arain MA, Chen YJ, Ciombor KK, et al. *NCCN clinical practice guidelines in oncology rectal cancer Version 1.2019.*; 2019. [cited 2019 Apr 25]. Available at: https://www.nccn.org/professionals/physician_gls/pdf/rectal.pdf.

8. Bujko K, Bujko M. Point: Short-course radiation therapy is preferable in the neoadjuvant treatment of rectal cancer. *Semin Radiat Oncol* 2011; **21:** 220-7. doi: 10.1016/j.semradonc.2011.02.008

9. Glynne-Jones R, Wyrwicz L, Tiret E, Brown G, Rödel C, Cervantes A, et al. Rectal cancer: ESMO Clinical Practice Guidelines for diagnosis, treatment and follow-up. *Ann Oncol* 2018; **29(Suppl 4):** iv263. doi: 10.1093/annonc/mdy161

10. But-Hadzic J, Anderluh F, Brecelj E, Edhemovic I, Secerov-Ermenc A, Hudej R, et al. Acute toxicity and tumor response in locally advanced rectal cancer after preoperative chemoradiation therapy with shortening of the overall treatment time using intensity-modulated radiation therapy with simultaneous integrated boost: a Phase 2 Trial. *Int J Radiat Oncol Biol Phys* 2016; **96:** 1003-10. doi: 10.1016/j.ijrobp.2016.08.031

11. Cancer Institute N. Common Terminology Criteria for Adverse Events (CTCAE) Common Terminology Criteria for Adverse Events v4.0 (CTCAE). 2009. [cited 2019 Apr 25]. Available at: http://evs.nci.nih.gov/ftp1/CTCAE/CTCAE_4.03_2010-06-14_QuickReference_5x7.pdf.

12. Edge SB, Compton CC. The american joint committee on cancer: The 7th edition of the AJCC cancer staging manual and the future of TNM. *Ann Surg Oncol* 2010; **17:** 1471-4. doi: 10.1245/s10434-010-0985-4

13. Dworak O, Keilholz L, Hoffmann A. Pathological features of rectal cancer after preoperative radiochemotherapy. *Int J Colorectal Dis* 1997; **12:** 19-23. PMID: 9112145

14. IBM Corp. Released 2018. *IBM SPSS Statistics for Windows, Version 26.0*. Armonk: IBM Corp; 2018.

15. Golo D, But-Hadzic J, Anderluh F, Brecelj E, Edhemovic I, Jeromen A, et al. Induction chemotherapy, chemoradiotherapy and consolidation chemotherapy in preoperative treatment of rectal cancer - Long-term results of phase II OIGIT-01 Trial. *Radiol Oncol* 2018; **52:** 267-74. doi: 10.2478/raon-2018-0028

16. Wang X, Yu Y, Meng W, Jiang D, Deng X, Wu B, et al. Total neoadjuvant treatment (CAPOX plus radiotherapy) for patients with locally advanced rectal cancer with high risk factors: A phase 2 trial. *Radiother Oncol* 2018; **129:** 300-5. doi: 10.1016/j.radonc.2018.08.027

17. Dewdney A, Cunningham D, Tabernero J, Capdevila J, Glimelius B, Cervantes A, et al. Multicenter randomized phase II clinical trial comparing neoadjuvant oxaliplatin, capecitabine, and preoperative radiotherapy with or without cetuximab followed by total mesorectal excision in patients with high-risk rectal cancer (EXPERT-C). *J Clin Oncol* 2012; **30:** 1620-7. doi:10.1200/JCO.2011.39.6036

18. But-Hadzic J, Velenik V. Preoperative intensity-modulated chemoradiation therapy with simultaneous integrated boost in rectal cancer: 2-year follow-up results of phase II study. *Radiol Oncol* 2018; **52:** 23-9. doi: 10.1515/raon-2018-0007

19. Kalady MF, De Campos-Lobato LF, Stocchi L, Geisler DP, Dietz D, Lavery IC, et al. Predictive factors of pathologic complete response after neoadjuvant chemoradiation for rectal cancer. *Ann Surg* 2009; **250:** 582-8. doi: 10.1097/SLA.0b013e3181b91e63

20. Francois BY, Nemoz CJ, Baulieux J, Vignal J, Grandjean J, Partensky C, et al. Influence of the interval between preoperative radiation therapy and surgery on downstaging and on the rate of sphincter-sparing surgery for rectal cancer: the Lyon R90-01 randomized trial. *J Clin Oncol* 1999; **17:** 2396-402. doi: 10.1200/JCO.1999.17.8.2396

21. Goodman KA. Total neoadjuvant therapy for rectal cancer. *Cancer Radiother* 2018; **22:** 459-65. doi: 10.1016/j.canrad.2018.01.004

22. George TJ, Allegra CJ, Yothers G. Neoadjuvant rectal (NAR) score: a new surrogate endpoint in rectal cancer clinical trials. *Curr Colorectal Cancer Rep* 2015; **11:** 275-80. doi: 10.1007/s11888-015-0285-2

23. Yothers G, George TJ, Allegra CJ, Bosset J-F, Bujko K, Collette L, et al. Predictive validity of NeoAdjuvant Rectal (NAR) Score and pathologic complete response (ypCR) for overall survival (OS) as surrogate endpoints in rectal cancer clinical trial. [Abstract]. *J Clin Oncol* 2016; **34(15 Suppl):** 3533. doi: 10.1200/JCO.2016.34.15_suppl.3533

24. Sclafani F, Peckitt C, Cunningham D, Tait D, Giralt J, Glimelius B, et al. Short- and long-term quality of life and bowel function in patients with MRI-defined, high-risk, locally advanced rectal cancer treated with an intensified neoadjuvant strategy in the randomized phase 2 EXPERT-C Trial. *Int J Radiat Oncol* 2015; **93:** 303-12. doi: 10.1016/j.ijrobp.2015.03.038

25. Schou J V., Larsen FO, Rasch L, Linnemann D, Langhoff J, Høgdall E, et al. Induction chemotherapy with capecitabine and oxaliplatin followed by chemoradiotherapy before total mesorectal excision in patients with locally advanced rectal cancer. *Ann Oncol* 2012; **23:** 2627-33. doi: 10.1093/annonc/mds056

26. Zaborowski A, Stakelum A, Winter DC. Systematic review of outcomes after total neoadjuvant therapy for locally advanced rectal cancer. *BJS* 2019; **106:** 979-87. doi: 10.1002/bjs.11171

27. Bosset JF, Calais G, Mineur L, Maingon P, Stojanovic-Rundic S, Bensadoun RJ, et al. Fluorouracil-based adjuvant chemotherapy after preoperative chemoradiotherapy in rectal cancer: Long-term results of the EORTC 22921 randomised study. *Lancet Oncol* 2014; **15:** 184-90. doi: 10.1016/S1470-2045(13)70599-0

28. Herrle F, Sandra-Petrescu F, Weiss C, Post S, Runkel N, Kienle P. Quality of life and timing of stoma closure in patients with rectal cancer undergoing low anterior resection with diverting stoma: A multicenter longitudinal observational study. *Dis Colon Rectum* 2016; **59:** 281-90. doi: 10.1097/DCR.0000000000000545

research article

A multi-institutional analysis of diffuse large B-cell lymphoma (DLBCL) treated with consolidative radiotherapy and the impact of cell-of-origin on outcomes

Chrishanthi Rajasooriyar[1], Jeremy Tey[2], Lea Choung Wong[2], Michelle Poon[3], Rao Nandini[4], Ivan Tham[2], Balamurugan Vellayappan[2]

[1] Department of Oncology, Teaching Hospital, Jaffna, Sri Lanka
[2] Department of Radiation Oncology, National University Cancer Institute Singapore, National University Health System, Singapore
[3] Department of Haematology-Oncology, National University Cancer Institute Singapore, National University Health System, Singapore
[4] Department of Pathology, Tan Tock Seng Hospital, Singapore

Radiol Oncol 2019; 53(4): 473-479.

Received 26 June 2019
Accepted 11 August 2019

Correspondence to: Assist. Prof. Balamurugan Vellayappan MBBS, FRANZCR, MCI, Department of Radiation Oncology, National University Cancer Institute Singapore, National University Health System, 1E Kent Ridge Road, Level 7 Tower Block, Singapore 119228.
E-mail: bala_vellayappan@nuhs.edu.sg

Disclosure: No potential conflicts of interest were disclosed.

Background. Patients with diffuse large B-cell lymphoma (DLBCL) with bulky disease and/or those who fail to achieve complete response benefit from the addition of radiotherapy (RT). We aim to review the outcome, as well as determine the impact of cell-of-origin, on patients undergoing consolidative RT.

Patients and methods. Patients with DLBCL treated with radical intent consolidative RT were included. Clinical, pathological and treatment characteristics were extracted from electronic medical records. Survival outcomes and factors that predict for disease-free survival (DFS) were analysed.

Results. Seventy-four patients were included in this analysis. The median follow up was 3 years (0.7–16 years). Fifty-eight percent of patients had stage I–II disease, and 61% received at least 6 cycles of chemotherapy. Cell-of-origin was discernible in 60% of patients, and approximately half were classified as Germinal centre origin. The 5-year overall survival (OS) of this group was excellent at 92% (median survival not reached). The 5-year DFS was 73% (95% CI 57–83%). Seven percent (n = 5) of patients experienced local recurrence at a median time of 6 months. Failure to achieve complete response post RT and/or initial bulky disease are significant predictors of inferior DFS. There was no association between cell-of-origin and DFS or OS.

Conclusions. The outcome of patients who received radiotherapy as consolidation is excellent. Patients who fail to achieve complete response after radiotherapy had poorer outcomes. Despite using radiotherapy, presence of bulky disease remains a significant predictor of disease recurrence. We did not find any association of poorer outcomes, with regards to cell-of-origin, in the use of consolidative RT.

Key words: lymphoma; cell-of-origin; radiotherapy; consolidation

Introduction

Diffuse large B-cell lymphoma (DLBCL) is the most common non-Hodgkin's lymphoma in adults, accounting for about 30–60% of all cases.[1] It has an aggressive natural history, with a prognosis of less than a year without treatment.[2] Radiotherapy (RT), historically, has been an integral part of DLBCL

treatment.[3] However, with the implementation of new systemic therapy agents, the use of RT has declined.[4,5] The discovery of the chimeric monoclonal antibody rituximab against CD20 receptors has greatly improved the control and cure of DLBCL.[6] Data from the MINT studies suggest that rituximab reduced the risk posed by bulky disease, but did not eliminate it.[7] In line with that, many studies have shown the improved outcome with the addition of RT, especially in the context of bulky disease.[8,9]

However, clinicians have noticed that the behaviour of DLBCL can be varied, and attempts have been made to better classify DLBCL.[10] Based on gene expression profiling studies, DLBCL can be divided into 2 distinct subtypes: Germinal Centre B cell (GCB) and non-Germinal Centre B- cell subtype (non-GCB).[11] Immunohistochemistry based algorithms have been shown to have good concordance with gene expression profiling for cell-of-origin classification.[12] Studies based on Western populations have suggested that GCB-subtypes are associated with improved outcomes.[13] However, these findings could not be replicated in the Asian population.[14] It is important to note that these patients were treated primarily with chemotherapy, and the impact of cell-of-origin for patients undergoing consolidative RT is unclear.

The aim of this study is to report the outcome of patients with DLBCL treated with

rituximab, cyclophosphamide, hydroxydaunorubicin, oncovin, prednisone (R-CHOP) or R-CHOP like chemotherapy and consolidative RT. In addition, we classified patients according to cell-of-origin (where information available) and determined the impact on the outcomes.

Patients and methods

Patient selection criteria

This was a retrospective cohort study carried out at two tertiary hospitals in Singapore. (National University Hospital and Tan Tock Seng Hospital). Institutional review board approval was obtained and waiver of consent was granted. From June 2001 to August 2015, patients with histologically confirmed DLBCL, stages I–IV, who received R-CHOP, or R-CHOP like chemotherapy, and received consolidative RT were identified through the institutional RT database. Only patients treated with curative intent were included.

Staging was based on Ann Arbor Classification. Bulky disease was defined as any nodal or extra-nodal mass with a dimension of more than 7.5 cm in any direction. International prognostic index (IPI) score was based on age, Eastern Cooperative Oncology Group (ECOG) performance status, serum lactate dehydrogenase (LDH), stage of the disease and the number of extra-nodal sites.[15]

Patient records were carefully reviewed and the following parameters were extracted: Age, gender, ethnicity, stage, use of positron emission tomography / computed tomography (PET/CT) for staging, extra-nodal involvement, baseline PET standardized uptake value (SUV), Eastern Cooperative Oncology Group (ECOG) performance status, B symptoms, presence of bulky disease, elevated LDH, IPI score, number of cycles of chemotherapy, pre-RT response (complete response *vs.* not in complete response) and RT dose-fractionation. For cell-of-origin, patients were classified based on the Hans algorithm (Figure 1).

Treatment details

All patients received R-CHOP or R-CHOP like chemotherapy. Patients with IPI 0–1 and limited stage received 3–4 cycles of chemotherapy, whereas all other patients received 6 or more cycles of chemotherapy. All patients had a response assessment scan post-chemotherapy, before proceeding onto RT. The cell-of-origin did not influence the treatment decision.

The decision for RT was made based on consensus at the multidisciplinary board meeting, taking into account the bulky disease, number of chemotherapy cycles and response to chemotherapy (assessed on PET/CT or contrast-enhanced CT using established guidelines).[16] Patients with complete response were treated to a dose of 30–36 Gy, and patients with partial response or stable disease were treated to 40–50 Gy, both in 1.8–2 Gy fractions. RT was delivered using either using a 3-dimensional conformal or intensity-modulated tech-

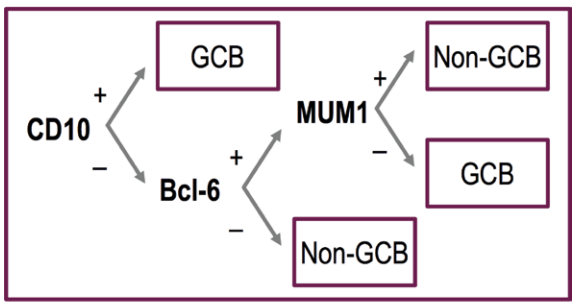

FIGURE 1. Hans classification.

nique, at the discretion of the treating physician. Involved-field radiotherapy (IFRT) was used in cases who were not staged by PET/CT.[17] Involved-site radiotherapy (ISRT), described below, was used in cases who were staged with PET/CT.[18] PET/CT staging was available from 2011 and routinely used from 2014. In both situations, the staging and post-chemotherapy scans were utilized to determine the target volume.

ISRT technique: The gross tumour volume [GTV] was the residual tumour post-chemotherapy. The clinical target volume [CTV] included the GTV, craniocaudal extent of the pre-chemotherapy tumour volume and the circumferential extent of the post-chemotherapy tumour volume with the addition of 1–1.5 cm craniocaudal margin and 0.5–1 cm of circumferential margin. When there was a complete response to chemotherapy, the CTV was based on pre-chemotherapy volumes respecting anatomical boundaries for lateral extent of tumour. The planning target volume [PTV] was created by adding 0.5–1cm to the CTV. Image guidance was performed primarily with electronic portal imaging. On-board kilovoltage cone beam CT was used for selected cases (available since 2011).

Follow up

Patients were followed up with PET/CT or contrast-enhanced CT scan 3 months after the completion of RT. The complete responders were reviewed every 3 months for the first 2 years alternating with the haematologist and for 6 months from 3rd to the 5th year. A full blood count and lactate dehydrogenase were checked at each follow-up, together with clinical history and examination for signs of recurrence. Re-imaging and further investigations were performed when there was a suspicion of recurrence.

Outcome assessment

Overall survival (OS) was defined as the time from diagnosis to death due to any cause. Disease-free survival (DFS) was defined as the time from diagnosis to recurrence, or death. Patterns of relapse: local in-field (*i.e.* within radiation field), in the nodal regions (out-of-field) and distant sites. The time to local relapse was studied time from date of completion of RT to date of relapse.

Prognostic factors examined

We analysed the influence of age, gender, ECOG performance status, stage, presence of B symptoms, LDH, IPI score, presence of bulky disease, baseline SUV on PET, number of chemotherapy cycles, radiation dose, response to radiation and cell-of-origin on OS and DFS.

Statistical analysis

Descriptive statistics were used to summarize clinical and treatment characteristics. DFS and OS were analyzed using the Kaplan-Meier methods and graphically presented. The actuarial 5-year survival rates were estimated. For DFS, patients without recurrence were censored at death or date of last follow up. For OS, patients who were still alive were censored at the date of last follow-up. Patterns of relapse were reported with descriptive statistics. Univariable analysis was carried out on factors that may influence outcomes such as DFS and OS. Univariable factors with a P-value of < 0.1 were included in the multivariable analysis. The Cox regression model was used to compare sur-

TABLE 1. Patient characteristics and treatment details

Variable	Level	Number of patients (%)
All patients		74 (100)
Age	Median (range)	61 (14–88)
Gender	Males Females	43 (58) 31 (42)
Ethnicity	Chinese Malay Indian Others	54 (73) 10 (14) 1 (1) 9 (12)
Stage	I–II III–IV	43 (58) 31 (42)
Staging PET/CT	No Yes SUV max ≤ 20 SUV max > 20	44 (59) 30 (41) 12 (40) 18 (60)
Involvement of extra-nodal sites	Nodal only Extra-nodal +/- nodal	19 (26) 55 (74)
ECOG	0 1 2 3	20 (27) 47 (64) 3 (4) 4 (5)
Bulky disease	≤ 7.5cm > 7.5 cm	37 (57) 28 (43)
IPI score	0–1 2 3 4–5	28 (38) 26 (35) 13 (18) 7 (9)
Number of chemotherapy cycles	< 6 ≥ 6	28 (39) 44 (61)
Radiotherapy dose	≤ 36 Gy > 36 Gy	45 (61) 29 (39)
Cell-of-origin	Germinal centre Non-germinal centre Unknown	20 (27) 22(30) 32 (43)

ECOG = Eastern Cooperative Oncology Group performance status; IPI = international prognostic index; SUV = standardized uptake value

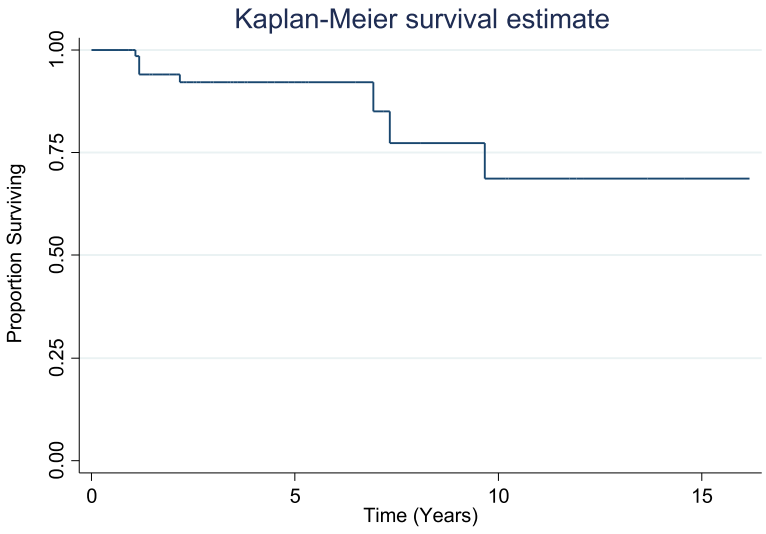

FIGURE 2. Overall survival.

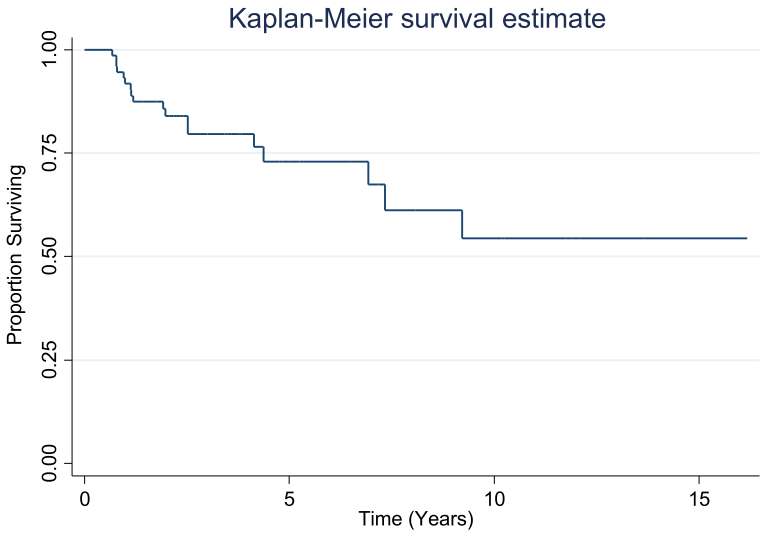

FIGURE 3. Disease-free survival.

vival estimates and calculate P values and hazard ratios. A P-value of < 0.05 was considered to be statistically significant. Statistical analysis was carried out using Stata Statistical Software (Release 14, College Station, TX: StataCorp LP)

Results

Seventy-four patients were included in the study and the demographic characteristics are shown in Table 1. The median age was 61 years ranging from 14–88 years. Fifty-eight percent were males and the same proportion had early-stage disease (Stage I–II). Bulky disease was seen in 43% of patients. About a third of the included patients had IPI scores of 0–1. Sixty-one percent had at least 6 cycles of chemotherapy. About two-thirds of the patients were treated to a dose of 36 Gy or less. Information on cell-of-origin was available in 60% of patients and was equally distributed between GCB and non-GCB origin. Median follow up of the cohort was 3 (0.7–16) years.

Survival and patterns of relapse

The 5-year OS was 92% (median survival not reached) (Figure 2) and 5-year DFS was 73% (median survival not reached) (Figure 3).

Fifty-three patients (72%) were in complete remission post-RT. Patients who achieved complete remission had a significantly better DFS (HR 11.05, 95% CI 4.11–29.69, P < 0.01). (Figure 4). The presence of initial bulky disease was associated with an inferior DFS (HR 3.16, 95% CI 1.02–9.78, P = 0.04) (Figure 5).

Uni-variable and multi-variable analysis for DFS and OS are presented in Table 2. Response to RT (P < 0.001) and tumour bulk (P < 0.02) were significant predictors of DFS. Only response to RT (P = 0.011) was a significant predictors of OS. There was no association between cell-of-origin and DFS or OS (P = 0.16, P = 0.61 respectively).

Patterns of relapse

In total 13 (18%) patients failed. Among those failed, 5 (7%) failed locally inside the treatment field, 11(15%) outside the treatment field in nodal regions and 10 (14%) at distant sites.

The median time for local recurrence was 6 [0–23] months. All five patients who recurred in-field, received doses between 36–40 Gy. These 5 patients also recurred in nodal regions outside the treatment field or at distant sites. Three of these patients were salvaged and were alive at the last follow up and two died due to progressive disease.

Discussion

DLBCL is an aggressive condition, which can behave variably.[10] The decision on whether to use consolidative RT remains controversial, especially in advanced stages where complete response has been achieved.[19] In this study, we report the outcomes of our patients treated with consolidative RT.

TABLE 2. UNI- and multivariable analysis for disease-free survival (DFS) and overall survival (OS)

Variable	DFS						OS		
	Univariable analysis			Multivariable analysis			Univariable analysis		
	HR	95% CI	P	HR	95% CI	P	HR	95% CI	P
Age (continuous)	1.03	1–1.06	0.081	1.02	0.98–1.06	0.37	1	0.96–1.05	0.86
Gender (ref: male)	1.78	0.70–4.51	0.23				1.38	0.34–5.51	0.65
ECOG (continuous)	1.64	0.92–2.95	0.096	0.42	0.18–1.00	0.05	1.05	0.35–3.15	0.93
Stage 1–2 (ref) *vs.* 3–4	1.19	0.46–3.01	0.71				1.84	0.44–.64	0.4
B symptoms (ref: yes)	0.51	0.8–1.48	0.22				0.25	0.5–1.23	0.088
Elevated LDH yes (ref) *vs.* no	1.06	0.34–3.34	0.92				2.38	0.28–20.18	0.43
IPI (ref) *vs.* 2–5	1.48	0.55–3.99	0.43				2.32	0.46–11.69	0.31
Bulk < 7.5 cm(ref) *vs.* ≥ 7.5 cm	3.16	1.02–9.78	**0.045**	6.10	1.34–27.87	**< 0.02**	3.19	0.46–22.15	0.24
Baseline PET SUV ≤ 20 (ref) *vs.* > 20	0.25	0.45–1.35	0.11				-	-	-
Chemotherapy < 6 cycles (ref) *vs.* ≥ 6 cycles	2.24	0.78–6.34	0.13				1.73	0.39–7.69	0.47
Dose < 36 Gy (ref) *vs.* ≥ 36 Gy	0.89	0.34–2.30	0.81				2.21	0.52–9.37	0.28
RT response CR(ref) *vs.* non CR	11.05	4.11–29.70	**<0.001**	5.64	2.78–11.45	**<0.001**	**6.26**	**1.53–25.7**	**0.011**
Cell of origin (ref GC) NGC unknown	 3.72 3.60	 0.74–18.54 0.79–16.50	 0.11 0.10				 2.57 3.77	 0.23–28.94 0.44–32.49	 0.44 0.23

ECOG = Eastern Cooperative Oncology Group performance status; GC = germinal centre B cell (GCB); IPI = international prognostic index; NGC = non-GC; RT = radiotherapy; SUV = standardized uptake value

TABLE 3. Survival outcomes of aggressive lymphoma treated with consolidative RT

Author	Year of publication	Limited/advanced disease	DFS	OS
Horning *et al*.	2004	Limited	73% (6 yr)	82% (6 yr)
Reyes *et al*.	2005	Limited	74 (5 yr)	81 (5 yr)
Bonnet *et al*.	2007	Limited	63% (5 yr)	68% (5 yr)
Held *et al*.	2014	Limited & advanced	68% (3 yr)	78% (3 yr)
Aviles *et al*.	2018	Advanced	Not reported	91% (5 yr)
Lamy *et al*.	2018	Limited	92% (5 yr)	96% (5yr)
Pfreundschuh *et al*.	2018	Limited & advanced	84% (3 yr)	93% (3 yr)
Rajasooriyar et al.	2019	Limited & advanced	73% (5 yr)	92% (5 yr)

DFS = disease-free survival; OS = overall survival

We report encouraging survival and disease control rates in this cohort–5-year OS of 92% and 5-year DFS of 73%. Our results are congruent with other contemporary series[9,20-25], which are summarised in Table 3. While assessing for predictors for improved DFS, we found that patients who were in complete response (post-RT) had improved DFS on multivariable analysis (HR 5.64, 95% CI 2.78–11.45, P < 0.001). This was not an unexpected finding as it is likely suggestive of better tumour biology. In addition, patients who had bulky disease (> 7.5cm) had an increased risk of relapse (HR 6.1 95% CI 1.34–27.87, P < 0.02). Bulky disease (at initial presentation) is considered to be an indication for consolidative RT, although the definition of bulk has varied across studies, from 5 cm(8, 26) to 10 cm.[20] In our institution, we use 7.5 cm as a definition of bulk, in line with the MINT studies.[7] As such, it is likely that consolidative RT reduces the risk of disease recurrence, but does not prevent it. As for OS, only complete response (post-RT) was predictive of improved OS.

Secondly, we were able to classify about two-thirds of our patients by cell-of-origin (into GCB

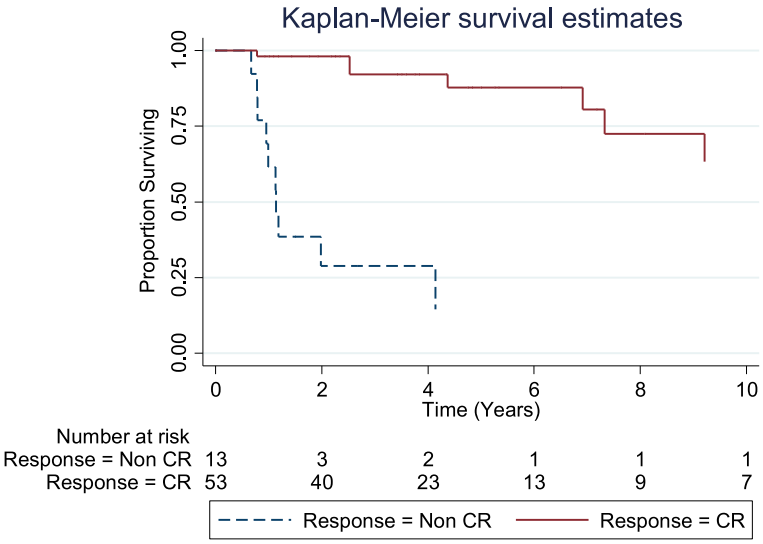

CR = complete response

FIGURE 4. Disease-free survival by response to radiotherapy.

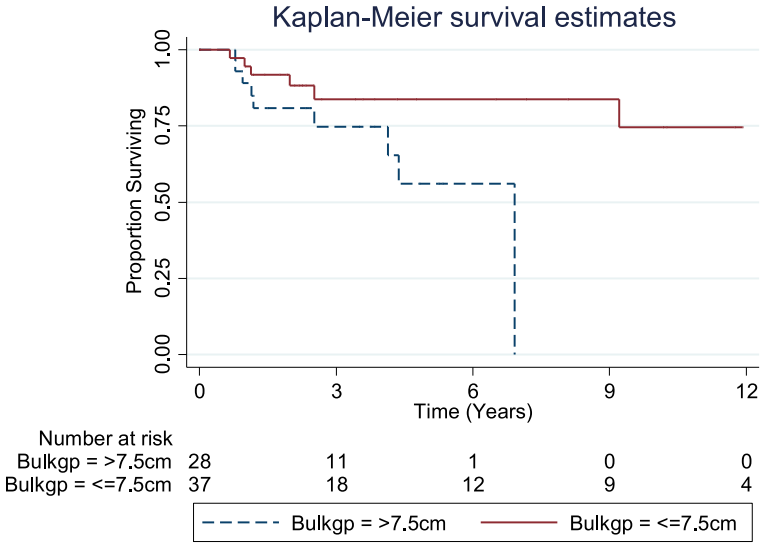

Bulkgp = the bulky disease greatest dimension of mass in any direction (where >7.5cm is considered bulky)

FIGURE 5. Disease-free survival by presence of initial bulky disease.

vs. non-GCB). IHC markers of CD10, BCL-6 and MUM-1 were routinely performed from 2013. As such, 27% were classified to have GCB, 29% non-GCB and remainder were unclassified. Based on univariate analysis, non-GCB was not deemed to be a significant predictor of worse DFS or OS. (HR 3.72 95% CI 0.74–18.54, P = 0.11; HR 2.57 95% CI 0.23–28.94, P = 0.44), compared to GC. This should only be considered as hypothesis-generating as the number of events from our cohort is relatively small. In addition, we would like to qualify that there were no statistically significant differences between the GCB and non-GCB groups, in terms of initial bulky disease (P = 0.09) or response to RT (P = 0.27)

Thirdly, with regards to patterns of recurrence, some previous studies have analysed the patterns of failure in patients with DLBCL. Shi *et al.* analysed patients with DLBCL, who achieved complete remission after R-CHOP.[26] Almost half of the patients with advanced-stage DLBCL failed at the initial presenting sites even after achieving complete remission with R-CHOP. In addition, around half of such local failures occurred at initial bulky or bony sites. The local failure rate was 44% in the R-CHOP alone group compared to 7% with R-CHOP plus consolidative RT. Our series echoes the findings of Shi *et al.*, where only 7% of patients failed inside the treatment field with a local control rate of 93%. However, it is important to note that these were not isolated local failures. As such, RT continues to provide excellent local control for bulky and/or residual disease.

The UNFOLDER study examining the role of consolidative RT (for bulky and/or extranodal sites) in patients who had achieved complete response to chemotherapy underwent early termination of the no-RT arm, due to increased number of recurrences.[27] The full results are eagerly awaited.

Our study has several strengths. Our data is well-curated, as all the patients were treated at two institutions which rely on electronic medical records, electronic PACS (picture archiving and communication system), and where the management of majority of the cases are discussed at the weekly lymphoma tumour board meetings. Moreover, the patients were regularly followed up by haematologists and radiation oncologists. Secondly, we are the first to examine the clinical relevance of cell-of-origin on RT outcomes. However, we acknowledge the limitations of our study. Despite close follow-up, there are patients with missing data, as with any retrospective study. In addition, we captured all patients who received consolidative RT - and this included patients with both limited and advanced disease, where the outcomes can be different. Our data spans over 15 years, where staging methodology, chemotherapy choices and response assessment modalities have evolved. Moreover, there is evidence to show that the survival of DLBCL patients has improved over the years.[28] Lastly, the overall number of events (recurrence or death) in our analysis was small, so it is possible

that we had insufficient power to detect prognostic factors (type II error). It would also have been useful to have a control group of patients who were treated with chemotherapy alone.

Conclusions

Although DLBCL is considered to be an aggressive form of non-Hodgkin's Lymphoma, it has an excellent outcome with modern treatment. RT contributes significantly towards local control and survival in patients with bulky disease or residual disease following first-line chemotherapy. The cell-of-origin, by Hans algorithm, may not be a relevant prognostic factor in patients undergoing consolidative RT. A well-designed randomised controlled trial, comparing patients treated with chemotherapy alone, would be useful to determine the additional benefit of RT.

References

1. Tilly H, Gomes da Silva M, Vitolo U, Jack A, Meignan M, Lopez-Guillermo A, et al. Diffuse large B-cell lymphoma (DLBCL): ESMO Clinical Practice Guidelines for diagnosis, treatment and follow-up. *Ann Oncol* 2015; **26(Suppl 5):** v116-25. doi: 10.1093/annonc/mdv304
2. Fisher RI, Miller TP, O'Connor OA. Diffuse aggressive lymphoma. *Hematology Am Soc Hematol Educ Program* **2004;** 221-36. doi: 10.1182/asheducation-2004.1.221
3. Bush RS, Gospodarowicz M, Sturgeon J, Alison R. Radiation therapy of localized non-Hodgkin's lymphoma. *Cancer Treat Rep* 1977; **61:** 1129-36. PMID: 332347
4. Haque W, Dabaja B, Tann A, Khan M, Szeja S, Butler EB, et al. Changes in treatment patterns and impact of radiotherapy for early stage diffuse large B cell lymphoma after rituximab: a population-based analysis. *Radiother Oncol* 2016; **120:** 150-5. doi: 10.1016/j.radonc.2016.05.027
5. Vargo JA, Gill BS, Balasubramani GK, Beriwal S. Treatment selection and survival outcomes in early-stage diffuse large B-cell lymphoma: do we still need consolidative radiotherapy? *J Clin Oncol* 2015; **33:** 3710-7. doi: 10.1200/JCO.2015.61.7654
6. Coiffier B, Lepage E, Briere J, Herbrecht R, Tilly H, Bouabdallah R, et al. CHOP chemotherapy plus rituximab compared with CHOP alone in elderly patients with diffuse large-B-cell lymphoma. *N Engl J Med* 2002; **346:** 235-42. doi: 10.1056/NEJMoa011795
7. Pfreundschuh M, Kuhnt E, Trumper L, Osterborg A, Trneny M, Shepherd L, et al. CHOP-like chemotherapy with or without rituximab in young patients with good-prognosis diffuse large-B-cell lymphoma: 6-year results of an open-label randomised study of the MabThera International Trial (MInT) Group. *Lancet Oncol* 2011; **12:** 1013-22. doi: 10.1016/S1470-2045(11)70235-2
8. Phan J, Mazloom A, Medeiros LJ, Zreik TG, Wogan C, Shihadeh F, et al. Benefit of consolidative radiation therapy in patients with diffuse large B-cell lymphoma treated with R-CHOP chemotherapy. *J Clin Oncol* 2010; **28:** 4170-6. doi: 10.1200/JCO.2009.27.3441
9. Held G, Murawski N, Ziepert M, Fleckenstein J, Poschel V, Zwick C, et al. Role of radiotherapy to bulky disease in elderly patients with aggressive B-cell lymphoma. *J Clin Oncol* 2014; **32:** 1112-8. doi: 10.1200/JCO.2013.51.4505
10. Chapuy B, Stewart C, Dunford AJ, Kim J, Kamburov A, Redd RA, et al. Molecular subtypes of diffuse large B cell lymphoma are associated with distinct pathogenic mechanisms and outcomes. *Nat Med* 2018; **24:** 679-90. doi: 10.1038/s41591-018-0016-8
11. Alizadeh AA, Eisen MB, Davis RE, Ma C, Lossos IS, Rosenwald A, et al. Distinct types of diffuse large B-cell lymphoma identified by gene expression profiling. *Nature* 2000; **403:** 503-11. doi: 10.1038/35000501
12. Hans CP, Weisenburger DD, Greiner TC, Gascoyne RD, Delabie J, Ott G, et al. Confirmation of the molecular classification of diffuse large B-cell lymphoma by immunohistochemistry using a tissue microarray. *Blood* 2004; **103:** 275-82. doi: 10.1182/blood-2003-05-1545
13. Lenz G, Wright G, Dave SS, Xiao W, Powell J, Zhao H, et al. Stromal gene signatures in large-B-cell lymphomas. *N Engl J Med* 2008; **359:** 2313-23. doi: 10.1056/NEJMoa0802885
14. Chong VC, Yap ES, Xin L, Chin ST, Jeyasekharan A, Chee Y-L, et al. Immunophenotypic and genetic characteristics of diffuse large B-cell lymphoma (DLBCL), and prognostic significance of cell of origin (COO) in a southeast Asian cohort. *Blood* 2018; **132(Suppl 1):** 4222. doi: 10.1182/blood-2018-99-119672
15. International Non-Hodgkin's Lymphoma Prognostic Factors Project. A predictive model for aggressive non-Hodgkin's lymphoma. *N Engl J Med* 1993; **329:** 987-94. doi: 10.1056/NEJM199309303291402
16. Cheson BD, Fisher RI, Barrington SF, Cavalli F, Schwartz LH, Zucca E, et al. Recommendations for initial evaluation, staging, and response assessment of Hodgkin and non-Hodgkin lymphoma: the Lugano classification. *J Clin Oncol* 2014; **32:** 3059-68. doi: 10.1200/JCO.2013.54.8800
17. Yahalom J, Mauch P. The involved field is back: issues in delineating the radiation field in Hodgkin's disease. *Ann Oncol* 2002; **13(Suppl 1):** 79-83. doi: 10.1093/annonc/13.s1.79
18. Illidge T, Specht L, Yahalom J, Aleman B, Berthelsen AK, Constine L, et al. Modern radiation therapy for nodal non-Hodgkin lymphoma-target definition and dose guidelines from the International Lymphoma Radiation Oncology Group. *Int J Radiat Oncol Biol Phys* 2014; **89:** 49-58. doi: 10.1016/j.ijrobp.2014.01.006
19. Specht L. Does radiation have a role in advanced stage Hodgkin's or Non-Hodgkin lymphoma? *Curr Treat Options Oncol* 2016; **17:** 4. doi: 10.1007/s11864-015-0377-x
20. Horning SJ, Weller E, Kim K, Earle JD, O'Connell MJ, Habermann TM, et al. Chemotherapy with or without radiotherapy in limited-stage diffuse aggressive non-Hodgkin's lymphoma: Eastern Cooperative Oncology Group study 1484. *J Clin Oncol* 2004; **22:** 3032-8. doi: 10.1200/JCO.2004.06.088
21. Reyes F, Lepage E, Ganem G, Molina TJ, Brice P, Coiffier B, et al. ACVBP versus CHOP plus radiotherapy for localized aggressive lymphoma. *N Engl J Med* 2005; **352:** 1197-205. doi: 10.1056/NEJMoa042040
22. Bonnet C, Fillet G, Mounier N, Ganem G, Molina TJ, Thieblemont C, et al. CHOP alone compared with CHOP plus radiotherapy for localized aggressive lymphoma in elderly patients: a study by the Groupe d'Etude des Lymphomes de l'Adulte. *J Clin Oncol* 2007; **25:** 787-92. doi: 10.1200/JCO.2006.07.0722
23. Aviles A, Nambo MJ, Calva A, Neri N, Cleto S, Silva L. Adjuvant radiotherapy in patients with diffuse large B-cell lymphoma in advanced stage (III/IV) improves the outcome in the rituximab era. *Hematology* 2019; **24:** 521-5. doi: 10.1080/10245332.2018.1423880
24. Lamy T, Damaj G, Soubeyran P, Gyan E, Cartron G, Bouabdallah K, et al. R-CHOP 14 with or without radiotherapy in nonbulky limited-stage diffuse large B-cell lymphoma. *Blood* 2018; **131:** 174-81. doi: 10.1182/blood-2017-07-793984
25. Pfreundschuh M, Murawski N, Ziepert M, Altmann B, Dreyling MH, Borchmann P, et al. Radiotherapy (RT) to bulky (B) and extralymphatic (E) disease in combination with 6xR-CHOP-14 or R-CHOP-21 in young good-prognosis DLBCL patients: results of the 2x2 randomized UNFOLDER trial of the DSHNHL/GLA. *J Clin Oncol* 2018; **36(15 Suppl):** 7574. doi: 10.1200/JCO.2018.36.15_suppl.7574.
26. Shi Z, Das S, Okwan-Duodu D, Esiashvili N, Flowers C, Chen Z, et al. Patterns of failure in advanced stage diffuse large B-cell lymphoma patients after complete response to R-CHOP immunochemotherapy and the emerging role of consolidative radiation therapy. *Int J Radiat Oncol Biol Phys* 2013; **86:** 569-77. doi: 10.1016/j.ijrobp.2013.02.007
27. Fridrik MA. ASCO update on lymphoma. *Memo* 2017; **10:** 218-9. doi: 10.1007/s12254-017-0372-y
28. Issa DE, van de Schans SA, Chamuleau ME, Karim-Kos HE, Wondergem M, Huijgens PC, et al. Trends in incidence, treatment and survival of aggressive B-cell lymphoma in the Netherlands 1989-2010. *Haematologica* 2015; **100:** 525-33. doi: 10.3324/haematol.2014.107300

research article

Definitive radiochemotherapy in esophageal cancer - a single institution experience

Franc Anderluh, Miha Toplak, Vaneja Velenik, Irena Oblak, Ajra Secerov Ermenc, Ana Jeromen Peressutti, Jasna But-Hadzic, Marija Skoblar Vidmar

Department of Radiotherapy, Institute of Oncology Ljubljana; Ljubljana, Slovenia

Radiol Oncol 2019; 53(4): 480-487.

Received 22 March 2019
Accepted 20 September 2019

Correspondence to: Anderluh Franc, M.D., M.Sc., Institute of Oncology Ljubljana, Zaloška 2, SI-1000 Ljubljana, Slovenia.
E-mail: fanderluh@onko-i.si

Disclosure: No potential conflicts of ineterst were disclosed.

Background. Definitive radiochemotherapy is the preferred treatment option in patients with the cancer of the cervical esophagus and a viable treatment option in patients with the cancer of lower two thirds of the esophagus, who decline proposed surgical treatment. The purpose of the study was to evaluate the treatment results with definitive radiochemotherapy of patients with esophageal cancer, treated in a single institution in the period from 2010 to 2017.

Patients and methods. All available medical data for 55 patients with esophageal cancer, who were treated with definitive radiochemotherapy with curative intent, were analyzed retrospectively. Patients were irradiated to a total dose to the tumor of 70 Gy (2 Gy per fraction) in upper third (cervical) tumors or to the mean total dose of 57.6 Gy (1.8 Gy per fraction) in middle third (intrathoracic) tumors. All but one patient received concomitant chemotherapy, with the majority of them (41 patients; 74.5%) receiving concomitant chemotherapy with 5-fluorouracil in continuous 96 hours infusion and cisplatin. The main endpoints of the study were overall survival (OS; death of any cause), loco-regional control (LRC; local and/or regional disease recurrence) and disease-free survival (DFS; recurrence of any kind and/or new primary malignoma). Univariate analysis testing the impact of different parameters on survivals and analysis of treatment related side effects were performed as well.

Results. The mean age of patients was 62 years (SD 9 years; range: 29–80 years). Majority of them had squamous cell cancer (53 patients; 96.4%) in the stage T3 or T4 (47 patients; 85.5%) and/or N+ disease (35 patients; 63.6%). Median follow-up time for the whole group of patients was 16.8 months (range: 0.3–81.8 months). At the time of analysis 14 (25.5%) patients were still alive. Rates for OS, LRC and DFS at two and five years were as follows: 47% and 19.4%; 43.7% and 41%; 32.1% and 11.5%, respectively.

Conclusions. The study results of treatment with definitive radiochemotherapy in patients with esophageal cancer are similar to the results of other studies. Majority of patients ended the treatment according to the protocol, which at least in part can be attributed to the adequate and well organized supportive treatment in our institution.

Key words: esophageal cancer; definitive radiochemotherapy; survival; loco-regional control

Introduction

Nowadays, the preoperative radiochemotherapy (pRCT) followed by surgery is the standard treatment for squamous cell cancer and adenocarcinoma of the esophagus in the stage ≥ T1b–2N0M0, with perioperative chemotherapy being one of the treatment options for adenocarcinoma, as well.[1,2] Based on the results of the RTOG 85-01 study, since the late nineties of the last century, definitive radiochemotherapy (dRCT) became another viable treatment option for patients with locoregionally advanced esophageal cancer.[3] It is reserved for the patients who are not fit for surgery or decline it and is a preferable treatment option for patients with tumors located in the upper third of the esophagus (cervical tumors), since surgery procedures in these patients can be associated with significant postoperative morbidity and mortality.[1,2] Before that, patients with inoperable esophageal cancer

were usually treated with paliative intent or best supportive care only. Survival results for pRCT followed by surgery can reach up to 50% at five years with a locoregional control rate of up to 85%.[4] For dRCT five year survival is around 25% and locoregional control is about 40–60%.[5] In recent years, in patients treated with dCRT, there was not much improvement in survivals, but with multidisciplinary approach, use of modern radiotherapy techniques (such as intensity modulated radiotherapy [IMRT] or volumetric arc therapy [VMAT]) and different chemotherapy regimens given (paclitaxel/carboplatin), there was improvement in reducing treatment related toxicity with consequent better quality of life during and after the treatment.[1,2,6-8]

In Slovenia, in all newly diagnosed esophageal cancer patients, the treatment decisions are provided by multidisciplinary board committees. If the treatment with radical intent is proposed, all the patients are treated in the Institute of Oncology Ljubljana (IOL) which provides the chemo- and radiotherapy part of the treatment protocols and/or in the University Clinical Centers in Ljubljana and Maribor, where surgical procedures are performed. The selection of patients suitable for dCRT is based on the results of pretreatment diagnostic procedures (tumor location, histology, TNM stage), performance stage (WHO stage ≤ 2) and eventual comorbidities (*e.g.* significant renal, hepatic or bone marrow impairment), which could have an impact on the chemotherapy given.

The aim of this retrospective study was to evaluate the treatment results of dRCT for patients treated in the IOL in the period from the beginning of 2010 to the end of 2017.

Patients and methods

Patients and tumors

According to the data of Cancer Registry of Republic of Slovenia and hospital based Cancer Registry of the IOL, in the period from 2010 to 2017, 412 new patients with esophageal cancer were referred for the treatment to the IOL. Of these, based on the multidisciplinary board committee's decision, 55 (13.3%) patients were treated with dRCT with curative intent. Others were treated with pRCT, systemic treatment only or with palliative intent. All available medical data (including demographical data, pretreatment characteristics, treatment specifics and treatment related side effects) of patients treated with dCRT were collected retrospectively. The TNM stage was based on NCCN 7th tumor staging edition. In 1 (1.8%) patient the disease was staged as M1 with neck lymph nodes considered as metastatic, all other patients had a non-metastatic disease. At the start of the treatment 8 (14.5%) patients had synchronous esophageal and different head and neck cancers and 1 (1.8%) patient had synchronous esophageal and operable colon cancers.

Radiotherapy and chemotherapy

All patients were treated on one of IOL's linear accelerators with high energy photons. The total dose to the tumor was defined according to the position of the primary tumor. Patients with tumors located exclusively in the upper third of the esophagus (cervical tumors) were irradiated to the total dose of 70 Gy (2 Gy per fraction), whereas in patients with the intrathoracic tumors (middle third), the prescribed median total dose to the primary tumor was 57.6 Gy in 1.8 Gy per fraction. The radiation techniques varied according to the time period: 3-D treatment planning was used for patients treated in 2010 and the first half of 2011, IMRT technique with single dose level to the planning target volume from the second half of 2011 onward and VMAT or IMRT with synchronous integrated boost (IMRT-SIB) techniques with two or three dose levels for patients treated from 2015 onward. All but one patient received some sort of concomitant chemotherapy, as well. The sort and intensity of the applied chemotherapy varied according to patients' general condition and comorbidities or eventual synchronous cancer.

Endpoints

The main endpoints of the study were overall survival (OS; death of any cause), locoregional control (LRC; local and/or regional disease recurrence) and disease-free survival (DFS; recurrence of any kind and/or new primary malignoma). Data on treatment related side effects were analyzed as well.

Statistics

Statistical analysis was performed using software statistical package SPSS (SPSS Inc., USA). The survival of patients was computed from the date of diagnosis to the close-out date (February 8th, 2019). Survival probability was calculated using Kaplan-Meyer estimate. Univariate analysis was performed as well, with log-rank test used to evaluate the differences between individual groups of

patients and p-value of ≤ 0.05 considered as statistically significant. If any of tested parameters would prove as statistically significant, multivariate analysis (with 95% confidence intervals specified and risk ratios calculated) was planned as well.

The study was approved by the Institutional Review Board Committee and has been conducted in accordance with the declaration of Helsinki.

Results

Patients and tumors

The mean age of 55 patients included in the study was 62 years (SD 9 years, range: 29-80 years). Majority of patients were male (45 patients – 81.8%) in a good performance status (WHO performance stage 0-1 in 50 patients – 90.9%) and had squamous cell cancer (53 patients - 96.4%) in the stage T3 or T4 (47 patients - 85.5%) and/or N+ disease (35 patients - 63.6%). Patients' and tumors' characteristics are presented in Table 1.

The mean time from the onset of symptoms to diagnosis was 17.2 weeks (range 4–56 weeks). At diagnosis 4 (7.3%) patients had no problems swallowing, 11 (20%) had problems with swallowing solid food, 32 (58.1%) could only swallow soft food or liquids, 6 (10.9%) were aphagic and for 2 (3.6%) patients no data on swallowing status was available. Before the start of dRCT 33 (60%) patients needed surgical intervention for establishing the adequate nutritional pathway; in 1 dilation of primary tumor's stenosis was performed, in 6 patients an esophageal stent was placed on the site of the primary tumor and in 26 patients gastric or jejunal feeding tube was inserted. In 6 (10.9%) patients no weight loss was detected before the start of the specific treatment, 11 (20%) patients lost ≤ 5% of the baseline weight, 8 (14.5%) patients lost 5–10% of the baseline weight and 24 (34.6%) patients lost > 10% of the baseline weight. All patients were presented at the multidisciplinary board committee for the decision on the sort of specific treatment. The median time from diagnosis to the start of any kind of specific treatment was 5.7 weeks (range: 2–18.6 weeks).

TABLE 1. Patients' and tumors' characteristics

	N (%)
Gender	
male	45 (81.8)
female	10 (18.2)
Age at diagnosis (years)	mean: 62 (SD 9 years, range: 29–80 years)
WHO performance stage	
0	24 (43.6)
1	26 (47.3)
2	5 (9.1)
Risk factors	
none	13 (23.6)
active or ex-smokers	31 (56.4)
gastroesophageal reflux	2 (3.6)
gastroesophageal reflux and smoking	3 (5.5)
unknown	6 (10.9)
T stage	
T X	1 (1.8)
T 1	1 (1.8)
T 2	6 (10.9)
T 3	36 (65.5)
T 4	11 (20)
N stage	
N 0	20 (36.4)
N 1	20 (36.4)
N 2	12 (21.8)
N 3	3 (5.5)
Histology	
squamous cell cancer	53 (96.4)
adenocarcinoma	1 (1.8)
verified carcinoma, unspecified	1 (1.8)
Grade	
G 1	3 (5.5)
G 2	28 (50.9)
G 3	12 (21.8)
unknown or not specified	12 (21.8)
Upper border of the tumor	
≤ 18 cm from the incisors	32 (58.2)
18–32 cm from the incisors	23 (41.8)

SD = standard deviation

Radiochemotherapy

Definitive radiochemotherapy was advised by multidisciplinary board committee in 49 (89.1%) patients and in 6 (10.9%) patients pRCT was proposed. In these 6 patients, after completion of the preoperative treatment with radiochemotherapy with the total dose of 45 Gy (1.8 Gy per fraction) to the tumor bed, 1 patient refused the proposed surgical procedure and in the remaining 5 patients, the surgery was declined according to thoracic surgeons' decisions based on evaluation diagnostic procedures. Four patients were treated with additional radiochemotherapy and in 2 patients only careful follow up was advised. The radiation techniques used were as follows: in 6 (12.2%) patients 3-D treatment planning was used, in 11 (22.4) patients IMRT and in 32 (58.1%) patients VMAT or IMRT-SIB, respectively. PET-CT for treatment planning was used in 25 (45.5%) patients. Median total radiation dose applied to the tumor bed was 57.6 Gy (range: 23.4–70 Gy), the median number of fractions was 32 (range: 13–36 fractions) and the median duration of the radiotherapy treatment was 45 days (range: 17–57 days). In none of the patients, the correction of total dose to the tumor bed due to

TABLE 2. Different chemotherapy regimens used

Chemotherapy regimen used	N (%)
5-FU in continuous 96 hours infusion + cisplatin	41 (74.5)
Weekly cisplatin only during RT	3 (5.5)
Paclitaxel + carboplatin	2 (3.6)
5-FU + carboplatin	2 (3.6)
Induction TCF followed by weekly cisplatin during RT	1 (1.8)
Induction 5-FU + cisplatin followed by weekly carboplatin during RT	1 (1.8)
Induction paclitaxel + carboplatin followed by weekly carboplatin during RT	1 (1.8)
Induction weekly cisplatin followed by weekly carboplatin during RT	1 (1.8)
Induction paclitaxel + carboplatin followed by 5-FU + cisplatin during RT	1 (1.8)
Induction capecitabine + cisplatin followed by weekly cisplatin during RT	1 (1.8)
No chemotherapy given	1 (1.8)

FU = fluorouracil; RT = radiotherapy; TCF = docetaxel, cisplatin and 5-FU

TABLE 3. Side effects of concomitant radiochemotherapy (according to EORTC Common Toxicity Criteria version 4)

Side effect	Grade			
	0	1	2	3
Esophagitis	6 (10.9)	21 (38.2)	17 (30.9)	10 (18.2)
Radiodermatitis	35 (63.3)	8 (14.5)	7 (12.7)	4 (7.3)
Nausea	40 (72.7)	9 (16.4)	4 (7.3)	1 (1.8)
Vomiting	50 (90.9)	1 (1.8)	3 (5.5)	0
Neutropenia	25 (45.5)	8 (14.5)	10 (18.2)	12 (21.8)
Thrombocytopenia	20 (36.4)	21 (38.2)	8 (14.5)	6 (10.9)
Anemia	6 (10.9)	27 (49.1)	21 (38.2)	1 (1.8)

TABLE 4. Median, two- and five years survivals

	OS	LRC	DFS
Median	20.5 months (95% CI 8.2–32.8)	16.6 months (95% CI 7.3–26)	12.9 months (95% CI 9.8-16.1)
2-year	47%	43.7%	32.1%
5-year	19.4%	41%	11.5%

CI = confidence interval; DFS = disease-free survival; LRC = locoregional control; OS = overall survival

toxic side effects of the treatment was needed. One patient finished the intended treatment prematurely after receiving 23.4 Gy because of severe deterioration of general performance status due to comorbidities and continued with palliative treatment in a regional general hospital. Another patient finished with radiochemotherapy prematurely after receiving the dose of 48 Gy due to esophagus perforation, which in our opinion was not attributed to the treatment received but was one of the possible rare complications in the natural course of the disease. All, but 1 patient also received some sort of concomitant chemotherapy, with the majority of them (41 patients; 74.5%) receiving concomitant chemotherapy with 5-fluorouracil (5-FU) in continuous 96 hours infusion and cisplatin. Ten different chemotherapy regimens used are presented in Table 2. The median number of chemotherapy applications received was 3 (range: 0–8 applications). In 45 (81.8%) patients no adjustment of the dose or number of chemotherapy applications was needed, whereas in the remaining 9 (16.4%) patients chemotherapy regimen was adjusted due to treatment toxic side effects (renal impairment and/or neutropenia and/or thrombocytopenia).

Treatment side effects, which were graded according to EORTC Common Terminology Criteria for Adverse Events (CTCAE) version 4, are presented in Table 3.[9] At least one side effect of concomitant radiochemotherapy of any grade was recorded in all patients. Twenty-two (40%) patients had at least one side effect of grade III, with most common side effects of grade III being neutropenia in 12 (21.8%) and esophagitis in 10 (18.2%) patients. One treatment related death was recorded immediately after the completion of radiotherapy treatment due to fistula formation on the place of esophageal stent inserted before the start of radiochemotherapy, with consequent massive bilateral bronchopneumonia and cardiorespiratory failure.

Because of the treatment related side effects and/or severe deterioration of alimentary status 33 (60%) patients were hospitalized during radiotherapy for supportive treatment. During the treatment 25 (45.5%) patients received peroral nutritional supplements, 29 (52.7%) parenteral supplements and 1 (1.8%) patient didn't need any kind of nutritional support. Based on the weight at the start of the treatment, at the end of the specific treatment, no weight loss was recorded in 18 (32.7%) patients, 17 (30.9%) patients lost ≤ 5% of the weight, 7 (12.7%) patients 5–10% of the weight and in 9 (16.4%) patients the weight loss of > 10% was recorded. No data on the weight loss during the treatment was available in 4 (7.3%) patients. During or after the completion of dRCT 16 (29.2%) patients needed surgical intervention; in 4 dilation on the place of primary tumor was performed, in 3 esophageal stent was placed on the site of the pri-

TABLE 5. Results of univariate analysis testing the impact of different parameters on survivals

	OS (p)	LRC (p)	DFS (p)
Gender: male (N = 45) female (N = 10)	0.16	0.46	0.63
Age: ≤ 62 years (N = 29) > 62 years (N = 26)	0.16	0.6	0.85
WHO performance stage: 0–1 (N = 50) 2 (N = 5)	0.99	0.78	0.95
Risk factors: none present (N = 19) at least one present (N = 36)	0.67	0.24	0.23
Tumor localization: upper third - cervical (N = 32) middle third - intrathoracic (N = 23)	0.18	0.56	0.57
T stage: T 1+2 (N = 8) T 3+4 (N = 47)	0.38	0.76	0.37
N stage: N0 (N = 20) N+ (N = 35)	0.79	0.22	0.42
Treatment schedule: definitive radiochemotherapy (N = 49) preoperative radiochemotherapy without surgery and completion of the treatment with additional radio(chemo) therapy (N = 6)	0.66	0.55	0.46
TD on tumor: ≤ 57.6 Gy (N = 35) > 57.6 Gy (N = 20)	0.61	0.52	0.79

DFS = disease-free survival; LRC = locoregional control; OS = overall survival; p = p value; TD = total dose

mary tumor, in 1 patient a stent was placed in the trachea due to the formation of tracheoesophageal fistula and in 8 patients gastric or jejunal feeding tube was inserted.

Survival

Median follow-up time for the whole group of patients was 16.8 months (range: 0.3–81.8 months). At the time of analysis 14 (25.5%) patients were still alive. Of 41 (74.5%) patients who died, 31 died due to the esophageal cancer, 6 of other causes and for 4 patients no data on the cause of death was available. Median survivals and survivals at two and five years are presented in Table 4 and survival curves in Figures 1–3.

In univariate analysis none of the tested parameters reached statistical significance for their impact on survivals (Table 5). Therefore, multivariate analysis was not performed.

After the end of the treatment, the recurrence of the disease was recorded in 35 (63.6%) patients in the median time of 6.2 months (range: 0–57.8 months). The disease recurred locally in 26 (72.2%) patients, regionally in 15 (42.8%) patients and in 14 (40%) patients systemic spread was detected. Ten (28.6%) patients received some sort of additional specific treatment and in others best supportive care was advised by the multidisciplinary board committee.

Discussion

Esophageal cancer is a disease which predominantly affects older men with a history of smoking and alcohol abuse (squamous cell cancer) or patients with obesity and history of gastroesophageal reflux and/or Barret's esophageal metaplasia (adenocarcinoma).[7] Nowadays, dRCT is one of the possible treatment strategies used in esophageal cancer of both histologies. The indications for its use are well defined in national and international guidelines for the treatment of patients with esophageal cancer.[1,2,10] It is reserved for patients with inoperable tumors of the lower two thirds of the esophagus, patients who decline surgery and is a preferable treatment option in patients with tumors located in the cervical esophagus. Since dRCT can be accompanied by serious treatment side-effects, the careful selection of patients is necessary. In our group of patients, 58.2% of them had tumors in the cervical esophagus and/or synchronous head and neck cancers and in the remaining 23 patients, the tumor was locally advanced (T3 or T4) in 20 (86.9%) patients. 90.9% of all the patients included in our study were in a good general performance (performance stage 0-1 according to WHO scale). In the retrospective study of Haefner *et al*. in the group of 93 patients treated with dCRT the tumor was located in cervical, upper or mid esophagus in 66.7% of patients.[11] Seventy-two (77.2%) patients had T3-4 tumors and most of them were in a relatively good general condition with the mean Karnofsky performance status of 86 (range: 70–100).

Because of the natural course of the disease which primarily affects the swallowing, special attention needs to be addressed to patients' pretreatment evaluation of alimentary status and adequate nutritional support during the treatment.[12] In our group of patients, 49 (89.1%) patients had problems with swallowing and/or were aphagic at diagnosis and consequently in 60% of patients some kind of surgical intervention (dilation or esophageal stent insertion or gastric-/jejunal feeding tube insertion) was needed before the start of dRCT. In the study of Bedenne *et al*., in patients treated with

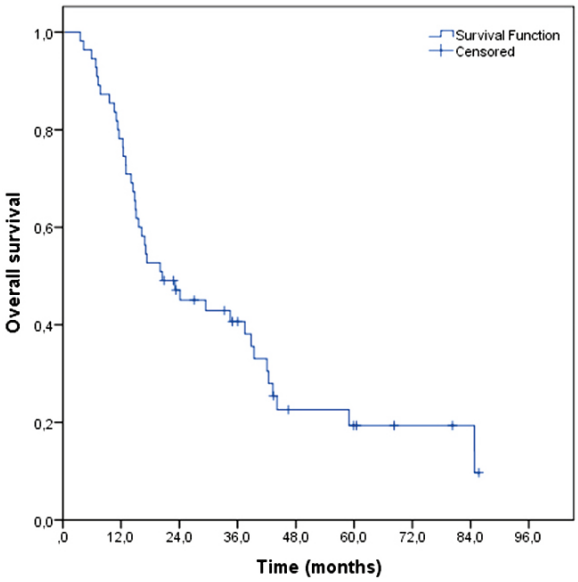

FIGURE 1. Overall survival curve.

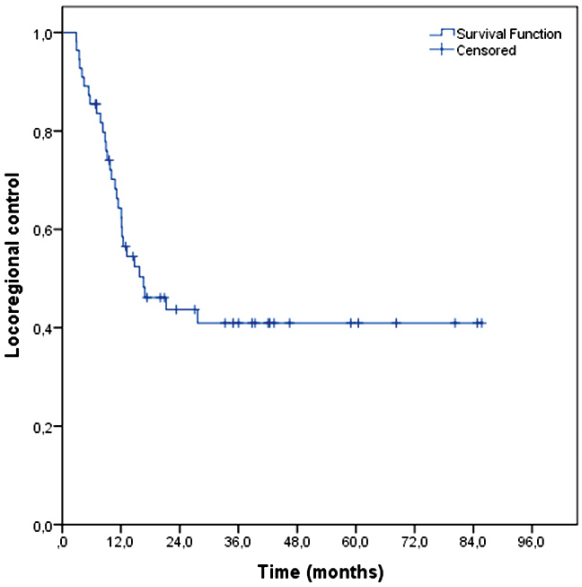

FIGURE 2. Locoregional control curve.

dCRT, 90.8% had problems swallowing before the start of any treatment.[13] However, no data on surgical procedures performed before the start of the treatment to establish adequate nutritional pathway is reported. During dRCT all the patients were carefully monitored by attending physician and the staff of IOL's supportive care Unit for clinical nutrition and diethotherapy, as well. In this way, we were able to select patients who needed special attention. All but one patient received either peroral or parenteral nutritional supplements during treatment and 60% of all the patients were hospitalized during dRCT for appropriate supportive treatment. Good supportive care reflects in the facts that in only 29.1% of all the patients the additional weight loss of >5% was recorded during treatment and that majority of patients could complete their treatment with the intended radiation dose to the primary tumor.

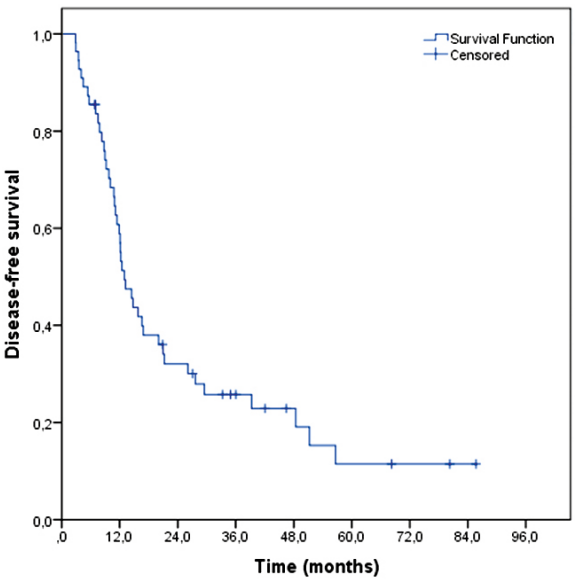

FIGURE 3. Disease-frees survival curve.

All but one patient included in the study received some sort of concomitant chemotherapy during irradiation, with 10 different chemotherapy schedules being used (see Table 2). The sort of chemotherapy used was determined by the multidisciplinary board committee's decision taking into account the extent of the disease, patients' general condition, comorbidities and possible synchronous tumors (8 patients with synchronous esophageal and head and neck cancers and 1 patient with synchronous esophageal and colorectal cancers). The intensity of applied chemotherapy was adjusted because of the comorbidity and/or treatment related side effects (renal impairment and/or changes in blood count) in 16.4% of patients. All others received the dose planned at the start of the treatment, which at least in part can be attributed to the good supportive care during the treatment. Majority of patients (74.5%) in our study received concomitant chemotherapy with 5-FU in continuous 96 hours infusion and cisplatin which in many countries is still the gold standard in dRCT, although according to the results of CROSS trial, nowadays many authors believe that concomitant chemotherapy with paclitaxel and carboplatin should be used in dRCT as well.[6,14]

In our study the total dose of 70 Gy to the primary tumor (in fractions of 2 Gy) was used in patients with tumors located exclusively in the upper third of the esophagus, whereas in patients with cervical tumors which extended in the thorax or with intrathoracic tumors, in order to avoid unacceptable toxicity, different fractionations were used with the median total dose to the primary tumor of 57.6 Gy in 32 fractions. Today, the topic of the radiation dose in dRCT is still controversial and highly debated. In the USA doses of 50-50.4 Gy are advised although many authors believe that, in order to increase the chance of better local control and survival, higher doses to the primary tumor should be used, which indeed is the case in Europe and some other parts of the world. [1,2,5,7,15]

The treatment with dRCT in our group of patients was relatively well tolerated. As expected with such a treatment, in all the patients at least one treatment side effect was recorded (Table 3), with 40% of patients having at least one side effect of grade III. The most common side effects of grade III were neutropenia in 21.8% and esophagitis in 18.2% of patients, which is concordant with the data from the literature.[7,8] However, despite the treatment related side effects and because of good supportive treatment, the tolerability of the treatment in our group of patients was good, since majority of patients received the prescribed radiation dose to the tumor and in only 9 (16.4%) patients any kind of adjustments on the dose and/or number of chemotherapy applications were needed. One treatment related death was recorded at the end of dRCT in the patient in whom tracheoesophageal fistula formed on the place of esophageal stent inserted before the start of the dRCT. The problem of dose perturbations in the area of inserted metallic stents is well known.[16] In our opinion, due to the relatively high radiation dose applied to the primary tumor, insertion of metallic stents before the start of the dRCT should be avoided. However, since no clinical reports on effects of stents on radiotherapy dose distribution in esophageal cancer exist, any clinical recommendations should be made with caution.

The OS in our group of patients (19.4% - see Table 4) was a bit lower if compared with the results from the literature, according to which the 5-years OS after dRCT is around 25%. On the other hand, 5-year LRC of 41% in our study, is concordant with the data from the literature with 5-year LRC after dRCT of 40-60%.[3,17-20] The slightly lower OS in our study can be attributed to unfavourable stage distribution since 85.5% of our patients had T3 or T4 disease and 63.6% N+ disease and the fact that of 35 patients in whom the recurrence of the disease was recorded, only 10 patients received some sort of additional specific treatment. In esophageal cancer some of the factors (such us gender, age at diagnosis, T and N stage, WHO performance stage, radiation dose received, etc.) are well recognized as the risk factors for worse treatment outcome.[7,21,22] However, in our study in univariate analysis none of the analyzed factors reached statistical significance for their impact on survivals, which in our opinion can be attributed to relatively small overall number of patients and uneven distribution of patients in different subgroups tested.

Conclusions

Our results of treatment with definitive radiochemotherapy in patients with esophageal cancer are concordant with the results of other studies. Due to the high intensity of existing treatment protocols, multidisciplinary approach with adequate supportive treatment is needed, and in our opinion treatment of patients with dCRT should be centralized and performed in institutions with sufficient experience and workload. Majority of our patients ended the treatment according to the protocol, which at least in part can be attributed to the adequate and well organized supportive treatment in our institution. However, the results of dRCT in general are still not satisfactory. With the increasingly widespread use of modern radiotherapy treatment techniques, such as IMRT or VMAT, there is not much room for improvement in radiotherapy part of the treatment protocols. Most probably there is still room for improvement in systemic treatment in means of intensifying chemotherapeutics given and/or with the addition of target drugs and immunotherapy, but further prospective studies addresing this subject are needed.

References

1. NCCN clinical practice guidelines in oncology (NCCN Guidelines®). Esophageal and esophagogastric junction cancers, version 1. 2019. [cited 2019 Jan 15]. Available at: https://www.nccn.org/professionals/physician_gls/pdf/esophageal.pdf
2. Lordick F, Mariette C, Haustermans K, Obermannova R, Arnold D. Oesophageal cancer: ESMO clinical practice guidelines for diagnosis, treatment and follow-up. *Ann Oncol* 2016; **27(Suppl 5):** v50-7. doi: 10.1093/annonc/mdw329
3. Cooper JS, Guo MD, Herskovic A, Macdonald JS, Martenson JA, Al-Sarraf M, et al. Chemoradiotherapy of locally advanced esophageal cancer: long-term follow-up of a prospective randomized trial (RTOG 85-01). Radiation Therapy Oncology Group. *JAMA* 1999; **281:** 1623-7. doi: 10.1001/jama.281.17.1623

4. van Hagen P, Hulshof MCCM, van Lanschot JJB, Steyerberg EW, van Berge Henegouwen MI, Wijnhoven BPL, et al. Preoperative chemoradiotherapy for esophageal or junctional cancer. *N Engl J Med* 2012; **366:** 2074-84. doi: 10.1056/NEJMoa1112088

5. Jeene PM, van Laarhoven HWM, Hulshof MCCM. The role of definitive chemoradiation in patients with non-metastatic oesophageal cancer. *Best Pract Res Clin Gastroenterol* 2018; **36-37:** 53-9. doi: 10.1016/j.bpg.2018.11.011

6. Shapiro J, van Lanschot JJB, Hulshof MCCM, van Hagen P, van Berge Henegouwen MI, Wijnhoven BPL, et al. Neoadjuvant chemoradiotherapy plus surgery versus surgery alone for oesophageal or junctional cancer (CROSS): long-term results of a randomised controlled trial. *Lancet Oncol* 2015; **16:** 1090-8. doi: 10.1016/S1470-2045(15)00040-6

7. Czito BG, DeNittis AS, Palta M. Esophageal Cancer. In: Halperin EC, Wazer DE, Perez CA, Brady LW, editors. *Principles and practice of radiation oncology*. 6th edition. Philadelphia: Lippincott Williams&Wilkins; 2013. p. 995-1023.

8. Adebahr S, Schimek-Jasch T, Nestle U, Brunner TB. Oesophagus side effects related to the treatment of oesophageal cancer or radiotherapy of other thoracic malignancies. *Best Pract Res Clin Gastroenterol* 2016; **30:** 565-80. doi: 10.1016/j.bpg.2016.07.003

9. Common Terminology Criteria for Adverse Events (CTCAE), version 4.0. [cited 2019 Jan 15]. Available at: https://www.eortc.be/services/doc/ctc/CTCAE_4.03_2010-06-14_QuickReference_5x7.pdf

10. Guidelines for the treatment of esophageal and esophagogastric junction cancers. [Slovenian]. Anderluh F, But Hadžić J, Crnjac A, Gačevski G, Hlebanja Z, Jeromen A, et al, editors. [cited 2019 Jan 15]. Available at: https://www.onko-i.si/fileadmin/user_upload/Smernice_za_zdravljenje_raka_poziralnika_in_EGS_splet.pdf

11. Haefner MF, Lang K, Verma V, Koerber SA, Uhlmann L, Debus J, et al. Neoadjuvant versus definitive chemoradiotherapy for locally advanced esophageal cancer. Outcomes and patterns of failure. *Strahlentherapie Oncol* 2018; **194:** 116-24. doi: 10.1007/s00066-017-1211-0

12. Jordan T, Mastnak DM, Palamar N, Kozjek NR. Nutritional therapy for patients with esophageal cancer. *Nutr Cancer* 2018; **70:** 23-9. doi: 10.1080/01635581.2017.1374417

13. Bedenne L, Michel P, Bouche O, Milan C, Mariette C, Conroy T, et al. Chemoradiation followed by surgery compared with chemoradiation alone in squamous cancer of the esophagus: FFCD 9201. *J Clin Oncol* 2007; **25:** 1160-8. doi: 10.1200/JCO.2005.04.7118

14. Tomasello G, Ghidini M, Barni S, Passalacqua R, Petrelli F. Overview of different available chemotherapy regimens combined with radiotherapy for the neoadjuvant and definitive treatment of esophageal cancer. *Expert Rev Clin Pharmacol* 2017; **10:** 649-60. doi: 10.1080/17512433.2017.1313112

15. Luo Y, Mao Q, Wang X, Yu J, Li M. Radiotherapy for esophageal carcinoma: dose, response and survival. *Cancer Manag Res* 2017; **10:** 13-21. doi: 10.2147/CMAR.S144687

16. Li XA, Chibani O, Greenwald B, Suntharalingam M. Radiotherapy dose perturbation of metallic esophageal stents. *Int J Radiat Oncol Biol Phys* 2002; **54:** 1276-85. doi: 10.1016/S0360-3016(02)03803-8

17. Stahl M, Stuschke M, Lehkmann N, Meyer H-J, Walz MK, Seeber S, et.al. Chemoradiation with and without surgery in patients with locally advanced squamous cell carcinoma of the esophagus. *J Clin Oncol* 2005; **23:** 2310-7. doi: 10.1200/JCO.2005.00.034

18. Minsky BD, Pajak TF, Ginsberg RJ, Pisansky TM, Martenson J, Komaki R, et al. INT 0123 (Radiation Therapy Oncology Group 94-05) phase III trial of combined-modality therapy for esophageal cancer: high dose versus standard-dose radiation therapy. *J Clin Oncol* 2002; **20:** 1167-74. doi: 10.1200/JCO.2002.20.5.1167

19. Versteijne F, van Laarhoven HWM, van Hooft JE, van OS RM, Geijsen ED, van Berge Henegouwen MI, et al. Definitive chemoradiation for patients with inoperable and/or unresectable esophageal cancer: locoregional recurrence pattern. *Dis Esophagus* 2015; **28:** 453-9. doi: 10.1111/dote.12215

20. Teoh AYB, Chiu PWY, Yeung WK, Liu SYW, Wong SKH, Ng EKW. Long-term survival outcomes after definitive chemoradiation versus surgery in patients with resectable squamous carcinoma of the esophagus: results from a randomized controlled trial. *Ann Oncol* 2013; **24:** 165-71. doi: 10.1093/annonc/mds206

21. Huang FL, Yu SJ. Esophageal cancer: Risk factors, genetic association, and treatment. *Asian J Surg* 2018; **41:** 210-5. doi: 10.1016/j.asjsur.2016.10.005

22. Domper Arnal MJ, Ferrandez Arenas A, Lanas Arbeloa A. Esophageal cancer: Risk factors, screening and endoscopic treatment in Western and Eastern countries. *World J Gastroenterol* 2015; **21:** 7933-43. doi: 10.3748/wjg.v21.i26.7933

research article

Dose-volume derived nomogram as a reliable predictor of radiotherapy-induced hypothyroidism in head and neck cancer patients

Marin Prpic[1,2], Ivan Kruljac[3], Davor Kust[1], Petar Suton[2,4], Neva Purgar[1], Lora Kirigin Bilos[3], Marin Gregov[1], Iva Mrcela[1], Maja Franceschi[1,2,5], Nikola Djakovic[1,2], Ana Frobe[1,6]

[1] Department of Oncology and Nuclear Medicine, University Hospital Center Sestre Milosrdnice, Zagreb, Croatia
[2] School of Medicine, University of Zagreb, Zagreb, Croatia
[3] Department of Endocrinology, Diabetes and Metabolic Diseases Mladen Sekso, University Hospital Center Sestre Milosrdnice, Zagreb, Croatia
[4] Department of Radiotherapy and Medical Oncology, University Hospital for Tumors, University Hospital Center Sestre Milosrdnice, Zagreb, Croatia
[5] Faculty of Medicine, Josip Juraj Strossmayer University of Osijek, Osijek, Croatia
[6] School of Dental Medicine, University of Zagreb, Zagreb, Croatia

Radiol Oncol 2019; 53(4): 488-496.

Received 31 July 2019
Accepted 4 October 2019

Correspondence to: Marin Prpić, M.D., Ph.D., Department of Oncology and Nuclear Medicine, University Hospital Center Sestre Milosrdnice, Vinogradska cesta 29, 10000 Zagreb, Croatia. E-mail: marin.prpic@kbcsm.hr

Disclosure: No potential conflicts of interest were disclosed.

Background. The aim of this study was to determine the possible predictive value of various dosimetric parameters on the development of hypothyroidism (HT) in patients with head and neck squamous cell carcinoma (HNSCC) treated with (chemo)radiotherapy.

Patients and methods. This study included 156 patients with HNSCC who were treated with (chemo)radiotherapy in a primary or postoperative setting between August 2012 and September 2017. Dose-volume parameters as well as V10 toV70, D02 to D98, and the VS10 to VS70 were evaluated. The patients' hormone status was regularly assessed during follow-up. A nomogram (score) was constructed, and the Kaplan-Maier curves and Log-Rank test were used to demonstrate the difference in incidence of HT between cut-off values of specific variables.

Results. After a median follow-up of 23.0 (12.0–38.5) months, 70 (44.9%) patients developed HT. In univariate analysis, VS65, Dmin, V50, and total thyroid volume (TTV) had the highest accuracy in predicting HT. In a multivariate model, HT was associated with lower TTV (OR 0.31, 95% CI 0.11–0.87, P = 0.026) and Dmin (OR 9.83, 95% CI 1.89–108.08, P = 0.042). Hypothyroidism risk score (HRS) was constructed as a regression equation and comprised TTV and Dmin. HRS had an AUC of 0.709 (95% CI 0.627–0.791). HT occurred in 13 (20.0%) patients with a score < 7.1 and in 57 (62.6%) patients with a score > 7.1.

Conclusions. The dose volume parameters VS65, Dmin, V50, and TTV had the highest accuracy in predicting HT. The HRS may be a useful tool in detecting patients with high risk for radiation-induced hypothyroidism.

Key words: head and neck cancer; thyroid; radiation therapy; hypothyroidism; dose volume parameters

Introduction

A significant proportion of patients with head and neck squamous cell carcinoma (HNSCC) are treated with radiation therapy at some point during their disease. Despite the use of modern techniques and advances in radiotherapy delivery, the dose at organs at risk (OARs) in the head and neck region

is not negligible, and may result in significant side effects, such as oral mucositis, xerostomia, osteoradionecrosis, radiodermatitis and dysphagia.[1] The thyroid gland, as an OAR, is frequently involved in the treatment field due to its midline neck position, and the dose it receives often exceeds 50 Gy.[2] Thus, one of the potential consequences of neck irradiation is development of various thyroid disorders, mainly hypothyroidism (HT), which occurs in up to 50% of patients treated with radiotherapy for HNSCC.[3-5] HT is a subacute or chronic side effect of radiotherapy, with the time to development usually between 6 and 24 months after treatment. However, HT is often unpredictable and can develop at any time after completion of radiotherapy, with data showing a rising incidence with longer follow-up periods.[6]

Despite the growing body of evidence regarding possible damage to the thyroid during radiotherapy, there is still no generally accepted consensus on dose-volume parameters and constraints that could be used to spare the thyroid gland.[2,7-9] Moreover, the threshold dose on the thyroid gland, and the relationship between the radiation dose and induction of HT as the most important thyroid disorder resulting from radiotherapy is not well established.[10-12]

The aim of this study was to determine the possible predictive value of various dosimetric (dose-volume) parameters and clinical characteristics on the development of HT in patients with HNSCC treated with radiotherapy. Also, an additional effort was made to identify a subgroup of patients at high risk for HT development, using a combination of different factors (dose-volume nomogram).

Patients and methods

Patient selection

This study included 156 patients with HNSCC who were treated with (chemo) radiotherapy in a primary or postoperative setting between August 2012 and September 2017. Only clinically euthyroid patients were included in the study. Thyroid function was assessed during the pre-treatment diagnostic workup in all patients by evaluating the presence of thyroid-related symptoms and checking medical history, to identify possible pre-existing thyroid dysfunction. In patients with suspected HT, additional blood tests including thyroid-stimulating hormone (TSH), free thyroxine (fT4) / thyroxine (T4), and free triiodothyronine (fT3) / triiodothyronine (T3) were performed. Exclusion criteria were total thyroidectomy prior to the start of radiotherapy, patients who had irradiation to the head and neck in the past, and formerly detected thyroid disease. Additionally, patients receiving palliative radiotherapy or those with distant metastases were not included in the study, due to shorter life expectancy and thus insufficient time to develop HT. All included patients were regularly followed-up after the completion of therapy, and the study cut-off date for follow-up was March 31st 2018.

The study was conducted in accordance with ethical standards set by the institutional Ethics Committee and the Helsinki Declaration from 1975, as revised in 1983. Informed consent was not needed because all patients were treated according standard protocol used in HNSCC in our department. Thyroid gland contouring during the radiotherapy planning process, and analysis of its dosimetric parameters were two additional (non-standard) procedures, without effect on patient treatment.

Treatment

Prior to the start of radiotherapy, all patients underwent the radiation planning session (simulation) using computed tomography (CT, Toshiba Aquillion, Shimoishigami, Otawara- shi, Tochigi–ken, Japan), as per the institutional protocol. A thermoplastic mask (Orfit) with 5-point fixation was used for head and neck immobilization to ensure a reproducible setup. CT scan images were obtained at 2–3 mm slice thickness. After simulation, the data was transferred to the contouring system and the treatment planning system (Elekta Focal, XiO Maryland Heights, USA). Treatment was delivered using a linear accelerator (Elekta Synergy S, Elekta, Maryland Heights, USA) with 6 MV photons. Cone-beam CT was used before the first three fractions of radiotherapy and once per week afterwards for patient setup verification. Patients with adverse histopathological features (positive margins, perineural invasion, extranodal extension (ENE), multiple positive lymph nodes, stage pT3 or pT4) underwent postoperative irradiation. A dose of 46–50 Gy was given to the histologically negative and clinically undissected neck levels in daily fractions of 2 Gy. A boost of 60 Gy was applied to the tumor bed and metastases confined to the lymph node and a dose of 62–66 Gy was applied to regions of the neck with ENE and/or close/involved margins. These latter two features were indications for the addition of chemotherapy to adjuvant irradiation (concurrent chemoradiother-

apy). The chemotherapy regimen was cisplatin 80-100 mg/m^2 on days 1, 22, and 43. Patient treatment planning was done using the Elekta XiO planning system with the three-dimensional conformal radiotherapy ConPass technique[13], with an accepted planning goal of at least 95% of the planning target volume receiving more than 95% of the prescribed dose. The maximum dose was constrained to 107% of the prescribed dose. Delineated OARs were the spinal cord, parotid glands, optic nerves, retinas, eye globes, lenses, optic chiasm, cochleae, mandible and the brainstem. Additionally, the thyroid gland was contoured in all patients as an OAR, but with no specific dose constraints during treatment planning.

Dosimetric analysis

Basic thyroid gland dose-volume parameters included total thyroid volume (cm^3) - TTV, mean dose D_{mean}, minimum D_{min}, and maximum D_{max} dose. Furthermore, the proportion (%) of thyroid volume receiving a dose D (Gy) in the range of doses from 10 to 70 Gy (V10 to V70, respectively), the dose to percentage (ranging from 2 to 98%) of thyroid volume in cGy (D02 to D98, respectively), and the absolute thyroid volume spared from the dose D (Gy), again ranging from 10 Gy to 70 Gy in cm^3 (VS10 to VS70, respectively) were evaluated.

Clinical (non-dosimetric) parameters

In addition to dosimetric parameters, various clinical and demographic characteristics were analysed: age, gender, localization of the primary tumor, T status, N status, presence of metastases, chemotherapy and surgery involving thyroid gland.

Thyroid function assessment during and after HNSCC therapy

Thyroid function was evaluated in all patients prior to the start of radiotherapy by a thyroid disease specialist who evaluated the presence of thyroid-related symptoms and checked medical records to identify possible pre-existing hormonal imbalances. Patients with suspected thyroid dysfunction underwent further diagnostic tests to determine thyroid status. After the completion of therapy, the patients' hormone status was regularly assessed during follow-up using thyroid-stimulating hormone (TSH) and free thyroxine (fT4) assays. Thyroid hormone evaluation was done every 3 months for the first two years, and every 6 months afterwards. Patients were evaluated using chemiluminescent microparticle immunoassay method and Abbott Architect i2000 (Abbott Diagnostics, Abbott Park, Illinois, USA). The upper limit of normal for TSH at our laboratory is 5 mIU/L, so HT was defined as TSH >5 mIU/L. In patients with elevated TSH and clinical symptoms of HT, thyroid hormone replacement with levothyroxine was introduced.

Statistical analysis

Patient characteristics were assessed using descriptive statistics presented as a mean with standard deviation. Continuous variables were compared with t-test or Mann-Whitney U test when appropriate. Categorical variables were analysed using the Chi-squared test. Receiver operating characteristic (ROC) analysis was performed in order to determine the predictive accuracy of each variable in detecting HT. Interactions between the best predictors were analysed by using Pearson correlation analysis. The strongest predictors were then logarithmically transformed and their association with HT was analysed using the Cox proportional hazard models with a backward conditional stepwise approach. A nomogram (score) was constructed in the form of a regression equation based on unstandardized correlation coefficients derived from the final step of stepwise conditional backward Cox regression. Kaplan-Maier curves and Log-Rank test were used to demonstrate the difference in incidence of HT between cut-off values of specific variables. Two-sided P values of < 0.05 were considered statistically significant. The statistical analysis was done using SPSS version 20.0.

Results

The mean age of the study population was 59.8 ± 9.7 years and 137 (87.8%) were males. After a median follow-up of 23.0 (12.0–38.5) months at the study cut-off date, 70 (44.9%) patients developed HT (Figure 1, Table 1). The differences in general and dosimetric parameters between patients with and without HT are presented in Tables 2 and 3.

Since no significant differences in general characteristics between patients with and without HT were found, ROC analysis was performed for all dosimetric parameters (Table 4), and the strongest predictive variable was added into the multivariate model. Overall, the best predictive factor was VS65 with an area under curve (AUC) of 0.684 (95% confidence interval (CI) 0.600–0.768). Other predictive

TABLE 1. The incidence of hypothyroidism in the study population

Time (months)	N (%)
6	21 (13.5)
12	37 (23.7)
18	48 (30.8)
24	59 (37.8)
30	66 (42.3)
36	70 (44.9)
42	70 (44.9)

factors were Dmin - AUC of 0.673 (95% confidence interval (CI) 0.589–0.757) and V50 -AUC of 0.630 (95% confidence interval (CI) 0.543–0.717), while total thyroid volume (TTV) was analysed separately. Thyroid volume was analysed separately because it is an independent variable and is not associated with other dosimetric parameters.

Firstly, the interaction between these mentioned four parameters was analysed. A strong correlation was found between all variables. The strongest positive correlation was found between V50 and Dmin, and between VS65 and TTV (Table 5). In order to analyse their independent association with HT, variables were logarithmically transformed, after which a multivariate backwards conditional stepwise Cox regression was employed. In a multivariate model, HT was associated with lower TTV (OR 0.312, 95% CI 0.112–0.868, P = 0.026) and Dmin (OR 9.832, 95% CI 1.894–108.082, P = 0.042).

Secondly, we constructed a regression equation entitled hypothyroidism risk score (HRS) comprised of TTV and Dmin:

$$HRS = Log(10)\,Dmin \times 2.286 - Log(10)TTV \times 1.165$$

HRS substantially increased the accuracy of TTV in predicting HT (Figure 2). Log Rank X^2 of TTV was 8.73 (P = 0.003) and it increased to 25.68 (P < 0.001) when we replaced TTV with HRS. HRS had an AUC of 0.709 (95% CI 0.627–0.791) and a cut-off of > 7.1 had a sensitivity of 75.7% and a specificity of 64.0%. HT occurred in 13 (20.0%) patients with a score < 7.1 and in 57 (62.6%) patients with a score > 7.1.

Finally, we aimed to demonstrate the actual improvement in predictive accuracy when we applied HRS to a previously established predictive factor like V50. In our cohort of patients, V50 was also associated with HT as previously reported, but this association was not independent when considering other variables. V50 was capable of delineating only 14 patients with V50 < 60% as those with a lower risk of HT (Figure 3A). When we employed HRS in patients with V50 > 60%, additional 52 patients were categorized as those with lower risk of HT (Figure 3B).

Discussion

Severe side effects may occur in the treatment field in different organs at risk in patients with HNSCC who are receiving (chemo)radiotherapy with curative intent. The dose-volume constraints for the thyroid gland as an OAR are a matter of debate and not clearly defined.[10] Although the introduction of IMRT has marked a great advance in radiotherapy for HNSCC patients, with its ability to spare normal surrounding tissue from high radiation doses while delivering a highly conformal dose to the tumor, a significant radiation dose is still unavoidably delivered to the thyroid gland.[2] Furthermore, IMRT used for locally advanced head and neck cancer may increase the radiation dose to the thyroid compared with conventional conformal radiotherapy unless appropriate thyroid dose constraints are used.[3] Due

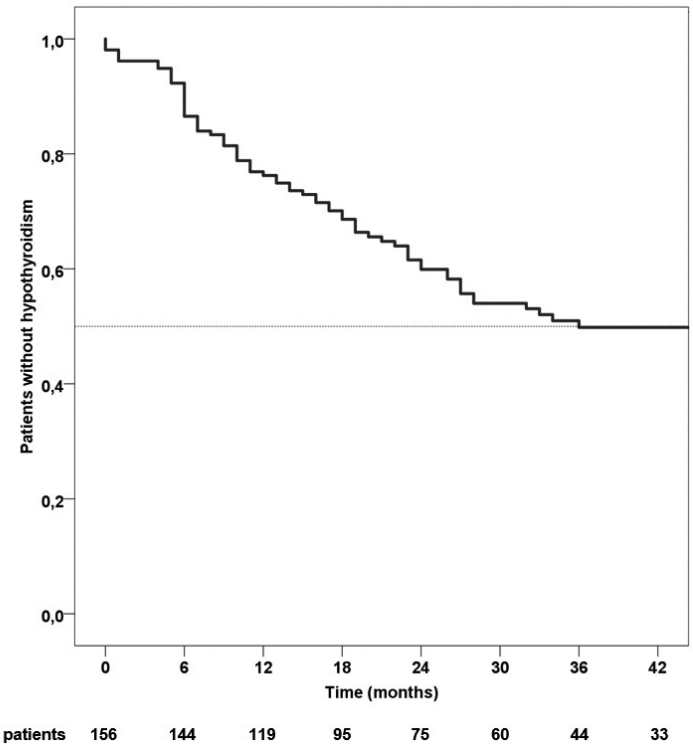

FIGURE 1. Kaplan-Maier curve showing the rate of hypothyroidism over time.

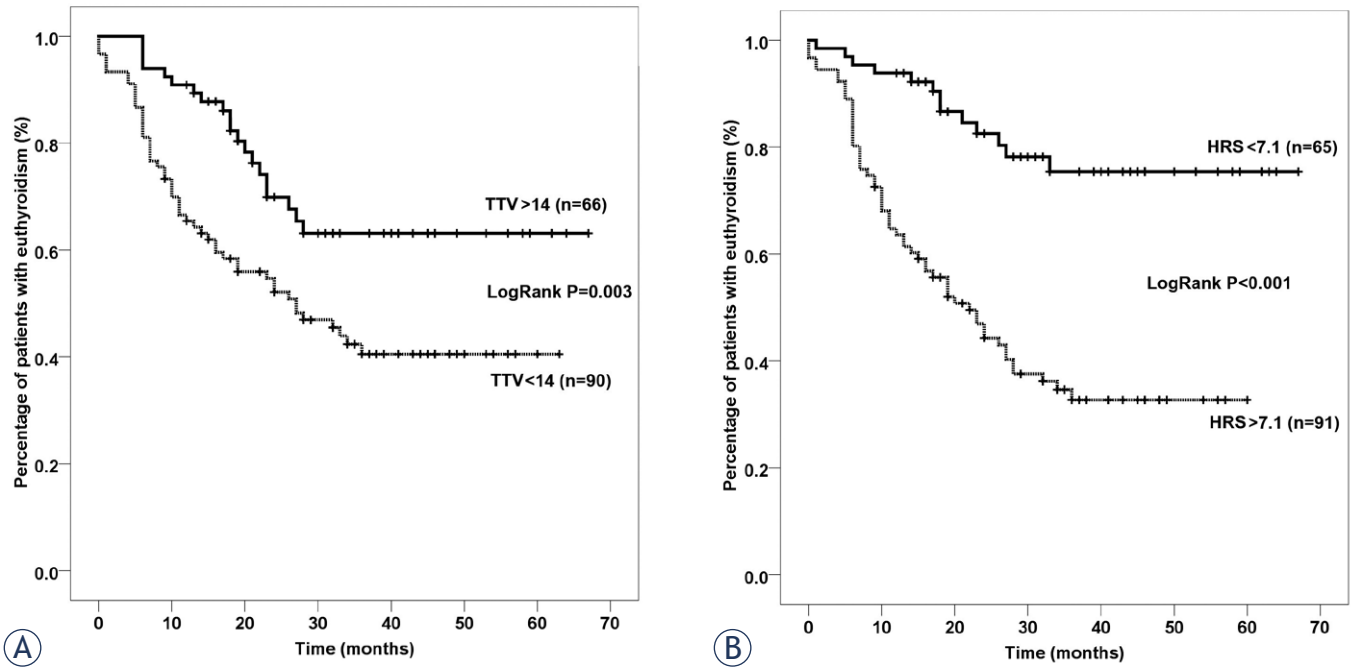

FIGURE 2. Kaplan Meier curves showing the difference in incidence of hypothyroidism between subgroups of patients divided based on specific cut-offs for total thyroid volume (TTV) **(A)** and Dmin **(B)**.

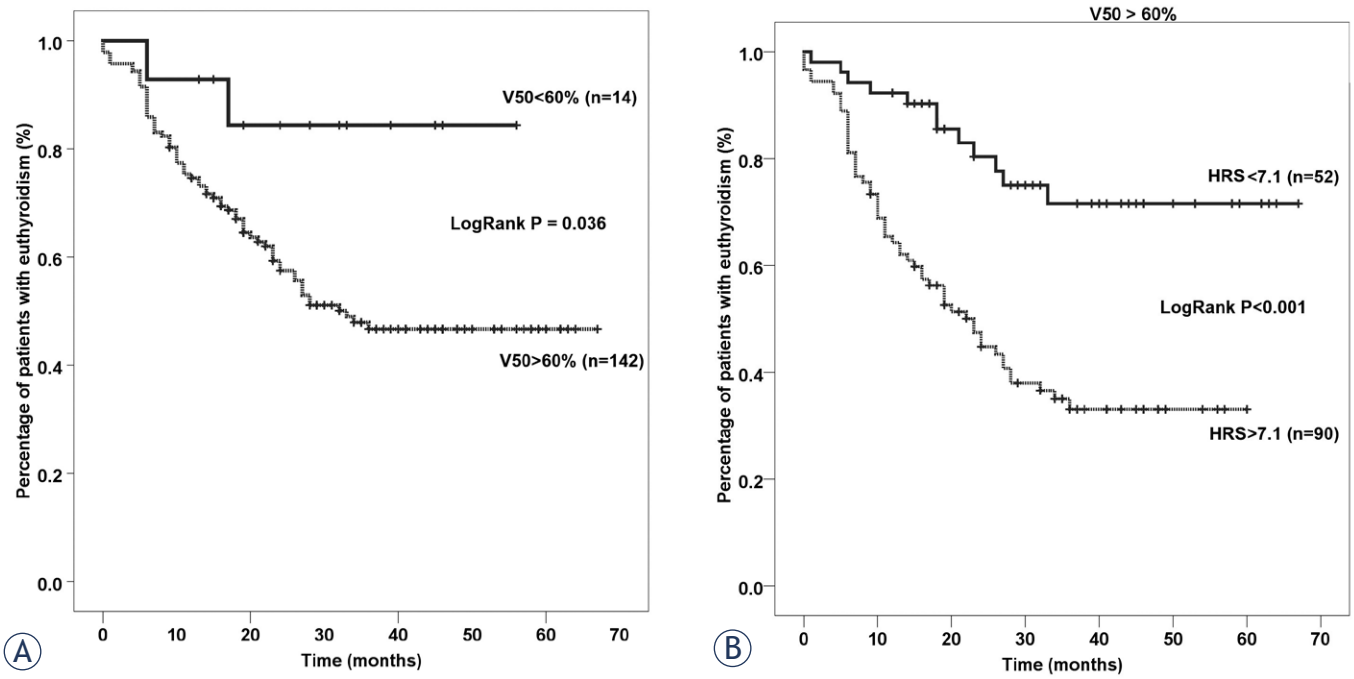

FIGURE 3. Kaplan-Meier curves showing the difference in incidence of hypothyroidism between subgroups of patients with V50 < 60% and > 60% **(A)**; Incidence of hypothyroidism in patients with V50 > 60% who were subdivided based on a novel hypothyroidism risks core (HRS) comprised of Dmin and TTV **(B)**.

to its proximity to other structures that are commonly included in the radiation field of these patients, sparing the thyroid gland can compromise final oncological outcome, especially in cases of suboptimal doses to areas which are at high-risk for recurrence. Thus, a significant proportion of patients receiving IMRT develops thyroid dysfunction, with HT being the most common complication. We observed

a high rate of HT (44% of patients) after a 2-year-follow-up period, which is consistent with previous reports.[4-5,14]

The relationship between the radiation dose delivered to the thyroid and the development of radiation-induced HT has been a matter of debate. Although previous studies have suggested that higher radiation doses to the thyroid gland are associated with a higher HT rate, a clear threshold radiation dose has not been defined.[15,16] Recent studies on patients with Hodgkin's lymphoma, breast cancer and head and neck cancer, proposed different dose-volumetric parameters for the prediction of HT development, mostly including the proportion of thyroid volume receiving some X dose (VX). In these studies, the defined VX threshold parameters ranged from V10 to V50.[2,4,11,17-20] However, the proposed proportion of thyroid volume that could receive VX dose was different among studies, making it difficult to draw strong conclusions.

In the study by Kim *et al.* V45 was the only parameter that independently predicted HT in multivariate analysis, and V45 of 50% was a threshold value.[4] In contrast, Akgun *et al.* found V30 to be useful in evaluating the risk of HT, since it was a statistically significant predictor of HT development.[17] In a large meta-analysis that examined dose-response data in 4 studies including a total of 1027 patients[10], final analysis showed that although there was a radiation dose-response relation with a 50% risk of HT at a dose of 45 Gy, there was considerable variation in the dose-response between studies (the dose of 50% radiotherapy induced HT probability varied from 33 Gy to 65 Gy), which was explained by the differences in follow-up. All authors agreed that although the threshold dose at which most patients will develop HT is still not defined, even low radiation doses have the potential to induce thyroid dysfunction. Thus, it is currently not possible to completely eliminate the risk of HT in patients treated with radiotherapy.

In the present study, V50 was found to be the best predictive factor for the development of HT among VX parameters. V50 is commonly reported in the literature as the parameter which is the most valuable in this setting; however, threshold V50 levels for the development of HT differ significantly between studies. The results of the present study are similar to those by Ling *et al.* which analysed radiotherapy dose parameters that corresponded with radiotherapy-induced thyroid dysfunction in 102 patients.[8] Their data showed that the incidence of HT was reduced when achieving D50 < 50 Gy, V50 <50%, and a mean dose of < 54.58 Gy. Sachdev *et al.* also reported that V50 was highly correlated with HT development, while other dosimetric parameters did not reach statistical significance. After a 50-month follow-up, the total rate of HT was 33%, and the proposed threshold was V50 > 60%.[11] A V50 threshold of <75% was proposed by Lin *et al.* as a useful guideline to avoid HT.[12] In the paper from Xu, the threshold level of V50 was set

TABLE 2. General characteristics of the study population; continuous variables are presented as mean ± SD and categorical ones as N (%)

	Euthyroidism N = 86		Hypothyroidism N = 70		P
Age	60.2	± 10.0	59.3	± 9.5	0.556
Male gender	79	(91.9)	58	(82.9)	0.087
Primary tumor					0.851
Unknown primary(C80)	5	(5.8)	2	(2.9)	
Hypopharinx	16	(18.6)	12	(17.1)	
Larynx	18	(20.9)	16	(22.9)	
Nasopharynx	3	(3.5)	5	(7.1)	
Oral cavity	11	(12.8)	9	(12.9)	
Oropharynx	28	(32.6)	24	(34.3)	
Other	5	(5.8)	2	(2.9)	
T status					0.106
1	10	(11.6)	14	(20.0)	
2	35	(40.7)	22	(31.4)	
3	16	(18.6)	21	(30.0)	
4	17	(19.8)	11	(15.7)	
x	8	(9.3)	2	(2.9)	
N status					0.508
N0	28	(32.6)	16	(22.9)	
N1	16	(18.6)	10	(14.3)	
N2a	1	(1.2)	3	(4.3)	
N2b	25	(29.1)	23	(32.9)	
N2c	12	(14.0)	13	(18.6)	
N3	4	(4.7)	5	(7.1)	
Neck metastases present	58	(67.4)	54	(77.1)	0.181
Chemotherapy	43	(50.0)	43	(61.4)	0.153
Surgery involving thyroid					0.758
None	18	(20.9)	14	(20.0)	
Lobectomy	10	(11.6)	11	(15.7)	
Non-thyroid	58	(67.4)	45	(64.3)	

C80 = patients with unknown primary tumor, with neck metastasis present (squamous cell carcinoma), primary tumor in head and neck region was not found by sensitive diagnostics;

No surgery = no surgery of primary tumor and/of lymph nodes, chemoradiotherapy was applied;

Surgery involving thyroid – none = thyroid resection is not included in operation protocol

Lobectomy = one lobe of the thyroid was removed

Non-thyroid = surgery of primary and/or lymph nodes was performed, without resection of the thyroid gland

TABLE 3. Dosimetric characteristics of the study population; continuous variables are presented as mean ± SD and categorical ones as n (%)

	Euthyroidism N = 86		Hypothyroidism N = 70		P
Dmin	4178	± 1652	5005	± 869	<0.001
Dmax	6298	± 704	6304	± 587	0.867
Dmean	5487	± 1055	5836	± 537	0.087
D02	6172	± 650	6222	± 582	0.765
D10	6041	± 663	6133	± 577	0.410
D20	5953	± 709	6062	± 567	0.373
D30	5818	± 884	5992	± 560	0.242
D40	5697	± 1003	5927	± 550	0.238
D50	5503	± 1168	5869	± 537	0.094
D60	5314	± 1414	5775	± 583	0.093
D70	5181	± 1495	5704	± 607	0.042
D80	5063	± 1540	5616	± 622	0.032
D90	4903	± 1595	5520	± 637	0.019
D98	4640	± 1663	5322	± 681	0.006
Total thyroid volume	15.951	± 8.399	11.461	± 4.513	<0.001
V10	96.85	± 11.27	100.00	± 0.00	0.005
V20	95.38	± 14.80	100.00	± 0.00	0.002
V30	94.40	± 16.57	99.64	± 2.99	0.005
V40	93.44	± 18.36	99.34	± 5.14	0.019
V45	92.70	± 19.66	98.99	± 5.51	0.040
V50	85.99	± 24.35	95.29	± 9.95	0.003
V55	53.15	± 41.84	65.72	± 40.89	0.053
V60	40.56	± 37.74	49.27	± 37.49	0.163
V65	12.82	± 25.13	13.61	± 26.67	0.888
V70	4.38	± 15.45	1.81	± 9.25	0.193
VS10	0.59	± 2.10	0.00	± 0.00	0.009
VS20	0.87	± 2.82	0.00	± 0.00	0.002
VS30	1.02	± 3.07	0.04	± 0.36	0.008
VS40	1.23	± 3.47	0.09	± 0.72	0.003
VS45	1.37	± 3.78	0.15	± 0.77	0.040
VS50	2.56	± 4.78	0.63	± 1.45	0.003
VS55	7.75	± 7.87	3.93	± 5.18	0.003
VS60	9.86	± 7.79	5.84	± 5.16	0.001
VS65	14.18	± 8.15	9.70	± 4.88	<0.001
VS70	15.32	± 8.00	11.23	± 4.62	<0.001

Dmin = minimum dose; Dmax = maximum dose; Dmean = mean dose; D02–D98 = the dose to percentage (ranging from 2 to 98%) to thyroid volume in cGy; V10–V70 = proportion (%) of thyroid volume receiving a dose D (Gy) in the range of doses from 10 to 70 Gy; VS10–VS70 = the absolute thyroid volume spared from the dose D (Gy) ranging from 10Gy to 70 Gy in cm^3; TTV = total thyroid volume (cm^3)

to 54.5%.[20] When all these results are analysed collectively, it can be concluded that the rate of HT is small in patients receiving < 50 Gy. In this study, it was shown that by employing our novel scoring system (HRS) it is possible to additionally stratify a cohort of patients with V50 > 60%, in order to predict the risk of HT development more precisely. Thus, this dose-volume derived nomogram could be a valuable tool in addition to the presently used parameters in everyday clinical practice.

VS is another less used dosimetric parameter which is important in estimating the amount of spared tissue. In paper by Lee *et al.* VS60 and VS45 of the thyroid were significant predictors of biochemical hypothyroidism.[21] Freedom from biochemical hypothyroidism was longer for those whose VS60 was ≥ 10 cm^3. Furthermore, in a paper by Chyan *et al.* VS30 Gy, VS40 Gy, and VS50 Gy were dosimetric parameters found to be statistically significant predictors of HT development.[7] In the present study, VS65 was independently associated with HT in multivariate analysis, and therefore could be a useful predictive factor for radiation-induced hypothyroidism.

Data from previous studies examining the role of chemotherapy on HT development are inconclusive. Some studies have found that concurrent chemotherapy application increased the probability of HT development.[8,19,22] In the study from Luo *et al.* chemotherapy was one factor contributing to the development of radiotherapy induced hypothyroidim, and was selected as one of the variables (risk factors), using the least absolute shrinkage and selection operator (LASSO).[19] On the other hand, in the literature-based meta-analysis, which included 15 studies, chemotherapy did not affect the risk of hypothyroidism.[10] However,these discrepancies may arise due to different chemotherapy doses and sequences and multi-agent chemotherapy regimens. We did not find a correlation between chemotherapy and HT, or an association between other patient and clinical characteristics (age, gender, extent of surgery, tumor site, thyroid surgery, and TNM status) and HT development. Earlier studies found that patients that underwent thyroid lobectomy had a higher incidence of HT.[23] However, prior lobectomy was not found to be a predictive factor of HT in our study.

This study has several limitations including its retrospective design and relatively small number of patients. On the contrary, we believe that developing a formula that determines the risk of hypothyroidism based on the radiated thyroid volume and the dose received is of great interest. In the

end, we would like to comment on the statistics used in this paper. Significant correlation exists between all dosimetric variables, making classical multivariate analysis impossible. We were aware of the fact that LASSO statistics was the most appropriate method to do the multivariate analysis in this case[19]. It might have been the most appropriate method from mathematical point of view, but it would substantially impair clarity of the results from a clinical point of view. We have performed an inferior type of LASSO statistics and decided to choose only one variable from each group which showed the strongest correlation with the onset of HT in univariate (ROC) analysis. Afterwards, we made a classical multivariate regression in order to calculate regression equation. Hence, we have made a less sophisticated variant of LASSO statistic in order to get clearer results from clinical point of view.

The nomogram presented in this paper can help in treatment decision-making, especially in HNSCC patients with a relative indication for postoperative radiotherapy. Omitting radiotherapy in some of these patients with low-risk disease (*i.e.* histologically negative neck, clinically negative contralateral neck in N1/N2a disease from well lateralized and small tumors) eliminates the unnecessary risk of radiation-induced side effects, including HT. In such cases, risk of radiation-induced HT predicted with the help of the nomogram (together with dosimetric constraints for other OAR) could be an important factor in treatment planning, in order to determine the best strategy for each individual patient.

The volumes and doses in head and neck radiotherapy depend mainly on the localization and extension of the local tumor as well as the levels of lymph node involvement. It is important to emphasize that sparing thyroid gland is not an option in cases when control of the tumor may be compromised. In these clinical circumstances, based on proposed nomogram, follow-up could be adjusted in those that are at highest risk for early HT development, which could lead to earlier management with hormone replacement therapy and subsequent higher quality of life.

Conclusions

In conclusion, the thyroid gland as an OAR remains a gray zone in radiotherapy. The thyroid gland is often neglected and has no priority in contouring, and because of its proximity to the tumor bed it

TABLE 4. Area under the curve for each variable in predicting hypothyroidism

Variable(s)	AUC	SE	P	95% Confidence Interval	
				Lower Bound	Upper Bound
Dmin	.673	.043	.000	.589	.757
Dmax	.508	.046	.867	.417	.599
Dmean	.580	.046	.087	.490	.669
D02	.514	.046	.765	.423	.605
D10	.538	.046	.410	.448	.629
D20	.542	.046	.373	.451	.632
D30	.555	.046	.242	.464	.645
D40	.555	.046	.238	.465	.645
D50	.578	.046	.094	.489	.668
D60	.578	.046	.093	.489	.668
D70	.595	.045	.042	.506	.683
D80	.600	.045	.032	.512	.688
D90	.609	.045	.019	.521	.697
D98	.627	.044	.006	.540	.714
VS					
VS10	.547	.046	.318	.456	.637
VS20	.564	.046	.170	.474	.654
VS30	.557	.046	.218	.468	.647
VS40	.569	.046	.140	.479	.658
VS45	.556	.046	.233	.466	.646
VS50	.623	.044	.008	.536	.710
VS55	.637	.044	.003	.550	.723
VS60	.655	.044	.001	.569	.740
VS65	.684	.043	.000	.600	.768
VS70	.672	.043	.000	.588	.757
Total thyroid volume					
TTV	.676	.043	.000	.592	.760
V					
V10	.552	.046	.262	.462	.642
V20	.564	.046	.170	.474	.654
V30	.563	.046	.177	.473	.653
V40	.562	.046	.182	.473	.652
V45	.564	.046	.168	.475	.654
V50	.630	.044	.005	.543	.717
V55	.589	.046	.057	.498	.679
V60	.565	.046	.166	.474	.655
V65	.495	.047	.906	.403	.586
V70	.470	.046	.519	.379	.561

Dmin = minimum dose; Dmax = maximum dose; Dmean = mean dose; D02–D98 = the dose to percentage (ranging from 2 to 98%) to thyroid volume in cGy; V10–V70 = proportion (%) of thyroid volume receiving a dose D (Gy) in the range of doses from 10 to 70 Gy; VS 10–VS70 = the absolute thyroid volume spared from the dose D (Gy) ranging from 10Gy to 70 Gy in cm^3; TTV = total thyroid volume

TABLE 5. Pearson correlation coefficients between strongest predictive variables. P< 0.001 for all correlations

	Dmin	TTV	VS65	V50
Dmin	1.000	-.398	-.537	.842
TTV	-.398	1.000	.853	-.331
VS65	-.537	.853	1.000	-.462
V50	.842	-.331	-.462	1.000

Dmin = minimum dose; TTV = total thyroid volume; VS65 = the absolute thyroid volume spared from the dose D (Gy) of 65 Gy; V50 = proportion (%) of thyroid volume receiving a dose D (Gy) of 50 Gy

has a high exposure to radiation, especially when it is used as primary therapy. Our comprehensive analysis of dose volume parameters suggests that proposed nomogram (HRS) may be a useful tool in predicting radiation-induced hypothyroidism, which may aid in the treatment planning process. Thyroid sparing may be optimized by using V50 < 60% as a dose-volumetric threshold when possible. In cases when V50 > 60% HRS may be helpful in predicting HT risk more precisely. Dose volume parameters should be incorporated into routine clinical practice. Although thyroid sparing should never compromise tumor coverage, hypothyroidism, as the most common manifestation of thyroid dysfunction should be anticipated and treated appropriately. These results should be tested in other studies and if validated through prospectively designed trials, could be incorporated in treatment planning and decision making in a subgroup of patients which are at low risk of recurrence when omitting radiotherapy.

References

1. Sroussi HY, Epstein JB, Bensadoun RJ, Saunders DP, Lalla RV, Migliorati CA, et al. Common oral complications of head and neck cancer radiation therapy: mucositis, infections, saliva change, fibrosis, sensory dysfunctions, dental caries, periodontal disease, and osteoradionecrosis. *Cancer Med* 2017; **6:** 2918-31. doi: 10.1002/cam4.1221
2. Sommat K, Ong WS, Hussain A, Soong YL, Tan T, Wee J, et al. Thyroid V40 predicts primary hypothyroidism after intensity modulated radiation therapy for nasopharyngeal carcinoma. *Int J Radiat Oncol Biol Phys* 2017; **98:** 574-80. doi: 10.1016/j.ijrobp.2017.03.007
3. Diaz R, Jaboin JJ, Morales-Paliza M, Koehler E, Phillips JG, Stinson Set, et al. Hypothyroidism as a consequence of intensity-modulated radiotherapy with concurrent taxane-based chemotherapy for locally advanced head-and-neck cancer. *Int J Radiat Oncol Biol Phys* 2010; **77:** 468-76. doi: 10.1016/j.ijrobp.2009.05.018
4. Kim MY, Yu T, Wu HG. Dose-volumetric parameters for predicting hypothyroidism after radiotherapy for head and neck cancer. *Jpn J Clin Oncol* 2014; **44:** 331-7. doi: 10.1093/jjco/hyt235
5. Mulholland GB, Zhang H, Nguyen NT, Tkacyzk N, Seikaly H, O'Connell D, et al. Optimal detection of hypothyroidism in early stage laryngeal cancer treated with radiotherapy. *J Otolaryngol Head Neck Surg* 2015; **44:** 34. doi: 10.1186/s40463-015-0085-3
6. Tell R, Lundell G, Nilsson B, Sjödin H, Lewin F, Lewensohn R. Long-term incidence of hypothyroidism after radiotherapy in patients with head-and-neck cancer. *Int J Radiat Oncol Biol Phys* 2004; **60:** 395-400. doi: 10.1016/j.ijrobp.2004.03.020
7. Chyan A, Chen J, Shugard E, Lambert L, Quivey JM, Yom SS. Dosimetric predictors of hypothyroidism in oropharyngeal cancer patients treated with intensity-modulated radiation therapy. *Radiat Oncol* 2014; **9:** 269. doi: 10.1186/s13014-014-0269-4
8. Ling S, Bhatt AD, Brown NV, Nguyen P, Sipos JA, Chakravarti A, et al. Correlative study of dose to thyroid and incidence of subsequent dysfunction after head and neck radiation. *Head Neck* 2017; **39:** 548-54. doi: 10.1002/hed.24643
9. Kanyilmaz G, Aktan M, Koc M, Demir H, Demir LS. Radiation-induced hypothyroidism in patients with breast cancer: a retrospective analysis of 243 cases. *Med Dosim* 2017; **42:** 190-6. doi: 10.1016/j.meddos.2017.03.003
10. Vogelius IR, Bentzen SM, Maraldo MV, Petersen PM, Specht L. Risk factors for radiation-induced hypothyroidism: a literature-based meta-analysis. *Cancer* 2011; **117:** 5250-60. doi: 10.1002/cncr.26186
11. Sachdev S, Refaat T, Bacchus ID, Sathiaseelan V, Mittal BB. Thyroid V50 highly predictive of hypothyroidism in head-and-neck cancer patients treated with intensity-modulated radiotherapy (IMRT). *Am J Clin Oncol*; **40:** 413-7. doi: 10.1097/COC.0000000000000165
12. Lin AJ, Zhang J, Cho-Lim J, Inouye W, Lee SP. Postradiation hypothyroidism in head and neck cancers: A Department of Veterans Affairs single-institution case-control dosimetry study. *Med Dosim* 2018; **44:** 56-60. doi: 10.1016/j.meddos.2018.02.001
13. Wiggenraad R, Mast M, van Santvoort J, Hoogendoorn M, Struikmans H. ConPas: a 3-D conformal parotidgland-sparing irradiation technique for bilateral neck treatment as an alternative to IMRT. *Strahlenther Onkol* 2005; **181:** 673-82. doi: 10.1007/s00066-005-1413-8
14. Colevas AD, Read R, Thornhill J, Adak S, Tishler R, Busse P, et al. Hypothyroidism incidence after multimodality treatment for stage III and IV squamous cell carcinomas of the head and neck. *Int J Radiat Oncol Biol Phys* 2001; **51:** 599-604. doi:10.1016/s0360-3016(01)01688-1
15. Boomsma MJ, Bijl HP, Langendijk JA. Radiation-induced hypothyroidism in head and neck cancer patients: a systematic review. *Radiother Oncol* 2011; **99:** 1-5. doi: 10.1016/j.radonc.2011.03.002
16. Alterio D, Jereczek-Fossa BA, Franchi B, D'Onofrio A, Piazzi V, Rondi E, et al. Thyroid disorders in patients treated with radiotherapy for head-and-neck cancer: a retrospective analysis of seventy-three patients. *Int J Radiat Oncol Biol Phys* 2007; **67:** 144-50. doi: 10.1016/j.ijrobp.2006.08.051
17. Akgun Z, Atasoy BM, Ozen Z, Yavuz D, Gulluoglu B, Sengoz M, et al. V30 as a predictor for radiation-induced hypothyroidism: a dosimetric analysis in patients who received radiotherapy to the neck. *Radiat Oncol* 2014; **9:** 104. doi: 10.1186/1748-717X-9-104
18. Cella L, Conson M, Caterino M, De Rosa N, Liuzzi R, Picardi M, et al. Thyroid V30 predicts radiation-induced hypothyroidism in patients treated with sequential chemo-radiotherapy for Hodgkin's lymphoma. *Int J Radiat Oncol Biol Phys* 2012; **82:** 1802-8. doi: 10.1016/j.ijrobp.2010.09.054
19. Luo R, Li M, Yang Z, Zhan Y, Huang B, Lu J, et al. Nomogram for radiation-induced hypothyroidism prediction in nasopharyngeal carcinoma after treatment. *Br J Radiol* 2017; **90:** 20160686. doi: 10.1259/bjr.20160686.
20. Xu Y, Shao Z, Tang T, Liu G, Yao Y, Wang J, et al. A dosimetric study on radiation-induced hypothyroidism following intensity-modulated radiotherapy in patients with nasopharyngeal carcinoma. *Oncol Lett* 2018; **16:** 6126-32. doi: 10.3892/ol.2018.9332
21. Lee V, Chan SY, Choi CW, Kwong D, Lam KO, Tong CC, et al. Dosimetric predictors of hypothyroidism after radical intensity-modulated radiation therapy for non-metastatic nasopharyngeal carcinoma. *Clin Oncol (R Coll Radiol)* 2016; **28:** e52-60. doi: 10.1016/j.clon.2016.05.004
22. Luo R, Wu VWC, He B, Gao X, Xu Z, Wang D et al. Development of a normal tissue complication probability (NTCP) model for radiation-induced hypothyroidism in nasopharyngeal carcinoma patients. *BMC Cancer* 2018; **18:** 575. doi: 10.1186/s12885-018-4348-z
23. Jereczek-Fossa BA, Alterio D, Jassem J, Gibelli B, Tradati N, Orecchia R. Radiotherapy induced thyroid disorders. *Cancer Treat Rev* 2004; **30:** 369-84. doi: 10.1016/j.ctrv.2003.12.003

Radiol Oncol 2019: 53(4): 373-387.
doi: 10.2478/raon-2019-0040

Multidisciplinarni tim za gastroenteropankreatične nevroendokrine tumorje: izziv za radiologa

Granata V, Fusco R, Setola SV, de Lutio di Castelguidone E, Camera L, Tafuto S, Avallone A, Belli A, Incollingo P, Palaia R, Izzo F, Petrillo A

Izhodišča. Gastroenteropankreatični nevroendokrini tumorji (GEP-NET) so heterogena skupina tumorjev. Učinkovita diagnostika zahteva multidisciplinarni pristop, ki presoja klinične simptome, ravni hormonov, radiološke in nuklearnomedicinske posnetke in histologijo. Slikanje ima ključno vlogo v diagnostiki nevroendokrinih tumorjev, zdravljenju in prognozi, zato so radiologi pomembni člani multidisciplinarnega tima. Med diagnostično obdelavo sta prisotni dve zahtevi: prva je potreba potrditi prisotnost tumorja in druga opredeliti mesto primarnega tumorja in oceniti prisotnost področnih in oddaljenih zasevkov.

Zaključki. Najprimernejša slikovna tehnika je odvisna od tipa nevroendokrinega tumorja in razpoložljivosti specializiranih slikovnih tehnik in strokovnega znanja. Konsenza glede najučinkovitejšega slikovnega algoritma ni, kar se odraža v izzivu zanesljive prepoznave teh tumorjev.

Radiol Oncol 2019: 53(4): 388-396.
doi: 10.2478/raon-2019-0036

Napredki pri obravnavi kraniofaringeoma pri otrocih in odraslih

Jensterle M, Jazbinšek S, Bošnjak R, Popović M, Zadravec Zaletel L, Vipotnik Vesnaver T, Faganel Kotnik B, Kotnik P

Izhodišča. Kraniofaringeom v otroški in odrasli dobi je redek tumor embrionalnega izvora, ki leži v selarnem, supraselarnem in paraselarnem področju. Kljub velikemu odstotku preživelih je zaradi lokacije in posledic zdravljenja tumorja obolevnost zaradi endokrinoloških izpadov, prizadetosti vida, presnovnih zapletov, kognitivnih in psihosocialnih posledic velika. Posledično je kakovost življenja bolnikov pomembno znižana. Trenutno ni splošno sprejetih smernic za zdravljenje kraniofaringeoma. Subtotalna resekcija, ki ji sledi radioterapija, je priporočena pri tumorjih, ki že ob postavitvi diagnoze vraščajo v hipotalamus, da bi ne prišlo do dodatne poškodbe le tega. Novejša spoznanja na področju molekularne patologije tumorja ponujajo možnost uporabe tarčne terapije, ki bi v prihodnosti lahko zmanjšala obolevnost povzročeno z zdravljenjem.

Zaključki. Kraniofaringeom je kronična bolezen z doživljenjskim sledenjem. Za najboljši izhod bolnikov je že ob diagnozi ter načrtovanju zdravljenja potrebna multidisciplinarna obravnava, v kateri sodelujejo izkušeni nevrokirurgi, nevroradiologi, nevroonkologi, patologi in endokrinologi.

Radiol Oncol 2019: 53(4): 397-406.
doi: 10.2478/raon-2019-0057

Signaliziranje citokina CCL5 preko receptorja CCR5 v multiformnem glioblastomu

Koprivnikar Kranjc M, Novak M, Pestell RG, Lah TT

Izhodišča. Glioblastom ja najbolj pogost in agresiven možganski tumor. Bolniki imajo povprečno stopnjo preživetja med 12 do 15 mesecev po diagnozi. Vzrok so glioblastomske matične celice, ki so najbolj odporne proti zdravljenju in celična heterogenost tumorjev zaradi infiltracije raznih vrst celic gostitelja. Endotelijske celice, mezenhimske matične celice in njihovi progenitorji ter bolj ali manj diferencirane celice imunskega sistema tvorijo mikro-okolje možganskega tumorja. Tako so pomembni zgradba in mehanizmi signaliziranja citokina CCL5 in njegovega receptorja CCR5 v glioblastomu. CCR5 je z G-proteini povezan receptor, ki sodeluje v procesih razvoja tumorske heterogenosti, razvoju rakavih matičnih celic in pospešuje invazijo in metastaziranje raka. Važna je tudi vloga CCR5 kot so-receptorja pri vhodu virusa HIV v limfocite, medtem ko CCL5/CCR5 os v glioblastomu usmerja infiltracijo in interakcije med monociti oz. makrofagi ter mezenhimskimi matičnimi celicami, ki tudi tvorijo niše matičnih celic gliblastoma. Nedavne raziskave nedvomno kažejo na vlogo CCL5/CCR5 pri invaziji in metastaziranju drugih vrst raka. Klinične študije so podprle ciljana zdravljenja z monoklinskimi humaniziranimi protitelesi za CCR5 (leronlimab) metastatskega trojno negativnega raka dojk (TNBC) in pa uporabo majhne inhibitorne molekule (maraviroc) pri metastatskem raku črevesja.

Zaključki. Ker je CCR5 močno izražen v glioblastomu in povezan s slabo napovedjo preživetja, zna biti os CCL5/CCR5 odlična nova tarča pri zdravjenju glioblastoma in drugih vrst raka. Molekularni mehanizem, s katerim se ta citokin in njegov receptor odzivata na kompleksno tumorsko mikro-okolje, ki vzdržuje rakave matične celice in tumorsko heterogenost, bo potrebno upoštevati pri bodočih raziskavah.

Radiol Oncol 2019: 53(4): 407-414.
doi: 10.2478/raon-2019-0052

Anatomska oblika vprašaja pri MR slikanju cervikalno-torakalnega-ganglijskega-kompleksa. Ali nam lahko pomaga, da se pri slikanju z ^{68}Ga-PSMA-11 PET/MR izognemo lažnemu sumu na maligno obolenje?

Bialek EJ, Malkowski B

Izhodišča. Zaznaven privzem ^{68}Ga-PSMA-liganda v simpatične ganglije lahko potencialno vodi do zamenjave le teh za maligno lezijo. Namen raziskave je bil raziskati anatomijo cervikalno-torakalnega--ganglijskega-kompleksa (CTG-C) pri preiskavi MR kot del multimodalnega slikanja ^{68}Ga- PSMA-11 PET/MR . Pregledali smo faktorje PET-a, ki bi lahko vodili do napačne identifikacije lezij.

Bolniki in metode. Pri 106 pacientih smo na 212 mestih CTG-C retrospektivno pregledali privzem radiooznačevalca ($SUV_{max)}$, njegovo velikost, obliko, pozicijo, simetrijo lokacije in intenziteto vizualnega privzema. Asimetrija privzema PSMA-liganda in povečan privzem sta bila opredeljena kot faktor tveganja za malignost.

Rezultati. Pri 66 % levih (L) in 53,8 % desnih (D) CTG-C smo opazili obliko kompleksa, ki spominja na znak klicaja ali znak vprašaja ali delne oblike le teh, kar je opredeljeno kot tipična oblika. Tumorjem podobne oblike CTG-C (ovalna, binodularna ali longitudinalna) so bile zaznane pri 28,3 % L-CTG-C in 40,6 % D-CTG-C. Vizualna opredelitev na PET suspektne malignosti, po prepoznavi tipične oblike CTG-C na preiskavi MR, je vodila k dvigu natančnosti pravilne identifikacije (iz 34,4 % na 75 %, *$\chi 2(1) = 70.4; p < .001$). Prepoznava tipične oblike CTG-C na* preiskavi MR nam je omogočila klasifikacijo nesumljivih 61,9 % vseh CTG-C, ki so bili prej obravnavani kot suspektni ob samo PET preiskavi.

Zaključki. Karakteristična oblika CTG-C (znak vprašaja, klicaja ali delne oblike le teh) nam pomaga pri pravilni prepoznavi CTG-C na multimodalni preiskavi, ko bi privzem liganda lahko vodil k diagnostični napaki in dajal lažno pozitivne prepoznave malignosti.

Radiol Oncol 2019: 53(4): 415-426.
doi: 10.2478/raon-2019-0049

Radiološke spremembe prašičjih jeter po elektrokemoterapiji z bleomicinom

Brložnik M, Boc N, Serša G, Žmuc J, Gašljević G, Seliškar A, Dežman R, Edhemović I, Milevoj N, Plavec T, Erjavec V, Pavlin D, Bošnjak M, Brecelj E, Lampreht Tratar U, Kos B, Izlakar J, Štukelj M, Miklavčič D, Čemažar M

Izhodišča. Radiološke spremembe po elektrokemoterapiji velikih jetrnih žil ter zdravega jetrnega parenhima še niso bile opisane.

Materiali in metode. V prospektivno raziskavo na živalskem modelu z izdanim dovoljenjem smo vključili devet prašičev pitancev. Pri vsaki živali smo ultrazvočno vodeno elektroporirali štiri področja; v treh področij smo elektrode vstavili v svetline velikih jetrnih žil. Preizkusili smo dve vrsti elektrod; linearne in heksagonalne elektrode. Ultrazvočno smo tretirana mesta pregledali takoj in do dvajset minut po postopku. Dinamično računalniško tomografijo smo izvedli pred posegom, 60 do 90 minut po njem ter 1 teden kasneje.

Rezultati. Radiološke preiskave tretiranih področij so pokazale nepoškodovane žilne stene ter normalno prehodne žile; brez krvavitev ali strdkov. Tretirana področja so se ultrazvočno dinamično spreminjala od hiperehogenih mikromehurčkov vzdolž elektrod do hipoehogenosti tretiranega parenhima, difuzije hiperehogenih mikromehurčkov ter izginjanja hipoehogenosti. Ultrazvočni pregled s kontrastom je pokazal zmanjšanje perfuzije tretiranega področja. Dinamična računalniška tomografija od 60 do 90 minut po postopku je pokazala, da tretirana mesta privzemajo manj kontrasta. Celotna površina mest, ki slabše privzemajo kontrast, je bila v primeru heksagonalnih elektrod manjša kot v primeru linearnih elektrod.

Zaključki. Radiološke preiskave prašičjih jeter po elektrokemoterapiji z bleomicinom niso pokazale klinično pomembnih poškodb jeter navkljub tveganemu postopku vstavitve elektrod v svetline velikih jetrnih žil, kar pomeni, da je elektrokemoterapija za zdravljenje jetrnih novotvorb varna.

Radiol Oncol 2019: 53(4): 427-433.
doi: 10.2478/raon-2019-0056

Proučevanje možganskih trombov, ki smo jih odstranili z mehansko trombektomijo ter uporabili T_1 uteženo slikanje in slikanje karakterističnega časa transverzalne reakcije (T_2) in difuzijske konstante (ADC). Predhodni rezultati

Vidmar J, Bajd F, Milošević ZV, Kocijančič IJ, Jeromel M, Serša I

Izhodišča. Nedavne tehnološke izboljšave omogočajo, da je tudi na področju interventne radiologije magnetnoresonančna slikovna preiskava (MRI) vse bolj prednostna glede na preiskavo CT. Večparametrični MRI omogoča zajem večje količine podatkov, ki so pomembni za opredelitev možganskih trombov.

Bolniki in metode. V raziskavi smo proučevali možganske trombe, ki smo jih odstranili z mehansko tromektomijo pri 17 bolnikih z diagnozo akutne možganske kapi. Trombe smo analizirali na osnovi visokoločljivega 3D T_1 uteženega slikanja, s čimer smo opredelili njihovo morfologijo, kot tudi z meritvami difuzijske konstante (angl. *apparent diffusion coefficient*, ADC) in transverzalnega relaksacijskega časa (T_2). Rezultati slikanja MR podani z izmerjenimi parametri (povprečni ADC in T_2 vzorca, koeficient variacije ADC in T_2 v vzorcu ter dolžina tromba) smo analizirali glede možnih korelacij s parametri postopka trombektomije (čas rekanalizacije in števila prehodov).

Rezultati. Obe MRI tehniki slikanja sta omogočili dobro razlikovanje področij znotraj trombov, ki imajo različno mobilnost vode in so tudi različno kompaktni. Koeficient variabilnosti ADC znotraj vzorca je pri tem najobčutljivejši parameter za razlikovanje med trombi, pri katerih je trombektomija potekala v enkratnem poskusu ter trombi, pri katerih je trombektomija potekla v dveh ali več poskusih ($p = 0,03$). Ugotovili smo negativno zvezo med časom rekanalizacije in dolžino tromba ($\rho = -0,22$).

Zaključki. Predhodni rezultati kažejo, da bi začetna MRI ocena trombov pri bolnikih z možgansko kapjo lahko olajšala načrtovanje interventnega posega. Koeficient variabilnosti ADC znotraj vzorca lahko služi za napoved možnih zapletov med postopki trombektomije in s tem omogoča tudi njihovo preprečevanje.

Radiol Oncol 2019: 53(4): 434-442.
doi: 10.2478/raon-2019-0051

LncRNA NEAT1 spodbuja proliferacijo celic endometrijskega raka ter njihovo migracijo in invazijo z regulacijo poti miR-144-3p/EZH2

Wang W, Ge L, Xu XJ, Yang T, Yuan Y, Ma XL, Zhang XH

Izhodišča. Endometrijski rak je eden najpogostejših ginekoloških rakov na svetu. Dolga nekodirajoča molekula RNA (lncRNA) gena NEAT1 (angl. *nuclear enriched abundant transcript 1*) spodbuja proliferacijo, migracijo in invazijo celic endometrijskega raka. V raziskavi smo raziskali funkcijo NEAT1 v tkivu in celicah endometrijskega raka, ker molekularni mehanizmi NEAT1 še niso znani.

Materiali in metode. Tumorsko in okolno tkivo smo odvzeli bolnicam z endometrijskim rakom. HEC-1A in celice Ishikawa smo gojili v celični kulturi. Izražanje NEAT1 je bilo zmanjšano s transfekcijo kratke lasnične RNA (shRNA), s transfekcijo miR-144-3p pa se je izražanje le-te povečalo. Proliferacijo celic smo izmerili s pomočjo testa MTT in s testom klonogenosti. Migracijo in invazijo celic pa smo izmerili s testom transwell. Za določanje odnosa med NEAT1, EZH2 in miR-144-3p smo uporabili luciferazni reporterski test. Nivo izražanja RZH2 smo izmerili s pomočjo metode Western prenosa in qPCR.

Rezultati. Stopnja izražanja NEAT1 v celicah in tkivih endometrijskega raka je bila zelo povečana. Utišanje izražanja NEAT1 je zmanjšalo proliferecijo, migracijo in invazijo celic endometrijskega raka. Poleg tega je NEAT1 deloval kot ceRNA miR-144-3p RNA molekule, kar je vodilo v povečano ekspresijo EZH2. Čezmerno izražanje miR-144-3p je zavrlo proliferacijo in invazijo celic endometrijskega raka.

Zaključki. NEAT1 spodbuja proliferacijo in invazijo celic endometrijskega raka preko regulacije miR-144-3p/EZH2.

Radiol Oncol 2019: 53(4): 443-452.
doi: 10.2478/raon-2019-0048

LncRNA PVT1 spodbuja proliferacijo in invazijo celic raka maternične vratu s spodbujanjem izražanja Smad3 s spužvasto miR-140-5p

Chang QQ, Chen CY, Chen Z, Chang S

Izhodišča. Rak maternične vratu je eden najpogostejših rakov na svetu. Vedno več je podatkov, da so pri napredovanju in zasevanju bolezni udeležene dolge nekodirajoče RNA nukleinske kisline (lncRNA). Namen raziskave je bil preučiti učinek lncRNA plazmacitoma, ki ima varianto translokacije 1 (PVT1), pri napredovanju celic raka maternične vratu in njihov mehanizem delovanja.

Materiali in metode. Izražanje PVT1, miR-140-5p in Smad3 v celicah maternične vratu smo določali s qRT-PCR in barvanjem po Westernu. Naredili smo bioinformatsko analizo in test z luciferazo z namenom ugotoviti morebitno korelacijo med izražanjem PVT1, miR-140-5p in Smad3. Vlogo PVT1 v proliferaciji, migraciji in invaziji celic maternične vratu smo ugotavljali z transfekcijo sh-RNA in funkcionalnimi testi, kot so test klonogenosti, test celjenja ran in test migracije celic.

Rezultati. Ugotovili smo povečano izražanje PVT1 in Smad3, ter zmanjšano izražanje miR-140-5p v celicah maternične vratu. Zavora PVT1 lahko spodbudi izražanje miR-140-5p, zavre izražanje Smad3 in s tem značilno zavre proliferacijo, migracijo in invazijo celic maternične vratu. Transfekcija miR-1140-5p pa zavre ali deloma povrne opisane spremembe v celicah maternične vratu.

Zaključki. Rezultati kažejo, da PVT1 spodbuja proliferacijo in migracijo celic maternične vratu preko spodbujanja Smad3 izražanja s spužvasto miRNA-140-5p, ki pa naj bi bila napovedni dejavnik in terapevtska tarča za rak maternične vratu.

Radiol Oncol 2019: 53(4): 453-458.
doi: 10.2478/raon-2019-0053

Vključitev statusa mutacij EGFR v označevalec M nove klasifikacije TNM in vpliv na krivulje preživetja pri bolnikih z nedrobnoceličnim pljučnim rakom

Stanič K, Turnšek N, Vrankar M

Izhodišča. Osma izdaja sistema za določanje stadija (tumor- bezgavke- zasevki; TNM) pljučnega raka je uvedla revizijo označevalca M. Nova klasifikacija je pri napovedovanju poteka bolezni omejena, ker je osredotočena le na anatomsko razsežnost bolezni. Informacije o molekularnem statusu tumorja pomembno vplivajo na odgovor na zdravljenje in preživetje; vendar je podatkov, ki obravnavajo to vprašanje, malo. Pričujoča raziskava kaže vpliv mutacij receptorja za epidermalni rastni faktor (EGFR) pri bolnikih z nedrobnoceličnim pljučnim rakom (NSCLC) na preživetje z vidika novih označevalcev M klasifikacijskega sistema TNM.

Bolniki in metode. Retrospektivno smo pregledali medicinske zapise 479 zaporedno zdravljenih metastatskih bolnikov z NSCLC, ki smo jih zdravili med letoma 2009 in 2011 in so bili testirani na mutacije EGFR. Pri 355 bolnikih je zdravstvena dokumentacija vključevala dovolj informacij, da jih je bilo mogoče ustrezno razvrstiti v eno od novih podskupin v skladu z označevalcem M osme klasifikacije TNM. Med temi je bilo 89 (25,1 %) bolnikov, ki so imeli mutacije EGFR (EGFR-m).

Rezultati. Srednje celokupno preživetje (mOS) EGFR-m bolnikov je bilo znatno daljše od mOS bolnikov brez mutacij EGFR (20,6 meseca v primerjavi z 8,3 meseca, $p < 0,001$). Bolniki z omejeno obremenitvijo bolezni (podskupina M1b) so imeli najdaljše mOS tako med EGFR bolniki divjega tipa (EGFR-wt) kot tudi med EGFR-m bolniki, 14,4 meseca in 39,2 meseca. Četudi so imeli EGFR-m bolniki močno razširjeno metastatsko bolezen (M1c) je bil njihovo mOS (18,8 mesecev) daljše od mOS oligometastatskih EGFR-wt bolnikov (M1b), ki so imeli najnižjo obremenitev bolezni (14,4 meseca). Srednja vrednost spremljanja je bila 53,9 meseca.

Zaključki. Vključitev statusa mutacij EGFR pri napredovalem NSCLC še dodatno loči krivulje preživetja posameznih kategorij M v 8. klasifikaciji TNM in natančneje napoveduje preživetje kot število metastaz ali število metastatskih mest.

Radiol Oncol 2019: 53(4): 459-464.
doi: 10.2478/raon-2019-0050

Dejavniki, ki vplivajo na kakovost glasu pred in po obsevalnem zdravljenju zgodnjega raka glasilk

Mekiš J, Strojan P, Hočevar Boltežar I

Izhodišča. Radioterapija je uspešen način zdravljenja zgodnjega raka glasilk. Namen raziskave je bil oceniti kakovost glasu pred in po uspešnem obsevalnem zdravljenju zgodnjega raka glasilk ter ugotoviti dejavnike, ki vplivajo nanjo.

Bolniki in metode. Pred in 3 mesece po končanem obsevalnem zdravljenju glotisnega raka T1 smo subjektivno (pacientova ocena kakovosti glasu [VAS], vprašalnik indeksa glasovne prizadetosti [*voice handicap index*; VHI], foniatrova ocena stopnje glasovne motnje [G], hrapavosti [R] in zadihanosti [B] glasu) in objektivno (temeljna grlna frekvenca [F_0], perturbacija višine in amplitude glasu, maksimalni fonacijski čas [MPT]) ocenili kakovost glasu pri 50 bolnikih. Podatke o spolu, starosti, razsežnosti tumorja, načinu biopsije, kajenju, lokalnem stanju v grlu in radioterapiji smo povzeli iz medicinske dokumentacije.

Rezultati. Tri mesece po končanem obsevalnem zdravljenju so se vrednosti VAS, VHI, ocen G in R, F_0, in MPT pomembno izboljšale v primerjavi z oceno pred začetkom zdravljenja. Pred zdravljenjem je zajetost sprednje komisure s tumorjem pomembno poslabšala perturbacijo višine ($p = 0,044$), razširjenost raka na obe glasilki pa perturbacijo višine ($p = 0,003$) in amplitude ($p = 0,007$). Tri mesece po zdravljenju so imeli bolniki s ponovitvijo biopsije pomembno višjo F_0 kot ostali ($p = 0,047$). Pri bolnikih s poobsevalnimi spremembami je bila ocena B pomembno slabša kot pri tistih brez sprememb ($p = 0,029$).

Zaključki. Glede na večino načinov ocenjevanje se kakovost glasu pomembno izboljša tri mesece po končanem obsevalnem zdravljenju raka glasilk. Glavni vzrok za slabšo kakovost glasu pred zdravljenjem je razsežnost tumorja. Poobsevalne spremembe in ponovitev biopsije za potrditev raka povzročajo več brazgotinjenj v glasilkah, kar negativno vpliva na kakovost glasu po končanem obsevalnem zdravljenju.

Radiol Oncol 2019: 53(4): 465-472.
doi: 10.2478/raon-2019-0046

Kompletno neoadjuvantno zdravljenje bolnikov z lokalno napredovalim rakom danke in z dejavniki visokega tveganja za ponovitev bolezni

Tuta M, Boc N, Brecelj E, Omejc M, Anderluh F, Šečerov Ermenc A, Jeromen Peressutti A, Oblak I, Krebs B, Velenik V

Izhodišča. Zaradi visokega odstotka bolnikov, pri katerih se pojavijo oddaljen zasevki in nizkega deleža tistih, ki zdravljenje s pooperativno kemoterapijo tudi dokončajo, je kompletno neoadjuvantno zdravljenje lokalno napredovalega raka danke z visokim tveganjem za ponovitev bolezni postalo sodoben način zdravljenja. Na ta način želimo izboljšati odgovor na zdravljenje, kot tudi preživetje bolnikov. V članku predstavljamo učinkovitost in toksičnost takšnega zdravljenja v Sloveniji.

Bolniki in metode. V raziskavo smo vključili bolnike z rakom danke in stadijem bolezni II in III ter z vsaj enim od 4 naštetih dejavnikov visokega tveganja za ponovitev bolezni: T4, prisotnost ekstramuralne venske invazije (EMVI), prisotnost pozitivne ekstramezorektalne bezgavke ali prizadetost mezorektalne fascije (MRF). Bolniki so bili zdravljeni s štirimi krogi uvodne kemoterapije po shemi CAPOX/FOLFOX, nato so prejeli radiokemoterapijo s kapecitabinom in dva konsolidacijska kroga kemoterapije po shemi CAPOX/FOLFOX pred operacijo. Operacija je bila načrtovana 8–10 tednov po zaključku radiokemoterapije.

Rezultati. Od novembra 2016 do julija 2018 smo vključili 66 bolnikov. Vsi so imeli III. stadij bolezni, 24 (36,4 %) bolnikov je imelo T4 tumor, 46 (69,7 %) prisotnost EMVI in pri 47 (71,2 %) je bila s tumorjem zajeta MRF. Po uvodni kemoterapiji, ki jo je zaključilo 61 (92,4 %) bolnikov, smo ugotovili znižanje stadija T, N in celokupnega stadija, odsotnost EMVI in odsotnost prizadetosti MRF pri 42,4 %, 62,1 %, 36,4 %, 69,7 % in 68,2 % bolnikov. Vsi bolniki so zaključili obsevanje, nato pa je 54 (81,8 %) bolnikov prejelo oba kroga konsolidacijske kemoterapije. Toksične sopojave stopnje 3 pri zdravljenju s kombiniranim neoadjuvatnim zdravljenjem smo videli pri 4 (6 %) bolnikih. Pet bolnikov je zavrnilo operativno zdravljenje, od teh so trije imeli radiološko popoln odgovor na zdravljenje. Eden od njih ni imel dokončnega operativnega zdravljenja primarnega tumorja zaradi nepričakovanega srčnega zastoja nekaj dni po formaciji sigmoidne kolostome zaradi okužbe perinealnega predela. Od 60 operiranih bolnikov, jih je 23,3 % imelo popolni patohistološki odgovor na zdravljenje, 20 % pa skoraj popolni odgovor. Pri 96,7 % bolnikov je bila mogoča radikalna resekcija. Znižanje patohistološkega stadija T, N in celokupnega stadija smo ugotovili pri 65 %, 96,7 % in 83,4 % bolnikov. Perioperativne zaplete stopnje 3 smo videli pri 3 bolnikih z dehiscenco anastomoze, pri enem bolniku s pelvičnim abscesom in pri dveh bolnikih s paralitičnim ileusom. Delež popolnih patohistoloških odgovorov na zdravljenje pri bolnikih, ki so bili obsevani s 3D konformno tehniko, je znašal 12,1 %, pri bolnikih, ki so bili obsevani z intenzitetno modulirano ali volumetrično radioterapevtsko tehniko, pa je bil 37 % ($p < 0,05$). Edini dejavnik, ki je vplival na delež popolnih patohistoloških odgovorov na zdravljenje, je bila hipofrakcionacija z višjo dozo na frakcijo in simultanim integriranim dodatkom na tumor.

Zaključki. Kompletno neoadjuvatno zdravljenje bolnikov z lokalno napredovalim rakom danke z dejavniki visokega tveganja za ponovitev bolezni ima ob nizki toksičnosti visoko učinkovitost. Ta se je pokazala kot zniževanje stadija tumorja in bezgavk. Potrebno bo dolgoročno spremljanje tako zdravljenih bolnikov, ker bomo na ta način lahko ovrednotili morebitno vpliv na preživetje in zmanjšanje pojavnosti oddaljenih zasevkov.

Radiol Oncol 2019: 53(4): 473-479.
doi: 10.2478/raon-2019-0045

Multicentrična analiza difuznega velikoceličnega B-celičnega limfoma zdravljenega s konsodilirajočo radioterapijo in pomen njegovega izvora na izid zdravljenjnja

Rajasooriyar C, Tey J, Wong LC, Poon M, Nandini R, Tham I, Vellayappan B

Izhodišča. Bolnikom z difuznim velikoceličnim B-celičnim limfomom, ki imajo velike tumorje in ki se ne odzovejo na zdravljenje s popolnim odgovorom, lahko z dodatno radioterapijo izboljšamo potek bolezni. Namen raziskave je bil pregledati, kako konsodilirajoča radioterapija vpliva na izid zdravljenja glede na izvor tumorja.

Bolniki in metode. V raziskavo smo vključili bolnike z difuznim velikoceličnima B-celičnim limfomom, ki smo jih predvideli za radikalno zdravljenje in ki smo jih dodatno zdravili s konsodilirajočo radioterapijo. Iz zdravniške dokumentacije smo povzeli klinične in patohistološke podatke ter podatke o zdravljenju. Analizirali smo stopnjo preživetja in iskali dejavnike, ki so napovedovali preživetje brez znakov bolezni.

Rezultati. V analizo smo vključili 74 bolnikov. Srednji čas sledenja bolnikov je bil do 3 leta (0,7–16 let). Oseminpetdeset bolnikov je imelo I.-II. stadij bolezni in 61 % jih je dobilo vsaj 6 krogov kemoterapije. Izvor bolezni je bilo možno določiti pri 60 % bolnikov, približno polovica njih je imela germinalni izvor bolezni. Petletno celokupno preživetje je bilo 73 % (95 % interval zaupanja 57–83 %). Sedem odstotkov (n = 5) bolnikov je imelo lokalno ponovitev bolezni v srednjem času 6 mesecev. Krajši čas do ponovitve bolezni so imeli bolniki, kjer z dodatno radioterapijo nismo dosegli popolnega odgovora na zdravljenje ali so imeli na začetku razširjeno bolezen. Ni pa bilo nobene povezave med celokupnim preživetjem ali časom do ponovitve bolezni glede na izvor bolezni.

Zaključki. Uspešnost zdravljenja bolnikov, ki so prejeli dodatno radioterapijo, je bila odlična. Bolniki, pri katerih po radioterapiji nismo ugotovili popolni odgovor na zdravljenje, so imeli slabši izid zdravljenja. Ne glede na radioterapijo, je razširjenost bolezni ključno vplivala na izid zdravljneja in ostaja odločilen klični napovedni dejavnik. Nismo našli nobene povezave med izvorom bolezni in učinkom konsodilirajoče radioterapije.

Radiol Oncol 2019: 53(4): 480-487.
doi: 10.2478/raon-2019-0054

Definitivna radiokemoterapija pri raku požiralnika. Izkušnje posamične ustanove

Anderluh F, Toplak M, Velenik V, Oblak I, Šečerov Ermenc A, Jeromen Peressutti A, But-Hadžić J, Skoblar Vidmar M

Izhodišča. Definitivna radiokemoterapija je metoda izbora zdravljenja pri bolnikih z rakom vratnega dela požiralnika in eden od možnih načinov zdravljenja pri bolnikih z rakom spodnjih dveh tretjin požiralnika, ki zavračajo operativno zdravljenje. Namen naše raziskave je bil analizirati rezultate zdravljenja z definitivno radiokemoterapijo pri bolnikih z rakom požiralnika, ki so bili zdravljeni na Onkološkem inštitutu Ljubljana med leti 2010 in 2017.

Bolniki in metode. Retrospektivno smo pregledali in analizirali vso razpoložljivo medicinsko dokumentacijo 55 bolnikov z rakom požiralnika, ki smo jih z namenom ozdravitve zdravili z definitivno radiokemoterapijo. Bolnike z rakom zgornje tretjine požiralnika (vratnega požiralnika) smo na predel primarnega tumorja obsevali do skupne doze 70 Gy (1,8–2 Gy na frakcijo), tiste z rakom srednje tretjine (intratorakalne tumorje) pa do skupne srednje doze 57,6 Gy (1,8 Gy na frakcijo). Vsi, razen enega bolnika so prejeli tudi sočasno kemoterapijo, večina od njih (41 bolnikov; 74,5 %) sočasno kemoterapijo s 5-fluorouracilom v neprekinjeni 96 urni infuziji in cisplatinom. Primarni cilji raziskave so bili celokupno preživetje (smrt zaradi kateregakoli vzroka), lokoregionalna kontrola bolezni (ponovitev bolezni lokalno in/ali regionalno) in preživetje brez bolezni (ponovitev bolezni kjerkoli in/ali nov primarni tumor). Opravljeni sta bili univariatna analiza, v kateri smo ugotavljali učinek različnih dejavnikov na preživetje in analiza stranskih učinkov zdravljenja.

Rezultati. Povprečna starost v raziskavo vključenih bolnikov je znašala 62 let (standardna deviacija [SD] 9 let; razpon: 29–80 let). Večina bolnikov (53 bolnikov; 96,4 %) je imela ploščatocelični rak v stadiju T3 ali T4 (47 bolnikov; 85,5 %) in/ali N+ bolezen (35 bolnikov; 63,6 %). Srednji čas sledenja je znašal 16,8 meseca (razpon: 0,3–81,8 meseca). V času analize je bilo 14 (25,5 %) bolnikov še živih. Vrednosti dve- in petletnega celokupnega preživetja, dve- in petletne lokoregionalne kontrole bolezni in dve- in petletnega preživetja brez bolezni so znašale: 47 % in 19,4%; 43,7 % in 41 % ter 32,1 % in 11,5 %.

Zaključki. Rezultati zdravljenja v pričujoči raziskavi z definitivno radiokemoterapijo pri bolnikih z rakom požiralnika so primerljivi z rezultati drugih raziskav. Večina bolnikov je zdravljenje zaključila po protokolu, kar lahko vsaj delno pripišemo tudi ustreznemu in v naši ustanovi dobro organiziranemu podpornemu zdravljenju.

Radiol Oncol 2019: 53(4): 488-496.
doi: 10.2478/raon-2019-0055

Nomogram, ki ponazarja razmerje doza-volumen pri radioterapiji raka glave in vratu, je zanesljiv napovedni dejavnik za hipotiroidizem po radioterapiji

Prpić M, Kruljac I, Kust D, Suton P, Purgar N, Kirigin Biloš L, Gregov M, Mrcela I, Franceschi M, Frobe A, Djaković N

Izhodišča. Namen raziskave je bil ugotoviti možne napovedne dejavnike dozimetričnih meritev na razvoj hipotiroidizma pri bolnikih z skvamoznim rakom glave in vratu zdravljenih s kemoradioterapijo.

Bolniki in metode. V raziskavi smo analizirali podatke 156 bolnikov zdravljenih s kemoradioterapijo med avgustom 2012 in septembrom 2017. Analizirali smo parametre doza-volumen pri volumnih V10 do V70, dozah DO2 do D89 in zaščitenih volumnih VS10 do VS70. Redno smo sledili hormonski status bolnikov. Pripravili smo oceno sprememb (nomogram) ter za statistiko ostalih parametrov uporabili krivuljo Kaplan-Maier in test *Log-rank*.

Rezultati. V času sledenja (mediana vrednost 23,0 (12,0–38,5 mesecev) je 70 bolnikov (44,9 %) razvilo hipotiroidizem. Univariatna analiza je pokazala da imajo VS65, Dmin, V50 in celotni volumen ščitnice (TTV) največjo napovedno vrednost za hipotiroidizem. Multivariatna analiza pa je pokazala povezavo hipotiroidizma z manjšim TTV (razmerje obetov [OR] 0,31; 95 % interval zaupanja [CI] 0,11–0,87; P = 0,026) in Dmin (OR 9,83; 95 % CI 1,89–108,08; P = 0,042). Oceno tveganja hipotiroidizma (angl. *hypothyroidism risk score*, HRS) smo ovrednotili z regresijsko enačbo ki je zajemala TTV in Dmin. Površina pod krivuljo (AUC) pri HRS je bila 0,708 (95 % CI 0,627–0,791). Hipotiroidizem se je pojavil pri 13 bolnikih (20,0 %) z vrednostjo HRS < 7,1 in pri 57 bolnikih (62,6 %) z vrednostjo > 7,1.

Zaključki. Najvišjo napovedno vrednost za hipotiroidizem imajo parametri doze-volumna VS65, Dmin, V50 in TTV. HRS je lahko uporaben za odkrivanje bolnikov z visokim tveganjem za razvoj z obsevanjem povzročenega hipotiroidizma.

Fundacija "Docent dr. J. Cholewa"
je neprofitno, neinstitucionalno in nestrankarsko
združenje posameznikov, ustanov in organizacij, ki želijo
materialno spodbujati in poglabljati raziskovalno
dejavnost v onkologiji.

Dunajska 106
1000 Ljubljana

IBAN: SI56 0203 3001 7879 431

Activity of "Dr. J. Cholewa" Foundation for Cancer Research and Education – a report for the final quarter of 2019

Dr. Josip Cholewa Foundation for cancer research and education continues with its planned activities in the final quarter of 2019. Its primary focus remains the provision of grants, scholarships, and other forms of financial assistance for basic, clinical and public health research in the field of oncology. In parallel, it also makes efforts to provide financial and other support for the organisation of congresses, symposia and other forms of meetings to spread the knowledge about prevention and treatment of cancer, and finally about rehabilitation for cancer patients. In Foundation's strategy, the spread of knowledge should not be restricted only to the professionals that treat cancer patients, but also to the patients themselves and to the general public.

The Foundation continues to provide support for »Radiology and Oncology«, a quarterly scientific magazine with a respectable impact factor that publishes research and review articles about all aspects of cancer. The magazine is edited and published in Ljubljana, Slovenia. »Radiology and Oncology« is an open access journal available to everyone free of charge. Its long tradition represents a guarantee for the continuity of international exchange of ideas and research results in the field of oncology for all in Slovenia that are interested and involved in helping people affected by many different aspects of cancer.

The Foundation will continue with its activities in the future, especially since the problems associated with cancer affect more and more people in Slovenia and elsewhere. Ever more treatment that is successful reflects in results with longer survival in many patients with previously incurable cancer conditions. Thus adding many new dimensions in life of cancer survivors and their families.

Viljem Kovač M.D., Ph.D.
Borut Štabuc, M.D., Ph.D.
Tomaž Benulič, M.D.
Andrej Plesničar, M.D., M.Sc.

TANTUM VERDE®

benzidaminijev klorid

Za lajšanje bolečine in oteklin v ustni votlini in žrelu, ki so posledica radiomukozitisa

Bistvene informacije iz Povzetka glavnih značilnosti zdravila

Tantum Verde 1,5 mg/ml oralno pršilo, raztopina
Tantum Verde 3 mg/ml oralno pršilo, raztopina
Sestava 1,5 mg/ml: 1 ml raztopine vsebuje 1,5 mg benzidaminijevega klorida, kar ustreza 1,34 mg benzidamina. V enem razpršku je 0,17 ml raztopine. En razpršek vsebuje 0,255 mg benzidaminijevega klorida, kar ustreza 0,2278 mg benzidamina. **Sestava 3 mg/ml:** 1 ml raztopine vsebuje 3 mg benzidaminijevega klorida, kar ustreza 2,68 mg benzidamina. V enem razpršku je 0,17 ml raztopine. En razpršek vsebuje 0,51 mg benzidaminijevega klorida, kar ustreza 0,4556 mg benzidamina. **Terapevtske indikacije:** Samozdravljenje: Lajšanje bolečine in oteklin pri vnetju v ustni votlini in žrelu, ki so lahko posledica okužb in stanj po operaciji. Po nasvetu in navodilu zdravnika: Lajšanje bolečine in oteklin v ustni votlini in žrelu, ki so posledica radiomukozitisa. **Odmerjanje in način uporabe:** Odmerjanje 1,5 mg/ml: Odrasli: 4 do 8 razpršk 2- do 6-krat na dan (vsake 1,5 do 3 ure). Pediatrična populacija: Mladostniki, stari od 12 do 18 let: 4-8 razpršk 2- do 6-krat na dan. Otroci od 6 do 12 let: 4 razprški 2- do 6-krat na dan. Otroci, mlajši od 6 let: 1 razpršek na 4 kg telesne mase; do največ 4 razprške 2- do 6-krat na dan. Odmerjanje 3 mg/ml: Uporaba 2- do 6-krat na dan (vsake 1,5 do 3 ure). Odrasli: 2 do 4 razprški 2- do 6-krat na dan. Pediatrična populacija: Mladostniki, stari od 12 do 18 let: 2 do 4 razprški 2- do 6-krat na dan. Otroci od 6 do 12 let: 2 razprška 2- do 6-krat na dan. Otroci, mlajši od 6 let: 1 razpršek na 8 kg telesne mase; do največ 2 razprška 2- do 6-krat na dan. Starejši bolniki, bolniki z jetrno okvaro in bolniki z ledvično okvaro: Uporabo oralnega pršila z benzidaminijevim kloridom se svetuje pod nadzorom zdravnika. Način uporabe: Za orofaringealno uporabo. Zdravilo se razpriši v usta in žrelo. **Kontraindikacije:** Preobčutljivost na učinkovino ali katero koli pomožno snov. **Posebna opozorila in previdnostni ukrepi:** Če se simptomi v treh dneh ne izboljšajo, se mora bolnik posvetovati z zdravnikom ali zobozdravnikom, kot je primerno. Benzidamin ni priporočljiv za bolnike s preobčutljivostjo nasalicilno kislino ali druga nesteroidna protivnetna zdravila. Pri bolnikih, ki imajo ali so imeli bronhialno astmo, lahko pride do bronhospazma, zato je potrebna previdnost. To zdravilo vsebuje majhne količine etanola (alkohola), in sicer manj kot 100 mg na odmerek. To zdravilo vsebuje metilparahidroksibenzoat (E218). Lahko povzroči alergijske reakcije (lahko zapoznele). Zdravilo z jakostjo 3 mg/ml vsebuje makrogolglicerol hidroksistearat 40. Lahko povzroči želodčne težave in drisko. **Medsebojno delovanje z drugimi zdravili in druge oblike interakcij:** Študij medsebojnega delovanja niso izvedli. **Nosečnost in dojenje:** O uporabi benzidamina pri nosečnicah in doječih ženskah ni zadostnih podatkov. Uporaba zdravila med nosečnostjo in dojenjem ni priporočljiva. **Vpliv na sposobnost vožnje in upravljanja strojev:** Zdravilo v priporočenem odmerku nima vpliva na sposobnost vožnje in upravljanja strojev. **Neželeni učinki:** Neznana pogostnost (ni mogoče oceniti iz razpoložljivih podatkov): anafilaktične reakcije, preobčutljivostne reakcije, odrevenelost, laringospazem, suha usta, navzea in bruhanje, angioedem, fotosenzitivnost, pekoč občutek v ustih. Neposredno po uporabi se lahko pojavi občutek odrevenelosti v ustih in v žrelu. Ta učinek se pojavi zaradi načina delovanja zdravila in po kratkem času izgine. **Način in režim izdaje zdravila:** BRp-Izdaja zdravila je brez recepta v lekarnah in specializiranih prodajalnah.

Imetnik dovoljenja za promet: Aziende Chimiche Riunite Angelini Francesco – A.C.R.A.F. S.p.A., Viale Amelia 70, 00181 Rim, Italija **Datum zadnje revizije besedila:** 14. 10. 2019

Pred svetovanjem ali izdajo preberite celoten Povzetek glavnih značilnosti zdravila.

Samo za strokovno javnost.

Datum priprave informacije: november 2019

Odgovoren za trženje: Bonifar d.o.o.

ANGELINI

PR/BSI/BEN/2019/012

NOVO
pri HR+/
HER2- mBC

Verzenios™
abemaciklib

EDINI
zaviralec CDK4 & 6, ki se jemlje NEPREKINJENO VSAK DAN.[1, 2, 3]

SKRAJŠAN POVZETEK GLAVNIH ZNAČILNOSTI ZDRAVILA
▼Za to zdravilo se izvaja dodatno spremljanje varnosti. Tako bodo hitreje na voljo nove informacije o njegovi varnosti. Zdravstvene delavce naprošamo, da poročajo o katerem koli domnevnem neželenem učinku zdravila.
IME ZDRAVILA Verzenios 50 mg/100 mg/150 mg filmsko obložene tablete **KAKOVOSTNA IN KOLIČINSKA SESTAVA** Ena filmsko obložena tableta vsebuje 50 mg/100 mg/150 mg abemaciklib. Ena filmsko obložena tableta vsebuje 14 mg/28 mg/42 mg laktoze (v obliki monohidrata). **Terapevtske indikacije** Zdravilo Verzenios je indicirano za zdravljenje žensk z lokalno napredovalim ali metastatskim, na hormonske receptorje (HR – *Hormone Receptor*) pozitivnim in na receptorje humanega epidermalnega rastnega faktorja 2 (HER2 – *Human Epidermal Growth Factor Receptor 2*) negativnim rakom dojk v kombinaciji z zaviralcem aromataze ali s fulvestrantom kot začetnim endokrinim zdravljenjem ali pri ženskah, ki so prejele predhodno endokrino zdravljenje. Pri ženskah v pred- in perimenopavzi je treba endokrino zdravljenje kombinirati z agonistom gonadoliberina (LHRH – *Luteinizing Hormone–Releasing Hormone*). **Odmerjanje in način uporabe** Zdravljenje z zdravilom Verzenios mora uvesti in nadzorovati zdravnik, ki ima izkušnje z uporabo zdravil za zdravljenje rakavih bolezni. *Zdravilo Verzenios v kombinaciji z endokrinim zdravljenjem* Priporočeni odmerek abemaciklib je 150 mg dvakrat na dan, kadar se uporablja v kombinaciji z endokrinim zdravljenjem. Zdravilo Verzenios je treba jemati, dokler ima bolnica od zdravljenja klinično korist ali dokler se ne pojavi nesprejemljiva toksičnost. Če bolnica bruha ali izpusti odmerek zdravila Verzenios, ji je treba naročiti, da naj naslednji odmerek vzame ob predvidenem času; dodatnega odmerka ne sme vzeti. Obvladovanje nekaterih neželenih učinkov lahko zahteva prekinitev in/ali zmanjšanje odmerka. Sočasni uporabi močnih zaviralcev CYP3A4 se je treba izogibati. Če se uporabi močnih zaviralcev CYP3A4 ni mogoče izogniti, je treba odmerek abemaciklib zmanjšati na 100 mg dvakrat na dan. Pri bolnicah, pri katerih je bil odmerek zmanjšan na 100 mg abemaciklib dvakrat na dan in pri katerih se sočasnemu dajanju močnega zaviralca CYP3A4 ni mogoče izogniti, je treba odmerek abemaciklib dodatno zmanjšati na 50 mg dvakrat na dan. Pri bolnicah, pri katerih je bil odmerek zmanjšan na 50 mg abemaciklib dvakrat na dan in pri katerih se sočasnemu dajanju močnega zaviralca CYP3A4 ni mogoče izogniti, je mogoče z odmerkom abemaciklib nadaljevati ob natančnem spremljanju znakov toksičnosti. Alternativno je mogoče odmerek abemaciklib zmanjšati na 50 mg enkrat na dan ali prekiniti dajanje abemaciklib. Če je uporaba zaviralca CYP3A4 prekinjena, je treba odmerek abemaciklib povečati na odmerek, kakršen je bil pred uvedbo zaviralca CYP3A4 (po 3–5 razpolovnih časih zaviralca CYP3A4). Prilagajanje odmerka glede na starost in pri bolnicah z blago ali zmerno ledvično okvaro ter z blago (Child Pugh A) ali zmerno (Child Pugh B) jetrno okvaro ni potrebno. Pri dajanju abemaciklib bolnicam s hudo ledvično okvaro sta potrebna previdnost in skrbno spremljanje glede znakov toksičnosti. Način uporabe Zdravilo Verzenios je namenjeno za peroralno uporabo. Odmerek se lahko vzame s hrano ali brez nje. Zdravilo se ne sme jemati z grenivko ali grenivkinim sokom. Bolnice naj odmerke vzamejo vsak dan ob približno istem času. Tableto je treba zaužiti celo (bolnice je pred zaužitjem ne smejo gristi, drobiti ali deliti). **Kontraindikacije** Preobčutljivost na učinkovino ali katero koli pomožno snov. **Posebna opozorila in previdnostni ukrepi** Pri bolnicah, ki so prejemale abemaciklib, so poročali o nevtropeniji, o večji pogostnosti okužb kot pri bolnicah, zdravljenih s placebom in endokrinim zdravljenjem, o povečanih vrednostih ALT in AST. Pri bolnicah, pri katerih se pojavi nevtropenija stopnje 3 ali 4, je priporočljivo prilagoditi odmerek. Bolnice je treba spremljati za znake in simptome globoke venske tromboze in pljučne embolije ter jih zdraviti, kot je medicinsko utemeljeno. Glede na povečanje vrednosti ALT ali AST je mogoče potrebna prilagoditev odmerka. Driska je najpogostejši neželeni učinek. Bolnice je treba ob prvem znaku tekočega blata začeti zdraviti z antidiaroiki, kot je loperamid, povečati vnos peroralnih tekočin in obvestiti zdravnika. Sočasni uporabi induktorjev CYP3A4 se je treba izogibati zaradi tveganja za zmanjšano učinkovitost abemaciklib. Bolnice z redkimi dednimi motnjami, kot so intoleranca za galaktozo, popolno pomanjkanje laktaze ali malapsorpcija glukoze/galaktoze, tega zdravila ne smejo jemati. **Medsebojno delovanje z drugimi zdravili in druge oblike interakcij** Abemaciklib se primarno presnavlja s CYP3A4. Sočasna uporaba abemaciklib in zaviralcev CYP3A4 lahko poveča plazemsko koncentracijo abemaciklib. Uporabi močnih zaviralcev CYP3A4 sočasno z abemaciklibom se je treba izogibati. Če je močne zaviralce CYP3A4 treba dajati sočasno, je treba odmerek abemaciklib zmanjšati, nato pa bolnico skrbno spremljati glede toksičnosti. Pri bolnicah, zdravljenih z zmernimi ali šibkimi zaviralci CYP3A4, ni potrebno prilagajanje odmerka, vendar jih je treba skrbno spremljati za znake toksičnosti. Sočasni uporabi močnih induktorjev CYP3A4 (vključno, vendar ne omejeno na: karbamazepin, fenitoin, rifampicin in šentjanževko) se je treba izogibati zaradi tveganja za zmanjšano učinkovitost abemaciklib. Abemaciklib in njegovi glavni aktivni presnovki zavirajo prenašalce v ledvicah, in sicer kationski organski prenašalec 2 (OCT2) ter prenašalca MATE1. *In vivo* lahko pride do medsebojnega delovanja abemaciklib in klinično pomembnih substratov teh prenašalcev, kot je dofelitid ali kreatinin. Trenutno ni znano, ali lahko abemaciklib zmanjša učinkovitost sistemskih hormonskih kontraceptivov, zato se ženskam, ki uporabljajo sistemske hormonske kontraceptive, svetuje, da hkrati uporabljajo tudi mehansko metodo. **Neželeni učinki** Najpogostejši neželeni učinki so driska, okužbe, nevtropenija, anemija, utrujenost, navzea, bruhanje in zmanjšanje apetita. *Zelo pogosti:* okužbe, nevtropenija, levkopenija, anemija, trombocitopenija, driska, bruhanje, navzea, zmanjšanje apetita, disgevzija, omotica, alopecija, pruritus, izpuščaj, utrujenost, pireksija, povečana vrednost alanin-aminotransferaze, povečana vrednost aspartat-aminotransferaze *Pogosti:* limfopenija, povečano solzenje, venska trombembolija, suha koža, mišična šibkost *Občasni:* febrilna nevtropenija **Imetnik dovoljenja za promet z zdravilom**: Eli Lilly Nederland B.V., Papendorpseweg 83, 3528BJ, Utrecht, Nizozemska. Datum prve odobritve dovoljenja za promet: 27. september 2018 **Datum zadnje revizije besedila**: 2.11.2018 **Režim izdaje:** Rp/Spec - Predpisovanje in izdaja zdravila je le na recept zdravnika specialista ustreznega področja medicine ali od njega pooblaščenega zdravnika.

Reference
1. Povzetek glavnih značilnosti zdravila Verzenios. Datum zadnje revizije besedila: 2.11.2018. **2.** Povzetek glavnih značilnosti zdravila Ibrance. Dostop preverjen 22.11.2018. **3.** Povzetek glavnih značilnosti zdravila Kisqali. Dostop preverjen 22.11.2018.

Pomembno obvestilo
Pričujoče gradivo je namenjeno samo za strokovno javnost. Predpisovanje in izdaja zdravila Verzenios je le na recept zdravnika specialista ustreznega področja medicine ali od njega pooblaščenega zdravnika. Pred predpisovanjem zdravila Verzenios vas vljudno prosimo, da preberete celotni Povzetek glavnih značilnosti zdravila. Podrobnejše informacije o zdravilu Verzenios in o zadnji reviziji besedila Povzetka glavnih značilnosti zdravila so na voljo na sedežu podjetja Eli Lilly (naslov podjetja in kontaktni podatki spodaj) in na spletni strani European Medicines Agency (EMA): www.ema.europa.eu in na spletni strani European Commission http://ec.europa.eu/health/documents/community-register/html/alfregister.htm.

Eli Lilly farmacevtska družba, d.o.o., Dunajska cesta 167, 1000 Ljubljana, telefon 01 / 580 00 10, faks 01 / 569 17 05

PP-AL-SI-0001, 23.11.2018, Samo za strokovno javnost.

Lilly

KEYTRUDA®
(pembrolizumab, MSD)

Pomaga spreminjati pričakovanja o preživetju

- pri metastatskem NSCLC *,1,2
- in napredovalem melanomu[3]

*NSCLC – non-small cell lung cancer

Reference: 1. Gandhi L, Rodríguez-Abreu D, Gadgeel S, et. al.; for the KEYNOTE-189 investigators. Pembrolizumab plus chemotherapy in metastatic non–small-cell lung cancer. N Engl J Med. 2018;378(22):2078–2092. **2.** Keytruda EU SmPC **3.** Hamid O, Robert C, Daud A, et. al. 5-year survival outcomes for patients with advanced melanoma treated with pembrolizumab in KEYNOTE-001. Annals of Oncology 2019; 30: 582-588.

SKRAJŠAN POVZETEK GLAVNIH ZNAČILNOSTI ZDRAVILA
Pred predpisovanjem, prosimo, preberite celoten Povzetek glavnih značilnosti zdravila!
▼ Za to zdravilo se izvaja dodatno spremljanje varnosti.
Ime zdravila: KEYTRUDA 25 mg/ml koncentrat za raztopino za infundiranje vsebuje pembrolizumab. **Terapevtske indikacije:** Zdravilo KEYTRUDA je kot samostojno zdravljenje indicirano za zdravljenje: napredovalega (neoperabilnega ali metastatskega) melanoma pri odraslih; za adjuvantno zdravljenje odraslih z melanomom v stadiju III, ki se je razširil na bezgavke, po popolni kirurški odstranitvi; metastatskega nedrobnoceličnega pljučnega raka (NSCLC) v prvi liniji zdravljenja pri odraslih, ki imajo tumorje z ≥ 50 % izraženostjo PD-L1 (TPS) in brez pozitivnih tumorskih mutacij EGFR ali ALK; lokalno napredovalega ali metastatskega NSCLC pri odraslih, ki imajo tumorje z ≥ 1 % izraženostjo PD-L1 (TPS) in so bili predhodno zdravljeni z vsaj eno shemo kemoterapije, bolniki s pozitivnimi tumorskimi mutacijami EGFR ali ALK so pred prejemom zdravila KEYTRUDA morali prejeti tudi tarčno zdravljenje; odraslih bolnikov s ponovljenim ali neodzivnim klasičnim Hodgkinovim limfomom (cHL), pri katerih avtologna presaditev matičnih celic (ASCT) in zdravljenje z brentuksimabom vedotinom (BV) nista bila uspešna, in odraslih bolnikov, ki za presaditev niso primerni, zdravljenje z BV pa pri njih ni bilo uspešno; lokalno napredovalega ali metastatskega urotelijskega karcinoma pri odraslih, predhodno zdravljenih s kemoterapijo, ki je vključevala platino; lokalno napredovalega ali metastatskega urotelijskega karcinoma pri odraslih, ki niso primerni za zdravljenje s kemoterapijo, ki vsebuje cisplatin in imajo tumorje z izraženostjo PD-L1 ≥ 10, ocenjeno s kombinirano pozitivno oceno (CPS); ponovljenega ali metastatskega ploščatoceličnega karcinoma glave in vratu (HNSCC) pri odraslih, ki imajo tumorje z ≥ 50 % izraženostjo PD-L1 (TPS), in pri katerih je bolezen napredovala med zdravljenjem ali po zdravljenju s kemoterapijo, ki je vključevala platino. Zdravilo KEYTRUDA je v kombinaciji s pemetreksedom in kemoterapijo na osnovi platine indicirano za prvo linijo zdravljenja metastatskega neploščatoceličnega NSCLC pri odraslih, pri katerih tumorji nimajo pozitivnih mutacij EGFR ali ALK; v kombinaciji s karboplatinom in bodisi paklitakselom bodisi nab-paklitakselom je indicirano za prvo linijo zdravljenja metastatskega ploščatoceličnega NSCLC pri odraslih; v kombinaciji z aksitinibom je indicirano za prvo linijo zdravljenja napredovalega raka ledvičnih celic (RCC) pri odraslih. **Odmerjanje in način uporabe:** Testiranje PD-L1 pri bolnikih z NSCLC, urotelijskim karcinomom ali HNSCC: Pri bolnikih z NSCLC je priporočljivo opraviti testiranje izraženosti PD-L1 tumorja z validirano preiskavo. Bolnike s predhodno nezdravljenim urotelijskim karcinomom ali HNSCC je treba za zdravljenje izbrati na podlagi izraženosti PD-L1, potrjene z validirano preiskavo. Odmerjanje: Priporočeni odmerek zdravila KEYTRUDA za samostojno zdravljenje je bodisi 200 mg na 3 tedne ali 400 mg na 6 tednov, apliciran z intravensko infuzijo v 30 minutah. Priporočeni odmerek za kombinirano zdravljenje je 200 mg na 3 tedne, apliciran z intravensko infuzijo v 30 minutah. Za uporabo v kombinaciji glejte povzetke glavnih značilnosti sočasno uporabljenih zdravil. Če se uporablja kot del kombiniranega zdravljenja skupaj s kemoterapijo, je treba zdravilo KEYTRUDA aplicirati prvo. Bolnike je treba zdraviti do napredovanja bolezni ali nesprejemljivih toksičnih učinkov. Pri adjuvantnem zdravljenju melanoma je treba zdravilo uporabljati do ponovitve bolezni, pojava nesprejemljivih toksičnih učinkov oziroma mora zdravljenje trajati do enega leta. Če je aksitinib uporabljen v kombinaciji s pembrolizumabom, se lahko razmisli o povečanju odmerka aksitiniba nad začetnih 5 mg v presledkih šest tednov ali več. Pri bolnikih starih ≥ 65 let, bolnikih z blago do zmerno okvaro ledvic, bolnikih z blago okvaro jeter prilagoditev odmerka ni potrebna. Odložitev odmerka ali ukinitev zdravljenja: Za primere, kjer je treba zdravljenje zadržati, dokler se neželeni učinki ne zmanjšajo na stopnjo 0-1 in kadar je treba zdravilo KEYTRUDA trajno ukiniti, prosimo, glejte celoten Povzetek glavnih značilnosti zdravila. **Kontraindikacije:** Preobčutljivost na učinkovino ali katero koli pomožno snov. **Povzetek posebnih opozoril, previdnostnih ukrepov, interakcij in neželenih učinkov:** Imunsko pogojeni neželeni učinki (pnevmonitis, kolitis, hepatitis, nefritis, endokrinopatije, neželeni učinki na kožo in drugi): Pri bolnikih, ki so prejemali pembrolizumab, so se pojavili imunsko pogojeni neželeni učinki, vključno s hudimi in smrtnimi primeri. Večina imunsko pogojenih neželenih učinkov, ki so se pojavili med zdravljenjem s pembrolizumabom, je bila reverzibilnih in so jih obvladali s prekinitvami uporabe pembrolizumaba, uporabo kortikosteroidov in/ali podporno oskrbo. Pojavijo se lahko tudi po zadnjem odmerku pembrolizumaba in hkrati prizadanejo več organskih sistemov. V primeru suma na imunsko pogojene neželene učinke je treba poskrbeti za ustrezno oceno za potrditev etiologije oziroma izključitev drugih vzrokov. Glede na izrazitost neželenega učinka je treba zadržati uporabo pembrolizumaba in uporabiti kortikosteroide – za natančna navodila, prosimo, glejte Povzetek glavnih značilnosti zdravila Keytruda. Zdravljenje s pembrolizumabom lahko poveča tveganje za zavrnitev pri prejemnikih presadkov čvrstih organov. Pri bolnikih, ki so prejemali pembrolizumab, so poročali o hudih z infuzijo povezanih reakcijah, vključno s preobčutljivostjo in anafilaksijo. Pembrolizumab se iz obtoka odstrani s katabolizmom, zato presnovnih medsebojnih delovanj zdravil ni pričakovati. Uporabi sistemskih kortikosteroidov ali imunosupresivov pred uvedbo pembrolizumaba se je treba izogibati, ker lahko vplivajo na farmakodinamično aktivnost in učinkovitost pembrolizumaba. Vendar pa je kortikosteroide ali druge imunosupresive mogoče uporabiti za zdravljenje imunsko pogojenih neželenih učinkov. Kortikosteroide je mogoče uporabiti tudi kot premedikacijo, če je pembrolizumab uporabljen v kombinaciji s kemoterapijo, kot antiemetično profilakso in/ali za ublažitev neželenih učinkov, povezanih s kemoterapijo. Ženske v rodni dobi morajo med zdravljenjem s pembrolizumabom in vsaj še 4 mesece po zadnjem odmerku pembrolizumaba uporabljati učinkovito kontracepcijo, med nosečnostjo in dojenjem se ga ne sme uporabljati. Varnost pembrolizumaba pri samostojnem zdravljenju so v kliničnih študijah ocenili pri 4.948 bolnikih z napredovalim melanomom, kirurško odstranjenim melanomom v stadiju III (adjuvantno zdravljenje), NSCLC, cHL, urotelijskim karcinomom ali HNSCC s štirimi odmerki (2 mg/kg na 3 tedne, 200 mg na 3 tedne in 10 mg/kg na 2 ali 3 tedne). V tej populaciji bolnikov je mediani čas opazovanja znašal 7,3 mesece (v razponu od 1 dneva do 31 mesecev), najpogostejši neželeni učinki zdravljenja s pembrolizumabom so bili utrujenost (34,1 %), izpuščaj (22,7 %), navzea (21,7 %), diareja (21,5 %) in pruritus (20,2 %). Večina poročanih neželenih učinkov pri samostojnem zdravljenju je bila po izrazitosti 1. ali 2. stopnje. Najresnejši neželeni učinki so bili imunsko pogojeni neželeni učinki in hude z infuzijo povezane reakcije. Varnost pembrolizumaba pri kombiniranem zdravljenju s kemoterapijo so ocenili pri 791 bolnikih NSCLC, ki so v kliničnih študijah prejemali pembrolizumab v odmerkih 200 mg, 2 mg/kg ali 10 mg/kg na vsake 3 tedne. V tej populaciji bolnikov so bili najpogostejši neželeni učinki diareja (54 %), hipertenzija (45 %), utrujenost (38 %), hipotiroidizem (35 %), zmanjšan apetit (30 %), sindrom palmarno-plantarne eritrodisestezije (28 %), navzea (28 %), zvišanje vrednosti ALT (27 %), zvišanje vrednosti AST (26 %), disfonija (25 %), kašelj (21 %) in zaprtost (21 %). Pojavnost neželenih učinkov 3. do 5. stopnje je bila med kombiniranim zdravljenjem s pembrolizumabom 76 % in pri zdravljenju s sunitinibom samim 71 %. Za celoten seznam neželenih učinkov, prosimo, glejte celoten Povzetek glavnih značilnosti zdravila.
Način in režim izdaje zdravila: H – Predpisovanje in izdaja zdravila je samo na recept, zdravilo se uporablja samo v bolnišnicah. Imetnik dovoljenja za promet z zdravilom: Merck Sharp & Dohme B.V. , Waarderweg 39, 2031 BN Haarlem, Nizozemska. **Datum zadnje revizije besedila:** 26. avgust 2019

MSD

Merck Sharp & Dohme inovativna zdravila d.o.o.,
Šmartinska cesta 140, 1000 Ljubljana
tel: +386 1/ 520 42 01, fax: +386 1/ 520 43 50
Pripravljeno v Sloveniji, september 2019; SI-KEY-00035 EXP: 09/2021
Samo za strokovno javnost.
H - Predpisovanje in izdaja zdravila je le na recept, zdravilo pa se uporablja samo v bolnišnicah. Pred predpisovanjem, prosimo, preberite celoten Povzetek glavnih značilnosti zdravila Keytruda, ki je na voljo pri naših strokovnih sodelavcih ali na lokalnem sedežu družbe.

Več na
foundationmedicine.si

OBŠIREN VPOGLED ZA NAČRTOVANJE BOLNIKU PRILAGOJENEGA ZDRAVLJENJA[1-6]

Odkrijte možnosti visoko kakovostnih storitev obširnega genomskega profiliranja FoundationOne®, ki olajšajo odločitev o najustreznejšem zdravljenju za posameznega bolnika z rakom, v različnih kliničnih stanjih.[4-6]

FOUNDATIONONE® CDx

FOUNDATIONONE® LIQUID

FOUNDATIONONE® HEME

Viri: 1. Frampton GM s sod. Nat Biotechnol 2013; 31:1023-1031. 2. Clark TA s sod. J Mol Diagn 2018; 20:686-702. 3. He J s sod. Blood 2016; 127:3004-3014. 4. FoundationOne® CDx Technical Information; dostopano april 2019 na: https://assets.ctfassets.net/vhribv12lmne/6Rt6csmCPuaguuqmgi2iY8/e3a9b0456ed71a55d2e4480374695d95/FoundationOne_CDx.pdf. 5. FoundationOne® Liquid Technical Specifications; dostopano april 2019 na: https://assets.ctfassets.net/vhribv12lmne/3SPYAcbGdqAeMsOqMyKUog/d0eb51659e08d733bf39971e85ed940d/F1L_TechnicalInformation_MKT-0061-04.pdf. 6. FoundationOne® Heme Technical Specifications; dostopano april 2019 na: https://assets.ctfassets.net/vhribv12lmne/zBxaQC12cScqgsEk8seMO/abf6133874f1e5929403f66d90c3b900/F1H_TechnicalInformation_06_digital.pdf.

PM-0148-2019-FMI

Informacija pripravljena: oktober 2019. Samo za strokovno javnost.
DODATNE INFORMACIJE SO NA VOLJO PRI:
Roche farmacevtska družba d.o.o., Stegne 13g, 1000 Ljubljana
rocheprotiraku.si / foundationmedicine.si

FOUNDATION MEDICINE®

Roche

Lonsurf®

trifluridin/tipiracil

Več časa za trenutke, ki štejejo

Kolorektalni rak

Zdravilo Lonsurf je indicirano v monoterapiji za zdravljenje odraslih bolnikov z metastatskim kolorektalnim rakom (KRR), ki so bili predhodno že zdravljeni ali niso primerni za zdravljenja, ki so na voljo. Ta vključujejo kemoterapijo na osnovi fluoropirimidina, oksaliplatina in irinotekana, zdravljenje z zaviralci žilnega endotelijskega rastnega dejavnika (VEGF – Vascular Endothelial Growth Factor) in zaviralci receptorjev za epidermalni rastni dejavnik (EGFR – Epidermal Growth Factor Receptor).

Rak želodca

Zdravilo Lonsurf je indicirano v monoterapiji za zdravljenje odraslih bolnikov z metastatskim rakom želodca vključno z adenokarcinomom gastro-ezofagealnega prehoda, ki so bili predhodno že zdravljeni z najmanj dvema sistemskima režimoma zdravljenja za napredovalo bolezen

Družba Servier ima licenco družbe Taiho za zdravilo Lonsurf®. Pri globalnem razvoju zdravila sodelujeta obe družbi in ga tržita na svojih določenih področjih.

SERVIER

Skrajšan povzetek glavnih značilnosti zdravila: Lonsurf 15 mg/6,14 mg filmsko obložene tablete in Lonsurf 20 mg/8,19 mg filmsko obložene tablete

▼Za to zdravilo se izvaja dodatno spremljanje varnosti. Tako bodo hitreje na voljo nove informacije o njegovi varnosti. Zdravstvene delavce naprošamo, da poročajo o katerem koli domnevnem neželenem učinku zdravila. **SESTAVA*: Lonsurf 15 mg/6,14 mg:** Ena filmsko obložena tableta vsebuje 15 mg trifluridina in 6,14 mg tipiracila (v obliki klorida). **Lonsurf 20 mg/8,19 mg:** Ena filmsko obložena tableta vsebuje 20 mg trifluridina in 8,19 mg tipiracila (v obliki klorida). **TERAPEVTSKE INDIKACIJE*:** Kolorektalni rak – zdravilo Lonsurf je indicirano v monoterapiji za zdravljenje odraslih bolnikov z metastatskim kolorektalnim rakom, ki so bili predhodno že zdravljeni ali niso primerni za zdravljenja, ki so na voljo. Ta vključujejo kemoterapijo na osnovi fluoropirimidina, oksaliplatina in irinotekana, zdravljenje z zaviralci žilnega endotelijskega rastnega dejavnika (VEGF – Vascular Endothelial Growth Factor) in zaviralci receptorjev za epidermalni rastni dejavnik (EGFR – Epidermal Growth Factor Receptor). Rak želodca – zdravilo Lonsurf je indicirano v monoterapiji za zdravljenje odraslih bolnikov z metastatskim rakom želodca vključno z adenokarcinomom gastro-ezofagealnega prehoda, ki so bili predhodno že zdravljeni z najmanj dvema sistemskima režimoma zdravljenja za napredovalo bolezen. **ODMERJANJE IN NAČIN UPORABE*:** Priporočeni začetni odmerek zdravila Lonsurf pri odraslih je 35 mg/m^2/odmerek peroralno dvakrat dnevno na 1. do 5. dan in 8. do 12. dan vsakega 28-dnevnega cikla zdravljenja, najpozneje 1 uro po zaključku jutranjega in večernega obroka. Odmerjanje, izračunano glede na telesno površino, ne sme preseči 80 mg/odmerek. Možne prilagoditve odmerka glede na varnost in prenašanje zdravila: dovoljena so največ 3 zmanjšanja odmerka na najmanjši odmerek 20 mg/m^2 dvakrat dnevno. Potem ko je bil odmerek zmanjšan, povečanje ni dovoljeno. **KONTRAINDIKACIJE*:** Preobčutljivost na zdravilni učinkovini ali katero koli pomožno snov. **OPOZORILA IN PREVIDNOSTNI UKREPI*:** Supresija kostnega mozga: Pred uvedbo zdravljenja in po potrebi za spremljanje toksičnosti zdravila, najmanj pred vsakim ciklom zdravljenja, je treba pregledati celotno krvno sliko. Zdravljenja ne smete začeti, če je absolutno število nevtrofilcev < 1,5 x 10^9/l, če je število trombocitov < 75 x 10^9/l ali če se je pri bolniku zaradi predhodnih zdravljenj pojavila klinično pomembna nehematološka toksičnost 3. ali 4. stopnje, ki še traja. Bolnike je treba skrbno spremljati zaradi morebitnih okužb, uvesti je treba ustrezne ukrepe, kot je klinično indicirano. Toksičnost za prebavila: Potrebna je uporaba antiemetikov, antidiaroikov ter drugih ukrepov, kot je klinično indicirano. Če je potrebno, prilagodite odmerke. Ledvična okvara: Zdravilo Lonsurf ni primerno za uporabo pri bolnikih s hudo ledvično okvaro ali končno stopnjo ledvične okvare. Bolnike z ledvično okvaro je potrebno med zdravljenjem skrbno spremljati; bolnike z zmerno ledvično okvaro je treba zaradi hematoloških toksičnosti bolj pogosto spremljati. Jetrna okvara: Uporaba zdravila Lonsurf pri bolnikih z obstoječo zmerno ali hudo jetrno okvaro ni priporočljiva. Proteinurija: Pred začetkom zdravljenja in med njim je priporočljivo spremljanje proteinurije z urinskimi testnimi lističi. Pomožne snovi: Zdravilo vsebuje laktozo. **INTERAKCIJE*:** Zdravila, ki medsebojno delujejo z nukleozidnimi prenašalci CNT1, ENT1 in ENT2, zaviralci OCT2 ali MATE1, substrati humane timidin-kinaze (npr. zidovudinom), hormonskimi kontraceptivi. **PLODNOST*, NOSEČNOST IN DOJENJE*:** Ni priporočljivo. **KONTRACEPCIJA*:** Ženske in moški morajo uporabljati učinkovito metodo kontracepcije med zdravljenjem in do 6 mesecev po zaključku zdravljenja. **VPLIV NA SPOSOBNOST VOŽNJE IN UPRAVLJANJA STROJEV*:** Med zdravljenjem se lahko pojavijo utrujenost, omotica ali splošno slabo počutje. **NEŽELENI UČINKI*:** *Zelo pogosti:* nevtropenija, levkopenija, anemija, trombocitopenija, zmanjšan apetit, diareja, navzea, bruhanje, utrujenost. *Pogosti:* okužba spodnjih dihal, febrilna nevtropenija, limfopenija, hipoalbuminemija, disgevzija, periferna nevropatija, dispneja, bolečina v trebuhu, zaprtje, stomatitis, bolezni ustne votline, hiperbilirubinemija, sindrom palmarne plantarne eritrodisestezije, izpuščaj, alopecija, pruritus, suha koža, proteinurija, pireksija, edem, vnetje sluznice, splošno slabo počutje, zvišanje jetrnih encimov, zvišanje alkalne fosfataze v krvi, zmanjšanje telesne mase. *Občasni:* septični šok, infekcijski enteritis, pljučnica, okužba žolčevoda, gripa, okužba sečil, gingivitis, herpes zoster, tinea pedis, okužba s kandido, bakterijska okužba, okužba, nevtropenična sepsa, okužba zgornjih dihal, konjunktivitis, bolečina zaradi raka, pancitopenija, granulocitopenija, monocitopenija, eritropenija, levkocitoza, monocitoza, dehidracija, hiperglikemija, hiperkaliemija, hipokaliemija, hipofosfatemija, hipernatriemija, hiponatriemija, hipokalciemija, protin, anksioznost, nespečnost, nevrotoksičnost, disestezija, hiperestezija, hipoestezija, sinkopa, parestezija, pekoč občutek, letargija, omotica, glavobol, zmanjšana ostrina vida, zamegljen vid, diplopija, katarakta, suho oko, vrtoglavica, neugodje v ušesu, angina pektoris, aritmija, palpitacije, embolija, hipertenzija, hipotenzija, vročinski oblivi, pljučna embolija, plevralni izliv, izcedek iz nosu, disfonija, orofaringealna bolečina, epistaksa, kašelj, hemoragični enterokolitis, krvavitev v prebavilih, akutni pankreatitis, ascites, ileus, subileus, kolitis, gastritis, refluksni gastritis, ezofagitis, moteno praznjenje želodca, abdominalna distenzija, analno vnetje, razjede v ustih, dispepsija, gastroezofagealna refluksna bolezen, proktalgija, bukalni polip, krvavitev dlesni, glositis, parodontalna bolezen, bolezen zob, siljenje na bruhanje, flatulenca, slab zadah, hepatotoksičnost, razširitev žolčnih vodov, luščenje kože, urtikarija, preobčutljivostne reakcije na svetlobo, eritem, akne, hiperhidroza, žulj, bolezni nohtov, otekanje sklepov, artralgija, bolečina v kosteh, mialgija, mišično-skeletna bolečina, mišična oslabelost, mišični krči, bolečina v okončinah, ledvična odpoved, neinfektivni cistitis, motnje mikcije, hematurija, levkociturija, motnje menstruacije, poslabšanje splošnega zdravstvenega stanja, bolečina, občutek spremembe telesne temperature, kseroza, nelagodje, zvišanje kreatinina v krvi, podaljšanje intervala QT na elektrokardiogramu, povečanje mednarodnega umerjenega razmerja (INR), podaljšanje aktiviranega parcialnega tromboplastinskega časa (aPTČ), zvišanje sečnine v krvi, zvišanje laktatne dehidrogenaze v krvi, znižanje celokupnih proteinov, zvišanje C-reaktivnega proteina, zmanjšan hematokrit. *Post-marketinške izkušnje:* intersticijska bolezen pljuč. **PREVELIKO ODMERJANJE*:** Neželeni učinki, o katerih so poročali v povezavi s prevelikim odmerjanjem, so bili v skladu z uveljavljenim varnostnim profilom. Glavni pričakovani zaplet prevelikega odmerjanja je supresija kostnega mozga. **FARMAKODINAMIČNE LASTNOSTI*:** *Farmakoterapevtska skupina:* zdravila z delovanjem na novotvorbe, antimetaboliti, oznaka ATC: L01BC59. Zdravilo Lonsurf sestavljata antineoplastični timidinski nukleozidni analog, trifluridin, in zaviralec timidin-fosforilaze (TPaze), tipiracilijev klorid. Po privzemu v rakave celice timidin-kinaza fosforilira trifluridin. Ta se v celicah nato presnovi v substrat deoksiribonukleinske kisline (DNA), ki se vgradi neposredno v DNA ter tako preprečuje celično proliferacijo. TPaza hitro razgradi trifluridin in njegova presnova po peroralni uporabi je hitra zaradi učinka prvega prehoda, zato je v zdravilo vključen zaviralec TPaze, tipiracilijev klorid. **PAKIRANJE*:** 20 filmsko obloženih tablet. **NAČIN PREDPISOVANJA IN IZDAJE ZDRAVILA:** Rp/Spec. **Imetnik dovoljenja za promet:** Les Laboratoires Servier, 50, rue Carnot, 92284 Suresnes cedex, Francija. **Številka dovoljenja za promet z zdravilom:** EU/1/16/1096/001 (Lonsurf 15 mg/6,14 mg), EU/1/16/1096/004 (Lonsurf 20 mg/8,19 mg). **Datum zadnje revizije besedila: september 2019. *Pred predpisovanjem preberite celoten povzetek glavnih značilnosti zdravila. Celoten povzetek glavnih značilnosti zdravila in podrobnejše informacije so na voljo pri: Servier Pharma d.o.o., Podmilščakova ulica 24, 1000 Ljubljana, tel: 01 563 48 11, www.servier.si.**

Datum priprave informacije: november 2019.
LNF AD1 C1 19/20 Samo za strokovno javnost.

Podaljšajmo, kar lahko.

Dokazano podaljša celokupno preživetje (OS) na več kot 1 leto (12,6 mesecev VARGATEF® + docetaksel v primerjavi z 10,3 mesecev placebo + docetaksel; HR: 0,83 [95% CI 0,70 – 0,99]; P = 0,0359) pri bolnikih, ki ga prejemajo v kombinaciji z docetakselom, z lokalno napredovalim, metastatskim ali lokalno ponovljivim nedrobnoceličnim pljučnim rakom (non-small cell lung cancer – NSCLC) s histologijo adenokarcinoma po kemoterapiji prve izbire.[1,2]

Vargatef 100 mg mehke kapsule, Vargatef 150 mg mehke kapsule

Sestava: ena mehka kapsula vsebuje 100 mg nintedaniba oz. 150 mg nintedaniba (v obliki esilata). Vsebuje 1,2 mg oz. 1,8 mg sojinega lecitina .**Terapevtske indikacije:** indicirano v kombinaciji z docetakselom za zdravljenje odraslih bolnikov z lokalno napredovalim, metastatskim ali lokalno ponovljivim nedrobnoceličnim pljučnim rakom (*NSCLC*) s histologijo adenokarcinoma po kemoterapiji prve izbire. **Odmerjanje in način uporabe:** zdravljenje mora uvesti in nadzirati zdravnik, ki ima izkušnje z uporabo onkoloških zdravil. Priporočeni odmerek nintedaniba je 200 mg 2x/dan, ki ga je treba jemati v približno 12-urnem razmiku, od 2. do 21. dne standardnega 21-dnevnega cikla zdravljenja z docetakselom. Bolnik ne sme vzeti Vargatefa istega dne, ko prejme kemoterapijo z docetakselom (to je 1. dne). Če bolnik pozabi vzeti priporočeni odmerek nintedaniba, naj ga začne ponovno jemati ob naslednjem načrtovanem času. Posameznih dnevnih priporočenih odmerkov nintedaniba ni dovoljeno povečati, zato da bi nadomestili pozabljene odmerke. Ne smete prekoračiti niti največjega priporočenega dnevnega odmerka 400 mg. Bolniki lahko z zdravljenjem z nintedanibom nadaljujejo po prekinitvi docetaksela, dokler so vidne klinične koristi ali do pojava nesprejemljive toksičnosti. ***Prilagajanje odmerka:*** začetni ukrep za obravnavo neželenih učinkov je začasna prekinitev zdravljenja z nintedanibom, dokler specifični neželeni učinek ne bo izzvenel do ravni, ki omogoča nadaljevanje zdravljenja (do 1. stopnje ali izhodiščnega stanja). Zdravljenje lahko nadaljujete z zmanjšanim odmerkom; priporočljivo je postopno prilagajanje odmerka po 100 mg na dan (to je zmanjšanje za 50 mg na odmerek) na podlagi individualne varnosti in prenašanja. Kadar neželeni učinki ne izginejo, tj. če bolnik ne prenaša odmerka po 100 mg 2x/dan, je treba zdravljenje trajno ukiniti. V primeru specifičnih povišanih vrednosti AST/ALT na > 3 x ULN v povezavi s povečanjem celokupnega bilirubina na ≥ 2 x ULN in ALKP < 2 x ULN je treba zdravljenje prekiniti. Če ni ugotovljen drug razlog, je treba zdravljenje trajno ukiniti. ***Posebne skupine bolnikov:*** varnost in učinkovitost pri otrocih, starih 0 do 18 let, še nista dokazani. Pri starejših bolnikih (≥ 65 let) pa na splošno niso opazili razlike. Začetnega odmerka ni treba prilagajati bolnikovi starosti. Podatki o varnosti za črnce in Afroameričane so omejeni. Bolnikom z blago do zmerno ledvično okvaro ali z blago jetrno okvaro začetnega odmerka ni treba prilagajati. Začetnega odmerka pri bolnikih z blago jetrno okvaro (Child Pugh A) na podlagi kliničnih podatkov ni treba prilagajati. Zdravljenje bolnikov z zmerno (Child Pugh B) in hudo (Child Pugh C) jetrno okvaro z Vargatefom ni priporočeno. Kapsule Vargatefa je treba zaužiti cele z vodo, najbolje s hrano; ne sme se jih žvečiti ali drobiti. **Kontraindikacije:** preobčutljivost za nintedanib, arašide ali sojo ali katerokoli pomožno snov. **Previdnostni ukrepi in opozorila:** bolezni prebavil (driska, ki tesno sovpada z dajanjem docetaksela; resni primeri driske s posledično dehidracijo in elektrolistkimi motnjami, navzea in bruhanje; zdravljenje je zato včasih treba prekiniti, zmanjšati odmerek ali trajno ukiniti), nevtropenija in sepsa (potrebno je spremljati krvno sliko), delovanje jeter (večja izpostavljenost pri Child Pugh A, zdravljenje pri Child Pugh B ali C pa ni priporočeno, opažene poškodbe jeter (vključno s hudo poškodbo jeter s smrtnim izidom), tveganje za povečanje ravni jetrnih encimov), delovanje ledvic (pozornost ob ledvični okvari/odpovedi), krvavitev (blaga do zmerna epistaksa, večina usodnih krvavitev je bila povezanih s tumorjem. Poročali so o resnih in neresnih krvavitvah (tudi smrtni izid), ki vključujejo prebavila, dihala in organe osrednjega živčnega sistema, najbolj pogoste pa so krvavitve v dihalih.V primeru krvavitve je treba razmisliti o prilagoditvi odmerka, prekinitvi ali trajni ukinitvi zdravljenja na podlagi klinične ocene), terapevtska antikoagulacija, metastaza v možganih (stabilne in aktivne metastaze v možganih), venska trombembolija (povečano tveganje za vensko trombembolijo, vključno s pljučno embolijo in globoko vensko trombozo), arterijski trombembolični dogodki (pri bolnikih z IPF, z večjim srčnožilnim tveganjem, vključno z znano koronarno arterijsko boleznijo), anevrizme in disekcije arterij (pred uvedbo Vargatefa je treba tveganje spodbude nastanka anevrizme in/ali diskeskij arterij skrbno preučiti pri bolnikih z hipertenzijo ali anamnezo anevrizme), predrtje prebavil, zapleti s celjenjem ran, vpliv na interval QT, alergijska reakcija (alergija na sojo in arašidove beljakovine), posebne populacije (izpostavljenost se veča z bolnikovo starostjo in obratno korelira s telesno maso, večja pri bolnikih azijske rase). **Interakcije:** močni zaviralci P-gp (ketokonazolom, eritromicin), močni induktorji P-gp (rifampicin, karbamazepin, fenitoin in šentjanževka), encimi citokroma (CYP), sočasno dajanje z drugimi zdravili (sočasno dajanje nintedaniba z docetakselom ni spremenilo farmakokinetike nobenega od zdravil v pomembnem obsegu). **Neželeni učinki:** ***Zelo pogosti:*** nevtropenija (vključno s febrilno nevtropenijo), zmanjšan apetit, neravnovesje elektrolitov, periferna nevropatija, krvavitev, driska, bruhanje, navzea, trebušna bolečina, povečana vrednost ALT, AST in ALKP, mukozitis (vključno s stomatitisom) in izpuščaj. ***Pogosti:*** febrilna nevtropenija, abscesi, sepsa, trombocitopenija, dehidracija, zmanjšanje telesne mase, venska trombembolija, hipertenzija, hiperbilirubinemija, povečana vrednost GGT in pruritus. ***Občasni:*** miokardni infarkt, perforacija, pankreatitis, z zdravilom povzročena poškodba jeter in ledvična odpoved. ***Neznana pogostnost***: anevrizme in disekcije arterij, kolitis. **Imetnik dovoljenja za promet:** Boehringer Ingelheim International GmbH, Binger Str. 173, D-55216 Ingelheim am Rhein, Nemčija. **Način in režim izdaje:** Rp. **Za podrobnejše informacije glejte SPC, z dne 08/2019.**

Literatura: 1. VARGATEF® Povzetek glavnih značilnosti zdravila 2019 **2.** Reck M et al. Lancet Oncol. 2014;15:143-55.

V kolikor imate medicinsko vprašanje v povezavi z zdravilom podjetja Boehringer Ingelheim, Podružnica Ljubljana,
Vas prosimo, da pokličete na telefonsko številko 01/5864-000 ali pošljete vaše vprašanje na elektronski naslov: medinfo@boehringer-ingelheim.com.

Boehringer Ingelheim

Boehringer Ingelheim RCV
podružnica Ljubljana
Šlandrova 4b, 1231 Ljubljana Črnuče

PC-SL-100109
Samo za strokovno javnost.
Datum priprave informacije: oktober 2019

VARGATEF® NINTEDANIB

Instructions for authors

The editorial policy

Radiology and Oncology is a multidisciplinary journal devoted to the publishing original and high quality scientific papers and review articles, pertinent to diagnostic and interventional radiology, computerized tomography, magnetic resonance, ultrasound, nuclear medicine, radiotherapy, clinical and experimental oncology, radiobiology, radiophysics and radiation protection. Therefore, the scope of the journal is to cover beside radiology the diagnostic and therapeutic aspects in oncology, which distinguishes it from other journals in the field.

The Editorial Board requires that the paper has not been published or submitted for publication elsewhere; the authors are responsible for all statements in their papers. Accepted articles become the property of the journal and, therefore cannot be published elsewhere without the written permission of the editors.

Submission of the manuscript

The manuscript written in English should be submitted to the journal via online submission system Editorial Manager available for this journal at: **www.radioloncol.com**.

In case of problems, please contact Sašo Trupej at **saso.trupej@computing.si** or the Editor of this journal at **gsersa@onko-i.si**

All articles are subjected to the editorial review and when the articles are appropriated they are reviewed by independent referees. In the cover letter, which must accompany the article, the authors are requested to suggest 3-4 researchers, competent to review their manuscript. However, please note that this will be treated only as a suggestion; the final selection of reviewers is exclusively the Editor's decision. The authors' names are revealed to the referees, but not vice versa.

Manuscripts which do not comply with the technical requirements stated herein will be returned to the authors for the correction before peer-review. The editorial board reserves the right to ask authors to make appropriate changes of the contents as well as grammatical and stylistic corrections when necessary. Page charges will be charged for manuscripts exceeding the recommended length, as well as additional editorial work and requests for printed reprints.

Articles are published printed and on-line as the open access (**https://content.sciendo.com/raon**).

All articles are subject to 700 EUR + VAT publication fee. Exceptionally, waiver of payment may be negotiated with editorial office, upon lack of funds.

Manuscripts submitted under multiple authorship are reviewed on the assumption that all listed authors concur in the submission and are responsible for its content; they must have agreed to its publication and have given the corresponding author the authority to act on their behalf in all matters pertaining to publication. The corresponding author is responsible for informing the coauthors of the manuscript status throughout the submission, review, and production process.

Preparation of manuscripts

Radiology and Oncology will consider manuscripts prepared according to the Uniform Requirements for Manuscripts Submitted to Biomedical Journals by International Committee of Medical Journal Editors (www.icmje.org). The manuscript should be written in grammatically and stylistically correct language. Abbreviations should be avoided. If their use is necessary, they should be explained at the first time mentioned. The technical data should conform to the SI system. The manuscript, excluding the references, tables, figures and figure legends, must not exceed 5000 words, and the number of figures and tables is limited to 8. Organize the text so that it includes: Introduction, Materials and methods, Results and Discussion. Exceptionally, the results and discussion can be combined in a single section. Start each section on a new page, and number each page consecutively with Arabic numerals.

The Title page should include a concise and informative title, followed by the full name(s) of the author(s); the institutional affiliation of each author; the name and address of the corresponding author (including telephone, fax and E-mail), and an abbreviated title (not exceeding 60 characters). This should be followed by the abstract page, summarizing in less than 250 words the reasons for the study, experimental approach, the major findings (with specific data if possible), and the principal conclusions, and providing 3-6 key words for indexing purposes. Structured abstracts are required. Slovene authors are requested to provide title and the abstract in Slovene language in a separate file. The text of the research article should then proceed as follows:

Introduction should summarize the rationale for the study or observation, citing only the essential references and stating the aim of the study.

Materials and methods should provide enough information to enable experiments to be repeated. New methods should be described in details.

Results should be presented clearly and concisely without repeating the data in the figures and tables. Emphasis should be on clear and precise presentation of results and their significance in relation to the aim of the investigation.

Discussion should explain the results rather than simply repeating them and interpret their significance and draw conclusions. It should discuss the results of the study in the light of previously published work.

Charts, Illustrations, Images and Tables

Charts, Illustrations, Images and Tables must be numbered and referred to in the text, with the appropriate location indicated. Charts, Illustrations and Images, provided electronically, should be of appropriate quality for good reproduction. Illustrations and charts must be vector image, created in CMYK color space, preferred font "Century Gothic", and saved as .AI, .EPS or .PDF format. Color charts, illustrations and Images are encouraged, and are published without additional charge. Image size must be 2.000 pixels on the longer side and saved as .JPG (maximum quality) format. In Images, mask the identities of the patients. Tables should be typed double-spaced, with a descriptive title and, if appropriate, units of numerical measurements included in the column heading. The files with the figures and tables can be uploaded as separate files.

References

References must be numbered in the order in which they appear in the text and their corresponding numbers quoted in the text. Authors are responsible for the accuracy of their references. References to the Abstracts and Letters to the Editor must be identified as such. Citation of papers in preparation or submitted for publication, unpublished observations, and personal communications should not be included in the reference list. If essential, such material may be incorporated in the appropriate place in the text. References follow the style of Index Medicus, DOI number (if exists) should be included.

All authors should be listed when their number does not exceed six; when there are seven or more authors, the first six listed are followed by "et al.". The following are some examples of references from articles, books and book chapters:

Dent RAG, Cole P. In vitro maturation of monocytes in squamous carcinoma of the lung. *Br J Cancer* 1981; **43:** 486-95. doi: 10.1038/bjc.1981.71

Chapman S, Nakielny R. *A guide to radiological procedures*. London: Bailliere Tindall; 1986.

Evans R, Alexander P. Mechanisms of extracellular killing of nucleated mammalian cells by macrophages. In: Nelson DS, editor. *Immunobiology of macrophage.* New York: Academic Press; 1976. p. 45-74.

Authorization for the use of human subjects or experimental animals

When reporting experiments on human subjects, authors should state whether the procedures followed the Helsinki Declaration. Patients have the right to privacy; therefore the identifying information (patient's names, hospital unit numbers) should not be published unless it is essential. In such cases the patient's informed consent for publication is needed, and should appear as an appropriate statement in the article. Institutional approval and Clinical Trial registration number is required. Retrospective clinical studies must be approved by the accredited Institutional Review Board/Committee for Medical Ethics or other equivalent body. These statements should appear in the Materials and methods section.

The research using animal subjects should be conducted according to the EU Directive 2010/63/EU and following the Guidelines for the welfare and use of animals in cancer research (Br J Cancer 2010; 102: 1555 – 77). Authors must state the committee approving the experiments, and must confirm that all experiments were performed in accordance with relevant regulations.

These statements should appear in the Materials and methods section (or for contributions without this section, within the main text or in the captions of relevant figures or tables).

Transfer of copyright agreement

For the publication of accepted articles, authors are required to send the License to Publish to the publisher on the address of the editorial office. A properly completed License to Publish, signed by the Corresponding Author on behalf of all the authors, must be provided for each submitted manuscript.

The non-commercial use of each article will be governed by the Creative Commons Attribution-NonCommercial-NoDerivs license.

Conflict of interest

When the manuscript is submitted for publication, the authors are expected to disclose any relationship that might pose real, apparent or potential conflict of interest with respect to the results reported in that manuscript. Potential conflicts of interest include not only financial relationships but also other, non-financial relationships. In the Acknowledgement section the source of funding support should be mentioned. The Editors will make effort to ensure that conflicts of interest will not compromise the evaluation process of the submitted manuscripts; potential editors and reviewers will exempt themselves from review process when such conflict of interest exists. The statement of disclosure must be in the Cover letter accompanying the manuscript or submitted on the form available on **www.icmje.org/coi_disclosure.pdf**

Page proofs

Page proofs will be sent by E-mail to the corresponding author. It is their responsibility to check the proofs carefully and return a list of essential corrections to the editorial office within three days of receipt. Only grammatical corrections are acceptable at that time.

Open access

Papers are published electronically as open access on **https://content.sciendo.com/raon**, also papers accepted for publication as E-ahead of print.

XALKORI® – 1. linija zdravljenja napredovalega, ALK pozitivnega nedrobnoceličnega pljučnega raka[1]

ALK = anaplastična limfomska kinaza

BISTVENI PODATKI IZ POVZETKA GLAVNIH ZNAČILNOSTI ZDRAVILA

XALKORI 200 mg, 250 mg trde kapsule

Sestava in oblika zdravila: Ena kapsula vsebuje 200 mg ali 250 mg krizotiniba. **Indikacije:** Monoterapija za: - prvo linijo zdravljenja odraslih bolnikov z napredovalim nedrobnoceličnim pljučnim rakom (NSCLC – *Non-Small Cell Lung Cancer*), ki je ALK (anaplastična limfomska kinaza) pozitiven; - zdravljenje odraslih bolnikov s predhodno zdravljenim, napredovalim NSCLC, ki je ALK pozitiven; - zdravljenje odraslih bolnikov z napredovalim NSCLC, ki je ROS1 pozitiven. **Odmerjanje in način uporabe:** Zdravljenje mora uvesti in nadzorovati zdravnik z izkušnjami z uporabo zdravil za zdravljenje rakavih bolezni. Preverjanje prisotnosti ALK in ROS1: Pri izbiri bolnikov za zdravljenje je treba pred zdravljenjem opraviti točno in validirano preverjanje prisotnosti ALK ali ROS1. Odmerjanje: Priporočeni odmerek je 250 mg dvakrat na dan (500 mg na dan), bolniki pa morajo zdravilo jemati brez prekinitev. Če bolnik pozabi vzeti odmerek, ga mora vzeti takoj, ko se spomni, razen če do naslednjega odmerka manjka manj kot 6 ur. V tem primeru bolnik pozabljenega odmerka ne sme vzeti. *Prilagajanja odmerkov:* Glede na varnost uporabe zdravila pri posameznem bolniku in kako bolnik zdravljenje prenaša, utegne biti potrebna prekinitev in/ali zmanjšanje odmerka pri bolnikih, ki se zdravijo s krizotinibom 250 mg peroralno dvakrat na dan (za režim zmanjševanja odmerka glejte poglavje 4.2 v povzetku glavnih značilnosti zdravila). Za prilagajanje odmerkov pri *hematološki in nehematološki toksičnosti* (povečanje vrednosti AST, ALT, bilirubina; ILD/pnevmonitis; podaljšanje intervala QTc, bradikardija, bolezni oči) glejte preglednici 1 in 2 v poglavju 4.2 povzetka glavnih značilnosti zdravila. *Okvara jeter:* Pri zdravljenju pri bolnikih z okvaro jeter je potrebna previdnost. Pri blagi okvari jeter prilagajanje začetnega odmerka ni priporočeno, pri zmerni okvari jeter je priporočeni začetni odmerek 200 mg dvakrat na dan, pri hudi okvari jeter pa 250 mg enkrat na dan (za merila glede klasifikacije okvare jeter glejte poglavje 4.2 v povzetku glavnih značilnosti zdravila). *Okvara ledvic:* Pri blagi in zmerni okvari prilagajanje začetnega odmerka ni priporočeno. Pri hudi okvari ledvic (ki ne zahteva peritonealne dialize ali hemodialize) je začetni odmerek 250 mg peroralno enkrat na dan; po vsaj 4 tednih zdravljenja se lahko poveča na 200 mg dvakrat na dan. *Starejši bolniki (≥ 65 let):* Prilagajanje začetnega odmerka ni potrebno. *Pediatrična populacija:* Varnost in učinkovitost nista bili dokazani. Način uporabe: Kapsule je treba pogoltniti cele, z nekaj vode, s hrano ali brez nje. Ne sme se jih zdrobiti, raztopiti ali odpreti. Izogibati se je treba uživanju grenivk, grenivkinega soka ter uporabi šentjanževke. **Kontraindikacije:** Preobčutljivost na krizotinib ali katerokoli pomožno snov. **Posebna opozorila in previdnostni ukrepi:** Določanje statusa ALK in ROS1: Pomembno je izbrati dobro validirano in robustno metodologijo, da se izognemo lažno negativnim ali lažno pozitivnim rezultatom. Hepatotoksičnost: V kliničnih študijah so poročali o hepatotoksičnosti, ki jo je povzročilo zdravilo (vključno s primeri s smrtnim izidom). Delovanje jeter, vključno z ALT, AST in skupnim bilirubinom, je treba preveriti enkrat na teden v prvih 2 mesecih zdravljenja, nato pa enkrat na mesec in kot je klinično indicirano. Ponovitve preverjanj morajo biti pogostejše pri povečanjih vrednosti stopnje 2, 3 ali 4. Intersticijska bolezen pljuč (ILD)/pnevmonitis: Lahko se pojavi huda, življenjsko nevarna ali smrtna ILD/pnevmonitis. Bolnike s simptomi ILD/pnevmonitisa je treba spremljati, zdravljenje pa prekiniti ob sumu na ILD/pnevmonitis. Podaljšanje intervala QT: Opažali so podaljšanje intervala QTc. Pri bolnikih z obstoječo bradikardijo, podaljšanjem intervala QTc v anamnezi ali predispozicijo zanj, pri bolnikih, ki jemljejo antiaritmike ali druga zdravila, ki podaljšujejo interval QT, ter pri bolnikih s pomembno obstoječo srčno boleznijo in/ali motnjami elektrolitov je treba krizotinib uporabljati previdno; potrebno je redno spremljanje EKG, elektrolitov in delovanja ledvic; preiskavi EKG in elektrolitov je treba opraviti čimbližje uporabi prvega odmerka, potem se priporoča redno spremljanje. Če se interval QTc podaljša za 60 ms ali več, je treba zdravljenje s krizotinibom začasno prekiniti in se posvetovati s kardiologom. Bradikardija: Lahko se pojavi simptomatska bradikardija (lahko se razvije več tednov po začetku zdravljenja); izogibati se je treba uporabi krizotiniba v kombinaciji z drugimi zdravili, ki povzročajo bradikardijo; pri simptomatski bradikardiji je treba prilagoditi odmerek. Srčno popuščanje: Poročali so o hudih, življenjsko nevarnih ali smrtnih neželenih učinkih srčnega popuščanja. Bolnike je treba spremljati glede pojavov znakov in simptomov srčnega popuščanja in ob pojavu simptomov zmanjšati odmerjanje ali prekiniti zdravljenje. Nevtropenija in levkopenija: V kliničnih študijah so poročali o nevtropeniji, levkopeniji in febrilni nevtropeniji; spremljati je treba popolno krvno sliko (pogostejše preiskave, če se opazijo abnormalnosti stopnje 3 ali 4 ali če se pojavi povišana telesna temperatura ali okužba). Perforacija v prebavilih: V kliničnih študijah so poročali o perforacijah v prebavilih, v obdobju trženja pa o smrtnih primerih perforacij v prebavilih. Krizotinib je treba pri bolnikih s tveganjem za nastanek perforacije v prebavilih uporabljati previdno; bolniki, pri katerih se razvije perforacija v prebavilih, se morajo prenehati zdraviti s krizotinibom; bolnike je treba poučiti o prvih znakih perforacije in jim svetovati, naj se nemudoma posvetujejo z zdravnikom. Vplivi na ledvice: V kliničnih študijah so opazili zvišanje ravni kreatinina v krvi in zmanjšanje očistka kreatinina. V kliničnih študijah in v obdobju trženja so poročali tudi o odpovedi ledvic, akutni odpovedi ledvic, primerih s smrtnim izidom, primerih, ki so zahtevali hemodializo in hiperkaliemiji stopnje 4. Vplivi na vid: V kliničnih študijah so poročali o izpadu vidnega polja stopnje 4 z izgubo vida. Če se na novo pojavi huda izguba vida, je treba zdravljenje prekiniti in opraviti oftalmološki pregled. Če so motnje vida trdovratne ali se poslabšajo, je priporočljiv oftalmološki pregled. Histološka preiskava, ki ne nakazuje adenokarcinoma: Na voljo so le omejeni podatki pri NSCLC, ki je ALK in ROS1 pozitiven in ima histološke značilnosti, ki ne nakazujejo adenokarcinoma, vključno s ploščatoceličnim karcinomom (SCC). **Medsebojno delovanje z drugimi zdravili in druge oblike interakcij:** Izogibati se je treba sočasni uporabi z močnimi zaviralci CYP3A4, npr. atazanavir, ritonavir, kobicistat, itrakonazol, ketokonazol, posakonazol, vorikonazol, klaritromicin, telitromicin in eritromicin (razen če morebitna korist za bolnika odtehta tveganje, v tem primeru je treba bolnike skrbno spremljati glede neželenih učinkov krizotiniba), ter grenivko i n grenivkinim sokom, saj l ahko povečajo koncentracije krizotiniba v plazmi. Izogibati se je treba sočasni uporabi z močnimi induktorji CYP3A4, npr. karbamazepin, fenobarbital, fenitoin, rifampicin in šentjanževka, saj lahko zmanjšajo koncentracije krizotiniba v plazmi. Učinek zmernih induktorjev CYP3A4, npr. efavirenz in rifabutin, še ni jasen, zato se je treba sočasni uporabi s krizotinibom izogibati. Zdravila, katerih koncentracije v plazmi lahko krizotinib spremeni (midazolam, alfentanil, cisaprid, ciklosporin, derivati ergot alkaloidov, fentanil, pimozid, kinidin, sirolimus, takrolimus, digoksin, dabigatran, kolhicin, pravastatin: sočasni uporabi s temi zdravili se je treba izogibati oziroma izvajati skrben klinični nadzor; bupropion, efavirenz, peroralni kontraceptivi, raltegravir, i rinotekan, morfin, nalokson, metformin, prokainamid). Zdravila, ki podaljšujejo interval QT ali ki lahko povzročijo Torsades de pointes (antiaritmiki skupine IA (kinidin, disopiramid), antiaritmiki skupine III (amiodaron, sotalol, dofetilid, ibutilid), metadon, cisaprid, moksifloksacin, antipsihotiki) – v primeru sočasne uporabe je potreben skrben nadzor intervala QT. Zdravila, ki povzročajo bradikardijo (nedihidropiridinski zaviralci kalcijevih kanalčkov (verapamil, diltiazem), antagonisti adrenergičnih receptorjev beta, klonidin, gvanfacin, digoksin, meflokin, antiholinesteraze, pilokarpin) – krizotinib je treba uporabljati previdno. **Plodnost, nosečnost in dojenje:** Ženske v rodni dobi se morajo izogibati zanositvi. Med zdravljenjem in najmanj 90 dni po njem je treba uporabljati ustrezno kontracepcijo (velja tudi za moške). Zdravilo lahko škoduje plodu in se ga med nosečnostjo ne sme uporabljati, razen če klinično stanje matere ne zahteva takega zdravljenja. Matere naj se med jemanjem zdravila dojenju izogibajo. Zdravilo lahko zmanjša plodnost moških in žensk. **Vpliv na sposobnost vožnje in upravljanja strojev:** Lahko se pojavijo simptomatska bradikardija (npr. sinkopa, omotica, hipotenzija), motnje vida ali utrujenost; potrebna je previdnost. **Neželeni učinki:** Najresnejši neželeni učinki so bili hepatotoksičnost, ILD/pnevmonitis, nevtropenija in podaljšanje intervala QT. Najpogostejši neželeni učinki (≥ 25 %) so bili motnje vida, navzea, diareja, bruhanje, edem, zaprtje, povečane vrednosti transaminaz, utrujenost, pomanjkanje apetita, omotica in nevropatija. Ostali zelo pogosti (≥ 1/10 bolnikov) neželeni učinki so: nevtropenija, anemija, levkopenija, disgevzija, bradikardija, bolečina v trebuhu in izpuščaj. **Način in režim izdaje:** Predpisovanje in izdaja zdravila je le na recept, zdravilo pa se uporablja samo v bolnišnicah. Izjemoma se lahko uporablja pri nadaljevanju zdravljenja na domu ob odpustu iz bolnišnice in nadaljnjem zdravljenju. **Imetnik dovoljenja za promet:** Pfizer Europe MA EEIG, Boulevard de la Plaine 17, 1050 Bruxelles, Belgija. **Datum zadnje revizije besedila:** 28.02.2019

Pred predpisovanjem se seznanite s celotnim povzetkom glavnih značilnosti zdravila.

Vir: 1. Povzetek glavnih značilnosti zdravila Xalkori, 28.02.2019

XALKORI® KRIZOTINIB

XAR-02-19 Samo za strokovno javnost

Pfizer Luxembourg SARL, GRAND DUCHY OF LUXEMBOURG, 51, Avenue J.F. Kennedy, L-1855,
Pfizer podružnica Ljubljana, Letališka cesta 29a, 1000 Ljubljana

Radiology and Oncology | Ljubljana | Slovenia | https://content.sciendo.com/raon

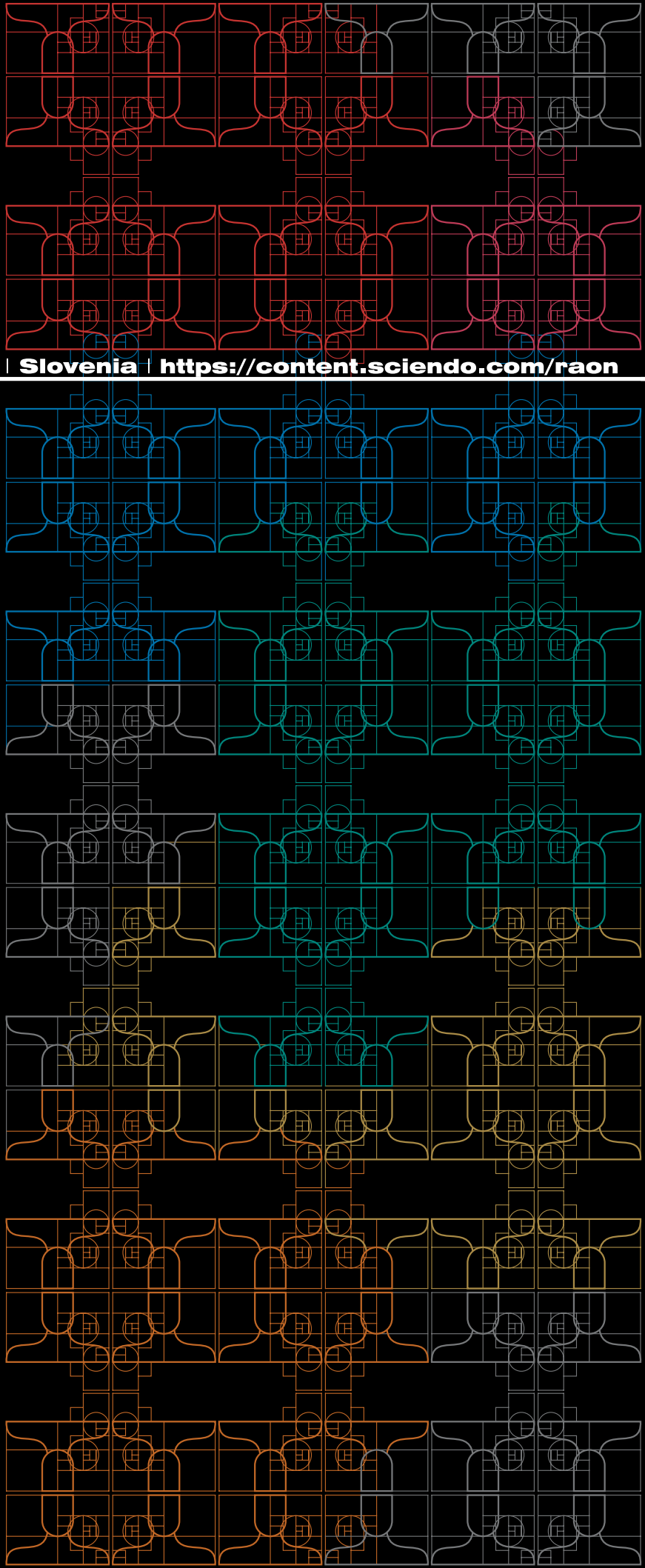

ISSN 1318 - 2099